Comprehensive Study on Impact of Climate Change on Water Flow Pattern Affecting the Generation of Hydropower Projects

TEAM

Sh. D.C. Rana, IAS
Member Secretary, HIMCOSTE, Shimla

Dr. Suresh C. Attri
Joint Member Secretary, HIMCOSTE, Shimla

Ms. Kalpana Kumari, Scientific Officer,
State Centre on Climate Change (SCCC), HIMCOSTE, Shimla

Ms. Neha Thakur, Scientific Professional
Ms. Monika Chauhan, Scientific Professional
Ms. Aditi Panatu, Scientific Professional
State Centre on Climate Change, HIMCOSTE, Shimla, H.P.

Sh. Raj Kumar, Project Associate
Ms. Anjana Bansal, Project Associate
Himachal Pradesh Remote Sensing Cell, HIMCOSTE, Shimla

Submitted by

State Centre on Climate Change
Himachal Pradesh Council for Science, Technology & Environment
Vigyan Bhawan, Kasumpti, Shimla-9

Submitted to

NJHPS, Satluj Jal Vidyut Nigam Limited (SJVNL)
Nathpa, Tehsil Nichar, District Kinnaur, HP

January, 2026

EXECUTIVE SUMMARY

The study investigates the impact of climate change on glacier dynamics, snow cover and hydrological flow in the Satluj basin. It assesses long-term trends in glacier retreat, snow cover variability, mass balance conditions and temperature discharge relationships to support climate-resilient planning. Multi-temporal satellite datasets (Landsat 7 ETM+ 2000, Resourcesat-2 LISS-III 2011, Landsat 8 OLI 2020), seasonal snow cover imagery (AWiFS 2010–2020) and ten years of discharge and temperature data (2010–2020) were used. Pre-processing, glacier delineation, spatial analysis and statistical modelling were carried out using ERDAS Imagine, analytical tools ArcGIS, Excel and SPSS.

The Satluj Basin shows rapid cryospheric change, with glacier area declining from 1481.75 km² (2000) to 1384.16 km² (2020), >80% of glaciers retreating at rates <10 m/year, especially in the Upper Satluj and Spiti sub-basins. Mass balance of 1,120 glaciers shifted from near-equilibrium in 2000 to widespread negative balance by 2020, while snow cover variability (35–72%) indicates shortened replenishment due to earlier melting and delayed snowfall.

With strong positive correlations between air temperature and river discharge hydrological analysis validates a shift toward temperature-driven runoff. These changes have an impact on hydropower generation, leading to higher flow variability, increased sediment load, turbine wear and lower late-season output. The risk of climate-related hazards like landslides rockfalls and GLOFs is also increased by accelerated glacier retreat.

The Satluj Basin is changing hydrologically and cryospherically. The sustainability of hydropower water security and hazard vulnerability are all at risk due to these changes. It is crucial to improve hydrological forecasting strengthen glacier and snow monitoring and put a climate-resilient adaptation plan into action. The Himalayan region is particularly vulnerable to climate-induced water stress because its rivers, which are fed by snow and glaciers, are a major source of freshwater, support hydropower and sustain livelihoods downstream.

ACKNOWLEDGEMENT

The Himachal Pradesh Council for Science, Technology & Environment (HIMCOSTE), Government of Himachal Pradesh, formally places on record its sincere gratitude to Satluj Jal Vidyut Nigam Limited (SJVNL) for commissioning and sponsoring the present study entitled as *"Comprehensive Study on Impact of Climate Change on Water Flow Pattern Affecting the Generation of Hydropower Projects"*. The study has been undertaken to generate scientific insights into climate-induced hydrological variability within the Satluj basin and to support informed understanding relevant to sustainable hydropower development and climate-resilient water resource management.

The Council also places on record its appreciation for the guidance, administrative support and facilitation provided by the Secretary (Environment, Science, Technology & Climate Change) Government of Himachal Pradesh**,** the Member Secretary (EC) and the Joint Member Secretary, Himachal Pradesh Council for Science, Technology & Environment (HIMCOSTE), which provided institutional support for the conduct of the assignment.

The study was undertaken under the aegis of the State Centre on Climate Change (SCCC) at HIMCOSTE, employing advanced Remote Sensing (RS) and Geographic Information System (GIS) methodologies, along with hydro-meteorological and statistical analyses, to assess climate induced variations in river discharge, seasonal flow regimes and runoff characteristics within the Satluj River system. The study contributes to the scientific and technical understanding of climate change impacts on hydrology and supports evidence-based planning for sustainable water resource and hydropower management in the region.

CONTENTS

LIST OF FIGURES

LIST OF TABLES

LIST OF ABBREVIATIONS

AAR	Accumulation Area Ratio
ABL	Ablation
ACC	Accumulation
ALOS	Advanced Land Observing Satellite
AWiFS	Advanced Wide Field Sensor
DEM	Digital Elevation Model
ELA	Equilibrium Line Altitude
ETM+	Enhanced Thematic Mapper Plus
GLOF	Glacier Lake outburst flood
LANDSAT	Land Remote Sensing Satellite
LISS III	Linear Imaging Self-Scanning Sensor III
OLI	Operational Land Imager
PALSAR	Phased Array type L-band Synthetic Aperture Radar
Q	Discharge
Temp.	Temperature
TM	Thematic Mapper
TOA	Top of Atmosphere

1. INTRODUCTION

Climate Change refers to long-term shifts in temperatures and weather patterns. As a result of the widespread consumption of fossil fuels like coal, oil and gas, human activity has been the primary cause of climate change since the 1800s. Fossil fuel combustion produces greenhouse gas emissions that encircle the earth like a blanket, trapping solar heat and driving up temperatures.

Climate change poses a serious and escalating threat to humanity. Average global temperatures have risen by 1.1°C between 2011 and 2020 compared to pre-industrial times, primarily due to greenhouse gas emissions from human activities. Carbon dioxide (CO_2), the main greenhouse gas, is produced through fossil fuel use, deforestation and industrial operations. These emissions have intensified global warming, affecting the Earth's temperature by altering the amount of sunlight it absorbs, reflects and traps in the atmosphere. Global warming is generating extensive changes: rising sea levels, melting glaciers and ice, changing precipitation patterns, more frequent and powerful extreme weather events (hot waves, heavy rainfall, droughts).

The impacts of climate change are evident and severe. Extreme weather events, including wildfires, droughts, floods and heat waves, are becoming more frequent and intense (WMO, 2022). Melting glaciers and ice caps are driving sea-level rise, threatening coastal regions. Vulnerable ecosystems and communities, particularly in poorer nations, are bearing the brunt of these changes. Global warming has diminished food and water security, increased the intensity and frequency of natural disasters and hindered progress toward the Sustainable Development Goals (IPCC, 2023). Rockstrom et al. (2009), pointed out that ecosystems and biodiversity are under tremendous stress due to climate change, which has already passed a safe level. The potential adverse effects of climate change will only intensify with further warming. Immediate and effective mitigation and adaptation measures are crucial to limiting the magnitude and rate of climate change and its associated hazards. Without decisive action, the risks to humanity and the planet will continue to grow.

CLIMATE CHANGE & MOUNTAIN ECOSYSTEM

Mountain ecosystems are intricate assemblages of living organisms, yet they remain highly delicate and vulnerable. Their sensitivity to climate change is amplified by steep temperature gradients and the presence of snow, ice, permafrost and other complex environmental features (Knight, 2022). The few remaining biological systems in these regions are increasingly threatened by climate and land-use changes, which also exert pressure on high-altitude forestry and agricultural practices (Notarnicola et al., 2024).

Major environmental challenges in mountainous areas include:

- Desertification,
- Landslides,
- Forest degradation,
- Reduction in snow cover and Glacier Lake Outburst Floods (GLOFs)

Although mountains cover approximately 25% of the Earth's surface, they harbor a substantial share of global biodiversity and cultural diversity. These ecosystems offer crucial services such as water supply, climate regulation and cultural significance (Foggin, 2016). Globally, more than 1.9 billion people directly or indirectly on water from mountain sources, making cryospheric change a critical threat to downstream water security (IPCC, 2022; Viviroli et al., 2007). Biodiversity loss, ecosystem degradation and ecological damage are already significant hazards worldwide and are set to worsen with every additional degree of warming. For instance, an 18 ± 13% loss of global glacier mass could disrupt water supplies for agriculture, hydropower and communities. A 2°C rise in temperature could reduce irrigation water in snowmelt-fed watersheds by 20%, with impacts potentially quadrupling at 4°C (IPCC, 2022). For the Himalayan regions, where millions depend on rivers fed by glaciers, such changes have significant ramifications.

As per WWF, over one-third of the world's glaciers will disappear by the year 2100, regardless of how we drastically reduce emissions in the decades that follow. Ninety-five percent of the Arctic's eldest and thickest ice sheet has long since disappeared.

THE HIMALAYAN CRYOSPHERE

Across the world, the cryosphere is melting be it the Arctic, Antarctic, Greenland or the Himalayas. Glaciers cover nearly 10% of the Earth's land surface and store about 77% of its fresh water, with over 96% of this ice concentrated in the polar regions (Dyurgerov & Meier, 2005). Outside the poles, the Indian Himalaya and the broader High Mountains of Asia contain the largest glacial extent collectively referred to as the "third pole" (Dyurgerov, 2001; Pant et al., 2018).

CRYOSPHERE

The cryosphere refers to all of Earth's frozen water, including glaciers, snow cover, ice, sea ice, frozen lakes and rivers and permafrost. It is a vital part of the planet's climate system because its high reflectivity (albedo) and large heat-storage capacity help regulate global temperatures. The cryosphere also acts as a major freshwater reservoir, storing nearly 77% of the world's fresh water in the form of ice. In mountain regions like the Himalayas, it plays a critical role in sustaining river flows, agriculture and livelihoods downstream.

Most Himalayan glaciers reside above 3700-4300 meters in relatively harsh terrain, making them significantly less explored and documented compared to polar or alpine glaciers. India contains over 9,500 glaciers across the Western, Central and Eastern Himalaya, with ISRO's latest inventory reporting 9,575 glaciers in the Indian Himalayan region (Raina & Srivastava, 2008; ISRO, 2021). Snow and glacial melt are vital components of Himalayan River systems, with the Himalayan cryosphere playing a major role in regulating the hydrological balance of the Ganges Valley.

Himalayan glaciers are retreating, though the rate and pattern vary across regions. Glaciers in Eastern and Central Himalaya exhibit clear retreat and mass loss (Bolch et al., 2012; Kargel et al., 2014). In contrast, the Karakoram anomaly highlights that some glaciers in the Karakoram region remain stable or are even advancing, driven by unique local climatic conditions (Hewitt, 2005; Gardelle et al., 2012). Long-term monitoring reveals significant recession of major glaciers, including the Gangotri Glacier, which has retreated by over 1 km in the past century and continues to experience rapid thinning (Dobhal et al., 2013). Similarly, the Chhota Shigri Glacier in Himachal Pradesh shows predominantly negative mass balance trends since systematic observations began (Wagnon et al., 2007; Azam et al., 2016). Additionally, satellite observations indicate a widespread

decline in snow cover duration, marked by earlier spring melt and reduced winter accumulation across the Himalaya (Bookhagen & Burbank, 2010; Jain et al., 2020). Together, these findings underscore the accelerating cryospheric changes impacting Himalayan hydrology and downstream water availability.

CLIMATE CHANGE IN INDIA: TRENDS AND PROJECTIONS

The Ministry of Earth Sciences reports that India has warmed by about 0.7 °C since 1901, with significant increases in extreme temperatures in recent decades. Future projections under high emissions suggest that temperatures could rise by up to 4.4 °C by 2100, posing major risks to agriculture, water resources and other climate-sensitive sectors. Rising temperatures are accelerating glacier melt, changing river flow patterns and increasing the risk of landslides, flash floods and GLOFs making the Himalayan region particularly at risk.

India's agriculture is primarily rain-fed, which makes it extremely susceptible to climate extremes and variability. Agricultural productivity and water availability are directly impacted by variations in monsoon timing, rainfall distribution, increased frequency of droughts and rising temperatures (MoES, 2020; Mishra et al., 2020). Based on scientific analyses, subject to the region and emission projections, predicted warming by 2080–2100 could lower national crop yields by 10%–40% (Aggarwal et al., 2019; Praveen & Sharma, 2019). Accordingly, net agricultural revenues could drop by 3% to 26%, reflecting losses brought on by climate change in all climate-sensitive zones (Birthal et al., 2015). Major crop yields are being destabilized by climate variability and rising temperatures, endangering food security and small and marginal farmers' livelihoods. Long-term water safety and crop yields are being further undermined by increasing water stress brought on by unpredictable monsoons and groundwater depletion (Ghosh et al., 2022; MoES, 2020). Through

few studies on health, urban systems, coastal zones and disaster resilience, climate research in India is still mostly concentrated on agriculture, leaving significant knowledge gaps (World Bank, 2022). In the meantime, rising temperatures, erratic rainfall and land-use pressures are putting more strain on forests, wetlands, watersheds and biodiversity hotspots (IPCC, 2022). Climate change increases vulnerability, displacement challenges and disparities in socioeconomic status, endangering livelihoods and food systems for communities reliant on climate-sensitive sectors (World Bank, 2022).

AN OVERVIEW: MOUNTAIN TERRAIN, SNOW REGIMES AND THE SATLUJ BASIN IN HIMACHAL PRADESH

HIMACHAL PRADESH: A HIGH-MOUNTAIN STATE IN THE WESTERN HIMALAYA

Himachal Pradesh is situated in the western Himalaya, primarily a mountainous state with varied climatic zones, rough terrain and steep altitudinal gradients. Different ecological and hydrological environments are created by elevations that vary from 350 meters in the Shivalik foothills to over 6,900 meters in the high Himalayan ranges. The Shivaliks, Lesser Himalaya, Greater Himalaya and Trans-Himalaya are the state's various physiographic zones, each of which is distinguished by its own geological features, climate and water regimes. Large snowfields, permafrost regions and snow-capped glaciers can be found in the Greater Himalaya and Trans-Himalaya, which includes districts like Kinnaur, Lahaul-Spiti and portions of Chamba and Kullu.

These regions experience long, severe winters, with temperatures often dropping below 20°C, while summer conditions remain cool and conducive to snowmelt runoff. The summer monsoon, which greatly increases rainfall at lower altitudes and winter western disturbances, which bring snowfall essential for glacier sustenance, are the state's two main sources of precipitation. Due to its hilly terrain, Himachal Pradesh is extremely vulnerable to climatic fluctuations; even minor shifts in temperature or precipitation patterns can have a big impact on river discharge, slope stability, snow accumulation and glacier mass balance. The state's snow-fed rivers and mountain landscapes are intricately linked to its economy, which is mostly reliant on hydropower, horticulture, agriculture and tourism. As a result, the region's ecological resilience, energy production and water security are all seriously threatened by continuous climate change.

SNOW AND GLACIER REGIMES OF HIMACHAL PRADESH

In the western Himalaya, Himachal Pradesh has one of the highest concentrations of seasonal snow and glaciers. More than 2,500 glaciers are dispersed over high-altitude areas including Lahaul–Spiti, Kinnaur, Chamba and Kullu and almost one-third of the state's land is covered by seasonal snow in the winter (Bhambri et al., 2011; ICIMOD, 2011). By holding winter precipitation and releasing meltwater gradually in the spring and summer, these glaciers and snowfields serve as natural freshwater reservoirs that control the base flow of rivers that are supplied by snow.

Major glaciers like Bara Shigri, Chhota Shigri and those in the Baspa Sub- basin are rapidly thinning and retreating due to warming and decreased snowfall, endangering the health of glaciers in Himachal Pradesh (Bolch et al., 2012; Azam et al., 2018, 2019; Wagnon et al., 2007). As warmer winters convert snowfall to rainfall, increasing the sensitivity of snow and glacier systems and changing downstream hydrology, satellite analysis in Himachal Pradesh reveal shorter snow-cover duration, earlier spring melt and lower winter snowpack (Rangra et al., 2023).

THE SATLUJ RIVER BASIN

One of the most significant transboundary river systems, the Satluj River Basin originates in the western Himalaya and provides Himachal Pradesh and northwest India with a vital lifeline. At an elevation of roughly 4,575 meters, the Satluj (sometimes written Sutlej) rises close to Rakhi Lake (Rakas Tal) in the Tibetan Plateau. It travels for almost 1,450 kilometers before entering the Indus River in Pakistan (Singh et al., 2021). The upper catchment lies in a cold and dry trans-Himalayan region with widespread permafrost, little vegetation and low annual precipitation, due to Western Disturbances (WDs). The Satluj Basin, which spans the districts of Kinnaur, Shimla, Kullu and Bilaspur in Himachal Pradesh, is home to a variety of landscapes, from steep forested intermediate ranges to desolate high-altitude deserts. The Baspa, Spiti and Kinnaur-Lahaul glacier systems are among the primary glaciers and snowfields that provide the river with meltwater, which greatly contributes to its discharge in late spring and summer (ICIMOD, 2011; Azam et al., 2019). The basin is one of the most snow-dependent hydrological systems in the western Himalaya due to its extensive seasonal snow cover.

The Satluj has a nivo-glacial hydrological regime, with peak flows from May to September brought on by glacier melt, snowmelt and monsoon rains. Research shows that snow and glacier melt, especially upstream of Bhakra Dam, account for 50–70% of the yearly flow in the upper Satluj (Sharma et al., 2018). Because precipitation is kept as snow instead of entering the river system, the discharge is noticeably reduced during the winter.

Major hydroelectric projects like Nathpa Jhakri (1,500 MW), Karcham Wangtoo (1,091 MW), Baspa II and Rampur hydropower stations are located along the river, which is also crucial to India's hydropower industry. Although recent changes in snow availability, rainfall patterns and glacier melt are changing flow regimes, the basin's steep topography and perennial snowmelt offer perfect conditions for electricity generation. The region's water supply, sediment load and hydropower output are becoming less reliable due to climate-induced changes such earlier snowmelt, decreasing glacier mass and sporadic high-intensity rains (Purohit et al., 2022). All things considered, the Satluj River Basin is a dynamic hydrological system that is extremely susceptible to changes in the climate. Because of its reliance on snow and ice melt, it is particularly susceptible to variations in temperature, winter precipitation and summer precipitation patterns, which can have a significant impact on hydropower generation and water security.

ROLE OF REMOTE SENSING AND GIS

Remote sensing plays a crucial role in the observation and analysis of cryospheric components such as glaciers, snow cover, permafrost and meltwater runoff. Satellite data provide systematic approach to monitor these environments at regional to global scales because high-mountain and polar regions are difficult to access and often lack continuous ground-based measurements. Remote sensing offers consistent, repeatable and long-term observations that help scientists track changes in the cryosphere under changing climatic conditions.

Advanced optical sensors (e.g., Landsat, Sentinel-2, MODIS) and microwave sensors (e.g., SAR from Sentinel-1) make it easier to delineation of glacier boundaries, mapping of accumulation and ablation zones and seasonal and interannual changes in snow cover extent. Digital Elevation Models (DEMs) is used to further enhance glacier inventory creation by enabling volumetric analysis and surface elevation change detection, which are critical for estimating geodetic mass balance.

Remote sensing algorithms such as NDSI (Normalized Difference Snow Index), spectral unmixing and SAR backscatter analysis are widely applied to discriminate snow, ice, debris-covered ice and supraglacial melt features. Integration of satellite-derived surface temperature, albedo and snow depth products supports energy-balance and degree-day modelling frameworks for quantifying melt contributions from snow and glaciers.

Overall, remote sensing provides a robust, cost-effective and scalable approach to monitoring cryospheric processes, assessing climate-driven changes in glacier and snow dynamics and improving water resource forecasting in data-scarce mountainous regions.

OBJECTIVES

The main objective of this study is to understand the influence of climate change on the water flow patterns in Himachal Pradesh. To achieve this, the following sub-objectives have been identified.

1. To estimate changes in snow and glacier extent using the past data (2000-2020)
2. To estimate the influence of snow, glacier and runoff changes on stream runoff.

STUDY AREA

The Satluj Basin is one of the most geomorphically active river systems in the western Himalaya, shaped by rapid tectonic uplift and fragile lithology that make it exceptionally prone to landslides, debris flows and flash-flood events (Dimri et al., 2020). Its upper reaches lie in a cold-desert cryosphere where permafrost, rock glaciers and thin snowpacks interact to control seasonal meltwater pulses—an attribute uncommon among Himalayan River basins. The basin also hosts several expanding proglacial lakes in the Spiti–Kinnaur region, which pose emerging GLOF risks under warming conditions (ICIMOD, 2021).

Ecologically, it forms a rare climate-transitional corridor, shifting from high-altitude desert vegetation to dense temperate forests within short altitudinal ranges, supporting sensitive biodiversity gradients (Rawat & Pandey, 2018). The Satluj has long served as a trans-Himalayan cultural route, where traditional glacier-fed irrigation channels (kulhs) still sustain agriculture in arid valleys (Singh & Singh, 2019). Furthermore, its steep gradients generate one of India's highest hydropower potentials, yet rising temperatures, altered snowfall regimes and increasing sediment

yields are creating uncertainties for long-term hydropower sustainability (Purohit et al., 2022). Overall, the Satluj Basin represents a rapidly changing mountain system where cryospheric, tectonic and socio-hydrological processes converge uniquely.

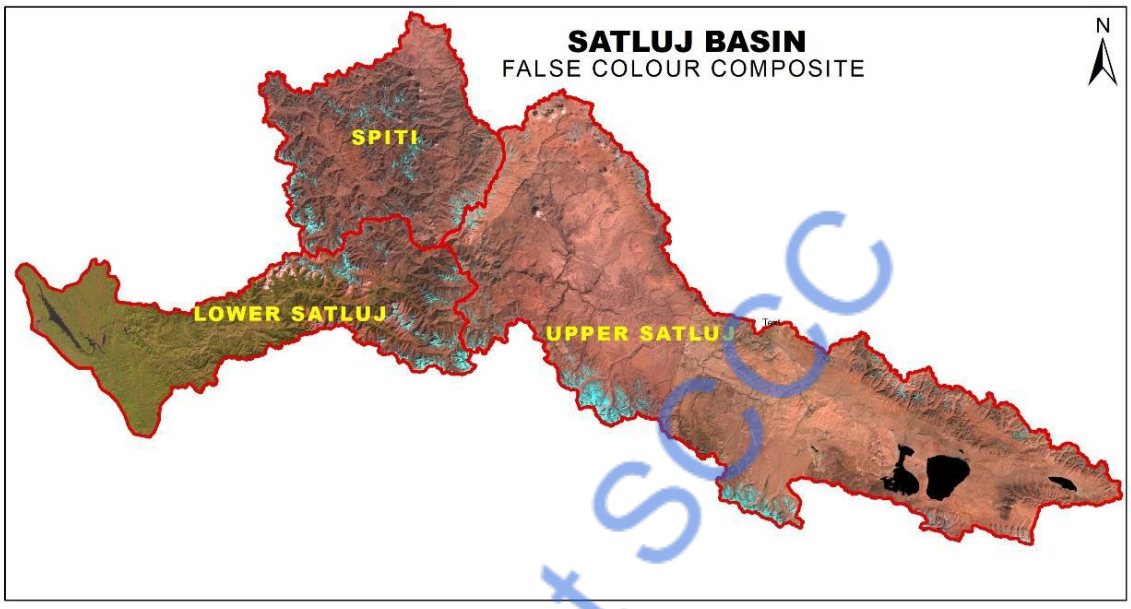

Figure 1.1 Study Area: Satluj River Basin, Western Himalaya

METHODOLOGY

High-mountain glaciers serve as silent climate recorders and accurate, multi-scale analytical tools are needed to comprehend their disappearance. This study uses a remote-sensing and GIS-based methodology to evaluate changes in Himachal Pradesh's glaciers and snow cover during a twenty-year period. Landsat TM/ETM+/OLI and Resourcesat-2 & 2A LISS-III/AWiFS were used to provide accurate temporal comparisons, cloud-free multi-sensor satellite datasets and seasonally consistent collections. Slope, aspect and elevation-dependent glacier behavior can be accurately interpreted thanks to terrain analysis enabled by digital elevation models like ALOS Palsar. In susceptible Himalayan terrain, where computerized indices frequently fail due to debris cover and shadow effects, glacier borders were mostly determined by manual visual interpretation. Calibrated reflectance imagery and regionally verified NDSI based thresholds were used for snow-cover mapping. Using visual interpretation technique, important glacier characteristics (area, length, elevation range, terminus position) were collected. Quantified area loss, retreat rates and decadal change patterns are shown in a multi-temporal comparison of glaciers. Accumulation Area Ratio (AAR) and Equilibrium Line Altitude (ELA) methods were used to estimate mass balance

indicators, relying on verified techniques used in studies of the Naradu Glacier. When taken as a whole, this integrated approach offers a solid scientific foundation for identifying glacier response to climate variability in the northwestern Himalaya.

SATELLITE DATA ACQUISITION

To prepare a multi-temporal glacier and snow-cover inventory, optical satellite images from multiple sensors were utilized:

- **LANDSAT 7 ETM+** imageries for 2000 (October/September)
- **LANDSAT 8 OLI** imageries for 2020 (October/September)
- **Resourcesat-2 LISS-III** imageries for 2011
- **AWiFS (Resourcesat-2)** imageries for snow-cover from **2010–2020** (October to May)
- **MODIS data (NASA) from Google Earth Engine**
- **DEM-** an integral component of satellite data acquisition for deriving glacier topography, hypsometry and mass-balance indicators.

These datasets were selected based on cloud-free conditions, comparable acquisition months and suitable spectral bands for glacier mapping.

PRE-PROCESSING OF SATELLITE IMAGERY

Radiometric and geometric corrections were conducted using ERDAS Imagine. This included:

- Radiometric calibration
- Geometric correction
- Image enhancement for improved visual and spectral discrimination

For higher-resolution analysis, LANDSAT MSS (30 m) was fused with PAN (15 m) using a resolution merge technique.

GLACIER DELINEATION AND CHANGE DETECTION

A detailed manual glacier-mapping workflow based on visual interpretation of multi-temporal satellite imagery and supported by DEM-derived slope and aspect enables accurate delineation of clean and debris-covered glaciers (Paul et al., 2013; Racoviteanu et al., 2009). High-

resolution seasonal imagery and expert interpretation help minimize errors from shadows, debris and complex terrain. Multi-temporal comparison of outlines (2000, 2011, 2020) provides reliable estimates of glacier area change and terminus retreat consistent with GLIMS and globally accepted Himalayan glacier-inventory standards (Bolch et al., 2010; Kaab et al., 2012).

NORMALIZED DELINEATION AND CHANGE DETECTION (NDSI)

The Normalized Difference Snow Index (NDSI), which employs the normalized ratio of green and SWIR reflectance, is widely used as an automated and robust method for snow-cover mapping, especially in mountainous regions where terrain shadows and cloud cover pose challenges. For this study, NDSI was derived using the green band (Band 2) and short-wave infrared band (Band 5) of the AWiFS sensor, following the standard formula:

$$NDSI = \frac{Band_{Green} - Band_{SWIR}}{Band_{Green} + Band_{SWIR}}$$

For AWiFS, the bands used were:

- Band 2 (Green)
- Band 5 (Short Wave Infra-Red)

To compute NDSI, the digital numbers (DNs) were first converted to top-of-atmosphere (TOA) reflectance, which required radiometric calibration (DN to radiance) and subsequent transformation to reflectance. This process utilizes key parameters such as minimum–maximum radiance values, exo-atmospheric solar irradiance for each band, satellite acquisition time, solar zenith and azimuth angles, solar declination and mean Earth–Sun distance (Markham & Barker, 1987; Srinivasulu & Kulkarni, 2004). Based on sensitivity analyses, an NDSI threshold of 0.4 is commonly adopted to distinguish snow from non-snow pixels.

For AWiFS data, TOA reflectance of Bands 2 and 5 was used to calculate NDSI without additional atmospheric correction. Field validation studies indicate that NDSI is largely insensitive to illumination conditions and can reliably discriminate snow even under varying slopes, terrain shadows and orientations typical of Himalayan environments (Kulkarni et al., 2006; Hall et al., 2015; Mahmoudi et al., 2020).

GLACIER MASS BALANCE ESTIMATION

Glacier mass balance was assessed using the Accumulation Area Ratio (AAR) method and Equilibrium Line Altitude (ELA) analysis. The AAR method quantifies the proportion of the glacier's accumulation zone relative to its total area. Higher AAR values typically indicate a positive or balanced mass state, whereas lower AAR values reflect net mass loss. Similarly, the ELA is representing the altitude separating accumulation and ablation zones, it serves as a sensitive indicator of glacier response to climatic variability; an upward shift in ELA generally signifies glacier thinning and negative mass balance (Sharma & Owen, 2015; Kumar et al., 2019). Studies on the Naradu Glacier have successfully demonstrated the use of AAR–ELA relationships for estimating long-term mass balance and climatic response, confirming consistent glacier thinning and an upward migration of ELA over recent decades (Kumar et al., 2019; Kumar et al., 2021). The following formulas were used:

$$AAR = \frac{\text{Accumulation Area of Glacier}}{Total\ area\ of\ Glacier}$$

$$Mass\ Balance = 273.01 * AAR * 120.187$$

MULTIVARIATE ANALYSIS OF GLACIER MELT RUNOFF

Multivariate analysis is a statistical approach used to examine the simultaneous influence of multiple independent variables on a single dependent variable (Joseph, 2010). In the present study, linear multivariate regression analysis was employed to evaluate the relationship between air temperature and glacier melt runoff. All statistical analyses were performed using IBM SPSS Statistics (Version 2020).

To assess the strength and direction of linear relationships between glacier melt runoff and temperature, Pearson's correlation coefficient was calculated. The coefficient ranges from −1 to +1, where −1 indicates a perfect negative linear relationship, +1 indicate a perfect positive linear relationship and 0 represents no linear relationship (Turney, 2022). This preliminary analysis helped identify statistically significant temperature variables influencing glacier melt runoff before regression modelling.

The effect of temperature variability on glacier melt runoff was quantified using multivariate linear regression analysis**.** The study utilized annual glacier discharge (runoff) data and corresponding air temperature data covering a 10-year period (2010–2020)**.** To minimize interannual bias and emphasize variability-driven responses, both discharge and temperature variables were expressed as anomalies, calculated as deviations from the mean of the study period.

The regression model is expressed as:

$$\Delta Q = \text{constant} + (\alpha \times \Delta Tmin) + (\beta \times \Delta Tmax)$$

Where:

- **ΔQ** → Anomaly in glacier melt discharge
- **ΔTmin** → Anomaly in minimum temperature
- **ΔTmax** → Anomaly in maximum temperature
- **α, β** → Regression coefficients representing the sensitivity of glacier melt runoff to minimum and maximum temperatures, respectively.

The regression coefficients indicate the relative contribution of each temperature parameter to variations in glacier melt runoff. The statistical significance of the model and individual predictors was evaluated at a **95% confidence level ($p < 0.05$)**. The **coefficient of determination (R^2)** was used to assess the proportion of variance in glacier melt runoff explained by temperature variability.

TOOLS & SOFTWARE

- ✓ **ERDAS Imagine**-Pre-processing, radiometric/geometric correction
- ✓ **ArcGIS**-Glacier delineation, spatial analysis, change detection
- ✓ **Excel/SPSS**-Temporal statistical analysis

2. GLACIER DISTRIBUTION IN THE SATLUJ BASIN

Glaciers are a fundamental component of high-mountain landscapes, exerting strong control on geomorphological, hydrological and climatic processes. Geomorphologically, glaciers shape mountain terrain through erosion and deposition, producing characteristic landforms such as moraines, cirques and U-shaped valleys (Benn and Evans, 2010; Alley et al., 2019). Although these processes usually operate over long timescales, abrupt and hazardous events such as moraine dam failures and debris flows may occur due to glacier retreat and fluvial undercutting, posing significant risks to downstream communities (Chiarle et al., 2007; O'Connor et al., 2001; Beason et al., 2018).

Hydrologically, glaciers function as natural reservoirs that regulate river discharge from seasonal to decadal scales (Fountain and Tangborn, 1985; Moore et al., 2009; Dussaillant et al., 2019). Glacier meltwater sustains streamflow during dry and warm periods, reduces seasonal runoff variability and helps moderate stream temperatures during late summer after seasonal snow has disappeared (Cadbury et al., 2008; Fellman et al., 2014). However, continued glacier shrinkage reduces this buffering capacity, increasing the vulnerability of glacier-fed basins to drought and long-term water scarcity (Huss and Hock, 2018; Pritchard, 2019). At the global scale, glacier mass loss is also a significant contributor to sea-level rise (Meier, 1984; Parkes and Marzeion, 2018; Zemp et al., 2019).

Glacier inventories play a critical role in quantifying glacier extent, monitoring changes over time and assessing glacier contributions to sea-level rise and regional hydrology (Hock et al., 2009; Moore et al., 2009; Pfeffer et al., 2014). They provide an essential baseline for evaluating past and future glacier changes. While updated glacier inventories are now available for many regions worldwide (Bolch et al., 2010; Smiraglia et al., 2015; Sun et al., 2018; Andreassen et al., 2022), significant data gaps and inconsistencies persist in several mountain regions.

In the Himalayan region, glaciers are of particular importance due to their role in sustaining major river systems that support millions of people downstream. Despite this significance, comprehensive and consistent digital glacier inventories for large parts of the Himalaya remain

limited (Bolch et al., 2012; Raina, 2009). Existing inventories often differ in data sources, mapping techniques, temporal coverage and formats, making it difficult to reliably assess glacier changes (Racoviteanu et al., 2009; Paul and Hendriks, 2010). Uncertainties are further amplified by challenges such as extensive debris cover, seasonal snow contamination, complex topography and limited field accessibility (Bhambri and Bolch, 2009; Racoviteanu et al., 2008).

Remote sensing has emerged as an indispensable tool for glacier mapping and monitoring in such remote and data-scarce regions. The integration of multispectral satellite imagery with digital elevation models (DEMs) has become a well-established approach for compiling glacier inventories and assessing glacier dynamics (Paul and Kaab, 2005; Andreassen et al., 2008; Bolch et al., 2010). Recent advances, including improved automated classification techniques and the use of radar coherence data, have enhanced the delineation of debris-covered glaciers and reduced mapping uncertainties (Atwood et al., 2010; Robson et al., 2020; Lu et al., 2022).

Considering the high climatic sensitivity of Himalayan glaciers and their designation as Essential Climate Variables (GCOS, 2004), the development of detailed and reliable glacier inventories is critically important for climate change assessment, hydrological modelling and water resource management (Cogley, 2009; Ohmura, 2009; Huss, 2011). In this context, the western Himalayas particularly glacierized basins such as the Satluj Basin represents a critical region where improved glacier inventories and mass balance assessments are essential for understanding cryospheric response to climate change and its implications for long-term water security.

SPATIAL-TEMPORAL DISTRIBUTION OF GLACIERS

The spatial-temporal variation in the number of glaciers in the Satluj basin, namely the Spiti, Baspa, Lower Satluj and Upper Satluj sub-basins, for the years 2000, 2011 and 2020 shows only slight changes over the two-decade period. It is evident from table and figure 2.1, a total of 1,699 glaciers in 2000 were mapped across all sub-basins, which reduced to 1,632 in 2011, indicating a net reduction in the number of glaciers due to cloud cover. However, by 2020 the total number increased to 1,709, slightly exceeding the 2000 level.

The Spiti sub- basin shows a minor decrease in glacier numbers from 696 in 2000 to 684 in 2011, followed by an increase to 699 in 2020, suggesting that few glaciers are fragmented or

identified during the later period. Whereas Baspa sub-basin remains unchanged, consistently recording 99 glaciers across all three decades, indicating relative stability in glacier inventory.

The number of glaciers in the Lower Satluj sub-basin declined from 313 in 2000 to 276 in 2011, largely attributable to data limitations arising from cloud and seasonal snow cover. However, by 2020 the glacier count increased to 314. A similar pattern was observed in the Upper Satluj Sub-basin, where the number of glaciers decreased from 591 in 2000 to 573 in 2011 and subsequently increased to 597 in 2020.

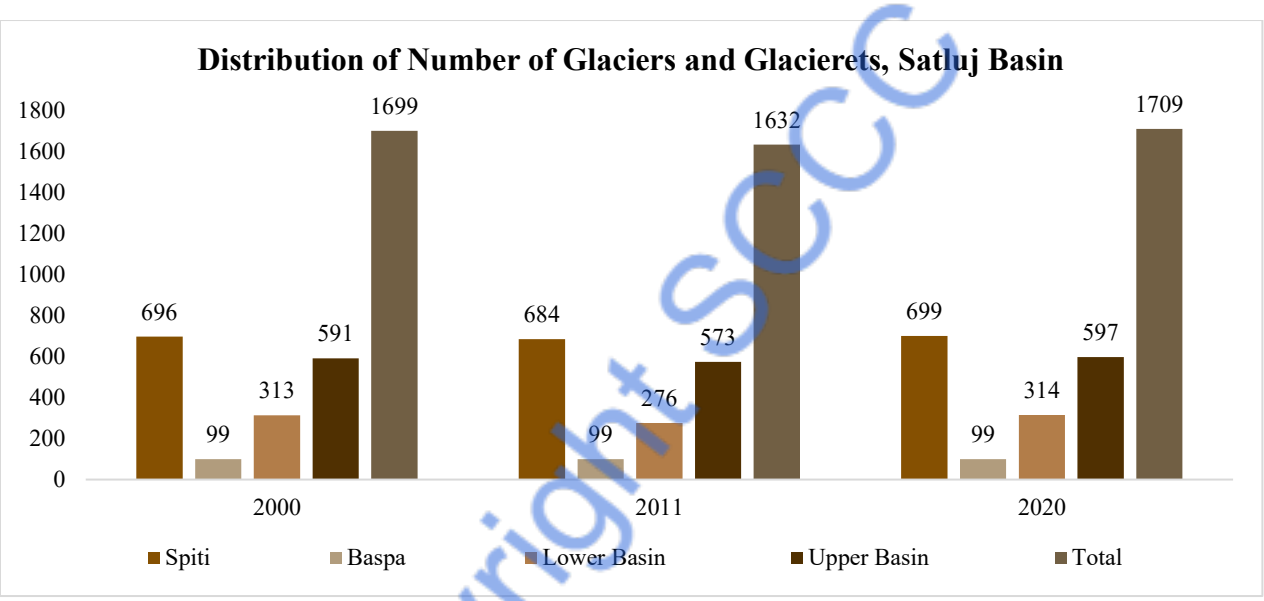

Figure 2.1 Distribution of Glaciers in Satluj Basin

Table 2.1 Decadal Distribution of Number of Glaciers and Glacierets, Satluj Basin

Year	2000	2011	2020
Spiti Sub-basin	696	684	699
Baspa Sub-basin	99	99	99
Lower Satluj Sub-basin	313	276	314
Upper Satluj Sub-basin	591	573	597
Total	**1699**	**1632**	**1709**

The observed increase in glacier numbers is not indicative of glacier growth but is consistent with ongoing glacier retreat, leading to the separation and independent delineation of tributary and feeder ice bodies from larger valley glaciers. It indicates dynamic glacier responses to climate change, including fragmentation, retreat and methodological differences in glacier mapping over

time. Thus, increased glacier melt may enhance river discharge. However, continued glacier loss leads to a long-term decline in meltwater contribution, threatening water availability for agriculture, hydropower and domestic use, especially during dry seasons.

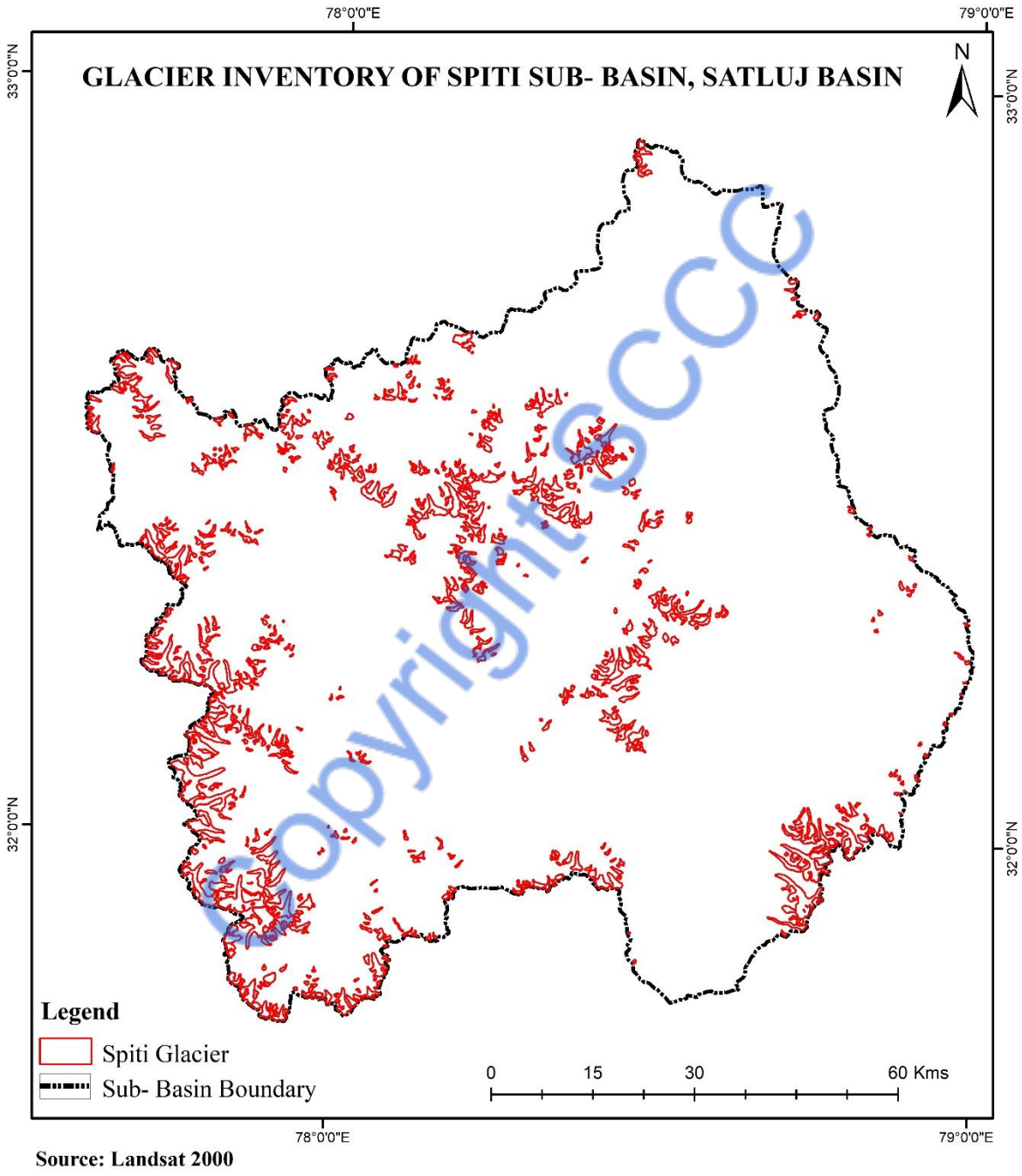

Figure 2.2 Glacier Inventory of Spiti sub-basin, Satluj Basin

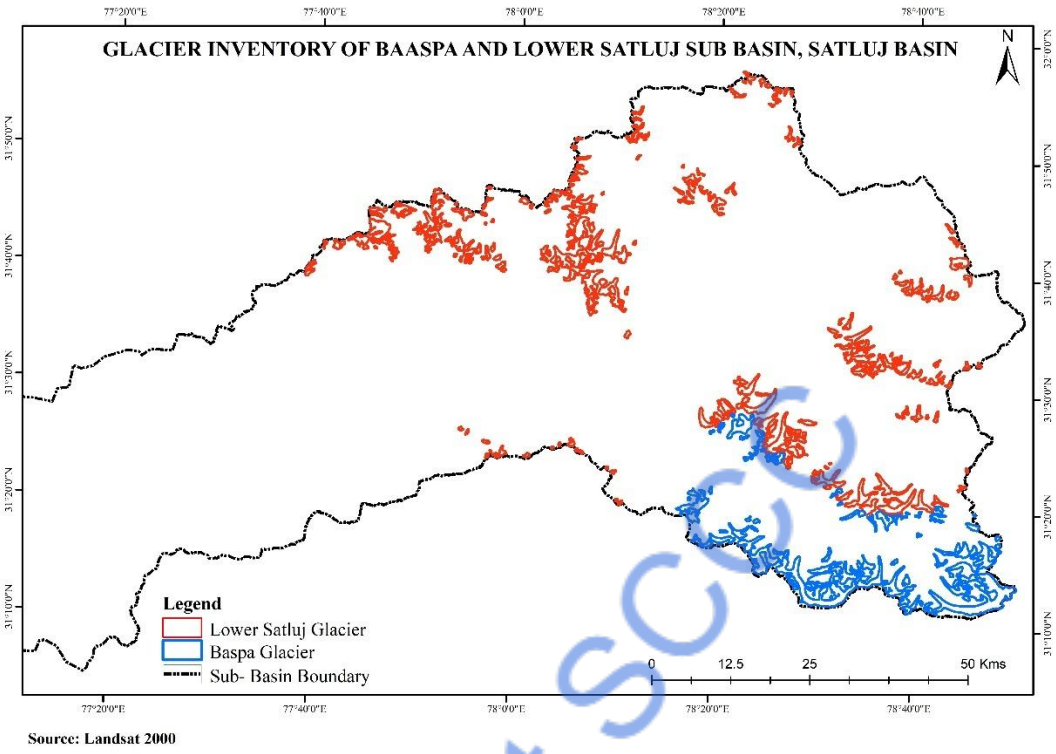

Figure 2.3 Glacier Inventory of Lower Satluj and Baspa sub-basin, Satluj Basin

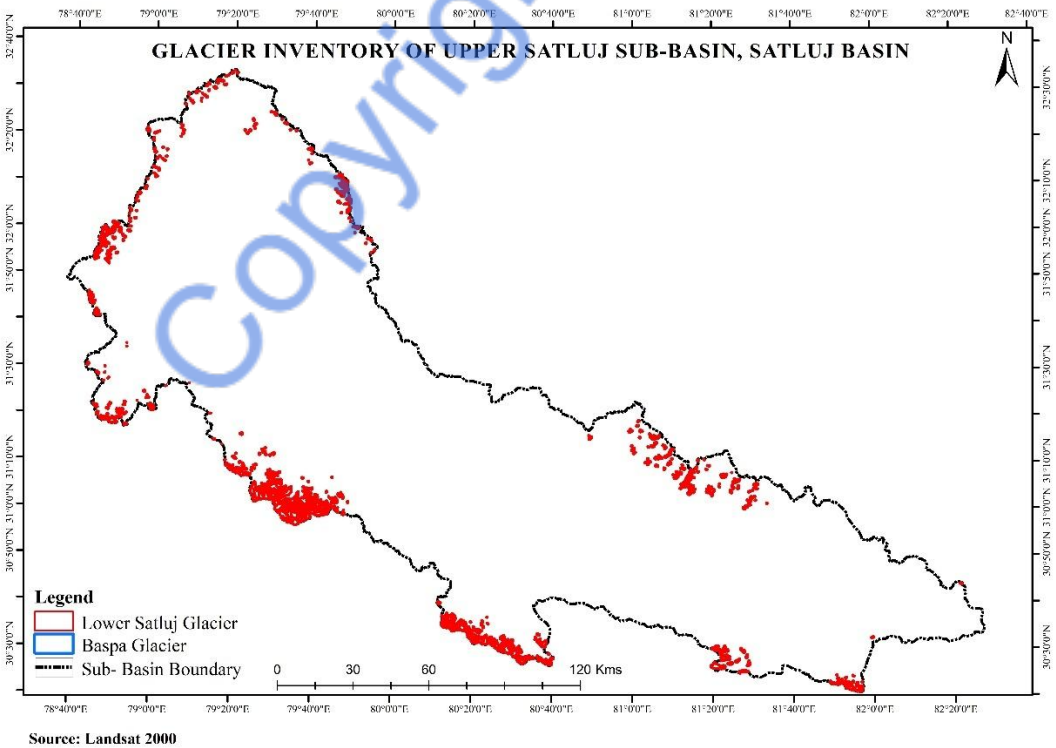

Figure 2.4 Glacier Inventory of Upper Satluj sub-basin, Satluj Basin

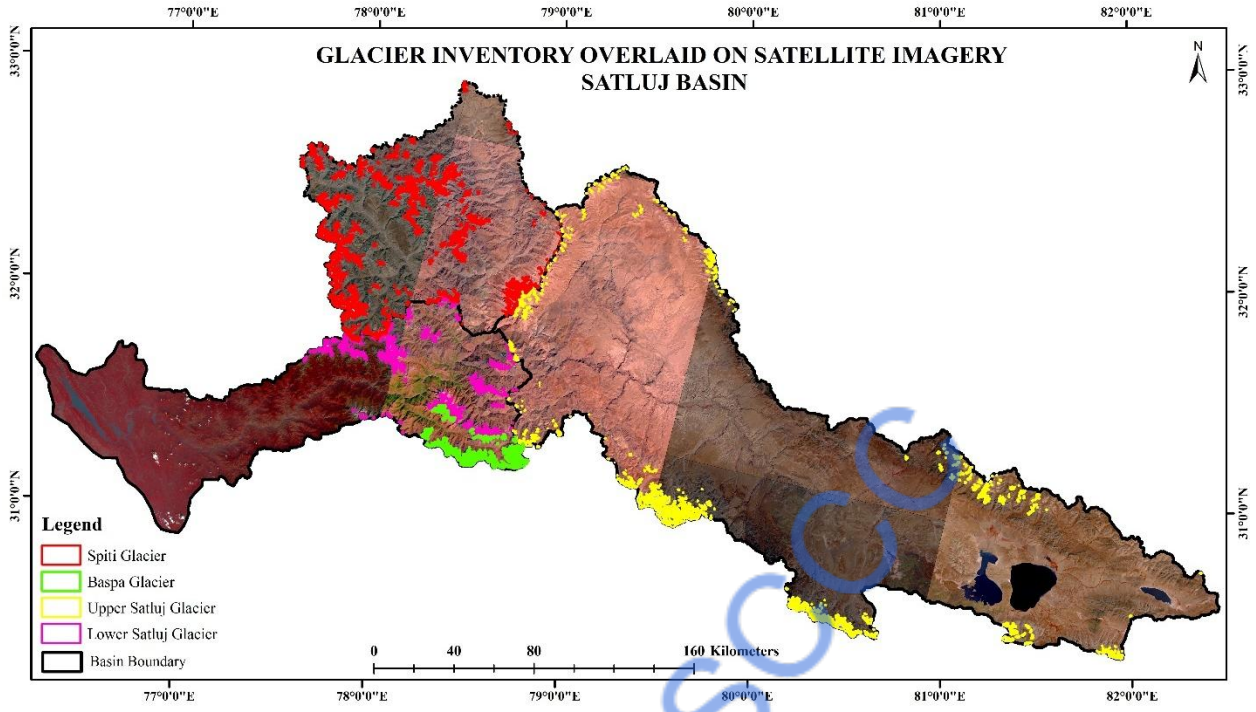

Source: LANDSAT Satellite data-2020

Figure 2.5 Glacier Inventory of Satluj basin

ASPECT-WISE DISTRIBUTION OF GLACIERS

The aspect-wise distribution of glaciers shows a strong dependence on slope orientation. A greater proportion of glacier area is concentrated on north and northeast facing slopes, which receive lower solar radiation and therefore experience reduced ablation. In contrast, south, southwest and west facing slopes exhibit limited glacier coverage due to higher insolation and enhanced melt rates. This pattern highlights the significant role of slope aspect in controlling glacier survival and spatial distribution (Evans, 2006; Scherler et al., 2011; Benn and Evans, 2010). The Elevation and aspect were derived and analysed using LANDSAT satellite data (2000 and 2020) and an ALOS PALSAR DEM. The aspect map is generated (Figure 2.6) by using ArcGIS tools and reclassifying it for classification of glaciers and glacierets directions.

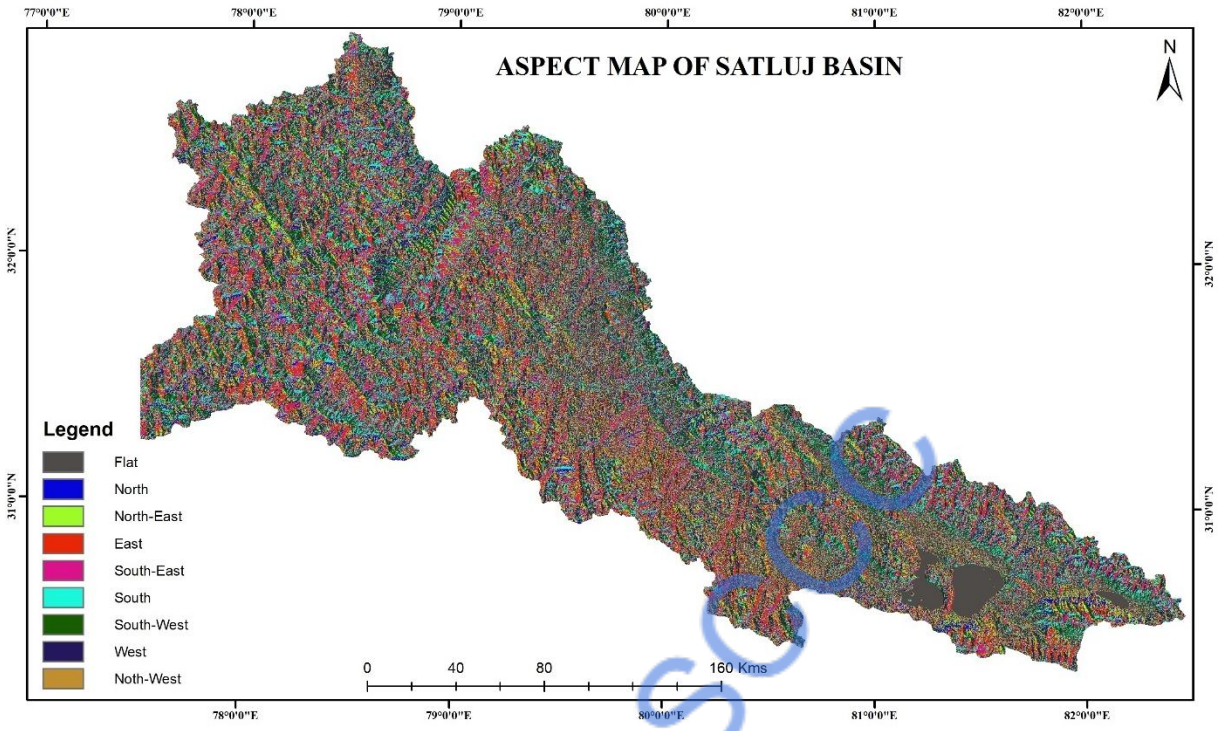

Figure 2.6 Aspect map of Satluj basin

ASPECT-WISE DISTRIBUTION OF GLACIERS AND GLACIERETS IN 2000

The aspect-wise distribution of glaciers in the Satluj basins divided into 4 sub-basins namely Spiti, Baspa, Lower Satluj and Upper Satluj Sub- basins for the year 2000 reveals a strong control of slope orientation on glacier occurrence and areal extent. A total of 1,699 glaciers and glacierets were mapped in the four sub-basins, covering an area of approximately 1,481.75 km².

Using LANDSAT ETM+ satellite imagery, 696 glaciers with a total area of 584.83 km² were identified and mapped in the Spiti sub- basin. North facing slopes dominate both in terms of glacier number (282) and area (280.11 km²), followed by northeast facing slopes (187 glaciers; 161.27 km²). The 82 glaciers were found in Northwest aspects; however, their areal extent is comparatively lower (37.02 km²). Limited glacier survival on sun-facing aspects is indicated by the small percentage of glacier coverage on south, southwest and west facing slopes, which are subjected to higher solar radiation and enhanced ablation (Benn and Evans, 2010; Bolch et al., 2012).

The Baspa Sub-basin contains 99 glaciers covering 174.17 km². Unlike Spiti, a significant proportion of glacier and glacierets area is concentrated on northwest-facing slopes (64.77 km²), despite a moderate number of glaciers (14). North facing slopes also show a notable glacier presence

(24 glaciers; 57.53 km²). Glaciers on southern and south-eastern aspects are fewer and occupy relatively small areas, reflecting enhanced ablation due to higher solar radiation.

In the Lower Satluj basin, 313 glaciers cover an area of 258.9 km². Northeast facing slopes host the highest number of glaciers (88) and a substantial area (80.5 km²), followed by north facing slopes (66 glaciers; 82.3 km²). Glaciers on southern and south-western aspects are limited both in number and area, emphasizing the role of aspect in controlling glacier distribution.

The Upper Satluj Sub- basin comprises 591 glaciers with a total area of 463.85 km². North and northeast facing slopes dominate, supporting 263 glaciers (169.21 km²) and 177 glaciers (173.11 km²), respectively. Northwest facing slopes also contribute significantly (83 glaciers; 28.85 km²). In contrast, glaciers on southern, south western and western aspects are sparse and occupy minimal area.

Overall, the analysis clearly indicates that north, northeast and northwest facing aspects collectively have the majority of glaciers and glacierets across all sub-basins, underscoring the strong influence of reduced solar insolation and favourable microclimatic conditions. South-facing aspects consistently show fewer and smaller glaciers, highlighting their higher vulnerability to melting under prevailing climatic conditions in the western Himalaya.

Table 2.2 Aspect-wise Distribution of Glaciers and Glacierets in 2000

Sub-basin	Spiti Sub-basin		Baspa Sub-basin		Lower Satluj Sub-basin		Upper Satluj Sub-basin	
Direction	Glaciers Number	Area in km²	Glaciers Number	Area in km²	Glaciers Number	Area in km²	Glaciers Number	Area in km²
North	282	280.11	24	57.53	66	82.3	263	169.21
Northeast	187	161.27	6	5.06	88	80.5	177	173.11
East	45	30.31	12	5.19	34	34.34	24	56.62
Southeast	57	57.25	12	3.19	43	14.9	19	19.18
South	13	7.68	14	20.41	19	6.68	9	3.42
Southwest	15	6.63	6	2.61	24	9.66	6	5.15
West	15	4.56	11	15.41	12	10.85	10	8.31
Northwest	82	37.02	14	64.77	27	19.67	83	28.85
Total	**696**	**584.83**	**99**	**174.17**	**313**	**258.9**	**591**	**463.85**

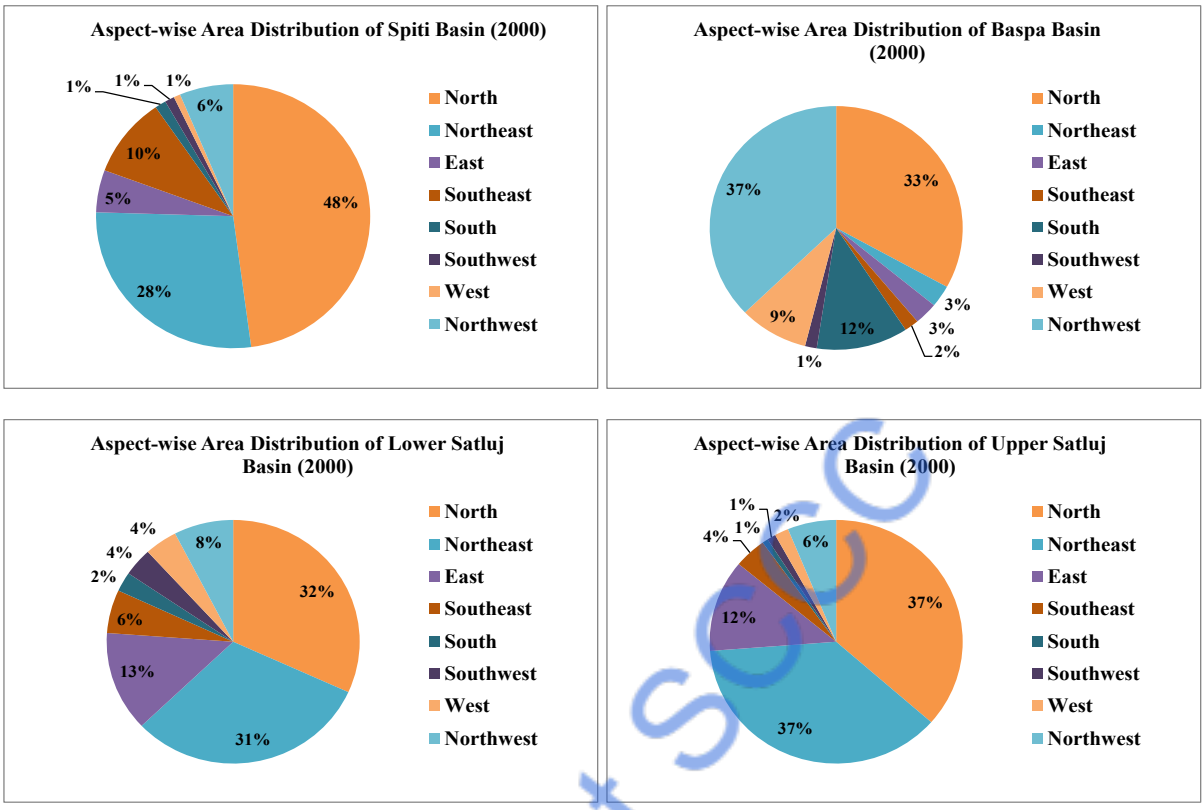

Figure 2.7 Aspect-wise distribution of glacier area in the Satluj basin for the year 2000

ASPECT-WISE DISTRIBUTION OF GLACIERS AND GLACIERETS IN 2011

The aspect-wise distribution of glaciers and glacierets across the Spiti, Baspa, Lower Satluj and Upper Satluj Sub-basins in 2011 in Table 2.3 and figure 2.8, highlights the continued dominance of glaciers on shaded slope orientations, along with a noticeable reduction in glacier area compared to 2000. In total, 1,632 glaciers and glacierets were mapped across the four basins, occupying a total area of approximately 1,414.36 km².

In the Spiti Sub-basin, 684 glaciers cover an area of 591.96 km². North facing slopes remain dominant, hosting 274 glaciers with a total area of 278.36 km², followed by northeast facing slopes with 184 glaciers covering 169.88 km². Northwest facing slopes also support a considerable number of glaciers (81), though with relatively smaller area (29.36 km²). Glaciers on southern and south-eastern aspects are fewer and fragmented, reflecting higher exposure to solar radiation.

The Baspa Sub-basin records 99 glaciers with a total area of 168.65 km². North facing slopes continue to contribute the largest share of glacier area (56.28 km²), while east facing slopes show a comparatively large glacier area (64.01 km²) despite a moderate glacier count. Glaciers on southern,

south-western and south-eastern aspects remain limited in areal extent, underscoring unfavourable ablation conditions.

In the Lower Satluj Sub-basin, 276 glaciers occupy an area of 237.37 km². Northeast facing slopes host the highest number of glaciers (80) with a substantial area of 74.89 km², followed closely by north facing slopes (62 glaciers; 76.64 km²). Northwest facing slopes also contribute significantly to glacier area (31.96 km²). South- and southeast-facing slopes show minimal glacier area, indicating strong aspect control.

The Upper Satluj Sub-basin comprises 573 glaciers with a total area of 416.38 km². North and northeast facing aspects dominate glacier distribution, accounting for 253 glaciers (147.42 km²) and 175 glaciers (161.65 km²), respectively. Northwest facing slopes support a moderate number of glaciers (81) with an area of 54.67 km². In contrast, glaciers on southern and western aspects are fewer and occupy limited areas.

Overall, the 2011 interpretation based on ALOS PALSOR DEM and Satellite data reveals that north, northeast and northwest facing slopes consistently host the majority of glaciers and glacierets area across all basins. As Compared to 2000, a decline in total glacier area is evident despite relatively stable glacier numbers, suggesting enhanced glacier thinning and fragmentation under the influence of regional climatic warming. It also affected due to cloud/ snow cover satellite data in the western Himalaya during 2011.

Table 2.3 Aspect-wise Distribution of Glaciers and Glacierets in 2011

Sub-basin	Spiti Sub-basin		Baspa Sub-basin		Lower Satluj Sub-basin		Upper Satluj Sub-basin	
Direction	**Glaciers Number**	**Area in km²**	**Glaciers Number**	**Area in km²**	**Glaciers Number**	**Area in km²**	**Glaciers Number**	**Area in km²**
North	274	278.36	24	56.28	62	76.64	253	147.42
Northeast	184	169.88	6	4.83	80	74.89	175	161.65
East	44	36.70	12	64.01	29	18.86	23	22.34
Southeast	58	7.68	12	18.22	35	4.67	17	2.16
South	13	58.78	14	3.09	13	11.44	8	16.42
Southwest	15	6.64	6	2.37	19	8.35	6	4.37
West	15	4.56	11	15.16	12	10.56	10	7.35
Northwest	81	29.36	14	4.69	26	31.96	81	54.67
Total	**684**	**591.96**	**99**	**168.65**	**276**	**237.37**	**573**	**416.38**

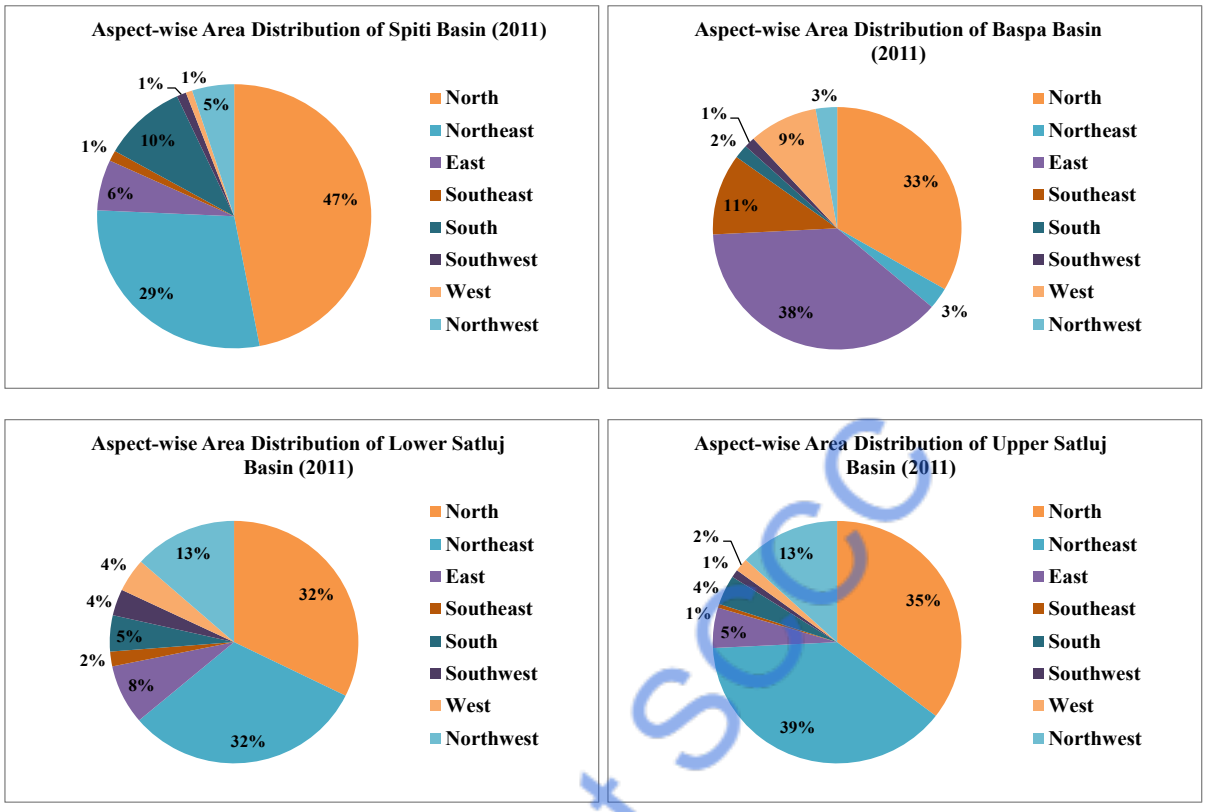

Figure 2.8 Aspect-wise distribution of glacier area in the Satluj basin for the year 2011

ASPECT-WISE DISTRIBUTION OF GLACIERS IN 2020

The aspect-wise distribution of glaciers across the Satluj basin is divided into 4 basins viz. Spiti, Baspa, Lower Satluj and Upper Satluj sub-basins in 2020 are based on LANDSAT 8 satellite data and DEM. It is evident from table 2.4 and figure 2.9, dominance of glaciers on shaded slope orientations, alongside an overall reduction in glacier area compared to earlier inventories (Table 2.4 and Figure 2.7). In total, 1,709 glaciers were mapped across the four basins, covering a combined area of approximately 1,384.16 km².

In the Spiti sub-basin, 699 glaciers occupy an area of 548.65 km². North facing slopes continue to host the largest glacier area (266.18 km²) and nearly the highest number of glaciers (281), followed by northeast-facing slopes with 191 glaciers covering 152.69 km². Northwest-facing slopes retain a substantial glacier count (82), although their total area has declined to 34.37 km². Southern, south-western and western aspects collectively account for a relatively small share of glacier coverage, indicating persistent unfavourable conditions for glacier survival on sun-facing slopes.

The Baspa Sub-basin shows a minute change in glacier numbers, maintaining 99 glaciers with a total area of 171.23 km². Northwest-facing slopes dominate in terms of area (65.38 km²), while north-facing slopes also support significant glacier coverage (56.33 km²). Glaciers on southern and south-eastern aspects remain limited in both number and area, reflecting strong aspect control and higher ablation on these slopes.

In the Lower Satluj Sub-basin, 314 glaciers cover an area of 248.94 km². Northeast-facing slopes again show the highest glacier concentration (88 glaciers; 77.22 km²), followed by north-facing slopes (67 glaciers; 79.56 km²). East and southeast-facing aspects support moderate glacier coverage, while south-facing and southwestern aspects host only small and fragmented glaciers.

The Upper Satluj sub-basin contains 597 glaciers with a total area of 416.34 km². North- and northeast-facing slopes continue to dominate glacier distribution, accounting for 264 glaciers (145.28 km²) and 179 glaciers (154.73 km²), respectively. Northwest facing slopes also show a notable presence in terms of glacier number (86), although their areal contribution is comparatively small (23.07 km²). Glaciers on the southern and western aspects remain few and are characterized by limited areal extent.

Overall, the 2020 analysis confirms that glacier occurrence and extent are strongly controlled by slope aspect, with north, northeast and northwest-facing slopes consistently supporting the majority of glaciers across all basins. Compared to 2000, while glacier numbers show marginal increase likely due to fragmentation the total glacier area has declined, highlighting ongoing glacier thinning and retreat under the influence of regional climatic warming in the western Himalaya.

Table 2.4 Aspect-wise Distribution of Glaciers and Glacierets in 2020

Sub-basin	Spiti Sub-basin		Baspa Sub-basin		Lower Satluj Sub-basin		Upper Satluj Sub-basin	
Direction	**Glaciers Number**	**Area in km²**	**Glaciers Number**	**Area in km²**	**Glaciers Number**	**Area in km²**	**Glaciers Number**	**Area in km²**
North	281	266.18	24	56.33	67	79.56	264	145.28
Northeast	191	152.69	6	5.28	88	77.22	179	154.73
East	45	27.29	12	4.6	34	32.42	24	61.83
Southeast	56	51.06	12	3.18	43	13.95	19	17.64
South	13	6.51	14	18.8	19	6.41	9	2.6
Southwest	16	6.33	6	2.38	24	9.46	6	4.03

West	15	4.22	11	15.28	12	10.56	10	7.16
Northwest	82	34.37	14	65.38	27	19.36	86	23.07
	699	548.65	99	171.23	314	248.94	597	416.34

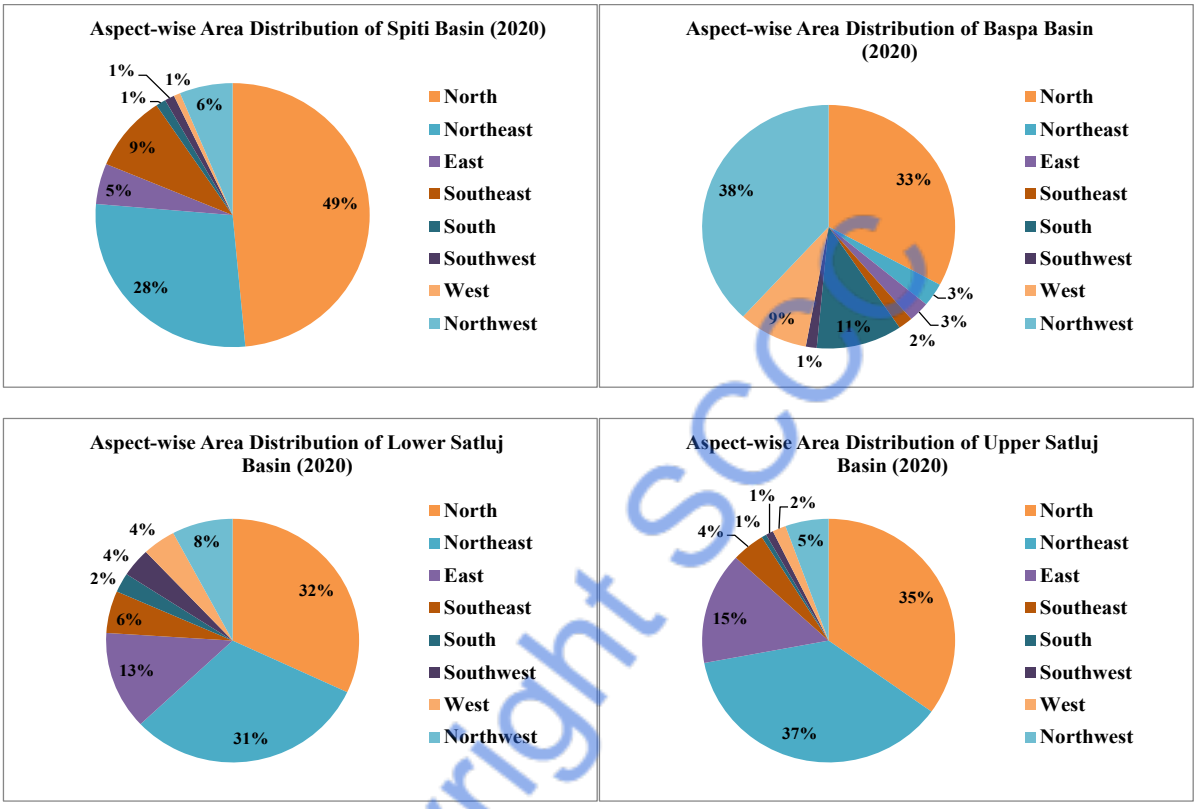

Figure 2.9 Aspect-wise Distribution of Glacier Area in the Satluj Basin for the year 2020

RETREATING GLACIER IN SATLUJ BASIN

The empirical approach, the snout-difference (terminus shift) method, is used to quantify glacier retreat by measuring changes in the position of the glacier snout over time. The basin-wise distribution of glacier retreat rates based on LANDSAT 5 ETM^{+}, 2000 and LANDSAT 8 OLI, 2020, highlights a rapid glacier retreat across the Satluj basin, divided into 4 sub-basins, i.e., Spiti, Baspa, Lower Satluj and Upper Satluj sub-basins. In 2000, out of 1699 glaciers and glacierets, 1,005 have shown major upward movement of snout, whereas 694 glaciers and glacierets have not shown significant snout variation. The rate of glacier retreat per year has been divided into four categories, viz., less than 10 m, 10-20 m, 20-40 m and more than 40 m. About 800 glaciers fall under the highest retreat class (<10 m/year), reflecting enhanced glacier recession across the Satluj River Basin.

As depicted in the figure 2.10 and table 2.5, 363 glaciers and glacierets in the Upper Satluj sub-basin has the highest number of glaciers in the less than 10 m/year category, followed by 315 glaciers and glacierets in the Spiti sub-basin (315). The 80 glaciers fall under the category of <10 m/year in Lower Satluj basin, while the Baspa sub-basin shows 46 rapidly retreating glaciers and glacierets. The spatial pattern of retreating glaciers and glacierets suggests that Upper Satluj and Spiti sub-basins have stronger sensitivity to glaciers in prevailing climatic conditions.

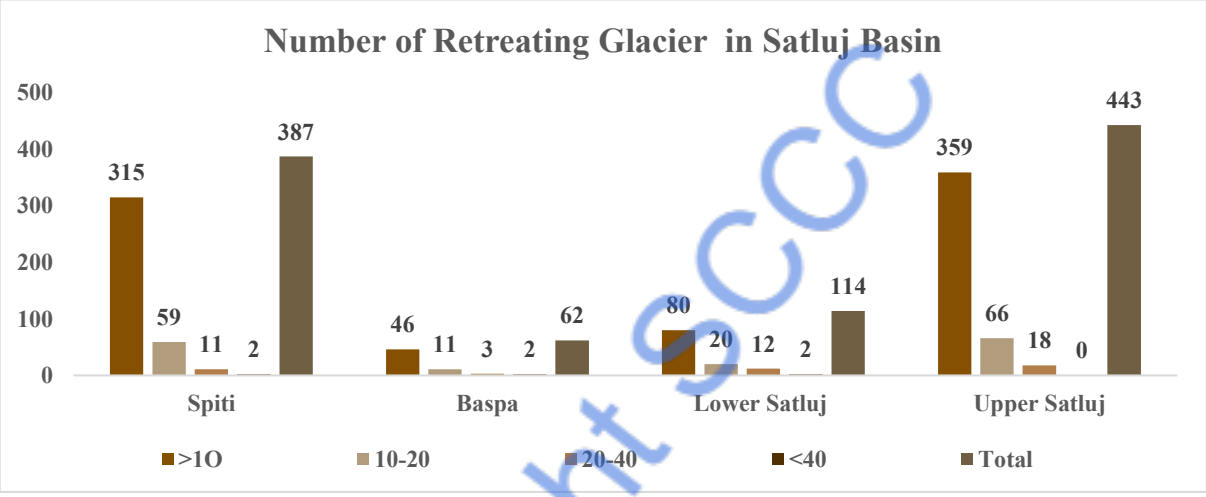

Figure 2.10 Number of retreating Glaciers in Satluj Basin

Table 2.5 Category-wise Number of Retreating Glaciers in Satluj Basin

Basin Name Classification	Spiti Sub-basin	Baspa Sub-basin	Lower Satluj Sub-basin	Upper Satluj Sub-basin	Satluj Basin
<10 (Lowest)	315	46	80	359	800
10-20 (Moderate)	59	10	20	66	155
20-40 (high)	11	3	12	18	44
>40 (Highest)	2	2	2	0	6
Total	387	61	114	443	1005

Glaciers and glacierets retreating at moderate rates (10–20 m/year) constitute 155 glaciers in all sub-basins. Among these, the Upper Satluj sub-basin again shows the maximum number (66), followed by Spiti (59), Lower Satluj (20) and Baspa (10). This indicates that while some glaciers are in transitional retreat phases, a large proportion has already shifted into higher retreat categories.

The 44 glaciers and glacierets analyzed in the category of higher retreat rates between 20–40 m/year, with 18 glaciers and glacierets in Upper Satluj and 12 glaciers and glacierets in Lower Satluj contributing the majority. The fastest retreat of glaciers and glacierets under the category of more than 40 m/year comprises only six glaciers with glacier ID 243, 526, 733, 781, 802 and 857 in Spiti, Baspa and Lower Satluj sub-basins, highlighting the scarcity of relatively stable glaciers in the region.

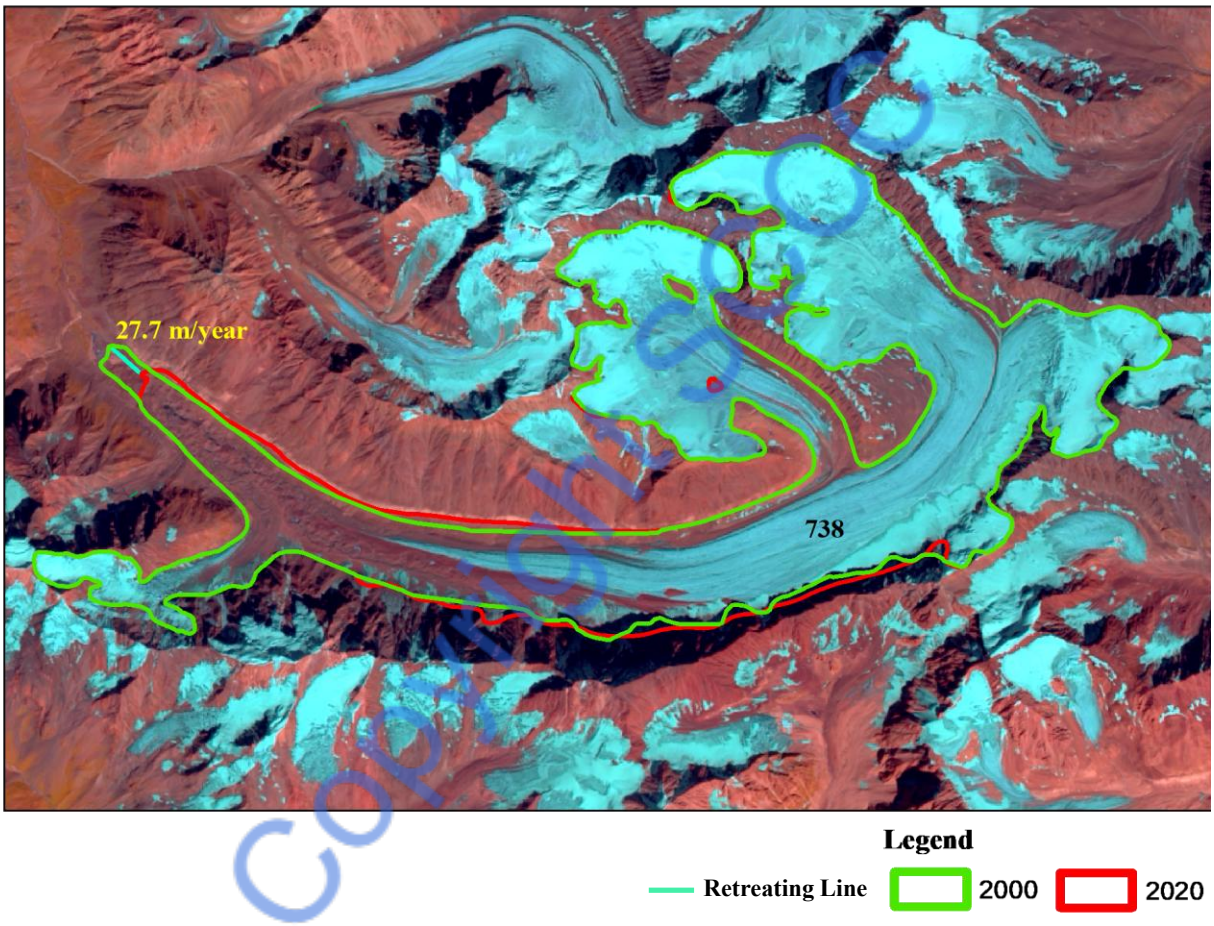

Figure 2.11 Glacier Retreat of Bamak Glacier, Baspa Basin, Himachal Pradesh

In the Satluj basin, Upper Satluj (443 glaciers) and Spiti (387 glaciers) sub-basins have contributed more than four-fifths of the glaciers. The retreating rate of glaciers and glacierets in Spiti, Baspa, Lower Satluj and Upper Satluj is shown in figure 2.11 to 2.15. The fastest retreat was observed in Glacier ID 243 in Spiti sub-basin, moving towards higher elevation at the rate of 73.7 m/year. The Bamak glacier (Glacier ID 738) in Baspa sub-basin, has been retreating 27.7 m/year since 2000 (Figure 2.9). The glacier ID 857, Lower Satluj sub-basin has been receding 60 m/year.

The figure 2.15 shows glacier ID 485 in Spiti sub-basin as one of the examples of fragmentation of glaciers. The overwhelming dominance of high retreat rates highlights the impact of rising temperatures, changing precipitation patterns and enhanced ablation processes in the western Himalaya. These changes have significant implications for long-term water resources and downstream hydrology.

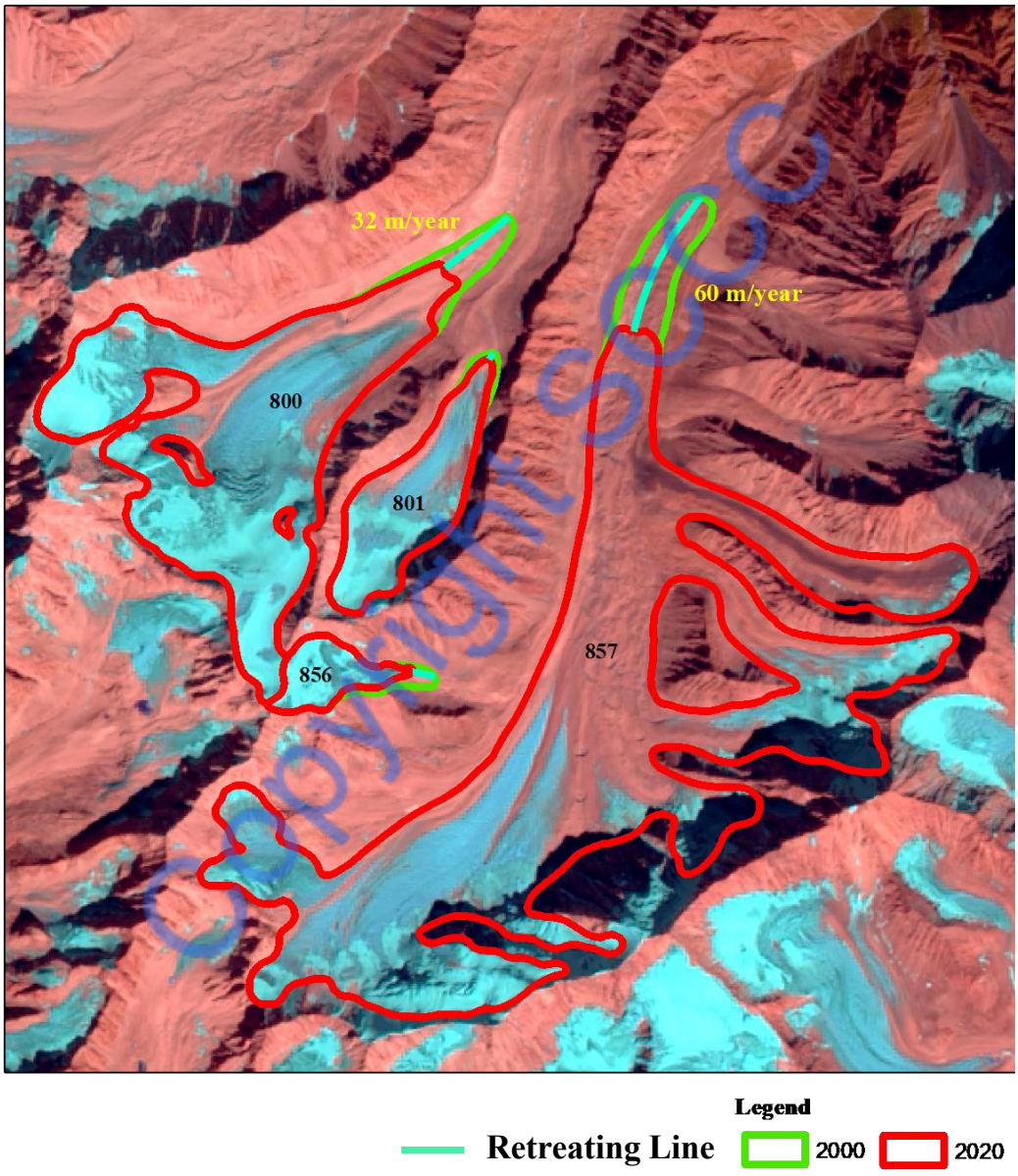

Figure 2.12 Glacier Retreat of Lower Satluj Sub-basin, Satluj Basin

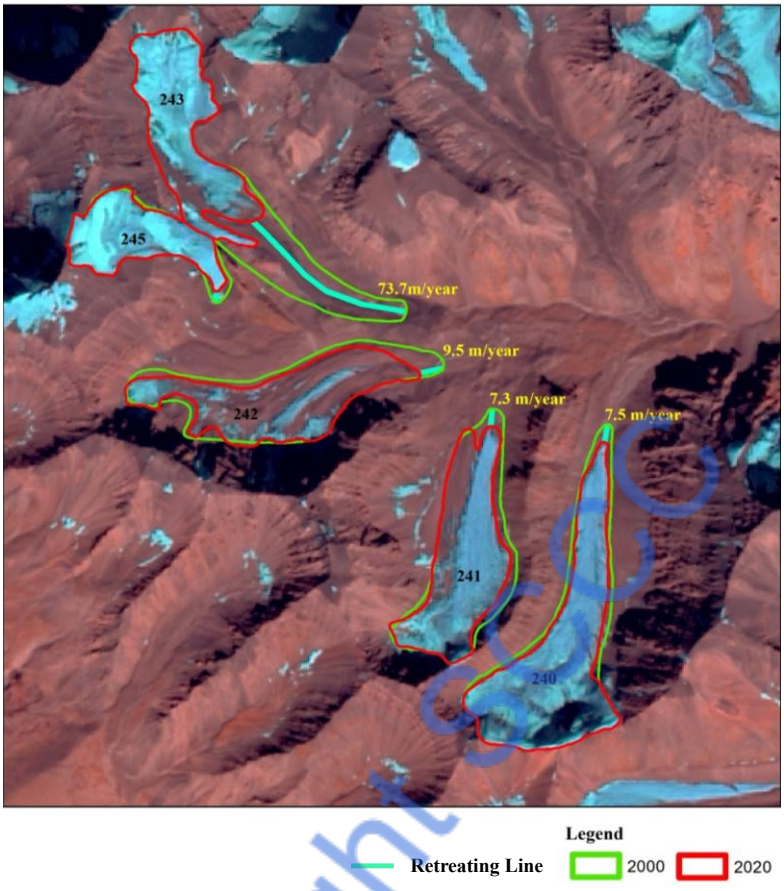

Figure 2.13 Retreating Glaciers, Spiti Sub-basin, Satluj Basin

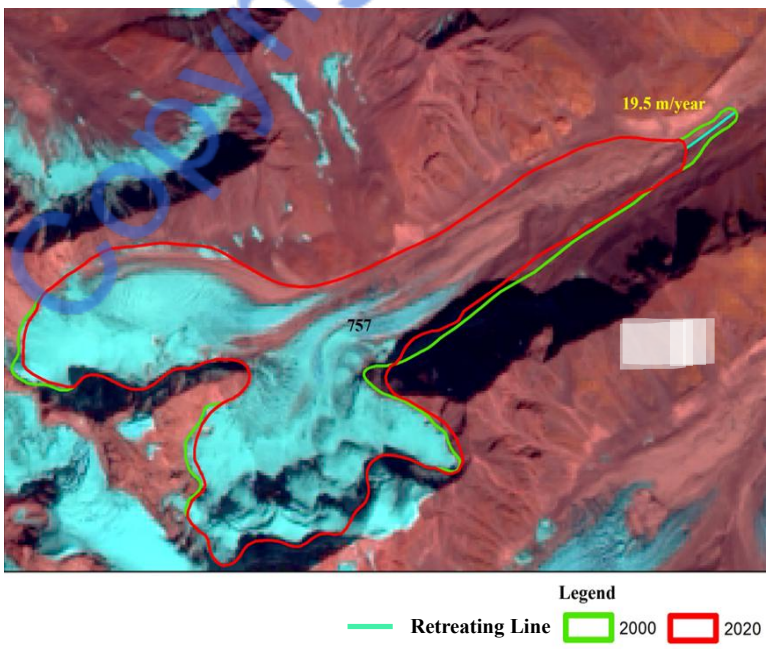

Figure 2.14 Nardu Glacier, Baspa Sub-basin, Satluj Basin

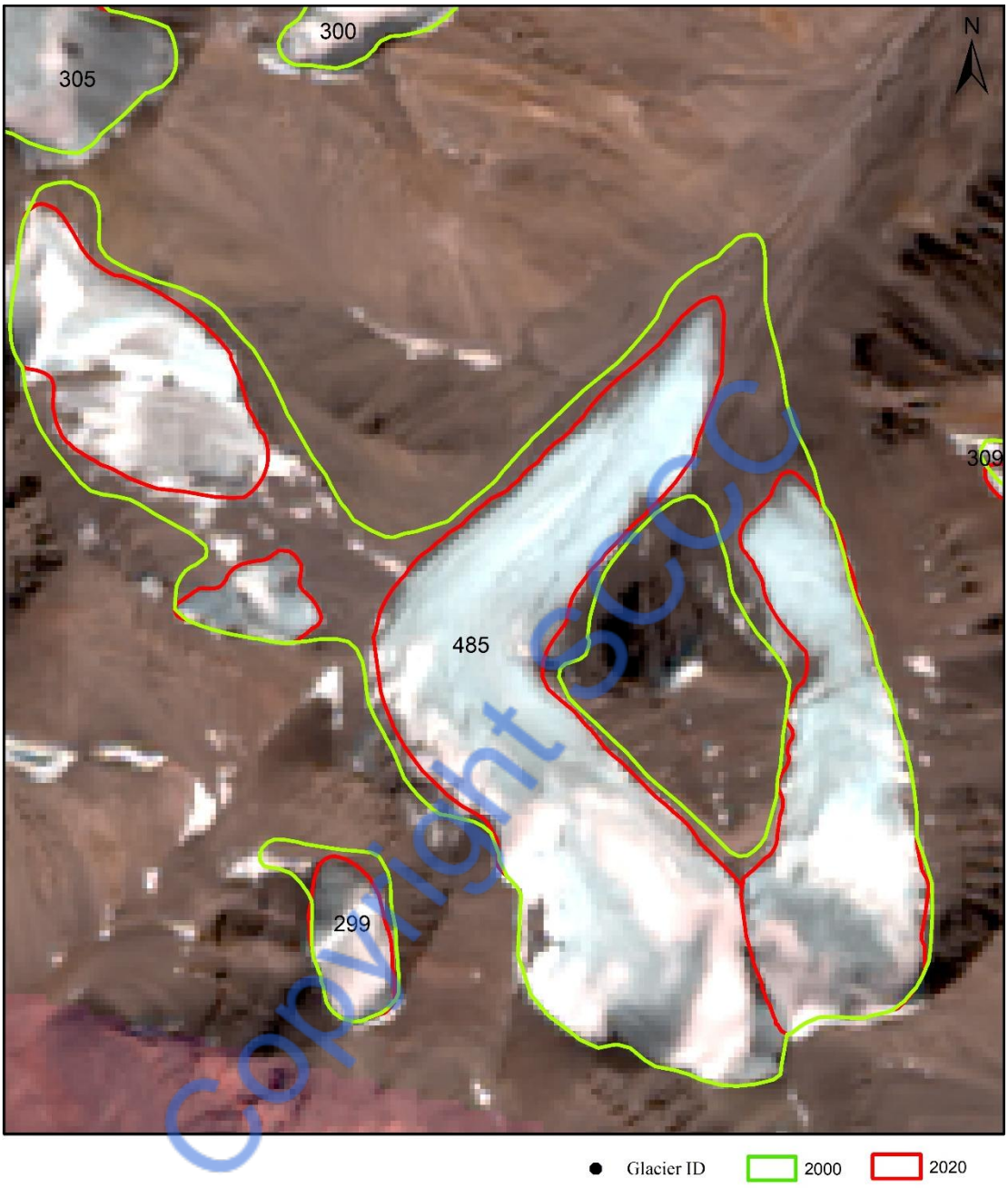

Figure 2.15 Fragmented glacier Spiti Sub basin, Satluj basin

3. SNOW COVER VARIABILITY IN SATLUJ BASIN

Mountain regions play a crucial role in the global hydrological cycle, acting as natural water towers that sustain downstream ecosystems and human populations. Among these regions, the Himalayas are of exceptional importance due to their extensive snow and glacier cover, which together form a dominant component of the cryosphere. Snow cover and glaciers serve as natural reservoirs, storing precipitation in solid form and releasing it gradually through melt processes. The timing, magnitude and variability of stream runoff in Himalayan river basins are therefore closely linked to snow accumulation, snowmelt dynamics and glacier mass balance.

Snow is a form of solid precipitation composed of crystalline ice particles that fall from clouds as snowflakes. Fresh snow generally exhibits low density values ranging from about 30–50 kg m^{-3}, which increase progressively through compaction, melting, refreezing and recrystallization processes (Paterson, 1994; Armstrong and Brun, 2008). When snow survives at least one ablation season, it transforms into firn, with densities typically ranging between 400 and 830 kg m^{-3} (Cuffey and Paterson, 2010). Continued densification over several years ultimately results in the formation of glacier ice, with densities between 830 and 910 kg m^{-3} (Benn and Evans, 2010). This gradual transformation demonstrates the intrinsic linkage between seasonal snow cover and long-term glacier formation, establishing snow as a critical input component of glacier mass balance (Dingman, 2015).

The atmospheric conditions required for snowfall are primarily met at higher latitudes and elevations, making mountainous regions particularly sensitive to changes in snow dynamics. Based on persistence, snow cover is classified into temporary, seasonal and permanent types. Temporary and seasonal snow covers occur mainly during winter, while permanent snow cover persists for many years and contributes to glacier nourishment. In terms of spatial extent, snow cover represents the second largest component of the cryosphere and covers approximately 40–50 per cent of the Earth's land surface during the Northern Hemisphere winter (Hall et al., 1995; Pepe et al., 2005). Due to its high reflectivity, snow cover strongly influences the Earth's radiation balance by

increasing surface albedo and regulating energy exchange between the land surface and the atmosphere (Foster and Chang, 1993).

In the Himalayan region, extensive snow cover develops during winter, particularly at higher elevations. The spatial and temporal variability of snow cover during winter and spring seasons plays a critical role in controlling river discharge. Rivers originating from the higher Himalayas derive a substantial proportion of their annual flow from snow and glacier melt. It has been estimated that approximately 30–50 per cent of the annual runoff in Himalayan rivers is contributed by snow and glacier meltwater (Agarwal et al., 1983). Snowmelt dominates streamflow during spring and early summer, while glacier melt provides a sustained contribution during late summer and dry periods, thereby regulating baseflow.

Snowcover ablation is highly sensitive to climatic variability, particularly changes in air temperature and precipitation patterns. Rising temperatures accelerate snowmelt, reduce snow cover duration and shift the timing of peak runoff towards earlier in the season. Such changes not only alter stream runoff patterns but also directly affect glacier mass balance. Seasonal snow accumulation constitutes the primary source of glacier nourishment, while enhanced ablation due to warming leads to negative mass balance conditions. Initially, increased glacier melt may result in higher runoff; however, persistent negative mass balance ultimately leads to glacier thinning and retreat, reducing long-term meltwater availability and increasing hydrological vulnerability.

Glacier mass balance represents the net gain or loss of ice over a specific period and is governed by the balance between accumulation (mainly snowfall) and ablation (melting, sublimation and calving). Snow cover variability directly influences glacier mass balance by controlling accumulation rates and surface energy conditions. Reduced snow cover lowers surface albedo, increases energy absorption and accelerates melt processes, thereby intensifying mass loss. Consequently, variations in snow cover, glacier dynamics and stream runoff are closely interconnected components of a single cryosphere–hydrology system.

Given the critical role of snow and glaciers in sustaining Himalayan river systems, accurate monitoring of snow cover extent, duration and reflectance is essential for hydrological modelling, glacier mass balance assessment and climate change impact studies. However, field-based monitoring of snow cover in rugged mountainous terrain such as the Himalayas is logistically

challenging, time-consuming and spatially limited. As a result, remote sensing techniques have become indispensable for snow and glacier monitoring.

Satellite-based snow cover monitoring began with the launch of the TIROS-1 satellite in 1960 (Singer and Popham, 1963). Since then, advancements in satellite technology have significantly enhanced the capability for operational snow mapping through improved spatial, temporal and radiometric resolutions. Snow exhibits distinct spectral reflectance characteristics in the visible and near-infrared regions, enabling reliable discrimination from other land cover types using optical satellite data (Hall et al., 1995). Sensors onboard polar-orbiting satellites such as Landsat, NOAA and MODIS have been widely used to map snow cover and analyze its seasonal and inter-annual variability.

India's Indian Remote Sensing (IRS) satellite programme has further strengthened snow monitoring capabilities in the Himalayan region. The RESOURCESAT-1 satellite, equipped with LISS-III, LISS-IV and AWiFS sensors, provides multi-resolution data suitable for regional and basin-scale snow cover analysis. AWiFS, an advanced version of the earlier WiFS sensor, offers improved spatial and spectral resolution while maintaining high temporal repetitivity, making it particularly effective for monitoring seasonal snow dynamics over large mountainous areas. In addition, geostationary satellites have also demonstrated their utility in near-real-time monitoring of snow-covered regions.

Satellite-derived snow cover information has been extensively used as an input for snowmelt runoff modelling and glacier mass balance studies (Kulkarni et al., 1997). Integration of snow cover data with meteorological observations and streamflow records enables improved estimation of meltwater contribution to runoff and enhances understanding of the hydrological response of glacier-fed river basins to climatic variability. Such integrated analyses are essential for predicting future water availability, managing water resources and assessing the long-term impacts of climate change in the Himalayan region.

TEMPORAL ANALYSIS OF SNOW COVER VARIATIONS IN SATLUJ BASIN

Seasonal snow cover is a vital hydrological component of Himalayan river basins, strongly influencing runoff generation and water availability. In this study, the spatial distribution of seasonal snow cover in the Satluj Basin in Himachal Pradesh excluding lower Satluj sub-basin

which covers an area about 11634 km^2 was analyzed using AWiFS satellite data (56 m resolution) (Figure 3.1) for the period 2010–11 to 2020–21, covering the winter season from October to May.

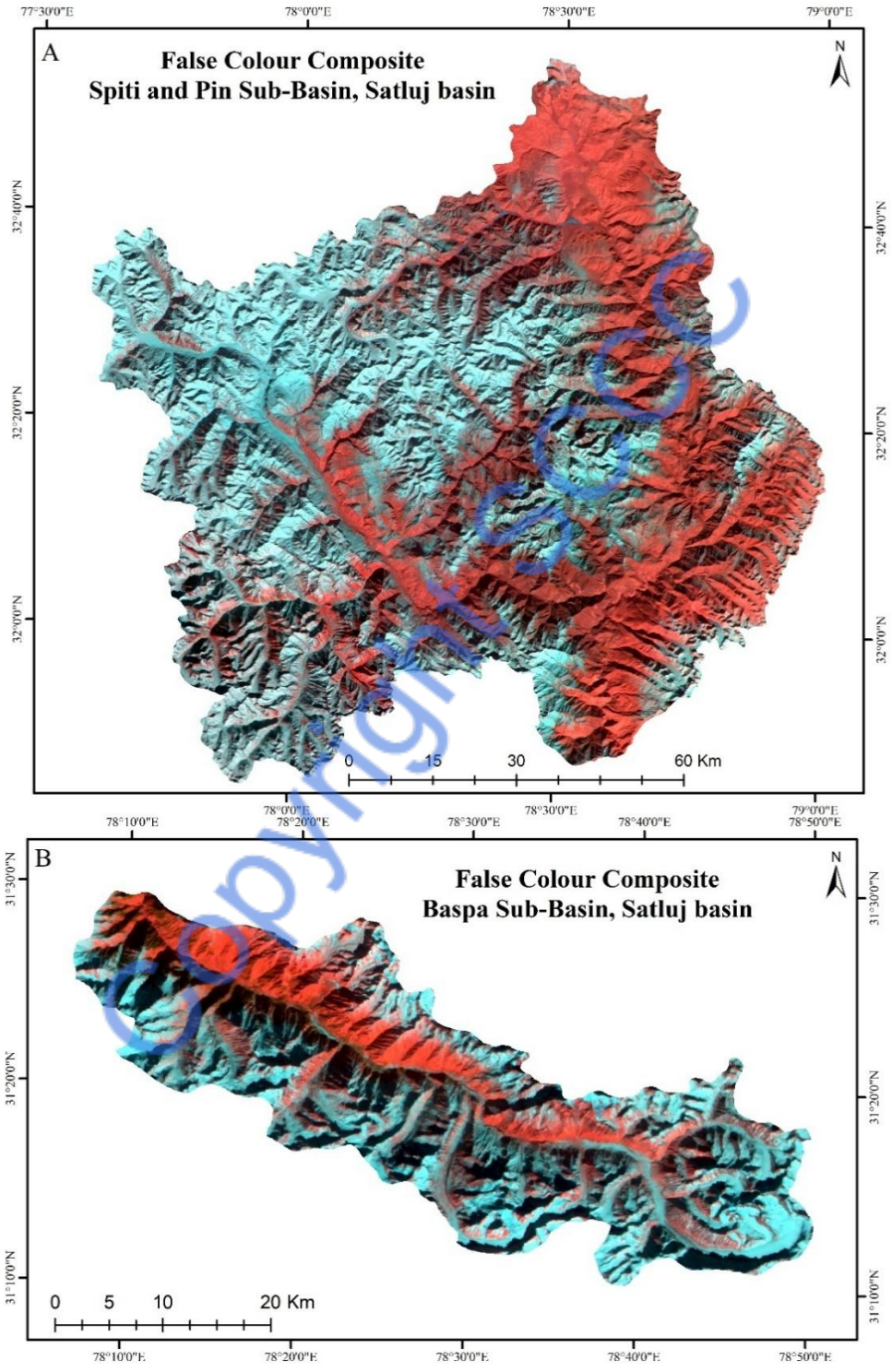

Source: IRS-AWiFS Satellite data-2012

Figure 3.1 False Color Composite Satluj basin (Himachal Pradesh)

There is significant seasonal variation in the monthly average snow cover. Snow accumulation typically starts in October, rises gradually through November and December, reaches its peak in January and February and then gradually decreases in the spring as a result of increased snowmelt and rising temperatures. The amount of snow cover in the early winter varies greatly from year to year due to variations in the start and intensity of snowfall.

The highest snow cover is usually recorded during the winter months, with January and February frequently surpassing 85–95% basin coverage in years with plenty of snow. March's high snow persistence emphasizes how crucial late-winter snow storage is to maintaining spring runoff. In the month of April and May reflects decrease in snow cover, alarming the basins in Himachal Pradesh is shifting from accumulation-dominated to melt-driven hydrological conditions.

TEMPORAL ANALYSIS OF SNOW COVER AREA, 2010–11

The snow cover conditions during 2010–11 (Figure 3.2 & 3.3) were characterized by low early-winter accumulation, a brief but intense mid-winter peak and rapid post-peak ablation, making this year one of the lower snow years in the study period. On the basis of AWiFs Satellite data, in October, snow cover extended over 30.17 % (3510 km²), indicating moderate early-season snowfall across higher elevations.

Table 3.1 Spatio-temporal Distribution of Snow cover, 2010-2011

Month	Area of Snow cover (Km²)	Area of Snow cover (%)
October	3510.00	30.17
November	3353.00	28.82
December	3115.00	26.77
January	10794.00	92.78
February	3366.00	28.93
March	3589.00	30.85
April	3021.00	25.97
May	1987.00	17.08
Average Area (Km²)	4091.88	35.17

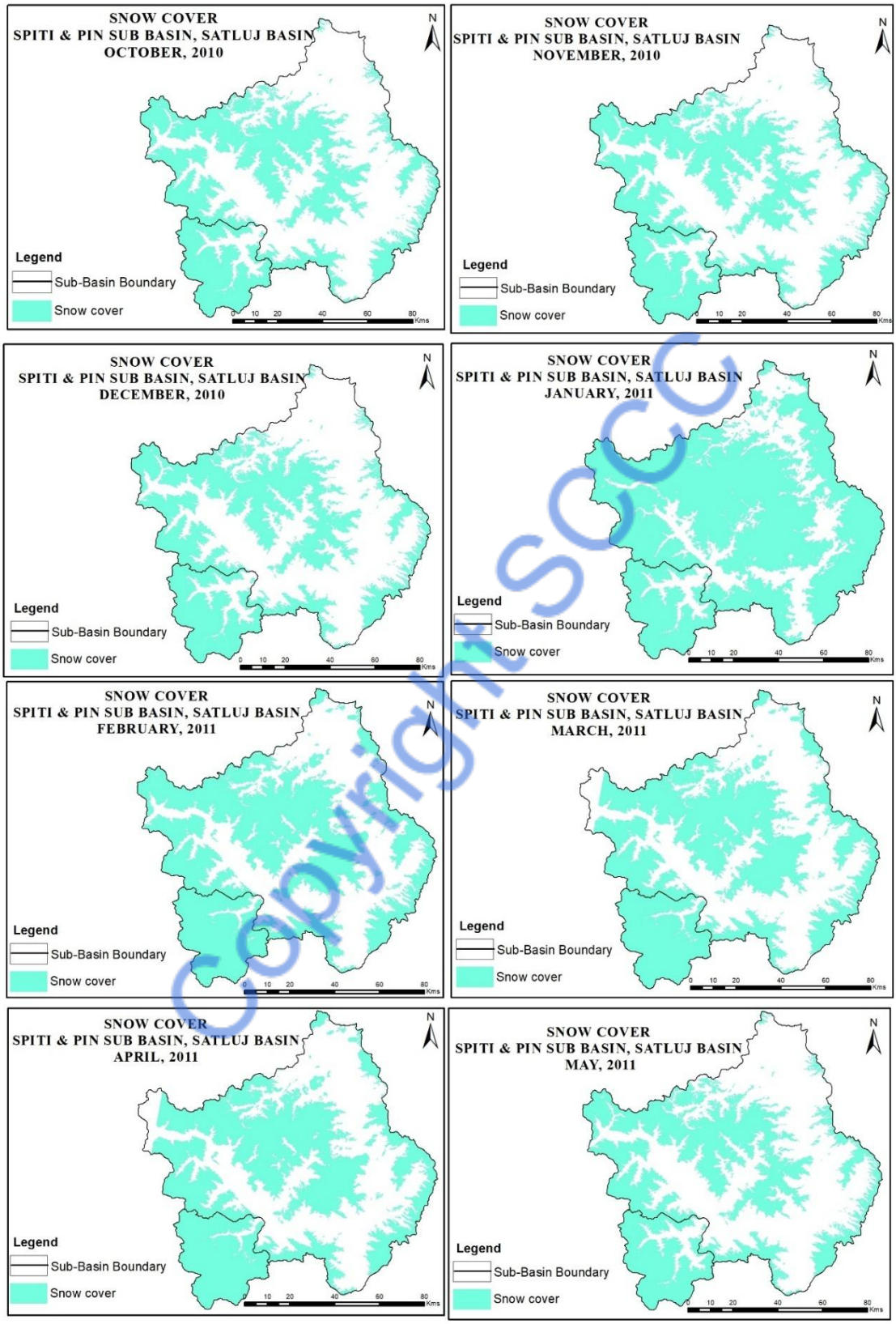

Figure 3.2 Distribution of snow cover in Spiti and Pin Sub-basin, 2010-2011

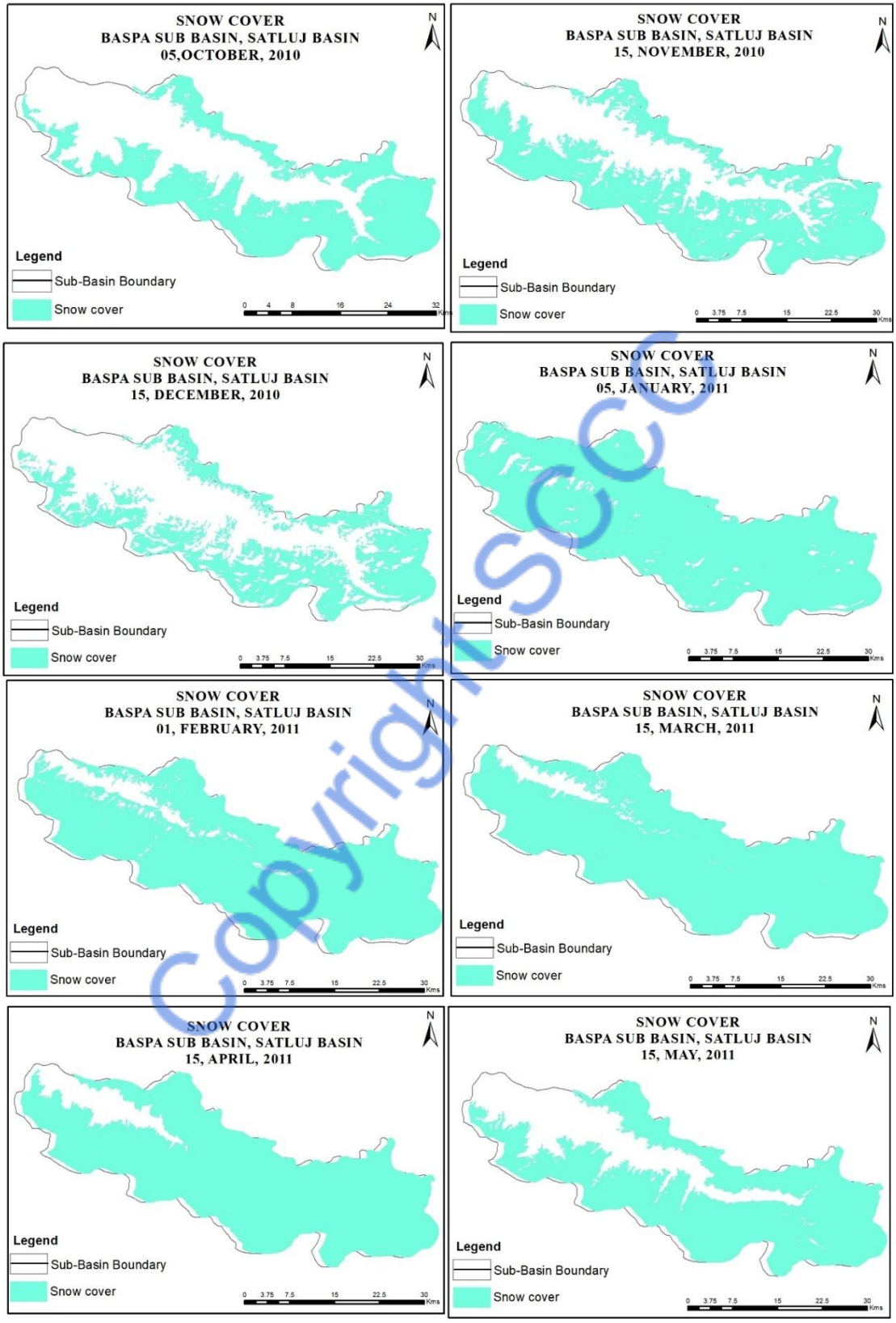

Figure 3.3 Distribution of snow cover in Baspa Sub-basin, 2010-2011

A gradual decline in snow cover was observed during November (3353.00 km²; 28.82%) and December (3115 km²; 26.77%), suggesting limited snowfall activity and possible early-season melting or compaction. A dramatic and abrupt increase occurred in January, when snow cover surged to 10794.00 km² (92.78%), representing near-complete basin coverage and indicating a major snowfall event during peak winter.

However, this extensive snow cover was short-lived. In February, snow cover declined sharply to 3366.00 km² (28.93%), reflecting rapid ablation or rainfall-induced melting. Moderate snow cover persisted during March (3589.00 km²; 30.85%) and April (3021.00 km²; 25.97%), indicating limited retention of winter snow.

By May, snow cover reduced further to 1987.00 km² (17.08%), signifying substantial depletion of seasonal snow across the basin. The annual average snow-covered area for 2010–11 was 4091.88 km² (35.17%), the lowest among all ana lyzed years, highlighting the overall weak snow conditions during this season.

TEMPORAL ANALYSIS OF SNOW COVER AREA, 2011–12

The snow cover conditions during 2011–12 exhibit a pattern of delayed early-winter accumulation followed by strong and sustained mid- to late-winter snow dominance, indicating a generally favorable snow season (Figure 3.4 and 3.5) . In October, snow cover was limited to 1861.62 km² (16.00%), reflecting weak early-season snowfall and a late onset of winter conditions (Table 3.2).

A further reduction was observed in November, when snow cover decreased to 1137.94 km² (9.78%), suggesting temporary warming or suppressed precipitation during early winter. However, a gradual accumulation phase began in December, with snow cover increasing to 2646.07 km² (22.74%), marking the initiation of more consistent winter snowfall at higher elevations (Table 3.2). A pronounced and rapid expansion of snow cover occurred in January, when the snow-covered area rose sharply to 62.23%, indicating widespread snowfall across the basin. Peak winter conditions were achieved during February, with snow cover reaching 93.60% and remained comparably high in March at 92.26 % (Table 3.2). These values demonstrate strong snow persistence and minimal ablation during the core winter months.

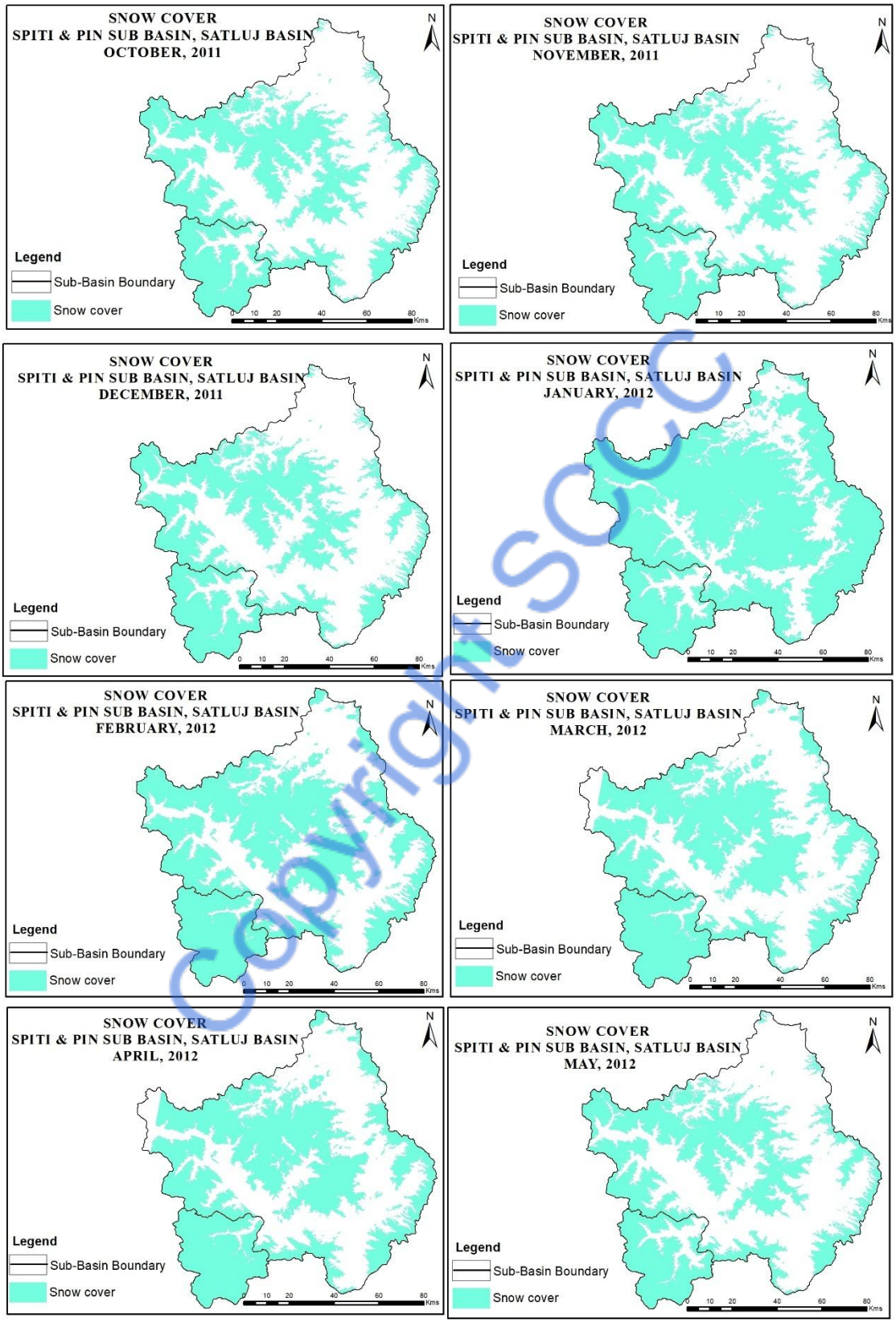

Figure 3.4 Distribution of snow cover in Spiti and Pin Sub-basin, 2011-2012

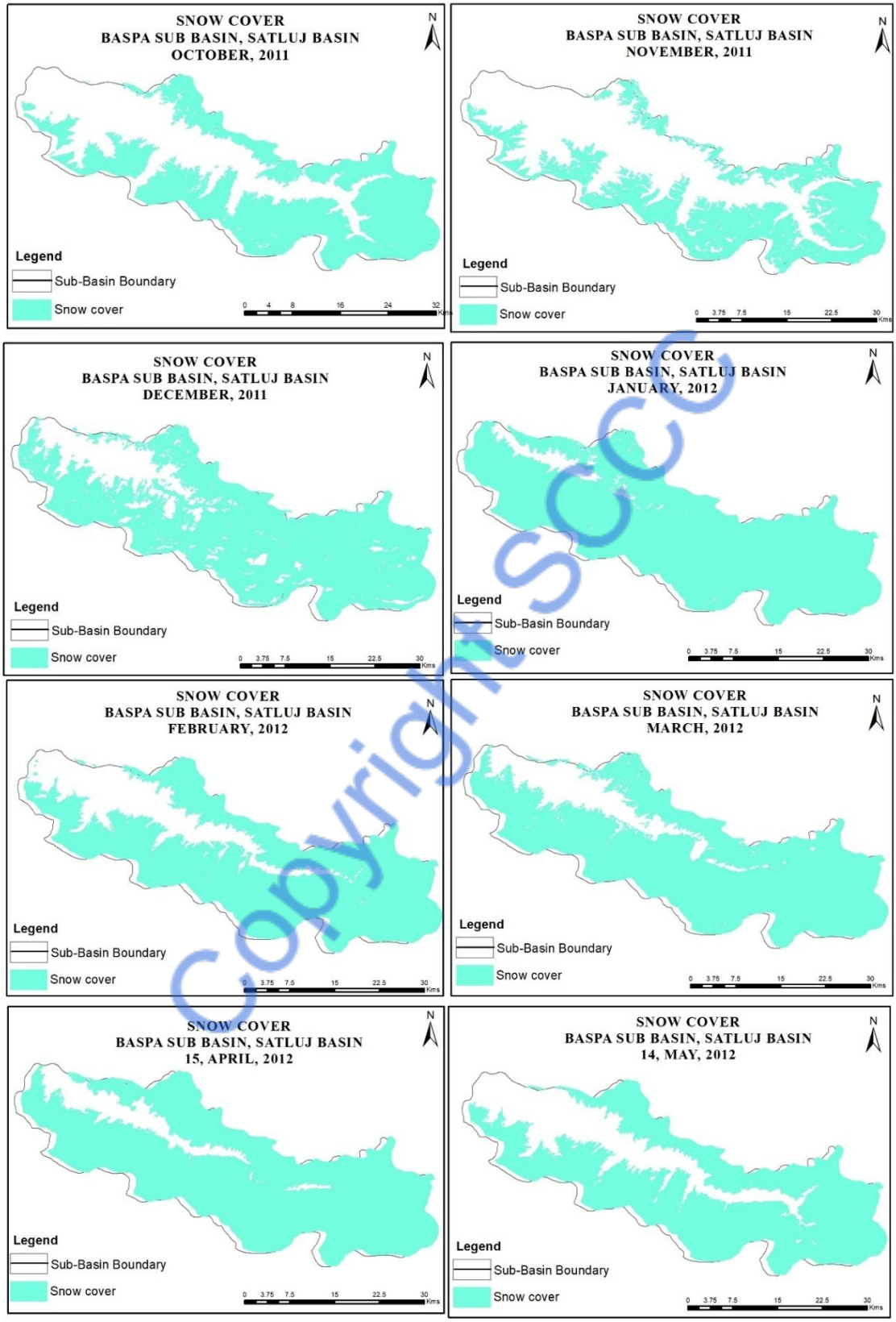

Figure 3.5 Distribution of snow cover in Baspa Sub-basin, 2011-2012

In April, snow cover declined moderately to 8165.83 km² (70.19%), reflecting the onset of spring warming and gradual melting at lower elevations. By May, snow cover had further reduced to 6330.00 km² (54.41%), indicating continued seasonal ablation while maintaining substantial snow storage at higher elevations. The annual average snow-covered area for 2011–12 was 6125.49 km² (52.65%), classifying this year as a moderate to high snow year within the overall temporal record.

Table 3.2 Spatio-temporal Distribution of Snow cover, 2011-2012

Month	Area of Snow cover (Km^2)	Area of Snow cover (%)
October	1861.62	16.00
November	1137.94	9.78
December	2646.07	22.74
January	7239.68	62.23
February	10888.96	93.60
March	10733.85	92.26
April	8165.83	70.19
May	6330.00	54.41
Average Area (Km^2)	6125.49	52.65

TEMPORAL ANALYSIS OF SNOW COVER AREA, 2012–13

It is evident in Table 3.3 that snow cover regime during 2012–13 was marked by early accumulation, exceptionally high peak winter coverage and strong seasonal persistence, identifying this year as one of the most snow-abundant years in the entire study period. In October, snow cover stretched over 2834.22 km² (24.36%), indicating an earlier initiation of snowfall compared to several adjacent years.

A slight reduction was observed in November, with snow cover decreasing marginally to 2614.57 km² (22.47%), likely reflecting short-term temperature fluctuations or limited early winter precipitation. However, a pronounced accumulation phase commenced in December, when snow cover increased sharply to 7831.31 km² (67.31%), signaling the establishment of widespread winter conditions across the basin.

Snow accumulation intensified further in January, with the snow-covered area expanding to 8604.56 km² (73.96%). Peak snow cover was achieved during February, reaching 11240.60 km² (96.62%), representing near-complete coverage of the basin. This extensive snow cover persisted

into March, with an area of 11066.03 km² (95.12%), indicating minimal ablation and highly stable winter conditions.

The annual average snow-covered area for 2012–13 was 7365.22 km² (63.31%), ranking this year among the highest snow-cover years in the dataset and reflecting sustained accumulation throughout the winter season.

Table 3.3 Spatio-temporal Distribution of Snow cover, 2012-2013

Month	Area of Snow cover (Km^2)	Area of Snow cover (%)
October	2834.22	24.36
November	2614.57	22.47
December	7831.31	67.31
January	8604.56	73.96
February	11240.60	96.62
March	11066.03	95.12
Average Area (Km^2)	7365.22	63.31

TEMPORAL ANALYSIS OF SNOW COVER AREA, 2013–14

The snow cover dynamics during 2013–2014 display a pattern of gradual early-winter accumulation followed by strong and sustained peak winter coverage, indicating a generally favourable snow season. In October, snow cover was relatively limited, covering 2127.58 km² (18.29%), which suggests a delayed onset of winter snowfall across the basin (Table 3.4).

The snow cover area extended in November to 4305.04 km² (37.00%), an increase was observed, reflecting the initiation of winter precipitation and gradual accumulation at higher elevations. However, a slight reduction occurred in December, with snow cover decreasing to 3521.17 km² (30.27%), possibly due to short-term warming or reduced snowfall activity during early winter (Table 3.4).

An accumulation phase of snow began in January, when snow cover increased to 10458.60 km² (89.90%), indicating widespread and intense winter snowfall. High snow coverage was sustained through February, with an extent of 10080.37 km² (86.65%) and continued into March, reaching 10353.60 km² (88.99%). These values demonstrate strong snow persistence during the core winter months, with minimal ablation (Table 3.4). The annual average snow-covered area for 2013–2014 was 6807.73 km² (58.52%), classifying this year as a moderately high snow year within the study period.

Table 3.4 Spatio-temporal Distribution of Snow cover, 2013-2014

Month	Area of Snow cover (Km^2)	Area of Snow cover (%)
October	2127.58	18.29
November	4305.04	37.00
December	3521.17	30.27
January	10458.60	89.90
February	10080.37	86.65
March	10353.60	88.99
Average Area (Km^2)	6807.73	58.52

TEMPORAL ANALYSIS OF SNOW COVER AREA, 2014–15

The snow cover interpretation during 2014–15 reflects a delayed onset of winter snowfall, followed by strong mid- to late-winter accumulation and moderate spring persistence using AWiFs satellite data (Figures 3.6 & 3.7). In October, snow cover was minimal, with an area of only 1109.69 km² (9.54%), indicating very limited early-season snowfall and relatively warm pre-winter conditions (Table 3.5).

A slight increase was observed in November, when snow cover expanded marginally to 1253.86 km² (10.78%), suggesting the initial arrival of winter precipitation; however, accumulation remained weak during early winter. A substantial increase occurred in December, with snow cover rising sharply to 6507.44 km² (55.93%), reflecting a major snowfall event that significantly enhanced basin-wide snow extent. Despite this increase, snow cover declined in January to 5572.49 km² (47.90%), indicating short-term melting or reduced snowfall. A strong accumulation phase resumed in February, with snow cover expanding markedly to 10184.24 km² (87.54%), signaling the establishment of peak winter conditions (Table 3.5).

The maximum snow cover was recorded in March, when the area reached 10894.98 km² (93.65%), indicating near-complete coverage of the basin. In April, snow cover declined moderately to 9190.70 km² (79.00%), reflecting the onset of spring ablation under increasing temperatures and solar radiation. By May, snow cover had reduced further to 5782.51 km² (49.70%), marking continued seasonal melting, particularly at lower and mid-elevation zones. The annual average snow-covered area for 2014–15 was 6311.99 km² (54.25%), classifying this year as a moderate to moderately high snow year (Table 3.5).

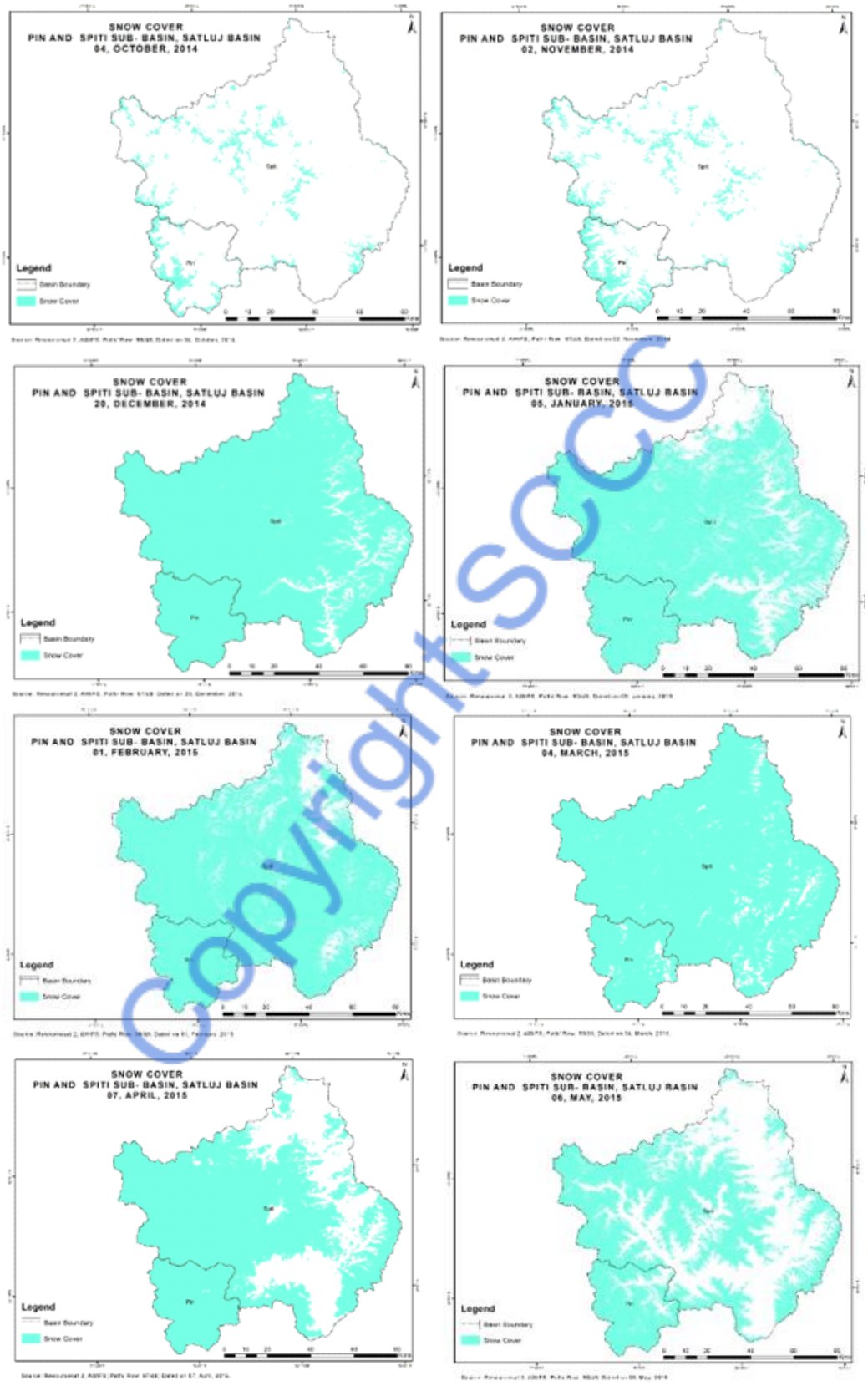

Figure 3.6 Distribution of snow cover in Spiti and Pin Sub-basin, 2014-2015

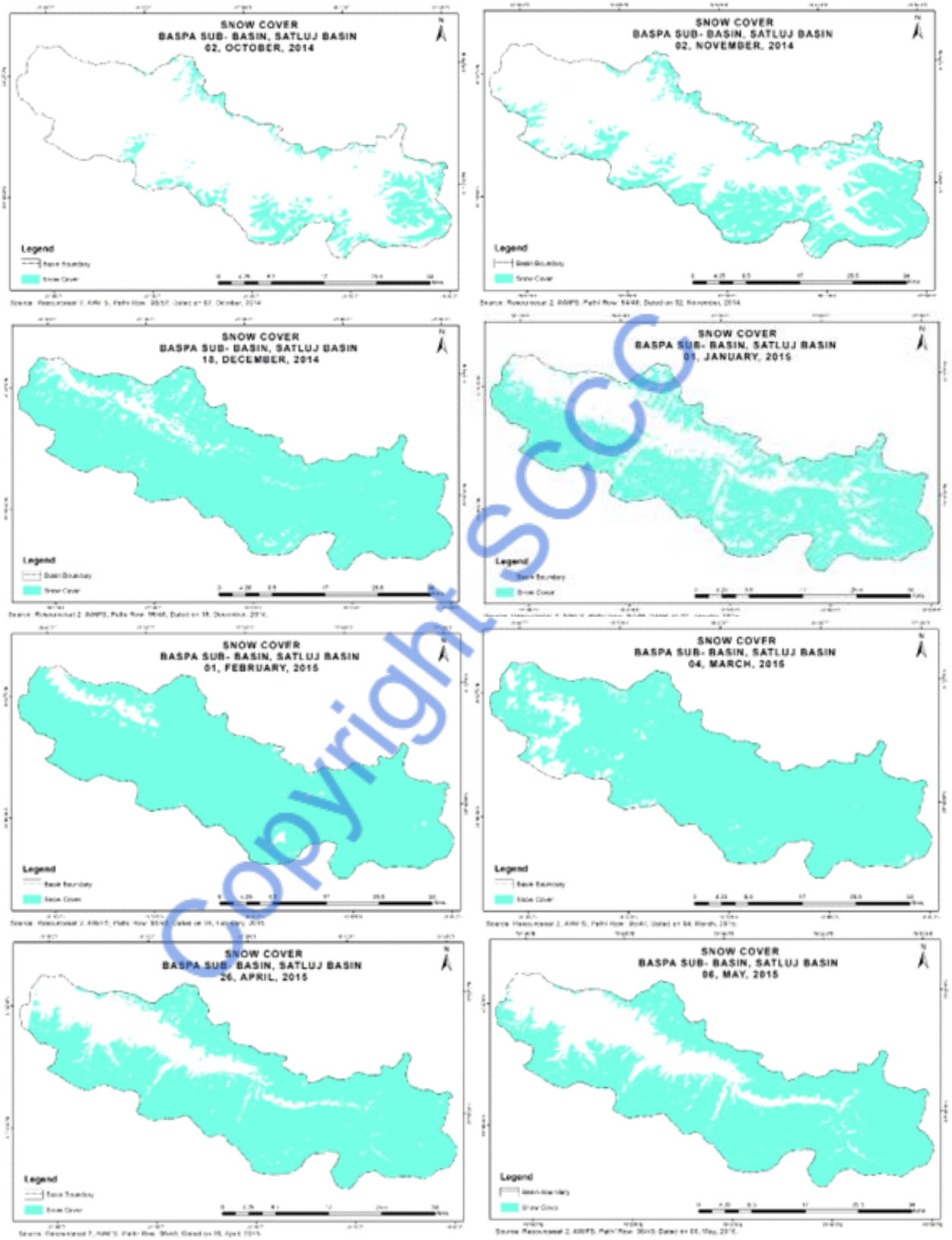

Figure 3.7 Distribution of snow cover in Baspa Sub-basin, 2014-2015

Table 3.5 Spatio-temporal Distribution of Snow cover, 2014-2015

Month	Area of Snow cover (Km^2)	Area of Snow cover (%)
October	1109.69	9.54
November	1253.86	10.78
December	6507.44	55.93
January	5572.49	47.90
February	10184.24	87.54
March	10894.98	93.65
April	9190.70	79.00
May	5782.51	49.70
Average Area (Km^2)	6311.99	54.25

TEMPORAL ANALYSIS OF SNOW COVER AREA, 2015–16

The snow cover dynamics during 2015–16 in figures 3.8 & 3.9 indicate a moderate snow year, characterized by gradual accumulation, a well-defined winter peak and relatively early spring ablation. Table 3.6 reflects that in October, snow cover was limited, with an area of 3332.54 km² (28.64%), reflecting weak early-season snowfall and delayed winter onset.

A substantial increase was observed in November, when snow cover expanded sharply to 6780.69 km² (58.28%), indicating the beginning of sustained winter precipitation. However, this increase was followed by a decline in December to 5291.69 km² (45.48%), suggesting temporary warming conditions or reduced snowfall during early winter (Table 3.6).

Snow cover recovered slightly in January, reaching 5499.77 km² (47.27%), though values remained lower than in November. A pronounced accumulation phase occurred in February, with snow cover increasing markedly to 7891.63 km² (67.83%), indicating strengthened winter conditions and widespread snowfall across higher elevations (Table 3.6). Peak snow cover was observed in March, when the snow-covered area reached 8391.38 km² (72.13%), representing the maximum spatial extent for the season. During April, snow cover declined moderately to 7311.37 km² (62.84%), reflecting the onset of seasonal ablation under rising temperatures (Table 3.6).

By May, snow cover had reduced sharply to 3682.30 km² (31.65%), indicating accelerated melting and rapid retreat of seasonal snow, particularly in lower and mid-elevation zones. The annual average snow-covered area for 2015–16 was 6022.67 km² (51.77%), placing this year in the category of a moderate snow year within the overall temporal record (Table 3.6).

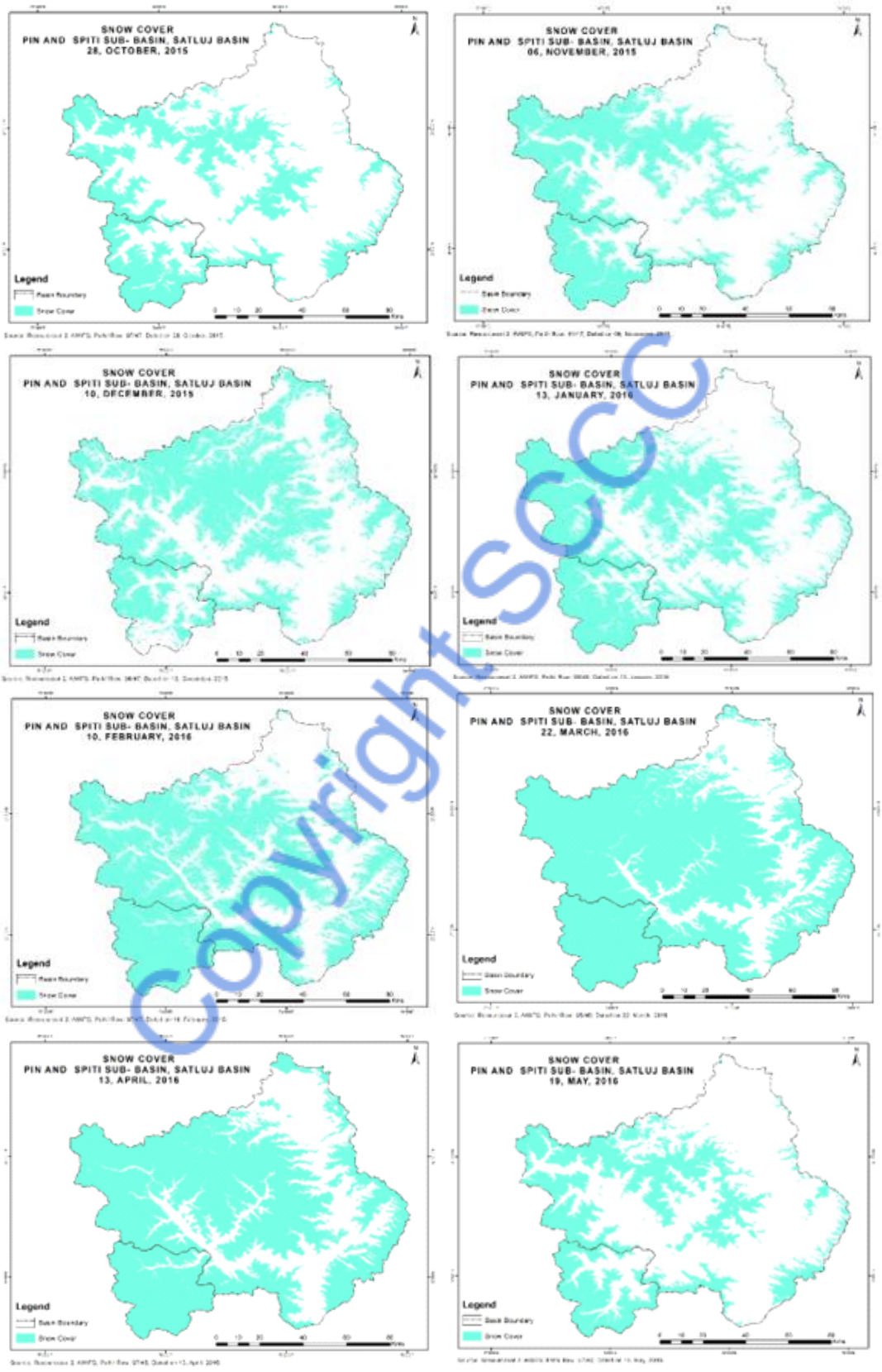

Figure 3.8 Distribution of snow cover in Spiti and Pin Sub-basin, 2015-2016

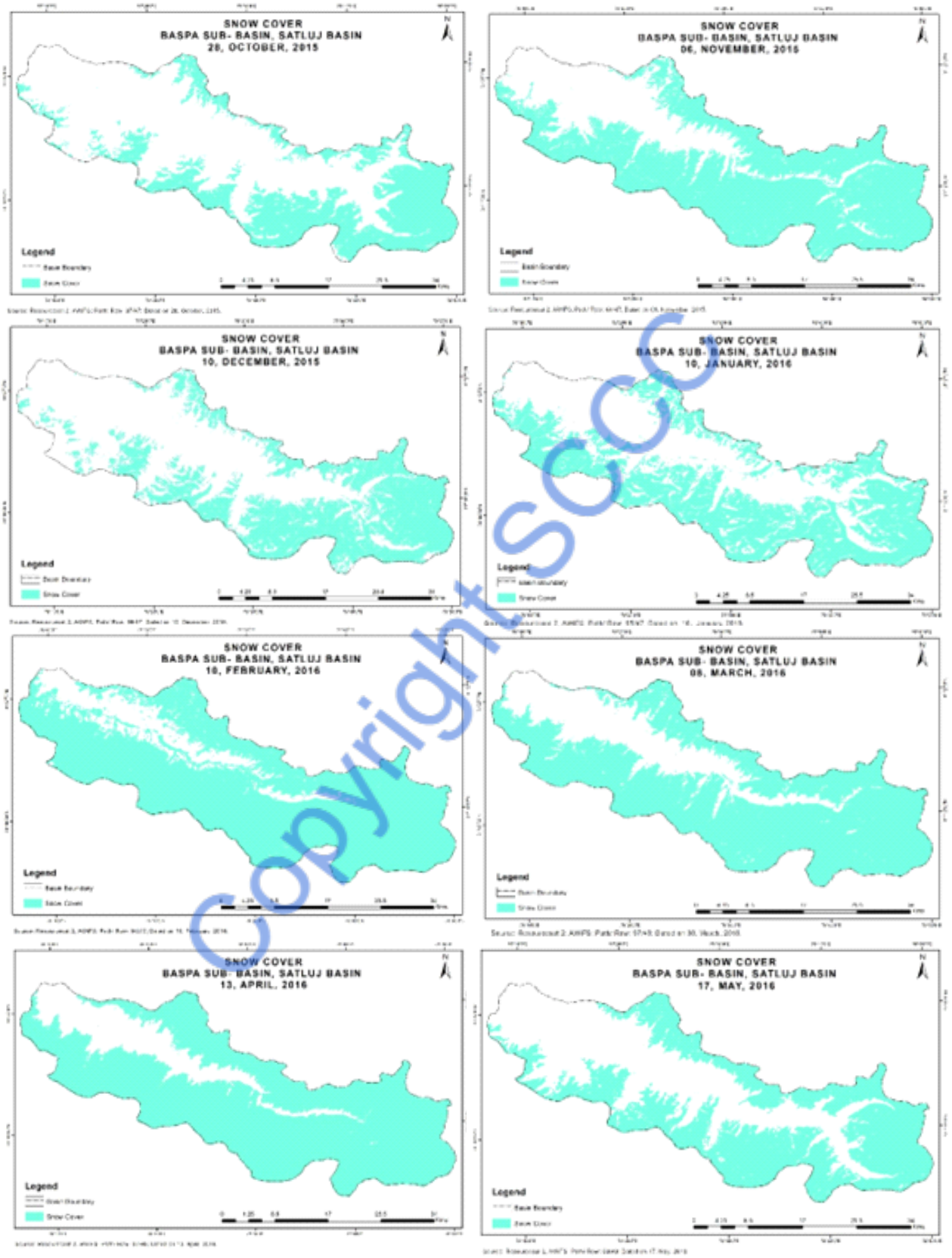

Figure 3.9 Distribution of snow cover in Baspa Sub-basin, 2015-2016

Table 3.6 Spatio-temporal Distribution of Snow cover, 2015-2016

Month	Area of Snow cover (Km^2)	Area of Snow cover (%)
October	3332.54	28.64
November	6780.69	58.28
December	5291.69	45.48
January	5499.77	47.27
February	7891.63	67.83
March	8391.38	72.13
April	7311.37	62.84
May	3682.3	31.65
Average Area (Km^2)	6022.671	51.77

TEMPORAL ANALYSIS OF SNOW COVER AREA, 2017–18

The snow cover conditions during 2017–18 was characterized by a delayed onset, high intra-seasonal variability and moderate overall snow persistence, distinguishing this year from both the preceding and succeeding snow-abundant years (Figure 3.10 & 3.11). In October, snow cover was minimal, with an area of only 1402.84 km² (12.06%), indicating weak early winter snowfall and relatively warmer pre-winter conditions (Table 3.7).

A slight increase was observed in November, when snow cover expanded to 2601.05 km² (22.36%), suggesting the initial establishment of winter precipitation, although accumulation remained limited. A pronounced and abrupt increase occurred in December, with snow cover rising sharply to 8849.71 km² (76.07%), reflecting a major snowfall event that significantly enhanced basin-wide snow extent (Table 3.7).

Despite this strong mid-winter accumulation, snow cover declined substantially in January to 4656.17 km² (40.02%), indicating either a temporary warming phase, rainfall-on-snow events, or redistribution and compaction of snow. During February, snow cover increased moderately to 5175.07 km² (44.48%), reflecting renewed snowfall but not reaching the extent observed in December (Table 3.7). A second accumulation phase occurred during March, when snow cover expanded markedly to 8340.93 km² (71.69%), followed by a further increase in April to 8731.69 km² (75.05%). This late-season enhancement suggests significant spring snowfall or persistent low temperatures that delayed ablation at higher elevations (Table 3.7).

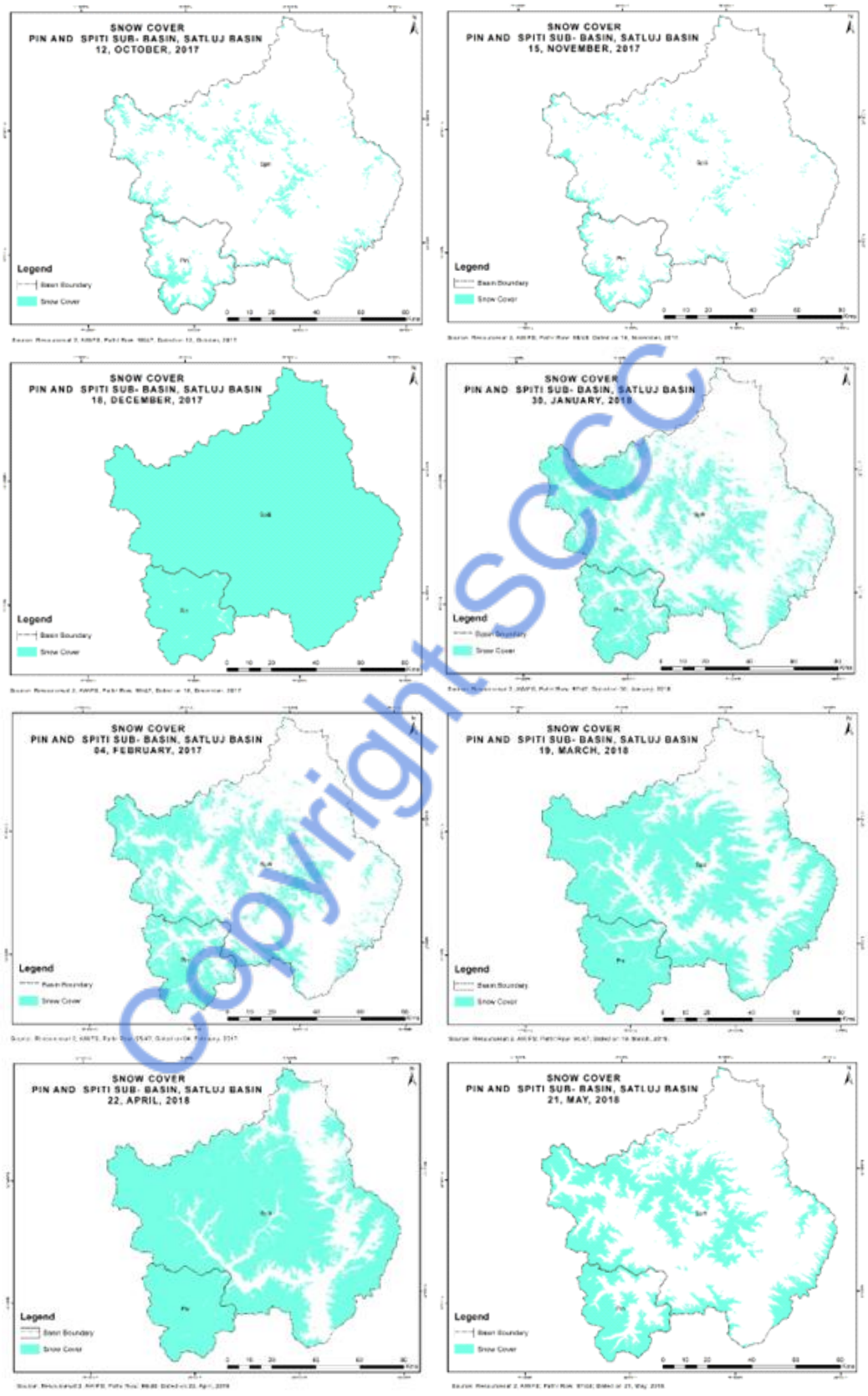

Figure 3.10 Distribution of snow cover in Spiti and Pin Sub-basin, 2017-2018

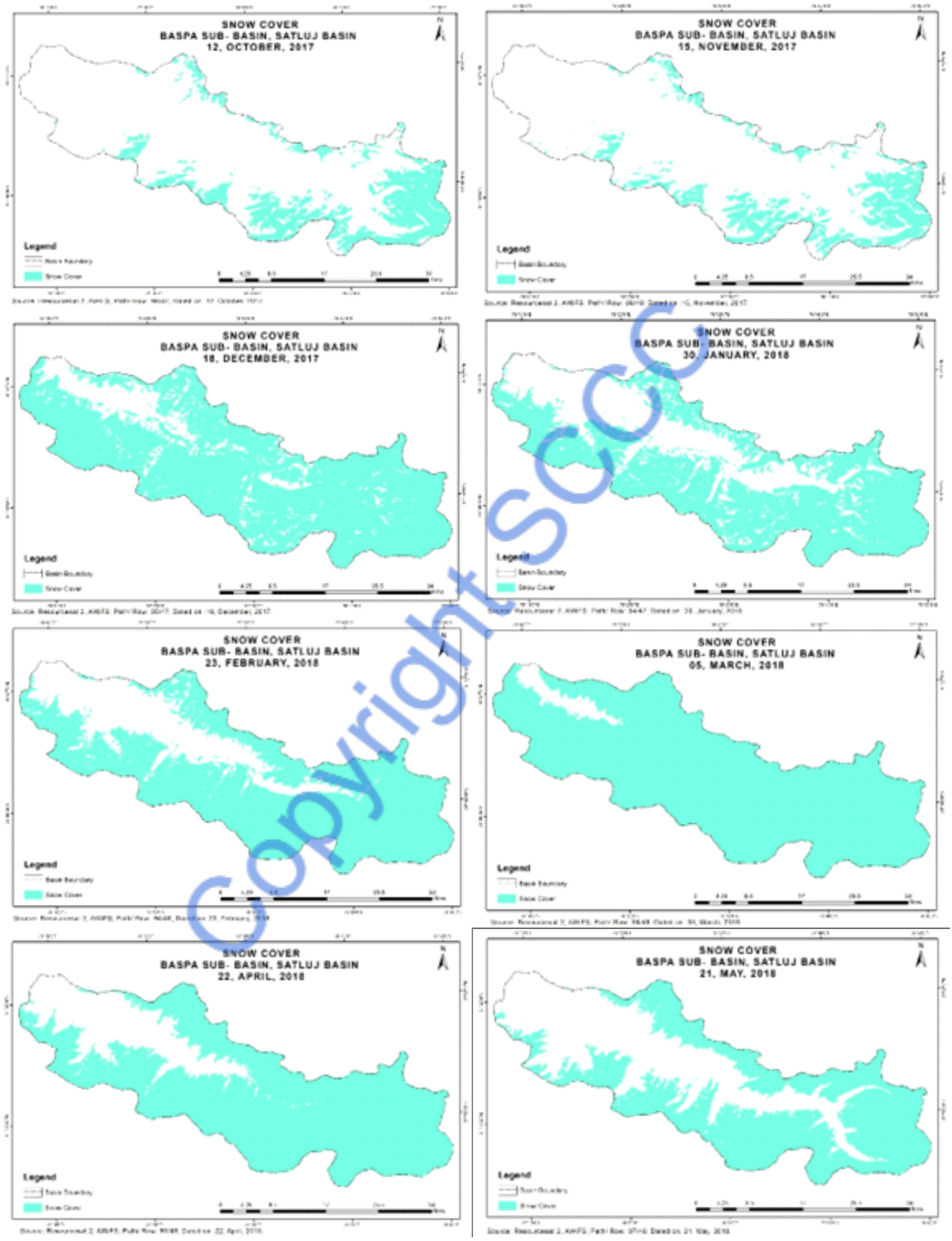

Figure 3.11 Distribution of snow cover in Baspa Sub-basin, 2017-2018

By May, snow cover reduced sharply to 4099.65 km² (35.24%), indicating a rapid onset of melting under rising temperatures. The annual average snow-covered area for 2017–18 was 5482.14 km² (47.12%), placing this year among the lower to moderate snow years in the overall temporal record.

Table 3.7 Spatio-temporal Distribution of Snow cover, 2017-2018

Month	Area of Snow cover (Km^2)	Area of Snow cover (%)
October	1402.84	12.06
November	2601.05	22.36
December	8849.71	76.07
January	4656.17	40.02
February	5175.07	44.48
March	8340.93	71.69
April	8731.69	75.05
May	4099.65	35.24
Average Area (Km^2)	5482.14	47.12

TEMPORAL ANALYSIS OF SNOW COVER AREA, 2018–19

The snow cover conditions during 2018–19 was marked by early accumulation, exceptionally high winter persistence and delayed seasonal ablation, making this year one of the most snow-abundant periods within the study timeframe (Figure 3.12 & 13). In October, snow cover was already substantial, with an area of 5664.57 km² (48.69%), indicating an early onset of snowfall and cooler pre-winter temperatures across the basin. Snow cover increased sharply in November, reaching 8427.46 km² (72.44%), reflecting widespread accumulation across mid- and high-elevation zones. Although a temporary reduction was observed in December (7113.45 km²; 61.14%), this decline likely represents short-term melting or snowfall variability rather than a sustained ablation phase (Table 3.8).

A renewed and stronger accumulation phase occurred in January, with snow cover expanding to 8582.61 km² (73.77%). Peak conditions were achieved during February, when snow cover reached 10943.97 km² (94.07%), indicating near-complete basin coverage. This extensive snow extent persisted into March, with values of 10662.87 km² (91.65%), suggesting stable winter conditions with limited melt. In April, snow cover remained exceptionally high at 10741.63 km² (92.33%), highlighting prolonged winter influence and delayed ablation (Table 3.8). Such persistence during early spring indicates sustained low temperatures and effective snow retention at

higher elevations. A sharp decline was observed only in May, when snow cover reduced to 5460.95 km² (46.94%), marking the onset of rapid seasonal melting.

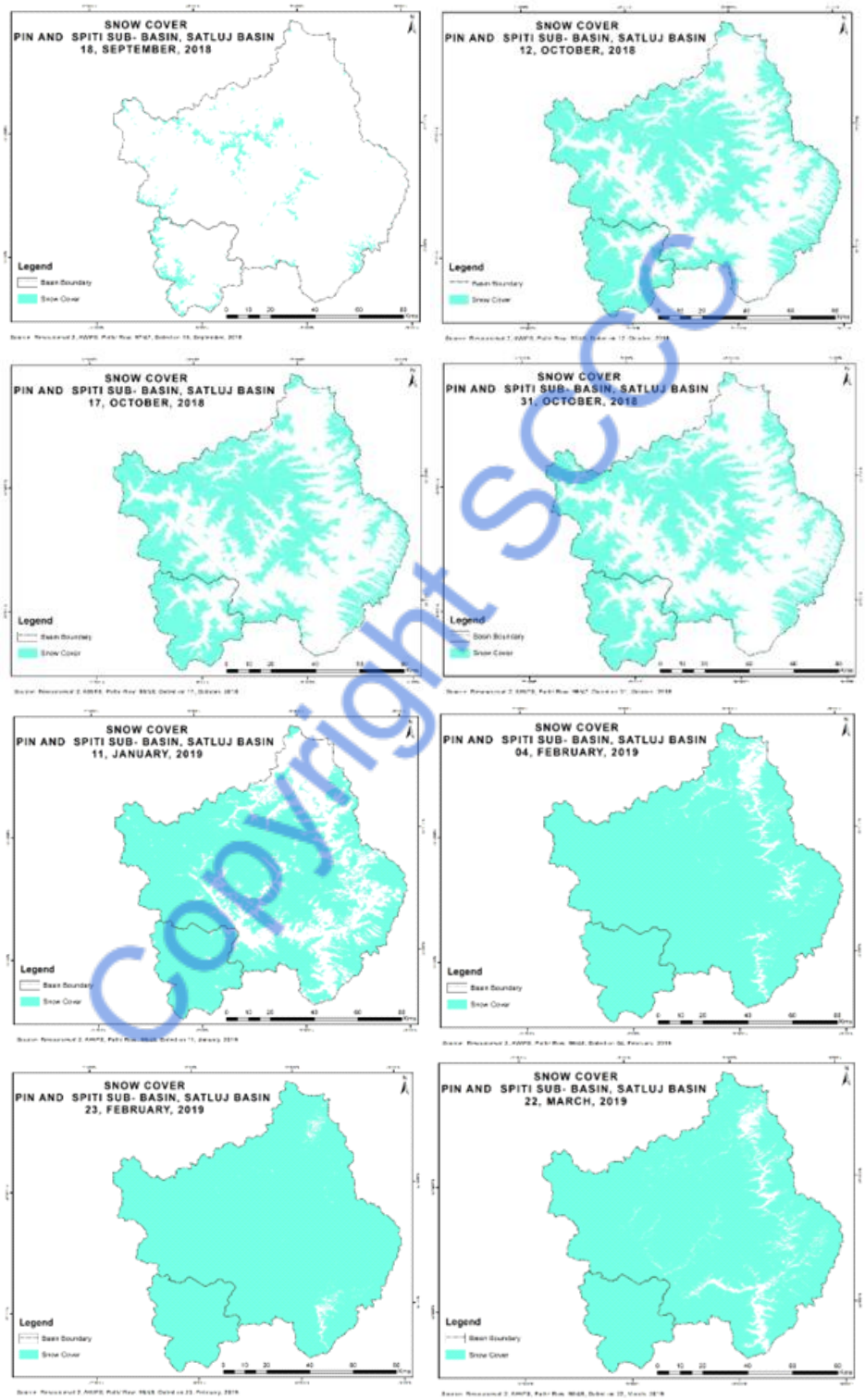

Figure 3.12 Distribution of snow cover in Spiti and Pin Sub-basin, 2018-2019

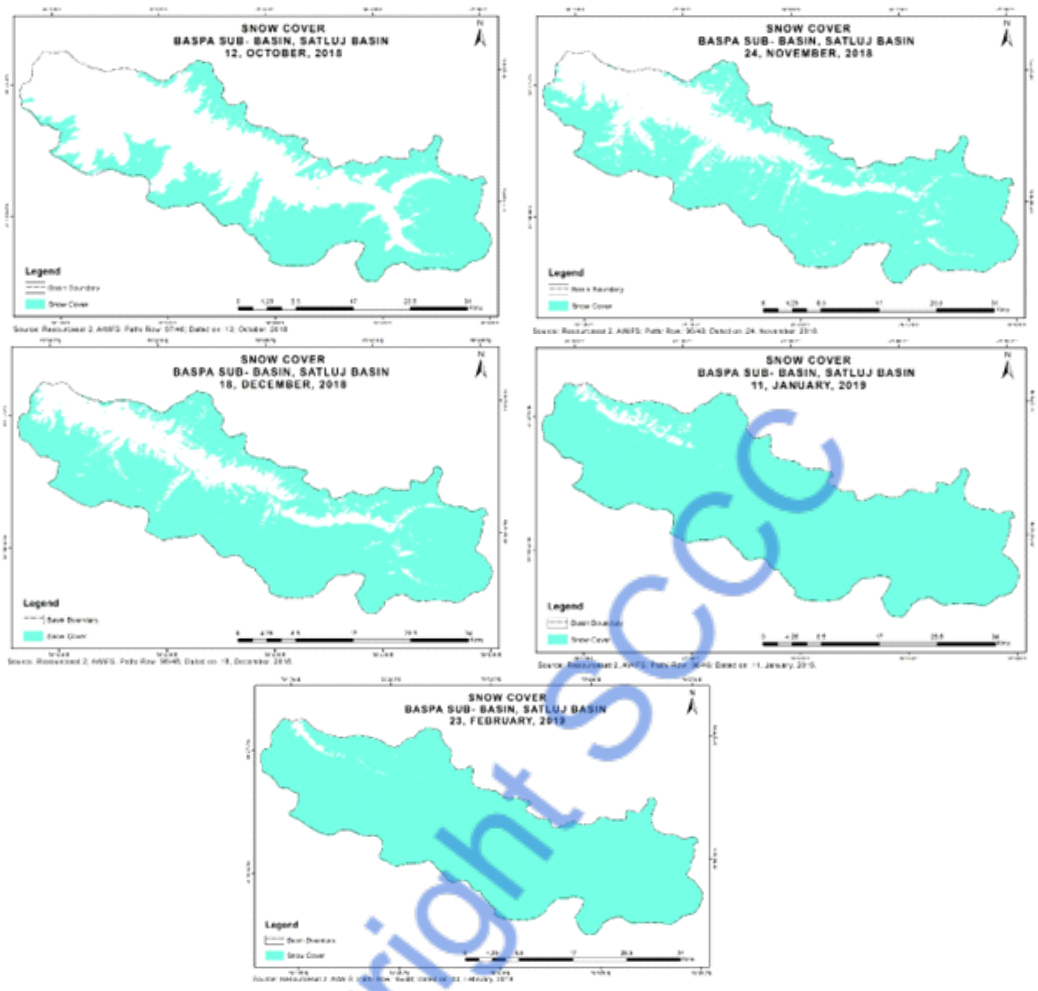

Figure 3.13 Distribution of snow cover in Baspa Sub-basin, 2018-2019

Table 3.8 Spatio-temporal Distribution of Snow Cover, 2018-2019

Month	Area of Snow cover (Km^2)	Area of Snow cover (%)
October	5664.57	48.69
November	8427.46	72.44
December	7113.45	61.14
January	8582.61	73.77
February	10943.97	94.07
March	10662.87	91.65
April	10741.63	92.33
May	5460.95	46.94
Average Area (Km^2)	8449.69	72.63

The annual average snow-covered area for 2018–19 was 8449.69 km² (72.63%), representing the highest average snow extent among all years analysed. This exceptionally high

average underscores the dominance of favourable snowfall and temperature conditions throughout the winter season.

TEMPORAL ANALYSIS OF SNOW COVER AREA, 2019–20

The snow cover conditions during 2019–20 was characterized by early onset, exceptional winter accumulation and prolonged persistence, making it one of the most snow-abundant years in the study period (Figure 3.14 & 3.15). In October, snow cover was already notable, with an area of 2889.05 km² (24.83%), indicating an earlier-than-normal commencement of seasonal snowfall compared to several previous years (Table 3.9).

A rapid and substantial increase in snow cover occurred in November, when the snow-covered area expanded sharply to 8136.86 km² (69.94%). This sudden rise reflects intense early winter precipitation and effective retention of snow across both higher and mid-elevation zones. The accumulation continued into December, reaching 10030.96 km² (86.22%), signifying near-basin-wide snow coverage (Table 3.9). Peak snow cover was recorded in January, with a maximum extent of 11168.11 km² (96.00%), indicating almost complete coverage of the basin. This exceptionally high value suggests persistent sub-freezing temperatures combined with repeated snowfall events, which significantly limited ablation processes. Although a marginal reduction was observed in February (10494.75 km²; 90.21%), snow cover remained extensively distributed, confirming sustained winter conditions (Table 3.9).

During March, snow cover decreased moderately to 9730.37 km² (83.64%), reflecting the onset of seasonal melting, particularly at lower elevations. However, the spatial extent remained considerably high, highlighting strong snow retention during the late winter phase. In April, snow cover declined further to 8377.84 km² (72.01%), indicating accelerated ablation driven by rising temperatures and increased solar radiation. By May, snow depletion became more pronounced, with snow cover reducing to 5924.74 km² (50.93%). Despite this decline, more than half of the basin remained snow-covered, demonstrating the exceptional persistence of snow during this year (Table 3.9). The annual average snow-covered area for 2019–20 was 8344.09 km² (71.72%), ranking this year as the second highest in terms of average snow extent, closely following 2018–19. The consistently high values across all winter and early spring months underscore the dominance of favourable climatic conditions during this period.

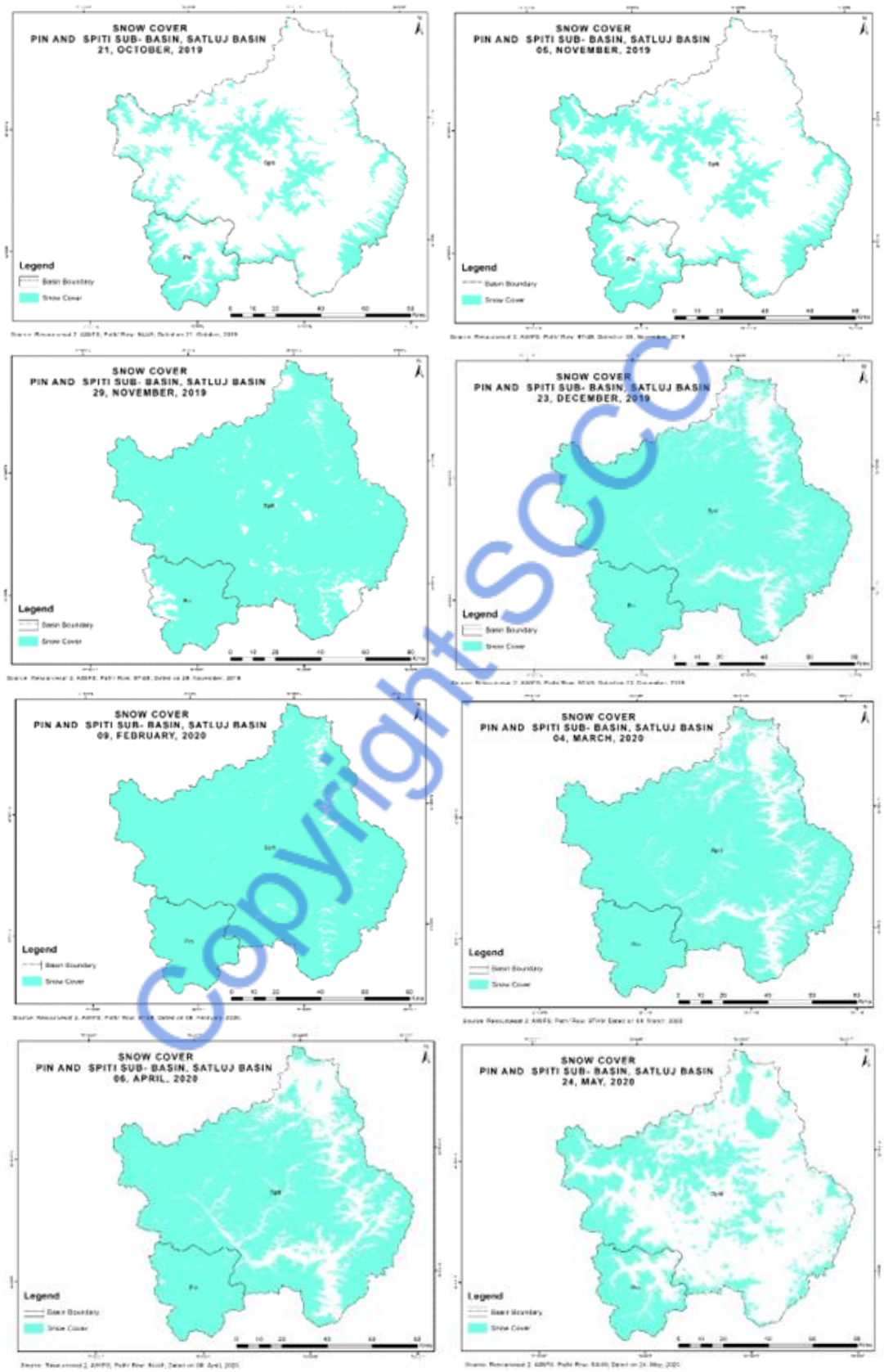

Figure 3.14 Distribution of snow cover in Spiti and Pin Sub-basin, 2019-2020

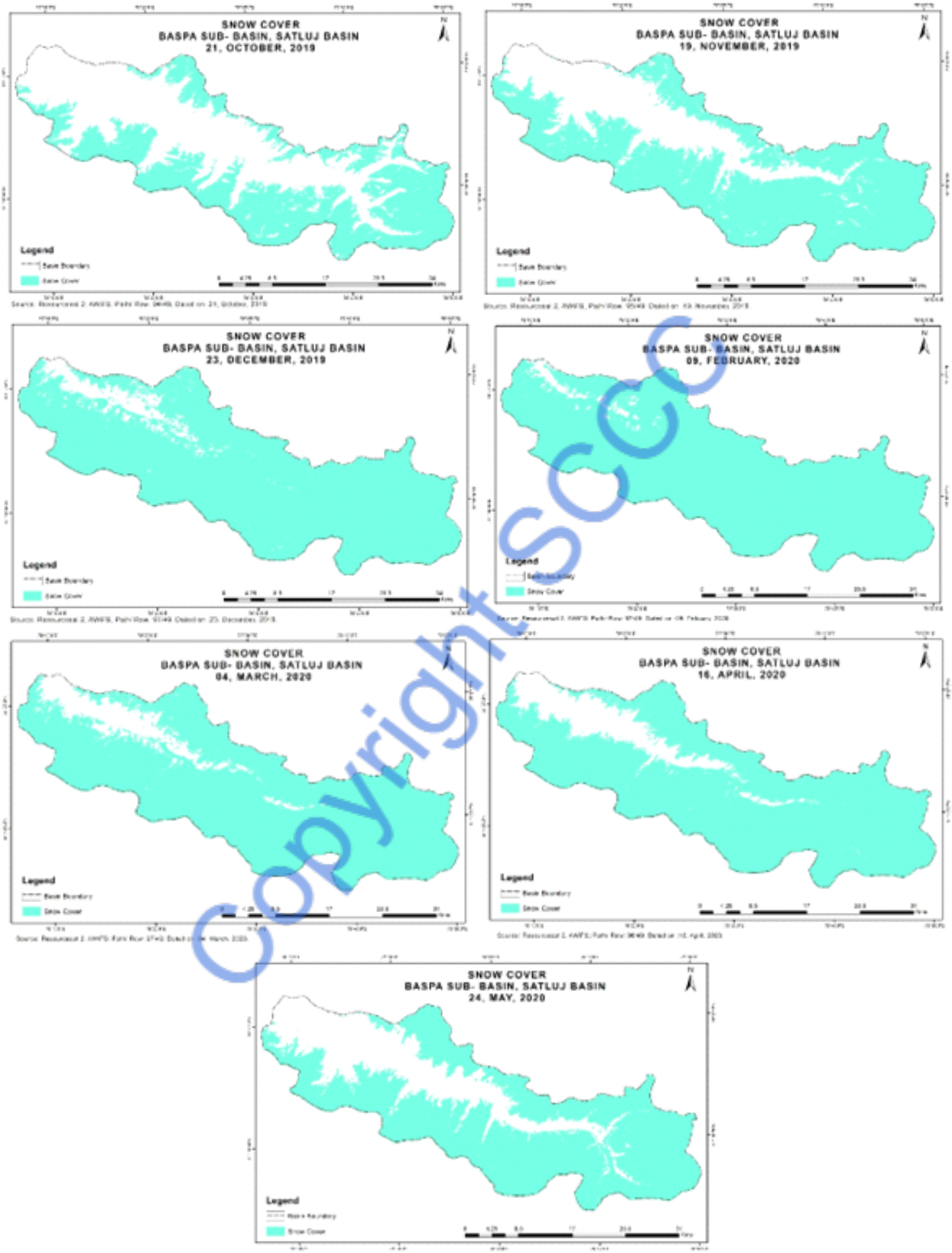

Figure 3.15 Distribution of snow cover in Baspa Sub-basin, 2019-2020

Table 3.9 Spatio-temporal distribution of Snow cover, 2019-2020

Month	Area of Snow cover (Km^2)	Area of Snow cover (%)
October	2889.05	24.83
November	8136.86	69.94
December	10030.96	86.22
January	11168.11	96.00
February	10494.75	90.21
March	9730.37	83.64
April	8377.84	72.01
May	5924.74	50.93
Average Area (Km^2)	8344.09	71.72

TEMPORAL ANALYSIS OF SNOW COVER AREA, 2020–21

The snow cover dynamics during 2020–21 exhibit a well-defined seasonal progression marked by delayed onset, strong mid-winter accumulation and gradual spring ablation (Figure 3.16 & 3.17). In October, snow cover was minimal, with an area of only 886.72 km² (7.62%), indicating limited early-season snowfall and relatively warmer pre-winter conditions. A substantial increase in snow cover was observed in November, when the snow-covered area expanded sharply to 6151.90 km² (52.88%), reflecting the onset of winter precipitation. This upward trend continued into December, with snow cover reaching 7425.85 km² (63.83%), suggesting widespread accumulation across higher elevations and progressive expansion to mid-altitude zones (Table 3.10).

Peak snow cover occurred during January, when the area increased further to 8996.18 km² (77.33%), representing the maximum spatial extent for the season. This peak indicates strong and sustained winter snowfall combined with favorable low-temperature conditions that limited melt processes. During February, snow cover showed a slight reduction to 7242.25 km² (62.25%), marking the initial phase of seasonal ablation, although coverage remained substantial. In March, snow cover remained relatively stable at 7408.96 km² (63.68%), indicating balanced conditions between accumulation at higher elevations and melt at lower altitudes. This stability suggests a gradual rather than abrupt transition from winter to spring. By April, snow cover declined further to 6379.64 km² (54.84%), reflecting enhanced melting under rising temperatures and increasing solar radiation. During May, snow depletion became more pronounced, with the snow-covered area reducing to 6109.62 km² (52.52%), indicating continued retreat of seasonal snow, particularly in

lower and mid-elevation zones (Table 3.10). Despite this decline, more than half of the basin remained snow-covered, highlighting the persistence of snow at higher elevations.

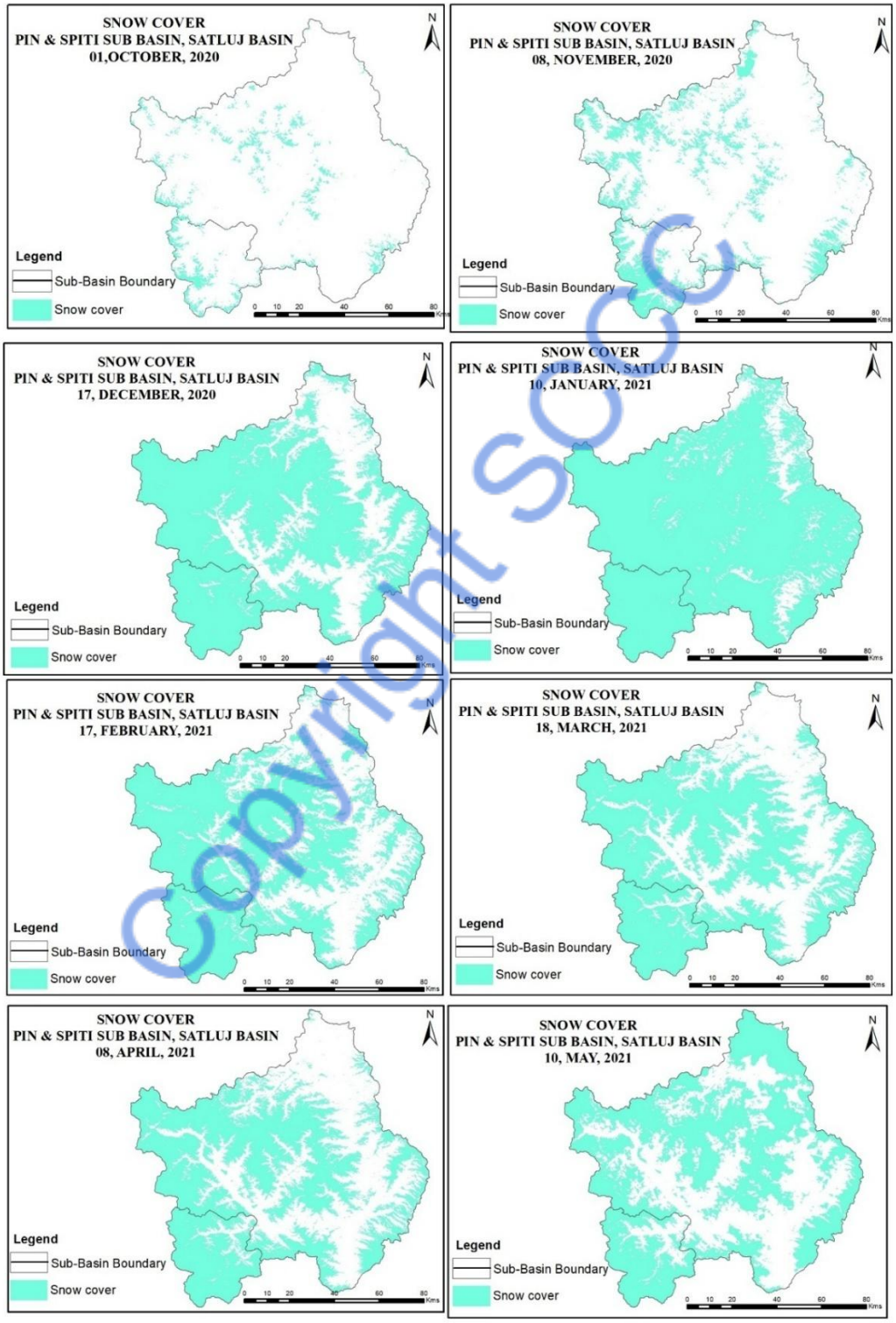

Figure 3.16 Distribution of snow cover in Spiti and Pin Sub-basin, 2020-2021

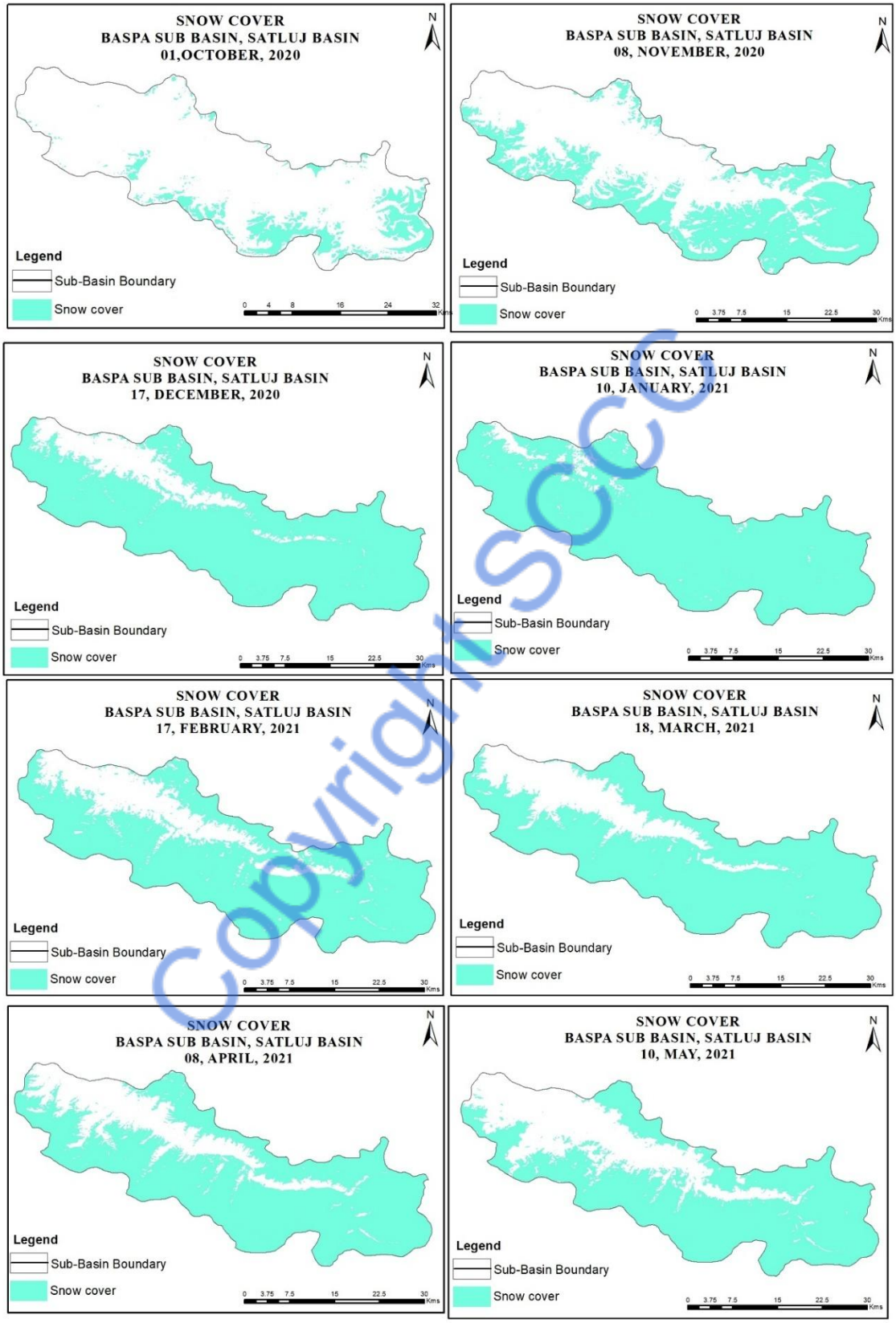

Figure 3.17 Distribution of snow cover in Baspa Sub-basin, 2020-2021

The annual average snow-covered area for 2020–21 was 6325.14 km² (54.37%), placing this year in the category of a moderate to moderately high snow year. Compared to preceding high-snow years such as 2018–19 and 2019–20, 2020–21 recorded slightly lower peak and average snow cover; however, it demonstrated relatively stable snow persistence during the core winter and early spring months.

Table 3.10 Spatio-temporal Distribution of Snow Cover, 2020-2021

Month	Area of Snow cover (Km^2)	Area of Snow cover (%)
October	886.72	7.62
November	6151.90	52.88
December	7425.85	63.83
January	8996.18	77.33
February	7242.25	62.25
March	7408.964	63.68
April	6379.64	54.84
May	6109.617	52.52
Average Area (Km^2)	6325.14	54.37

SPATIO-TEMPORAL ANALYSIS OF SNOW COVER (2010-11 TO 2020-2021)

The spatio-temporal variability in snow cover observed across the Satluj basin from 2010–11 to 2020–21 (Table 3.11 and Figure 3.18), has profound implications for hydropower generation, as snow cover acts as a critical intermediary between winter precipitation and seasonal runoff. The wide range in average snow-covered area, from approximately 4,092 km² (35.17%) to 8,450 km² (72.63%), highlights strong inter-annual climatic control and underscores the basin's sensitivity to variations in winter precipitation and temperature regimes.

The higher snow cover years, particularly 2012–13, 2018–19 and 2019–20, indicate enhanced winter snowfall and prolonged snow retention at higher elevations. Such conditions contribute positively to basin-scale water storage and ensure a sustained release of meltwater during the pre-monsoon and early summer months. For large reservoir-based hydropower projects, this translates into improved inflows, higher reservoir levels and greater operational flexibility. The extended melt period in high snow years helps maintain relatively stable discharge during the critical power demand season, thereby enhancing plant load factors and reducing dependence on erratic monsoon rainfall.

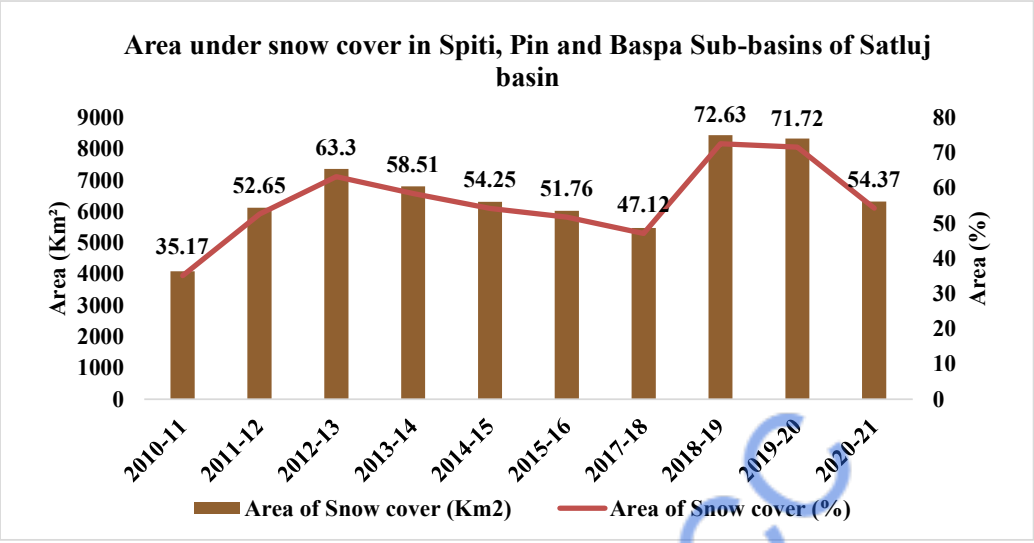

Figure 3.18 Spatio-temporal analysis of snow cover in Spiti, Pin and Baspa Sub-basins of Satluj basin

Table 3.11 Area Under snow cover in Spiti, Pin and Baspa Sub-basins of Satluj basin

Month	Area of Snow cover (Km^2)	Area of Snow cover (%)
2010-11	4091.88	35.17
2011-12	6125.494	52.65
2012-13	7365.215	63.30
2013-14	6807.727	58.51
2014-15	6311.989	54.25
2015-16	6022.671	51.76
2017-18	5482.139	47.12
2018-19	8449.689	72.63
2019-20	8344.085	71.72
2020-21	6325.139	54.37

During 2010–11, the basin experienced the lowest snow cover, with an average area of 4091.88 km² (35.17%), suggesting reduced winter snowfall or enhanced early-season melting. A sharp increase in snow cover is observed in 2011–12, where the area expanded to 6125.49 km² (52.65%), followed by a further rise in 2012–13, reaching 7365.22 km² (63.30%). This period reflects favourable accumulation conditions, likely associated with higher winter precipitation and lower temperatures. In 2013–14, snow cover slightly declined to 6807.73 km² (58.51%) and a continued decreasing trend is observed during 2014–15 and 2015–16, with snow cover percentages of 54.25% and 51.76%, respectively. This gradual reduction may indicate increased ablation or variability in winter snowfall. The declining trend persists into 2017–18, when snow cover further reduced to 5482.14 km² (47.12%), highlighting a phase of diminished snow persistence.

In contrast, low snow cover years, such as 2010–11 and 2017–18, reflect weaker winter accumulation and/or enhanced early-season ablation. These conditions limit snowmelt contribution during late spring and early summer, leading to reduced base flows during the lean season. Small run-of-river hydropower projects are particularly vulnerable under such conditions, as they lack storage capacity and depend directly on real-time flow availability. Reduced snowmelt in low-snow years can therefore result in decreased generation, frequent plant shutdowns and reduced economic viability of small hydropower schemes.

A pronounced increase in snow cover is evident during 2018–19, when the basin recorded the maximum snow-covered area of 8449.69 km², accounting for 72.63% of the basin. This exceptionally high snow extent continued into 2019–20, with 8344.09 km² (71.72%), indicating consecutive years of strong snow accumulation. Such anomalously high snow cover years are likely linked to enhanced winter precipitation and cooler temperature regimes. While this supports sustained hydropower generation over an extended period, it may also amplify sediment transport during the melt season. High snowmelt rates can mobilize large quantities of fine and coarse sediments from glacierized and periglacial zones, increasing turbine abrasion, reducing efficiency and raising operation and maintenance costs for both large and small hydropower plants.

In 2020–21, snow cover declined sharply to 6325.14 km² (54.37%), suggesting a sharp decline in snow cover observed indicates accelerated melting, likely driven by rising temperatures. Such rapid snow depletion can lead to short-term increases in runoff, potentially benefiting hydropower generation in the immediate term. However, this is often accompanied by heightened flow variability and increased flood risk, complicating reservoir operation, inflow forecasting and power scheduling. Sudden high-flow events may also impose stress on hydraulic structures, spillways and diversion works, increasing the risk of operational disruptions.

Overall, the absence of a consistent long-term increasing or decreasing trend in snow cover and the dominance of strong year-to-year variability, suggest that hydropower generation in the Satluj basin is increasingly exposed to climatic uncertainty. Changes in snow accumulation and melt timing not only affect the magnitude of runoff but also alter its seasonal distribution, with important consequences for firm power generation, sediment management and infrastructure safety. These findings highlight the necessity of incorporating continuous snow cover monitoring, improved snowmelt-runoff modeling and climate-adaptive reservoir operation strategies into

hydropower planning. Such measures are essential to enhance the resilience and long-term sustainability of hydropower development in this highly climate-sensitive Himalayan river basin.

CONCLUSION

The spatio-temporal analysis of snow cover in the Satluj basin from 2010–11 to 2020–21 demonstrates substantial inter-annual and seasonal variability, reflecting the basin's sensitivity to winter precipitation and temperature fluctuations. Years with higher snow accumulation, such as 2018–19 and 2019–20, enhance snowmelt contribution during the pre-monsoon and early summer months, supporting sustained inflows to reservoirs and improving hydropower generation potential. In contrast, years with lower snow cover, such as 2010–11 and 2017–18, reduce snowmelt contribution, particularly during lean seasons, negatively affecting base flows, firm power generation and the reliability of small run-of-river hydropower projects.

The observed variability in snow cover also influences sediment transport, flow timing and flood risk. Rapid snowmelt can temporarily boost runoff but increases sediment load and hydrological uncertainty, challenging reservoir operations, turbine efficiency and infrastructure safety. These patterns underscore that snow cover dynamics shaped by both climatic variability and long-term warming trends play a critical role in determining hydropower generation in glacier-fed Himalayan basins.

Therefore, ensuring sustainable and reliable hydropower development in the Satluj basin requires integrating continuous snow-cover monitoring, climate-informed hydrological modeling and adaptive water management strategies. Proactive planning that accounts for snow variability and melt-driven runoff is essential to safeguard energy security, maintain operational efficiency and enhance the resilience of hydropower infrastructure under changing climatic conditions.

4. MASS BALANCE DYNAMICS OF GLACIERS IN THE SATLUJ CATCHMENT

The Himalayan glaciers constitute the third-largest ice reserve in the world, following the Arctic and Antarctic regions and play a critical role in sustaining river systems that support large downstream populations. Rivers originating from these glaciers serve as a primary source of freshwater for domestic use, agriculture, hydropower generation and ecosystem maintenance. The magnitude and seasonal timing of glacier meltwater are strongly governed by regional precipitation patterns and air temperature variability (Barnett and others, 2005). Recent studies across the Himalayan region indicate that glacier melting is likely to intensify under future climate change scenarios, primarily due to rising temperatures and altered precipitation regimes (Immerzeel and others, 2012; Chaturvedi and others, 2014; Lutz and others, 2014; Shea and others, 2015).

Sustained glacier mass loss is expected to result in continued retreat of glacier area and volume until a new equilibrium with prevailing climatic conditions is attained. Such changes will significantly influence glacier-fed runoff, with projections suggesting an initial increase in meltwater contribution during the early decades of warming, followed by a progressive decline toward the end of the century as glacier reserves diminish (Huss and others, 2008; Immerzeel and others, 2012). In addition to climatic pressures, rapid population growth and increasing water demand in the Himalayan region underscore the necessity for efficient and informed water resource management. Consequently, understanding annual variations in glacier-stored water is essential for long-term planning and sustainable management. Basin-scale monitoring of glacier mass balance, integrated with local climatic observations, provides critical insights into trends and variability in glacier water storage.

Glacier mass balance is defined as the net difference between mass gains (accumulation) and mass losses (ablation) over a balance year (Paterson, 2000). Mass-balance information across multiple spatial and temporal scales is fundamental for assessing glacier–climate–hydrology interactions in mountainous regions. Methods for estimating glacier mass balance are broadly categorized into direct and indirect approaches. Direct, glaciological measurements rely on field-

based observations and are typically restricted to individual glaciers. In contrast, indirect methods—including geodetic, gravimetric and accumulation-area ratio (AAR) techniques—are widely employed to estimate mass balance at regional and basin scales in the Himalaya (Kulkarni and others, 2004; Berthier and others, 2007; Matsuo and Heki, 2010; Brahmbhatt and others, 2011; Gardelle and others, 2013; Vincent and others, 2013; Mir and others, 2014).

Among these approaches, the geodetic method is commonly used to quantify long-term, region-wide glacier mass balance by analyzing changes in glacier surface elevation derived from multi-temporal digital elevation models (Berthier and others, 2007; Gardelle and others, 2013; Vincent and others, 2013; Vijay and Braun, 2016). However, this method is limited in its ability to resolve annual mass-balance variations, owing to uncertainties in DEM accuracy and temporal data availability. Satellite-based gravimetric techniques can provide annual mass-change estimates over large regions, but their application is constrained by coarse spatial resolution (approximately 400 km). The AAR method offers a viable alternative for estimating mass balance at higher temporal resolution for individual glaciers, which can subsequently be upscaled to basin-level assessments. Nevertheless, the AAR approach is challenged by difficulties in accurately delineating the equilibrium line altitude (ELA), particularly due to cloud cover, intermittent snowfall events and data gaps in satellite imagery (Kulkarni, 1996; Rabatel and others, 2005; Tawde and others, 2016).

TEMPORAL ANALYSIS OF GLACIER MASS BALANCE IN THE SATLUJ BASIN

Glacier mass balance is a critical indicator of cryospheric response to climatic variability and long-term climate change. The present analysis evaluates the temporal evolution of glacier mass balance in the Satluj Basin using multi-temporal datasets for the years 2000, 2011 and 2020 (Figure 4.1). The glaciers were classified into positive mass balance, negative mass balance and non-comparable categories, allowing an assessment of both short-term variability and long-term trends in glacier health across the basin.

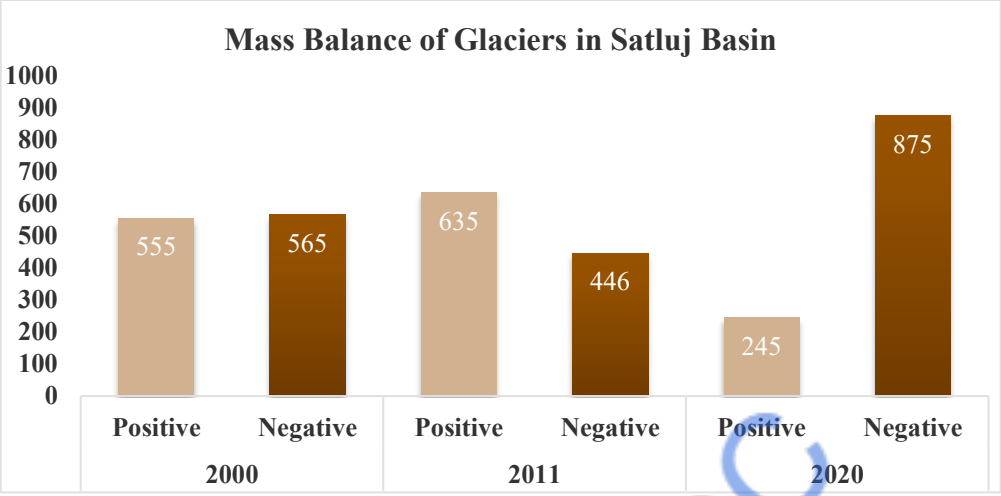

Figure 4.1 Mass Balance of Glaciers in Satluj Basin

Table 4.1 Mass Balance of Number of Glaciers in Satluj Basin

Year	Total Glaciers	Mass balance	No. of Glaciers
2000	1120	Positive Mass balance	555
		Negative Mass balance	565
2011	1081	Positive Mass balance	635
		Negative Mass balance	446
2020	1120	Positive Mass balance	245
		Negative Mass balance	875

MASS BALANCE STATUS IN 2000

In the year 2000, a total of 1,120 glaciers were analysed by using MODIS and Landsat TM Satellite data. Among these, 555 glaciers exhibited a positive mass balance, while 565 glaciers showed a negative mass balance. The near-equal distribution between positive and negative mass balance glaciers indicates a transitional phase in the cryospheric regime of the Satluj Basin.

This relatively balanced condition suggests that, during this period, accumulation and ablation processes were broadly comparable at the basin scale. Climatic conditions prevailing during the late 20th century likely supported sufficient winter snowfall at higher elevations to partially offset summer ablation. However, the slightly higher number of negatively balanced glaciers already points toward the incipient influence of warming trends, particularly at lower elevations and on south-facing slopes.

The spatial heterogeneity observed during this period implies that local topographic controls, such as elevation range, glacier hypsometry, aspect and debris cover, played a significant role in regulating mass balance behaviour. Larger valley glaciers and high-altitude cirque glaciers were more resilient, while smaller and low-lying glaciers were already vulnerable to negative mass balance conditions.

MASS BALANCE STATUS IN 2011

MODIS and Landsat Satellite data, 2010 and 2011 were interpreted, a noticeable shift in mass balance patterns is observed. Of the glaciers analysed, 635 glaciers recorded a positive mass balance, while 446 glaciers showed a negative mass balance and 39 glaciers could not be compared due to data limitations such as cloud and snow cover.

The increase in positively balanced glaciers during this period suggests a temporary or short-term improvement in accumulation conditions, potentially linked to inter-annual climatic variability, such as enhanced winter precipitation or episodic snowfall events at higher elevations. Such conditions may have temporarily lowered the equilibrium line altitude (ELA), enabling some glaciers to gain mass despite the broader warming trend.

However, this apparent improvement should be interpreted cautiously. The coexistence of a substantial number of negatively balanced glaciers indicates that climatic forcing was becoming increasingly heterogeneous, with accumulation gains limited to select elevation zones or glacier types. The presence of non-comparable glaciers also reflects ongoing morphological changes, fragmentation, or retreat, underscoring the dynamic nature of glacier systems during this period.

Overall, the 2011 scenario represents a short-lived stabilization phase, rather than a reversal of long-term mass loss trends. Such transient positive signals are consistent with observations from other western Himalayan basins, where inter-decadal variability can temporarily mask the underlying trajectory of glacier retreat.

MASS BALANCE STATUS IN 2020

The mass balance conditions in 2020 reveal a marked deterioration and fragmentation of glaciers across the Satluj Basin. Of the 1,120 glaciers analysed by using AWiFS (Advanced Wide Field Sensor) and LANDSAT Satellite data, only 245 glaciers exhibited a positive mass balance, whereas a dominant 875 glaciers recorded a negative mass balance.

This pronounced skew toward negative mass balance indicates a basin-wide dominance of ablation over accumulation, reflecting the cumulative impact of rising air temperatures, reduced snow persistence and upward migration of the ELA. The sharp decline in the number of positively balanced glaciers demonstrates that the buffering capacity observed in earlier periods has significantly weakened.

The high proportion of negatively balanced glaciers suggests that even high-altitude and previously stable glaciers are now experiencing sustained mass loss. Enhanced summer melt, reduced duration of snow cover and increased exposure of bare ice have likely amplified energy absorption, further accelerating glacier thinning and retreat.

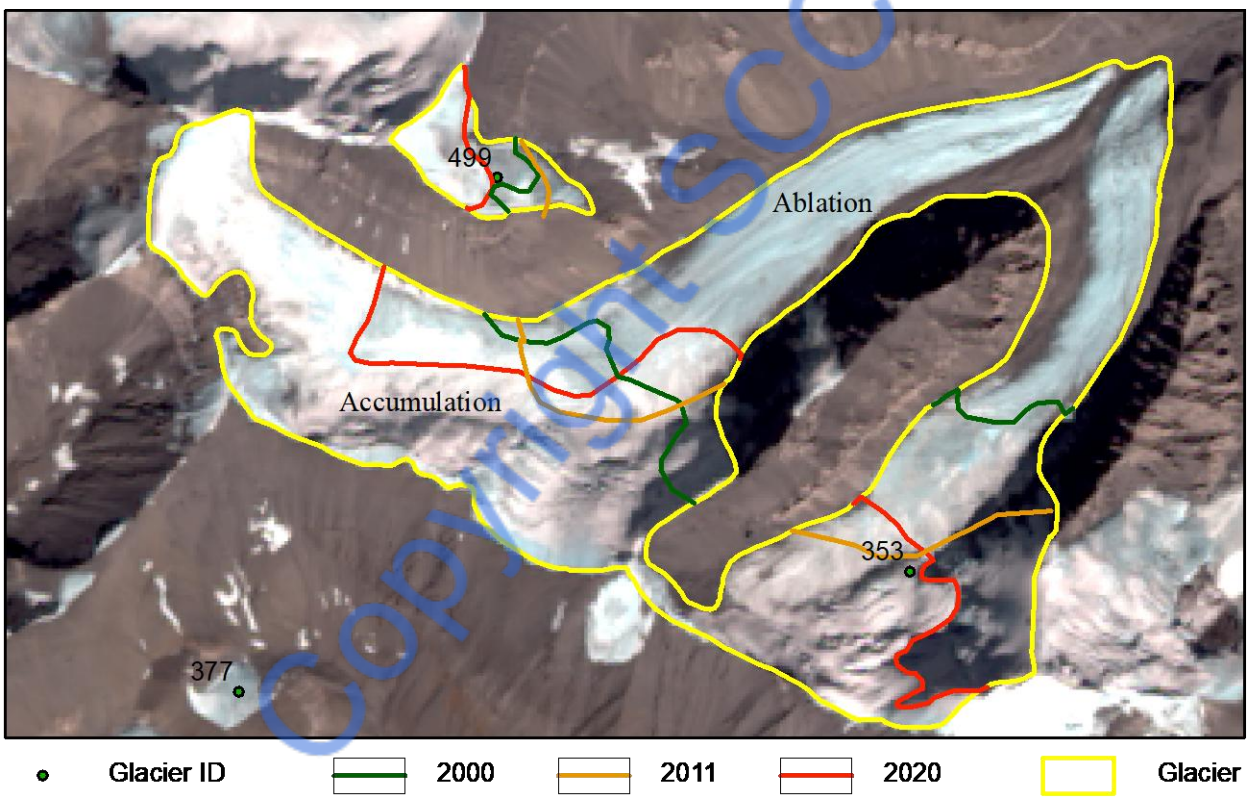

Figure 4.2 Shifting of ELA Line in Spiti Sub-basin, Satluj Basin

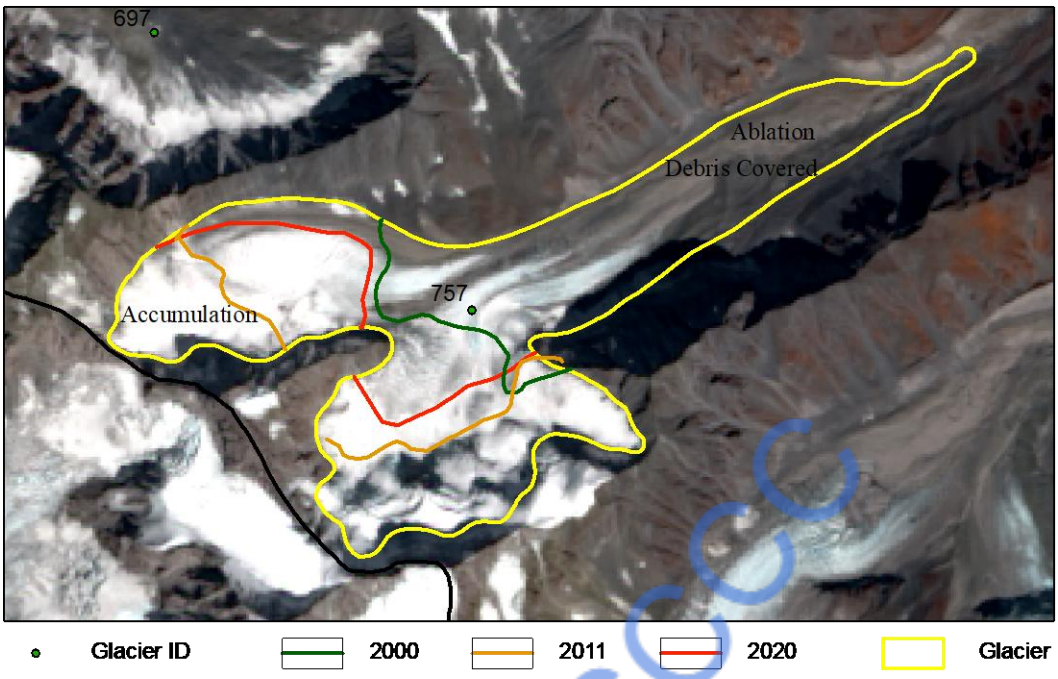

Figure 4.3 Shifting of ELA Line in Nardu Glacier, Baspa Sub-basin, Satluj Basin

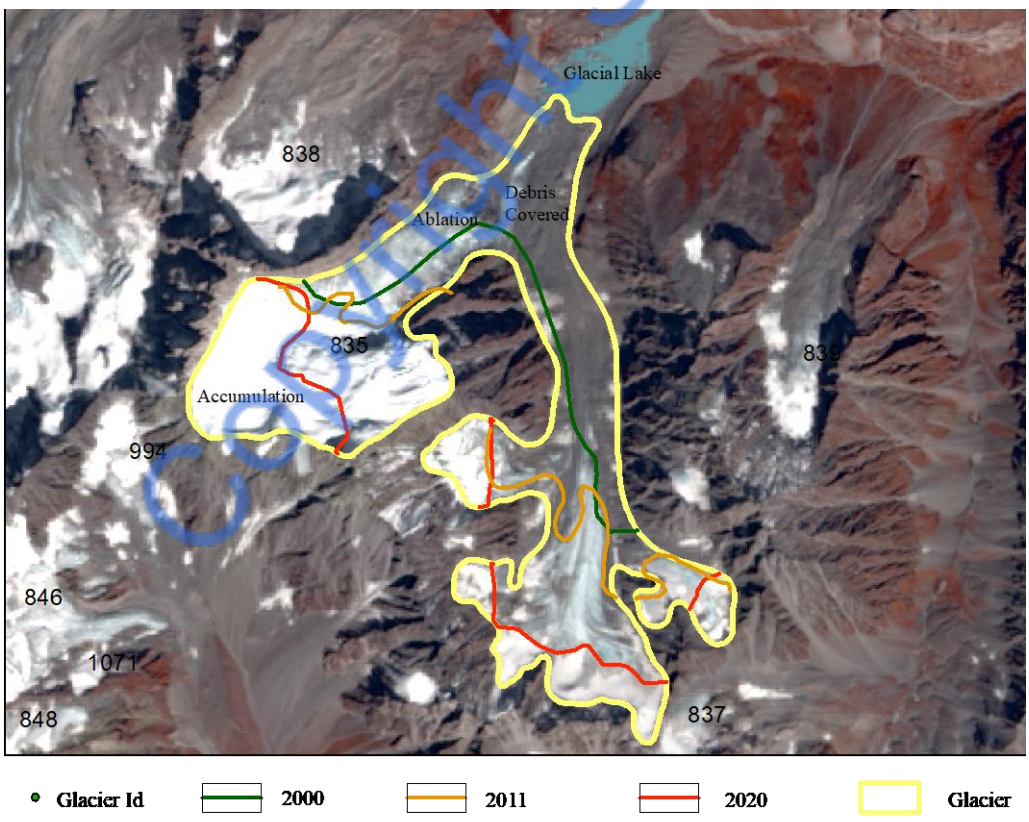

Figure 4.4 Shifting of ELA Line in Lower Satluj Sub-basin, Satluj Basin

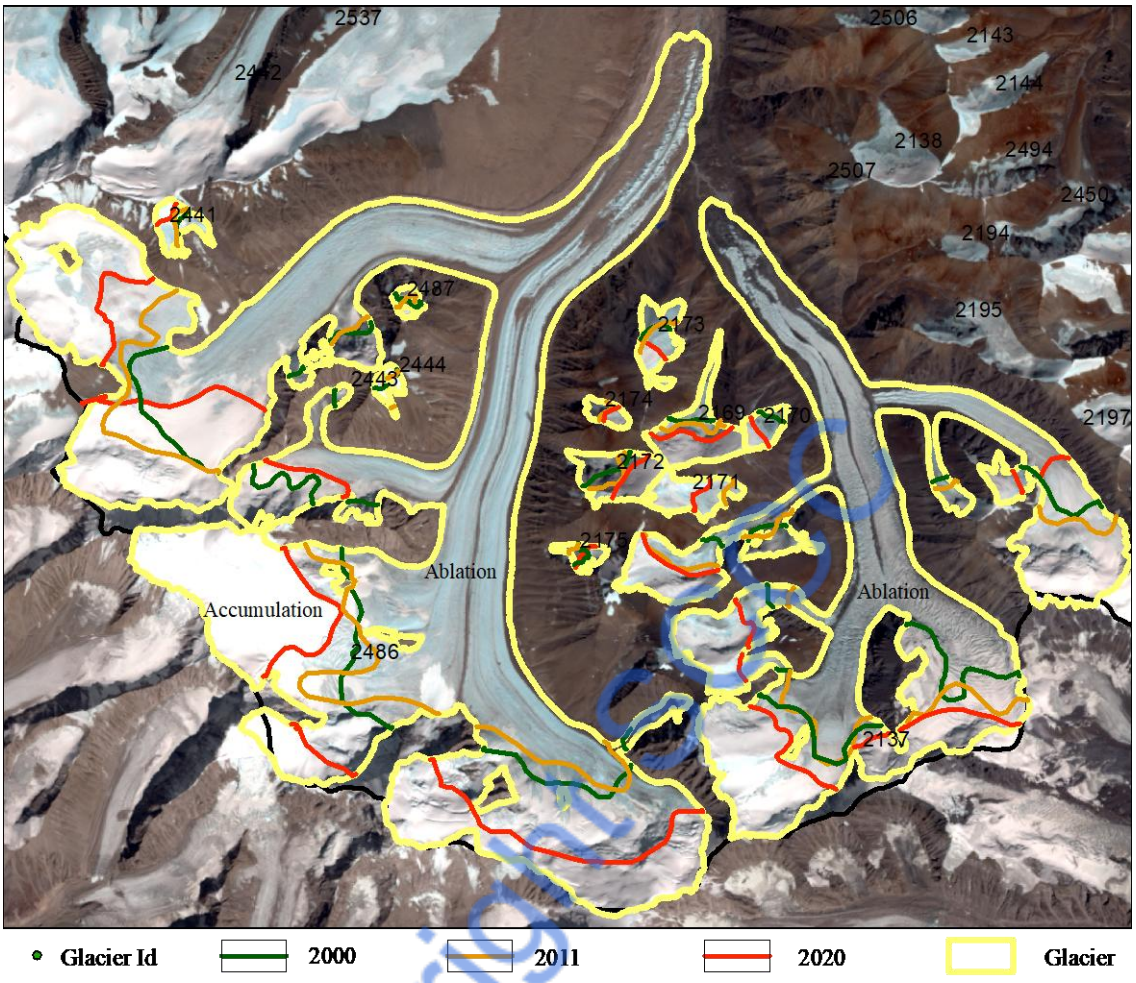

Figure 4.5 Shifting of ELA Line Upper Satluj Sub-basin, Satluj Basin

COMPARATIVE SPATIO-TEMPORAL TRENDS (2000–2020)

A comparative analysis based on Satellite data for the three decadal periods clearly indicates a progressive transition from near-equilibrium conditions. It highlights the dominance of negative mass balance in Satluj basin.

- In 2000, mass balance conditions were nearly balanced, highlighting early stages of climatic stress as it was the base year.
- By 2011, a temporary increase in positive mass balance glaciers suggested short-term climatic variability rather than long-term stabilization.
- By 2020, the mass balance had shifted decisively toward persistent and extensive mass loss.

This temporal interpretation highlights that ELA Line is shifting backward of glaciers due to climate change, where short-term accumulation gains cannot compensate for long-term warming trends. The increasing proportion of negatively balanced glaciers reflects a decline in glacier mass and storage capacity across the basin.

CLIMATIC AND TOPOGRAPHIC CONTROLS ON MASS BALANCE

On the basis of observation of mass balance trends are closely linked to regional climatic variations in the western Himalaya, affecting mean and minimum temperature, changes in precipitation phase (snow to rain) and reduced snow accumulation at lower and mid-elevations. The upward shift of the ELA has reduced accumulation and increased ablation area, especially for small and medium-sized glaciers. Glacial Lakes/ Waterbodies formation due to melting of Glaciers has also been increased in Satluj Basin.

Topographic factors continue to modulate glacier response at the local scale. Glaciers situated at higher elevations, with favourable aspect and shading, exhibit relatively better mass balance conditions. However, the overwhelming dominance of negative mass balance in 2020 indicates that climatic forcing now exceeds the buffering capacity of local controls.

HYDROLOGICAL AND ENVIRONMENTAL IMPLICATIONS

The dominance of negative mass balance glaciers has significant implications for the hydrology of the Satluj River system. The sustained glacier mass loss may initially enhance meltwater contribution, leading to increased summer discharge and flow variability. However, continued depletion of glacier ice reserves will eventually result in reduced long-term water availability in future, particularly during dry seasons.

Additionally, accelerated glacier retreat increases the risk of glacial lake formation in Moraine complexes with associated hazards, while also affecting sediment flux and downstream ecosystem stability. These hydrological and environmental changes gave rise to new obstacles for water resource management, hydropower generation and climate adaptation strategies in the Satluj basin.

MASS BALANCE IMPACT ON HYDROPOWER

The observed negative mass balance of glaciers in the Satluj Basin has direct and long-term implications for hydropower generation. In the short to medium term, enhanced glacier melt may

increase summer inflows to reservoirs, leading to higher seasonal power generation and greater flow variability. Such variability can complicate reservoir operation, sediment management and turbine efficiency, particularly during extreme melt or rainfall events.

Over the long term, continued depletion of glacier ice reserves is expected to reduce the dependable base flow of the Satluj River, especially during lean and dry seasons when glacier melt traditionally sustains river discharge. This decline in sustained flows may adversely affect firm power generation, reduce plant load factors and increase uncertainty in hydropower planning and design. Furthermore, increased sediment load from accelerated glacier retreat and moraine destabilization can enhance siltation of reservoirs and abrasion of turbine components, leading to higher maintenance costs and reduced project lifespan.

The growing risk of glacial lake outburst floods (GLOFs) and extreme hydrological events also poses a threat to hydropower infrastructure, including dams, diversion structures and transmission systems. Collectively, these impacts highlight the need for climate-resilient hydropower management strategies, incorporating adaptive reservoir operations, improved sediment handling, continuous cryospheric monitoring and integration of climate risk assessments in future hydropower development within the Satluj Basin.

CONCLUSION

The mass balance assessment of glaciers in the Satluj Basin for the years 2000, 2011 and 2020 indicates a clear and ongoing decline in glacier health, with a pronounced shift toward negative mass balance conditions. While short-term climatic variability may temporarily influence individual glacier behaviour, the long-term trend unequivocally points to sustained and basin-wide glacier mass loss.

The analysis of 1,120 glaciers reveals that approximately 78% are experiencing mass loss, whereas only 22% exhibit positive mass balance, underscoring the dominant influence of regional climatic warming on the cryosphere. This widespread negative mass balance is primarily driven by rising air temperatures, upward migration of the equilibrium line altitude (ELA) and a reduction in solid precipitation during winter months. In contrast, glaciers showing positive mass balance are generally confined to higher elevations and benefit from favourable hypsometry, aspect, debris cover and enhanced shading, which locally mitigate ablation processes.

This systematic loss of glacier mass has critical implications for long-term cryospheric sustainability, seasonal meltwater contribution and hydrological regimes of the Satluj River. Initially, glacier retreat may enhance meltwater discharge, but continued mass loss is expected to reduce base flow over time. These findings emphasize the need for long-term, high-resolution glacier monitoring and integrated climate–hydrology assessments to support adaptive water management strategies and ensure future water resource stability in the basin.

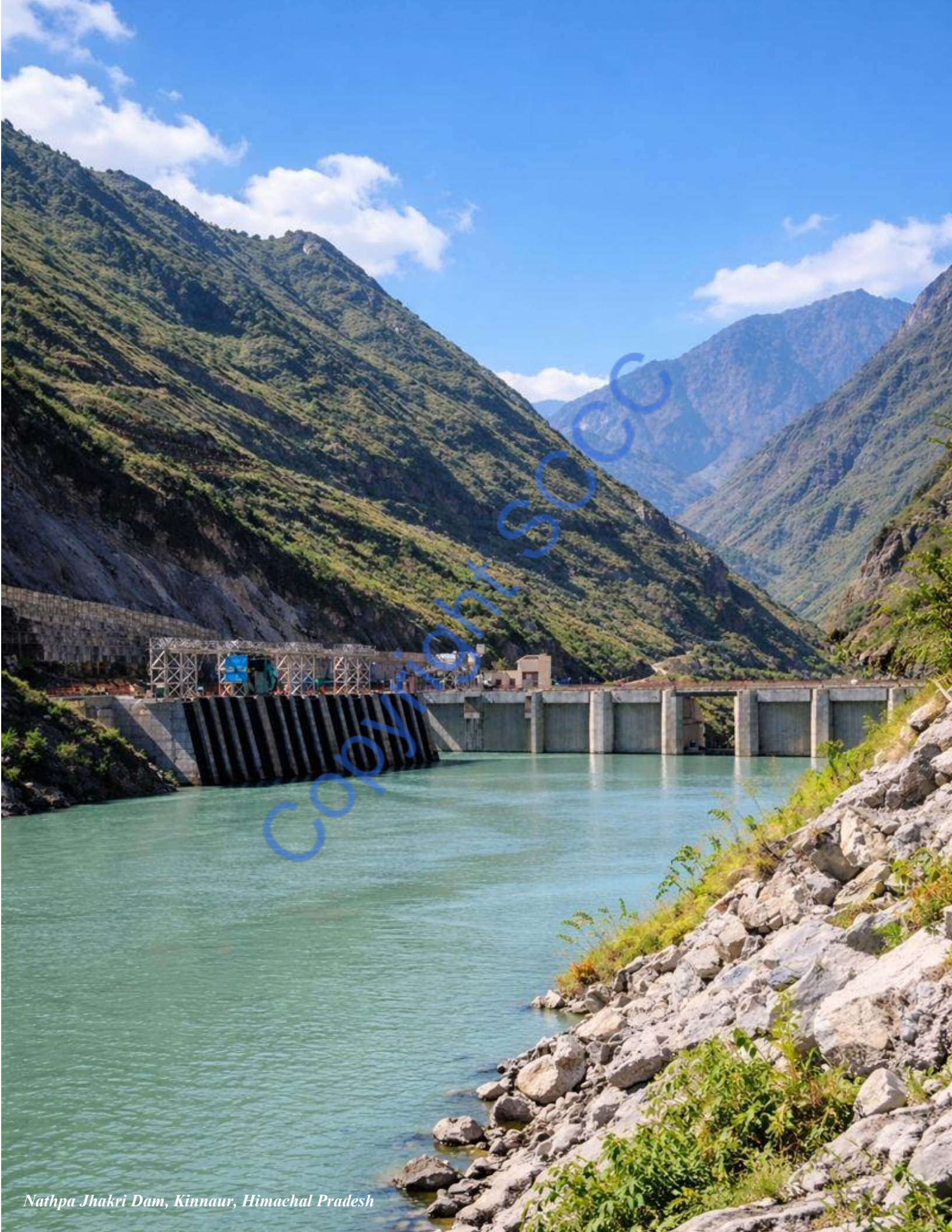

Nathpa Jhakri Dam, Kinnaur, Himachal Pradesh

5. GLACIER MELT RUNOFF AND IMPACT ON HYDROPOWER

Glacier melt runoff plays a critical role in sustaining river discharge in the high-altitude Himalayan basins, particularly during the dry and pre-monsoon seasons when rainfall contribution is limited. In the Satluj Basin, glacier and snow melt constitute an important component of the hydrological regime, directly influencing the availability, timing and variability of river flows that support major hydropower projects. Changes in glacier mass balance, therefore, have a direct bearing on the magnitude and reliability of meltwater contribution to hydropower generation (Bolch et al., 2012; IPCC, 2021).

Ongoing climatic warming has accelerated glacier retreat and induced widespread negative mass balance conditions across the western Himalaya, resulting in altered melt runoff regimes. In the short term, enhanced glacier melt may lead to increased summer discharge and higher flow variability, potentially benefiting seasonal hydropower generation. However, sustained loss of glacier ice reserves is expected to reduce long-term base flows, particularly during lean periods, thereby affecting firm power generation and operational reliability of hydropower plants (Immerzeel et al., 2010; NDMA, 2019). Additionally, increased sediment load due to intensified glacier erosion and the rising risk of glacier-related hazards such as glacial lake outburst floods (GLOFs) pose further challenges to the safety and sustainability of hydropower infrastructure in the Satluj Basin.

In hydrology and water resources science, discharge (Q) represents the volume of water flowing through a river or stream per unit time, usually expressed in cubic meters per second (m^3/s). Discharge integrates watershed responses to climatic, geological and land-use factors, serving as a critical indicator of water availability, ecosystem health and flood potential.

Temperature**,** particularly air temperature, is a fundamental climatic driver influencing hydrological processes. It governs snow and ice melt rates, evaporation, soil moisture and runoff timing. In glacierized or snow-dominated basins, warmer conditions accelerate meltwater

production, increasing streamflow. Conversely, in other regions, increased temperatures may enhance evaporation, reducing discharge.

Due to the intertwined control of climate on both temperature and discharge, examining their correlations helps understand watershed responses to climatic variability. Positive correlations often indicate meltwater-driven flows during snowmelt seasons, while negative correlations may arise where evaporation dominates runoff changes. Such analyses aid in characterizing watershed dynamics, predicting flow timing and volume, assessing climate change impacts and improving hydrological modeling for resource planning and management.

DESCRIPTIVE ANALYSIS OF TEMPERATURE DATA (2010–2020)

The dataset presents annual maximum and minimum temperature values for multiple stations over the period 2010–2020. Overall, the data indicate interannual variability with a general warming tendency in maximum temperatures until the mid-2010s, followed by a noticeable cooling in 2019–2020.

Across most stations, maximum temperatures between 2010 and 2015 remain relatively stable, generally ranging between 16°C and 18°C at the first station and between 10°C and 15°C at higher-elevation stations. A pronounced increase in maximum temperature is observed in 2016, where several stations record peak values (up to ~19.8°C), suggesting an anomalously warm year. This warming is also reflected in higher minimum temperatures during the same year, indicating reduced nocturnal cooling.

From 2017 to 2018, maximum temperatures remain elevated but show increased variability across stations. Minimum temperatures during these years fluctuate considerably, including sub-zero values at higher-altitude locations, highlighting strong altitudinal and topographic controls on thermal conditions.

A sharp decline in maximum temperature is evident in 2019 and 2020, particularly in 2020, where maximum values drop below 10°C at several stations and as low as ~0.5°C at one location. Minimum temperatures during this period also decrease, with several stations recording near-freezing or negative values, indicating colder conditions and possibly enhanced winter influence or anomalous climatic conditions.

Minimum temperature trends show greater variability than maximum temperatures, with frequent negative values throughout the study period, especially at high-elevation stations. This suggests strong sensitivity of nighttime temperatures to local factors such as elevation, snow cover and cloud conditions. Overall, the analysis reveals:

- Mid-decade warming (2015–2018) with peak temperatures in 2016
- High interannual variability, particularly in minimum temperatures
- A marked cooling phase during 2019–2020
- Clear indication of elevation-dependent temperature behaviour, with colder minima at certain stations

These temperature fluctuations are climatically significant, as variations in both maximum and minimum temperatures directly influence snow accumulation, melt processes, glacier mass balance and hydrological response in mountainous basins

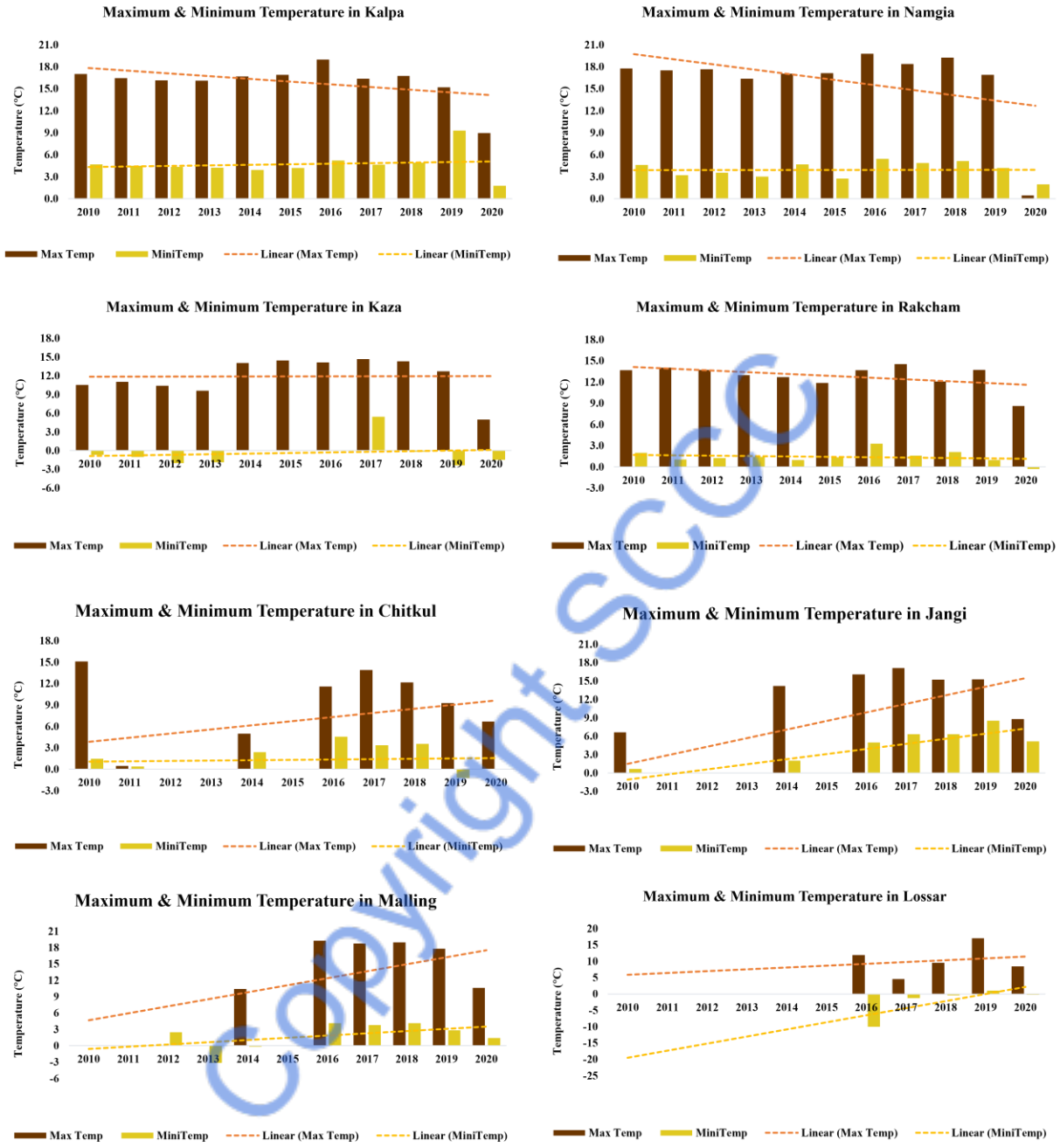

Figure 5.1 Minimum and Maximum temperature in 8 Stations in Satluj Basin, Himachal Pradesh

ANALYSIS OF AVERAGE DISCHARGE (2010–2020)

The average monthly discharge data from 2010 to 2020 (Table 5.1) exhibit a strong seasonal pattern, reflecting the combined influence of snowmelt, glacier melt and monsoonal precipitation in the basin.

Low-flow conditions prevail during the winter months (December–February), with average discharge generally ranging between 55 and 90 m^3/s. These months are characterized by low temperatures, minimal rainfall and reduced meltwater contribution, resulting in baseflow-dominated river discharge.

A gradual increase in discharge begins during March and April, corresponding to the onset of snowmelt. Mean discharge values during April typically range from 100 to 225 m^3/s, indicating the transition from less flow in winter to melt-dominated conditions.

Peak discharge occurs during the summer and monsoon months (June–August). June shows a sharp rise in discharge (approximately 426–1163 m^3/s), driven primarily by intensified snow and glacier melt. The highest discharge values are consistently recorded in July and August, with extreme peaks such as 1444 m^3/s in August 2010 and 1241 m^3/s in July 2015, reflecting strong monsoonal rainfall combined with enhanced meltwater input.

From September onwards, discharge begins to decline as monsoon rainfall weakens and meltwater contribution decreases. September discharge generally varies between 267 and 548 m^3/s, followed by a further reduction during October and November, marking the return to post-monsoon and early winter conditions.

Interannual variability is evident across the dataset, particularly during peak flow months, indicating sensitivity of river discharge to year-to-year variations in precipitation, temperature and melt intensity. Years such as 2010, 2013 and 2015 display notably higher summer discharge, suggesting episodes of intensified monsoon activity and/or enhanced glacier melt. Overall, the discharge regime is characteristic of a snow and glacier-fed Himalayan River system, with pronounced seasonality and strong dependence on climatic drivers.

The integrated analysis of temperature variability (2010–2020) and average river discharge (2007–2020) provides clear evidence of the strong climatic control on the hydrological behaviour of the basin. The temperature record reveals pronounced interannual variability, with a general warming tendency in maximum temperatures during the mid-2010s, peaking in 2016, followed by a distinct cooling phase during 2019–2020. Minimum temperatures exhibit greater fluctuations,

particularly at higher-elevation stations, underscoring the influence of elevation, snow cover and local topographic factors on nighttime thermal conditions.

Table 5.1 Analysis of Average Discharge (2010–2020) in m^3/sec

Months	2010	2011	2012	2013	2014	2015	2016	2017	2018	2019	2020
Jan	55	84	71	65	75	66	79	70	72	77	81
Feb	69	79	67	67	71	66	77	72	68	74	79
Mar	101	95	85	84	78	83	83	77	72	82	89
Apr	158	140	138	161	111	154	119	227	103	197	123
May	331	477	235	448	258	441	357	450	176	274	259
June	585	753	502	1163	692	620	627	572	426	516	694
July	1093	966	743	1131	1032	1241	775	1090	671	1080	845
Aug	1444	809	804	802	691	949	784	756	827	992	809
Sept	548	449	424	330	283	317	334	294	355	460	396
Oct	225	178	142	173	150	161	167	161	167	170	166
Nov	144	116	98	112	97	117	99	108	117	116	107
Dec	103	88	81	86	77	91	80	86	88	90	85

These temperature variations are closely reflected in the discharge regime of the river. The discharge data show a well-defined seasonal pattern typical of snow- and glacier-fed Himalayan river systems, with low winter flows dominated by baseflow, a gradual rise during spring due to snowmelt and peak flows during the summer and monsoon months driven by combined snowmelt, glacier melt and monsoonal precipitation. High interannual variability in peak discharge, especially during June to August, highlights the sensitivity of the basin to fluctuations in temperature and precipitation.

Years characterized by elevated summer discharge coincide with warmer conditions and/or intensified monsoon activity, indicating enhanced meltwater contribution and increased runoff generation. Conversely, cooler conditions and reduced melt intensity are associated with lower discharge during certain years, emphasizing the coupled response of cryospheric and hydrological processes to climatic forcing.

Overall, the findings demonstrate that temperature variability plays a critical role in regulating snow and glacier melt, which in turn governs seasonal and interannual discharge dynamics. Understanding these linkages is essential for assessing future water availability,

managing hydropower resources and evaluating climate change impacts on Himalayan river basins, particularly under scenarios of continued warming and increased hydro-climatic extremes.

RELATIONSHIP OF TEMPERATURE AND DISCHARGE (2010–2020)

This analysis examines the relationship between monthly mean temperature (°C) and average river discharge (m^3/s) over an eleven-year period (2010–2020). The objective is to compare seasonal and interannual variations in temperature and discharge and to assess how changes in temperature influence discharge patterns.

Across all years, temperature exhibits a strong seasonal cycle. The lowest temperatures occur during winter months (January–February and December), often falling below 0°C, while the highest temperatures are observed during summer (June–August), frequently exceeding 25°C in later years. Spring and autumn represent transitional periods with moderate temperatures.

A comparison across years indicates a gradual increase in summer and early autumn temperatures after 2014, suggesting a warming trend, particularly during peak summer months. Discharge also follows a pronounced seasonal pattern. Minimum flows occur in winter, corresponding to low temperatures and limited runoff. Discharge increases rapidly during spring (March–May), reaching peak values in summer (June–August). This pattern indicates the dominant influence of snowmelt and seasonal precipitation. Peak discharge values consistently occur in July or August, with extreme flows exceeding 1,000 m^3/s in several years (notably 2013, 2015, 2017 and 2019).

A positive relationship between temperature and discharge is evident, particularly from spring to summer. Rising temperatures accelerate snowmelt and enhance runoff, resulting in increased discharge. However, this relationship is not strictly linear. In some years, high temperatures do not correspond to proportionally high discharge, highlighting the additional role of precipitation variability and catchment conditions. For example, despite high summer temperatures in 2018, discharge values were lower than those observed in 2015 and 2017, indicating that temperature alone does not fully control flow magnitude.

During the period 2010–2013, the hydro-climatic regime was marked by relatively colder winter temperatures and moderate summer warming. Discharge during these years followed a

predictable seasonal pattern, with peak flows largely controlled by spring snowmelt and early summer runoff, resulting in comparatively stable and moderate discharge extremes. In contrast, the 2014–2017 period experienced noticeably higher summer temperatures alongside increased interannual variability in river discharge. Several of the highest peak flows in the dataset occurred during this interval, indicating enhanced runoff generation likely driven by intensified snowmelt and variable precipitation. The years 2018–2019 recorded the warmest summer temperatures of the entire study period, with discharge remaining generally elevated but exhibiting considerable variability, suggesting a stronger influence of short-term climatic events in addition to temperature. In 2020, however, temperature records for the latter months appear incomplete or anomalous, limiting the reliability of direct comparisons; therefore, hydrological interpretations for this year should be treated with caution. Overall, later years demonstrate greater hydrological variability, with more frequent extreme discharge events.

The long-term trends of dataset suggest a warming trend, especially during summer and autumn months. An increase in discharge variability, rather than a consistent upward or downward trend in mean discharge. A tendency toward more extreme peak flows in recent years, potentially linked to climatic variability. The observed increase in temperature and discharge variability has important implications for water resource management, flood risk assessment and ecosystem stability. Higher summer temperatures combined with episodic high flows may increase the frequency of flood events and alter seasonal water availability.

The comparative analysis reveals a strong seasonal coupling between temperature and discharge, with higher temperatures generally associated with increased river flow. However, inter-annual variations demonstrate that discharge is influenced by multiple factors beyond temperature alone. The warming trend and increased hydrological extremes observed after 2014 suggest a system becoming more sensitive to climate variability, emphasizing the need for adaptive water management strategies.

Table 5.2 Average Mean Monthly Temperature and Average discharge (2010-2020)

	2010		2011		2012		2013		2014		2015		2016		2017		2018		2019		2020	
Month	**Temp°C**	Avg Q (m^3/sec.)	**Temp°C**	Avg Q (m^3/sec.)	**Temp°C**	Avg Q (m^3/sec.)	**Temp°C**	Avg Q (m^3/sec.)	**Temp°C**	Avg Q (m^3/sec.)	**Temp°C**	Avg Q (m^3/sec.)	**Temp°C**	Avg Q (m^3/sec.)	**Temp°C**	Avg Q (m^3/sec.)	**Temp°C**	Avg Q (m^3/sec.)	**Temp°C**	Avg Q (m^3/sec.)	**Temp°C**	Avg Q (m^3/sec.)
Jan	1.3	55	-2.2	84	-2.0	71	-4.0	65	2.5	75	0.2	66	3.3	79	1.9	70	4.7	72	-0.9	77	-0.6	81
Feb	3.3	69	-1.1	79	-1.0	67	-4.1	67	3.0	71	0.6	66	4.8	77	2.7	72	4.5	68	-2.4	74	3.3	79
Mar	14.5	101	4.7	95	5.8	85	2.9	84	7.9	78	2.9	83	7.8	83	5.8	77	8.5	72	4.1	82	7.9	89
Apr	15.2	158	9.7	140	11.6	138	9.5	161	12.9	111	9.3	154	13.4	119	16.5	227	14.1	103	17.8	197	12.2	123
May	17.2	331	16.6	477	15.2	235	15.0	448	22.8	258	13.4	441	22.1	357	25.3	450	19.5	176	19.5	274	19.4	259
Jun	18.5	585	17.2	753	17.6	502	17.7	1163	28.6	692	13.4	620	26.8	627	27.5	572	28.0	426	25.6	516	24.2	694
Jul	22.5	1093	19.9	966	20.9	743	20.5	1131	19.7	1032	16.4	1241	27.5	775	27.0	1090	28.6	671	30.7	1080	28.0	845
Aug	23.5	1444	19.0	809	19.1	804	19.3	802	16.3	691	16.6	949	26.7	784	26.5	756	29.5	827	30.3	992	0.0	809
Sept	17.7	548	15.4	449	14.4	424	13.4	330	11.4	283	12.2	317	24.1	334	21.5	294	23.2	355	28.5	460	0.0	396
Oct	15.4	225	12.6	178	10.7	142	12.5	173	10.9	150	10.5	161	19.1	167	19.3	161	15.3	167	18.8	170	0.0	166
Nov	10.9	144	9.0	116	6.7	98	7.4	112	7.7	97	8.4	117	14.2	99	12.6	108	8.5	117	10.7	116	0.0	107
Dec	3.8	103	3.8	88	1.8	81	4.6	86	3.4	77	4.5	91	10.1	80	6.7	86	3.2	88	2.9	90	0.0	85

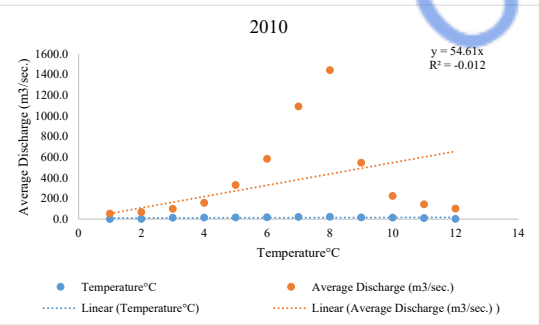

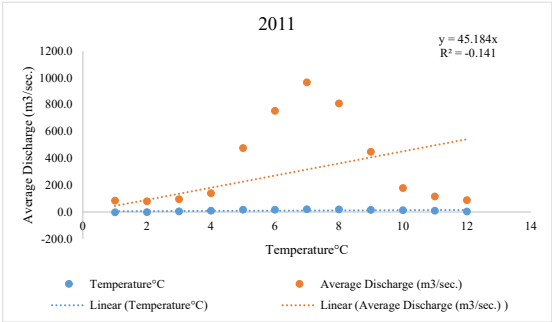

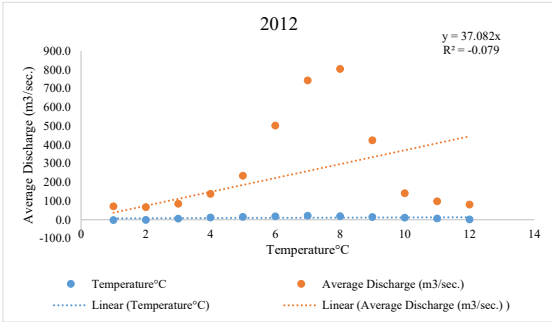

Figure 5.2 Scatter Plot of Temperature and Discharge (2010- 2020)

INTERPRETATION OF TEMPERATURE–DISCHARGE RELATIONSHIP (2010–2020)

The scatter plots for the period 2010–2020 illustrate the relationship between monthly temperature and average river discharge for individual years. Across all years, the regression lines generally show a positive slope, indicating that discharge tends to increase with rising temperature. This reflects the fundamental hydrological control of temperature on snowmelt and seasonal runoff generation. However, the strength of this relationship is consistently weak, as evidenced by the low and often negative R^2 values, which indicate that temperature alone explains only a small proportion of the variability in discharge.

During the early years (2010–2013), moderate positive slopes suggest that increasing temperatures contributed to higher discharge, particularly during spring and summer months. Nevertheless, the scattered distribution of data points and low R^2 values highlight significant variability, implying the influence of additional factors such as precipitation intensity, snowpack conditions and basin storage. In the mid-period (2014–2017), despite higher summer temperatures and some of the highest recorded discharge peaks, the temperature–discharge relationship remains weak. This suggests that extreme discharge events during these years were likely driven by combined effects of temperature-induced melt and enhanced precipitation rather than temperature alone.

In the later years (2018–2019), the warmest temperatures are observed and discharge remains relatively high, yet the dispersion of points increases. This further reinforces the non-linear and complex nature of the relationship. For 2020, although a positive trend is still indicated, anomalous or incomplete temperature data reduce the reliability of the regression and interpretations should therefore be treated with caution.

Overall, the figures demonstrate that while temperature is an important controlling factor for seasonal discharge**,** particularly through snowmelt processes, it does not independently govern river flow magnitude. The consistently low coefficients of determination emphasize the role of precipitation variability, catchment characteristics and climatic extremes, underscoring the multifactorial nature of river discharge dynamics.

Table 5.3 Year-wise R^2 Values and Dominant Runoff Processes (2010–2020)

year	R2	Description
2010	.600	Glacier and snow melt dominated
2011	.723	Glacier and snow melt dominated
2012	.708	Glacier and snow melt dominated
2013	.645	Glacier and snow melt dominated
2014	.525	Rainfall and Snow water melt
2015	.658	Glacier and snow melt dominated
2016	.749	Glacier and snow melt dominated
2017	.650	Glacier and snow melt dominated
2018	.768	Glacier and snow melt dominated
2019	.672	Glacier and snow melt dominated
2020	.282	Rainfall dominated

INTERPRETATION OF YEAR-WISE R^2 VALUES AND DOMINANT RUNOFF PROCESSES

The year-wise coefficients of determination (R^2) provide important insight into the dominant hydrological processes controlling river discharge from 2010 to 2020. During 2010–2013, relatively high R^2 values (0.600–0.723) indicate a strong relationship between temperature and discharge, suggesting that glacier and snowmelt were the primary contributors to river flow. In these years, rising temperatures consistently translated into increased discharge, reflecting melt-dominated hydrological conditions.

In 2014, the R^2 value declined to 0.525, indicating a weakened temperature–discharge relationship. This shift suggests a transition toward a mixed hydrological regime, where rainfall in combination with snowmelt played a more prominent role in controlling discharge variability. From 2015 to 2019, R^2 values again increased substantially (0.658–0.768), with 2016 and 2018 showing the strongest correlations. These high values confirm that glacier and snowmelt processes once again dominated runoff generation and temperature remained a key driver of seasonal discharge variability.

In contrast, 2020 exhibits a markedly low R^2 value (0.282), indicating a weak association between temperature and discharge. This suggests that rainfall-dominated processes were more influential during this year and discharge variations were largely independent of temperature

changes. Additionally, this weak relationship may also reflect data inconsistencies or anomalous climatic conditions. Overall, the R^2 analysis highlights that while glacier and snowmelt dominate runoff generation in most years, interannual climatic variability can shift the hydrological control toward rainfall-driven discharge, particularly in anomalous years such as 2020.

The analysis confirms that temperature-driven snow and glacier melt primarily regulate river discharge in the basin, especially during spring and summer. However, precipitation variability, basin storage and other climatic factors contribute significantly to discharge variability, limiting the explanatory power of temperature alone. Increased discharge variability and extreme flow events after 2014 highlight the system's sensitivity to climatic fluctuations, underscoring the need for comprehensive hydrological modeling that integrates multiple climatic inputs.

The temperature and discharge analysis from 2010 to 2020 reveals that glacier and snowmelt processes predominantly controlled seasonal discharge patterns, particularly during the periods 2010–2013 and 2015–2019. In contrast, certain years, notably 2014 and 2020, exhibited a greater influence of rainfall-driven runoff, indicating shifts in the dominant hydrological regime. The mid-decade period also showed a general warming trend, which coincided with increased hydrological variability and a higher frequency of extreme discharge events. These observations highlight the critical need to consider multiple climatic and hydrological factors when predicting runoff behavior in glacierized basins under changing climate conditions. Collectively, the findings underscore important implications for water resource management, flood risk mitigation and climate change adaptation in Himalayan River systems.

IMPACT OF GLACIER MELT ON SMALL AND LARGE HYDROPOWER PROJECTS IN THE SATLUJ BASIN

The temperature discharge relationships and runoff variability observed from 2010 to 2020 highlight important implications for hydropower generation in glacier-fed basins such as the Satluj. Rising temperatures have intensified glacier and snowmelt in most years, temporarily increasing summer runoff and enhancing short-term hydropower generation. However, the weak and highly variable temperature discharge relationships, reflected by fluctuating R^2 values, indicate growing hydrological uncertainty. Years dominated by rainfall-driven runoff demonstrate increasing dependence on extreme precipitation rather than melt processes, complicating inflow forecasting and reservoir operations.

In the long term, sustained glacier mass loss is expected to reduce meltwater contributions during lean seasons, adversely affecting firm power generation. Increased runoff variability also enhances sediment transport, leading to reservoir siltation, turbine abrasion and higher maintenance costs. Additionally, more frequent extreme discharge events elevate risks to hydropower infrastructure and operational stability. Overall, these trends underline the need for climate-resilient hydropower planning, incorporating adaptive reservoir management, improved hydro-climatic modelling and continuous cryosphere monitoring in Himalayan river basins.

ROLE OF GLACIERS IN THE SATLUJ BASIN HYDROLOGY

Glaciers and seasonal snowpacks act as natural water reservoirs in the Satluj basin, releasing meltwater during the dry and pre-monsoon periods when rainfall is limited. Estimates suggest that 40-50% of the annual discharge of the satluj river originates from snow and glacier melt, highlighting the basin's strong cryospheric control (National Institute of Hydrology, 2010; Prasad et al., 2019).

Rising temperatures in the Western Himalaya have led to:

- Increased ablation rates,
- Upward shifting of the equilibrium line altitude (ELA),
- Reduced accumulation areas, particularly for small and mid-sized glaciers.

Initially, enhanced melting increases runoff, a phenomenon often described as the **"peak water" phase**. However, as glacier volumes continue to decline, meltwater contribution is expected to decrease irreversibly, affecting long-term river flows and hydropower reliability (Schaefli et al., 2019).

IMPACTS ON LARGE HYDROPOWER PROJECTS

Short-Term Benefits

Large hydropower projects in the Satluj basin are mostly **reservoir-based systems**, allowing them to regulate river flows across seasons. During the current phase of accelerated glacier melt, these projects have benefited from:

- Increased summer and early monsoon inflows,
- Higher reservoir levels,
- Enhanced short-term power generation capacity.

Reservoirs such as **Bhakra** can store excess meltwater and release it during periods of low flow, partially offsetting hydrological variability (Schaefli et al., 2019).

Long-Term Challenges

Despite short-term gains, sustained glacier retreat poses serious long-term risks. As glacier volumes decline, meltwater contribution during lean seasons is projected to reduce significantly, affecting firm power generation and reservoir operation strategies. Climate model projections suggest that by mid-century nearly half of the glaciers in the Satluj basin may disappear, with smaller glaciers retreating most rapidly (Prasad et al., 2019).

Another major concern for large hydropower projects is sedimentation. Increased erosion from deglaciated terrain and unstable slopes results in higher sediment loads, which:

- Reduce reservoir storage capacity,
- Increase turbine abrasion,
- Raise operation and maintenance costs (Su et al., 2020).

Glacier-Related Hazards

Large hydropower infrastructure is also exposed to glacier-related hazards such as glacial lake outburst floods (GLOFs). The formation and expansion of glacial lakes due to rapid ice melt increase the risk of sudden flooding, which can damage dams, tunnels, powerhouses and downstream infrastructure (Environmental Science & Technology, 2015). Such events pose serious safety and financial risks, requiring enhanced monitoring and disaster preparedness.

IMPACTS ON SMALL HYDROPOWER PROJECTS

High Sensitivity to Flow Variability

Small hydropower projects in the Satluj basin are predominantly **run-of-river schemes** with minimal or no storage capacity. As a result, they are highly sensitive to changes in river discharge. Any fluctuation in glacier melt directly translates into variability in power generation, affecting project reliability and economic viability.

Earlier snowmelt and shifting meltwater peaks can cause:

- Excess flows during early summer,
- Reduced discharge during late summer and winter, which is particularly problematic for small projects that lack storage buffers (Su et al., 2020).

Sediment and Infrastructure Damage

Enhanced glacier melt is often accompanied by high sediment concentrations. For small hydropower projects, excessive sediment leads to:

- Rapid turbine wear and tear,
- Frequent shutdowns for desilting and maintenance,
- Reduced plant efficiency and lifespan.

Additionally, sudden flood events triggered by rapid melt, cloudbursts, or GLOFs can severely damage diversion weirs, canals, intake structures and penstocks. Compared to large dams, small hydropower projects typically lack robust protective infrastructure, making them more vulnerable to extreme events (Mishra, 2025).

Early Onset of Negative Impacts

Because of their limited adaptive capacity, small hydropower projects are expected to experience the negative impacts of glacier retreat **earlier and more intensely** than large projects. Declining base flows during dry seasons may render some projects economically unviable over time, especially in catchments dominated by small, rapidly retreating glaciers.

Changes in Flow Seasonality and Basin-Wide Implications

Glacier retreat not only affects total water availability but also alters the **seasonality of river flows**. Research indicates a shift toward:

- Earlier peak flows in spring and early summer,
- Reduced meltwater contribution during late summer and winter.

Such changes complicate reservoir operation for large projects and severely stress small run-of-river schemes that depend on consistent base flows. Altered flow regimes also affect downstream water users, irrigation demands and ecological flows, increasing competition for water resources within the basin (India Water Portal, 2026).

Implications for Hydropower Planning and Management

The long-term sustainability of hydropower development in the Satluj basin depends on integrating **glacier and climate change considerations** into planning and operations. Key measures include:

- Incorporating glacier mass balance and meltwater projections in hydropower design,
- Improving sediment management strategies,

- Strengthening GLOF monitoring and early warning systems,
- Adopting flexible reservoir operation policies to manage changing flow regimes.

Basin-scale planning that considers cumulative impacts of multiple hydropower projects is essential to reduce vulnerability and enhance resilience (Vimal Mishra, 2025).

6. CONCLUSION AND DISCUSSION

GLACIER DYNAMICS IN THE SATLUJ BASIN

The multi-temporal glacier inventory analysis clearly indicates that the Satluj Basin has undergone substantial cryospheric transformation during the last two decades**.** Although the total number of glaciers shows only marginal fluctuations between 2000, 2011 and 2020, a closer examination reveals that this numerical stability masks significant physical degradation of glaciers. The observed increase in glacier numbers in 2020 compared to 2011 is primarily a result of the non-availability of cloud and snow free satellite data. While the increase in glacier numbers in 2020 compared to 2000 is due to fragmentation is a well-documented response of glaciers undergoing sustained negative mass balance under warming climatic conditions.

The decline in glaciers and ice caps area across all sub-basin, i.e., Spiti, Baspa, Lower Satluj and Upper Satluj, demonstrates a persistent reduction in ice reserves**.** The Upper Satluj and Spiti sub-basins show the most pronounced changes, reflecting their higher elevation ranges, stronger dependence on winter snowfall and greater exposure to temperature rise. These findings are consistent with regional studies across the western Himalaya that report accelerated thinning and retreat of glaciers in cold-arid, high-altitude environments.

IMPACT OF TOPOGRAPHY AND ASPECT

The Aspect-wise analysis reveals that glacier distribution in the Satluj Basin is strongly controlled by slope orientation and incoming solar radiation. North, northeast and northwest facing slopes consistently host the majority of glacier area across all observation years. These aspects receive reduced solar insolation, resulting in lower surface energy availability for melt and more favourable microclimatic conditions for glacier persistence.

In contrast, glaciers located on south-, southwest- and west-facing slopes are sparse and significantly smaller in size. Their limited survival highlights the enhanced ablation associated with higher solar exposure and longer melt seasons. Importantly, even glaciers on traditionally favourable north-facing slopes exhibit measurable retreat, indicating that regional-scale atmospheric warming is now overriding local topographic buffering effects**.** This spatial pattern

reinforces the understanding that while topography modulates glacier sensitivity, it cannot fully offset the impacts of sustained climatic warming.

GLACIER RETREAT RATES AND CLIMATIC SENSITIVITY

The glacier retreat rate analysis between 2000 and 2020, based on LANDSAT satellite data by the snout difference method, provides compelling evidence of accelerated glacier recession across the Satluj Basin. A striking proportion of glaciers, approximately four-fifths of the analysed sample, fall within the lowest retreat class (<10 m/ yr^{-1}). Only a negligible number of glaciers exhibit high retreat rates, highlighting the near-absence of stable or equilibrium glaciers in the basin.

The Upper Satluj and Spiti sub-basins dominate the highest retreat categories, suggesting heightened sensitivity to rising temperatures and changing snowfall patterns. The Baspa sub-basin, while comparatively more stable, also displays consistent retreat, indicating that no part of the basin remains unaffected by climate change.

These retreat patterns reflect the combined influence of:

- Rising mean and minimum air temperatures,
- Reduced winter snowfall at lower elevations,
- Increased proportion of precipitation falling as rain instead of snow,
- Lengthening of the ablation season.

The spatial coherence of retreat across sub-basins suggests that glacier response is being driven by basin-scale climatic forcing rather than isolated local factors**.**

SNOW COVER VARIABILITY AND SEASONAL DYNAMICS

Seasonal snow cover analysis portrays high inter-annual variability, with pronounced differences in snow accumulation, peak extent and persistence based on AWiFS satellite data (October 2010- May, 2021). Snow cover typically begins accumulating in October, peaks during January–February and declines rapidly during April–May. However, the magnitude and duration of snow cover vary considerably between years.

The snow-abundant years such as 2012–13, 2018–19 and 2019–20 exhibit early accumulation, extensive winter coverage and delayed spring melt, resulting in higher average snow-covered areas. while years such as 2010–11 and 2017–18 are characterized by weak early-winter accumulation, abrupt mid-winter fluctuations and rapid post-peak ablation due to less snow precipitation.

The increasing frequency of years with delayed onset of snowfall and early spring melt suggests a shift toward more variable and less reliable snow regimes**.** This variability has important implications for both glacier mass balance and river hydrology.

IMPLICATIONS FOR GLACIER MASS BALANCE

Snow cover plays a crucial role in controlling glacier mass balance by governing accumulation rates and surface energy conditions. The reduced snow cover with time, lower glacier surface albedo, leading to enhanced absorption of solar radiation and accelerated melting. The observed snow cover variability, combined with widespread glacier retreat, indicates that glaciers in the Satluj Basin are experiencing persistent negative mass balance conditions.

The shifting of Equilibrium Line Altitudes (ELAs) towards higher elevation point to shrinking accumulation zones emphasizes that many glaciers are losing their capacity to regain mass during winter. While episodic snow-rich years may temporarily slow mass loss, they are insufficient to reverse the long-term negative trend. This pattern aligns with observations from benchmark glaciers in Himachal Pradesh, such as Naradu glaciers, which show sustained thinning despite inter-annual snowfall variability.

GLACIER MELT, FLOW VARIABILITY and HYDROPOWER SUSTAINABILITY IN THE SATLUJ BASIN

The analysis of glacier and snow dynamics in the Satluj Basin underscores the critical role of cryospheric processes in regulating hydropower generation. The strong dependence of both large and small hydropower projects on glacier-fed flows highlights the basin's vulnerability to climate-driven hydrological changes. Observed glacier retreat, reductions in glacier area and deglaciation of larger glaciers into smaller units indicate sustained negative mass balance, driven primarily by rising temperatures and extended ablation periods. While local topography such as

slope, aspect and elevation moderate's glacier response, the consistent retreat observed even on north and northeast facing slopes demonstrates that regional warming now overrides topographic buffering effects.

Large reservoir-based hydropower projects benefit from storage capacity that allows them to buffer short-term flow fluctuations caused by enhanced meltwater. This has led to temporary increases in summer inflows, reservoir levels and short-term power generation. However, sustained glacier retreat is projected to reduce late-season inflows, affecting firm power generation and operational reliability. Additionally, accelerated sediment transport from deglaciated terrain increases reservoir siltation, turbine abrasion and maintenance demands. Glacier-related hazards, particularly glacial lake outburst floods (GLOFs), further compound risk to infrastructure safety and operational stability, highlighting the necessity for robust monitoring and disaster preparedness.

Small run-of-river hydropower projects are inherently more sensitive to flow variability due to minimal storage and infrastructure limitations. Fluctuations in meltwater directly impact generation capacity, turbine efficiency and operational reliability. High sediment loads during peak melt periods accelerate wear and reduce plant lifespan, while sudden flood events from glacier melt or extreme weather can damage diversion structures and canals. The limited adaptive capacity of these systems means that small hydropower projects are likely to experience negative impacts earlier and more intensely than large reservoir-based projects.

The observed shifts in flow seasonality earlier peak flows in spring and early summer and reduced late-season discharge have basin-wide implications. Altered timing of water availability challenges reservoir operation strategies, complicates scheduling for large hydropower plants and stresses small run-of-river schemes that rely on consistent baseflows. These changes also affect downstream water users, irrigation systems and ecological flows, indicating that hydropower sustainability cannot be considered in isolation but must be integrated with broader water resource management.

From a planning and management perspective, the findings emphasize the importance of integrating glacier mass balance trends, snow cover variability and climate projections into

hydropower design and operation. Strategies such as adaptive reservoir management, enhanced sediment control and GLOF monitoring are critical to maintaining operational efficiency and infrastructure safety. Basin-scale planning that accounts for cumulative impacts of multiple hydropower projects is essential to enhance resilience and mitigate climate-related risks.

Overall, the discussion highlights a short-term benefit from accelerated glacier melt may temporarily enhance hydropower generation, the long-term reduction in meltwater, increasing flow variability and associated hazards present significant challenges. These findings underscore the urgent need for climate-sensitive hydropower planning and adaptive management strategies to ensure sustainable energy production and water security in the Satluj Basin and similar Himalayan river systems.

CONCLUSION

This study presents a detailed and integrated assessment of glacier dynamics and seasonal snow cover variability in the Satluj River Basin, offering important insights into the evolving cryospheric conditions of the western Himalaya under a changing climate. By combining multi-temporal glacier inventories, retreat rate analysis and long-term satellite-based snow cover observations, the research provides robust evidence of widespread and persistent glacier degradation across the basin. The analysis reveals that while the total number of glaciers has shown minor fluctuations over time, the overall glacierized area has consistently declined. This apparent contradiction is primarily the result of fragmentation of larger glaciers into smaller units, a clear indicator of sustained negative mass balance rather than glacier recovery. The continued reduction in glacier area and the dominance of high retreat rates across most glaciers reflect the strong influence of rising air temperatures, extended melt seasons and changing precipitation patterns in the region.

Topographic factors, particularly slope aspect and elevation, also play an important role in controlling glacier distribution, retreat and mass balance. Glaciers are predominantly concentrated on north- and northeast-facing slopes, where lower solar radiation provides relatively favourable conditions for ice preservation. However, the consistent retreat observed even on these climatically protected slopes highlights that regional-scale warming is now exceeding the mitigating influence

of local terrain. This finding emphasizes the increasing vulnerability of Himalayan glaciers, regardless of their topographic setting.

Further, seasonal snow cover analysis strengthens the understanding of glacier mass balance behaviour in the Satluj Basin. The study documents pronounced inter-annual variability in snow cover extent, accumulation timing and persistence. Although certain years exhibit enhanced snow accumulation, these episodic gains are insufficient to compensate for long-term mass losses driven by intensified ablation. The observed tendency toward delayed snowfall onset and earlier spring melting reduces the duration of snow cover, negatively affecting glacier accumulation and surface energy balance.

The combined effects of glacier retreat and altered snow regimes have significant hydrological consequences for the Satluj River system, with direct implications for hydropower generation. In the short term, increased melt from shrinking glaciers may lead to temporarily enhanced summer flows, benefiting reservoir-based hydropower projects such as Bhakra, Nathpa Jhakri and Karcham Wangtoo, by improving inflows and operational flexibility. However, as glacier volumes continue to diminish, meltwater contributions are expected to decline, reducing late-season baseflows and increasing reliance on monsoon precipitation. This shift is likely to increase inter-annual discharge variability, heighten sediment transport and elevate risks of turbine abrasion, reservoir siltation and structural stress during extreme flow events. Small run-of-river hydropower projects, which lack storage capacity, are particularly vulnerable to these hydrological changes, facing reduced generation reliability and increased operational challenges during low-flow periods.

In conclusion, the Satluj River Basin is undergoing a clear transition in its cryospheric and hydrological regime, driven by ongoing climate change. The persistent loss of glacier mass, recession of glacier snouts, increasing snow cover variability and shifting runoff patterns underscore the basin's growing vulnerability to climatic extremes. These changes have critical consequences for hydropower generation, water resource management and downstream livelihoods, emphasizing the urgent need for continuous cryospheric monitoring, integration of climate change projections into energy and water planning and the adoption of adaptive management strategies. The outcomes of this study provide valuable scientific evidence for

understanding Himalayan cryospheric change and offer a critical foundation for informed decision-making in climate-sensitive mountain river basins.

CONCLUDING REMARKS

The present study provides a comprehensive and basin-scale assessment of cryospheric changes in the Satluj River Basin, highlighting the growing influence of climate change on glacier dynamics, seasonal snow cover and associated hydrological processes. Through the integration of multi-temporal satellite data, geospatial analysis and mass balance indicators, the research establishes clear evidence of sustained glacier retreat, declining ice reserves and increasing variability in snow cover across the basin.

The findings demonstrate that although short-term fluctuations in snowfall may temporarily enhance snow cover and runoff, they do not offset the long-term trend of glacier mass loss driven by rising temperatures and extended ablation seasons. The apparent stability or increase in glacier numbers in recent years is largely a consequence of glacier fragmentation, masking the ongoing reduction in total glacier area and volume. This underscores the importance of using multiple indicators such as glacier area, retreat rates and accumulation characteristics rather than number of glaciers alone when assessing glacier health.

The strong control of topography, particularly slope aspect, on glacier distribution highlights the role of local terrain in moderating glacier response. However, the consistent retreat observed even on climatically favourable north-facing slopes indicates that regional atmospheric warming is now overwhelming these local buffering effects. Seasonal snow cover analysis further reveals increasing inter-annual variability, delayed accumulation and earlier spring melt, all of which negatively influence glacier nourishment and long-term mass balance.

From a hydrological perspective, the Satluj Basin appears to be undergoing a gradual transition from a traditionally nivo-glacially regulated system toward a more rainfall-dependent and hydrologically variable regime. While enhanced meltwater contributions may temporarily increase discharge in the near term, continued glacier shrinkage is expected to reduce late summer baseflow, increase flow variability and heighten the risk of water stress during dry periods.

These hydrological changes carry direct and significant implications for hydropower generation. Large reservoir-based projects, such as Bhakra, Nathpa Jhakri and Karcham Wangtoo, may temporarily benefit from increased early meltwater, improving summer power generation and reservoir storage. However, long-term reductions in glacier-fed inflows, coupled with greater flow variability, sediment load and increased frequency of extreme discharge events, pose risks to operational stability, turbine efficiency and infrastructure safety. Small run-of-river hydropower projects, which lack significant storage, are particularly vulnerable to these shifts, as declining baseflows and sudden high-flow events can compromise generation reliability and economic viability.

Overall, the study points out the vulnerability of the Satluj River Basin to ongoing and future climatic change. The results emphasize the need for sustained cryospheric monitoring, incorporation of climate-sensitive hydrological and hydropower planning and the development of adaptive strategies to ensure long-term water and energy security in the western Himalaya. The insights generated through this work provide a valuable scientific basis for informed decision-making and contribute to a broader understanding of climate change impacts on Himalayan river systems and their associated hydropower infrastructure.

KEY FINDINGS

- **Consistent Glacier Area Loss:** Multi-temporal satellite analysis (2000–2020) indicates a sustained decline in glacier area across the Satluj Basin, reflecting long-term cryospheric degradation.
- **Increase in Glacier Numbers Due to Fragmentation:** Minor increase in glacier count by 2020 is attributed to fragmentation of larger glaciers, not glacier regeneration.
- **Aspect-Controlled Glacier Distribution:** Glaciers are predominantly located on north, northeast and northwest-facing slopes, while south-facing slopes show significantly reduced glacier presence due to higher solar radiation.
- **Widespread Accelerated Glacier Retreat:** Over 80% of analyzed glaciers exhibit retreat rates exceeding 10 m/year, confirming basin-wide accelerated glacier recession.
- **Climate-Sensitive Hotspots Identified:** Upper Satluj and Spiti sub-basins contain the majority of rapidly retreating glaciers and require priority monitoring and intervention.

- **Persistent Negative Glacier Mass Balance:** ELA and AAR-based assessments indicate a clear transition from near-balanced mass conditions (2000) to dominant negative mass balance by 2020.
- **Decline in Snow Cover Duration:** Snow cover analysis (2010–2020) reveals high interannual variability, delayed snowfall onset and earlier seasonal melt, reducing glacier nourishment.
- **Shift Toward Temperature-Driven Runoff:** Strong positive correlations between air temperature and river discharge indicate increasing dominance of snow and glacier melt in controlling river flows.
- **Earlier Peak Discharge:** Peak river flows are occurring earlier in the melt season, reducing late-summer flow stability and natural buffering capacity.
- **Growing Uncertainty in Water Availability:** Continued glacier thinning may initially increase meltwater contribution, followed by long-term decline in baseflow during lean periods.
- **Impacts on Hydropower Generation:** Altered flow seasonality, increased discharge variability and higher sediment load adversely affect hydropower generation reliability and infrastructure sustainability.
- **Rising Climate-Induced Hazard Risks:** Accelerated glacier retreat increases susceptibility to landslides, slope instability and formation of potentially hazardous proglacial lakes.
- **Need for Strengthened Monitoring:** Continuous satellite-based cryosphere monitoring, integrated with field observations, is essential for informed climate adaptation and water-energy planning.
- **Satluj Basin as a Priority Climate Action Region:** High dependence on snow and glacier melt necessitates targeted adaptation strategies to ensure long-term water and energy security.

REFERENCES

Aggarwal, P.K., Rani, S. and Bala, A. (2019) 'Impact of climate change on agriculture in India: A review', *Current Science*, 116(12), pp. 1961–1967.

Alley, R.B., Cuffey, K.M. and Zoet, L.K. (2019) 'Glacial erosion: status and outlook', *Annals of Glaciology*, 60, pp. 1–13. https://doi.org/10.1017/aog.2019.38

Andreassen, L.M., Nagy, T., Kjøllmoen, B. and Leigh, J.R. (2022) 'An inventory of Norway's glaciers and ice-marginal lakes from 2018–19 Sentinel-2 data', *Journal of Glaciology*, 68, pp. 1085–1106. https://doi.org/10.1017/jog.2022.20

Armstrong, R.L. (1989) 'Mass balance history of Blue Glacier, Washington, USA', in Oerlemans, J. (ed.) *Glacier Fluctuations and Climatic Change*. Dordrecht: Springer, pp. 183–192. https://doi.org/10.1007/978-94-015-7823-3_12

Armstrong, R.L. and Brun, E. (2008) *Snow and Climate: Physical Processes, Surface Energy Exchange and Modeling*. Cambridge: Cambridge University Press.

Azam, M.F. et al. (2016) 'Review of the status and mass balance of Himalayan–Karakoram glaciers', *Frontiers in Earth Science*, 4, 37.

Azam, M.F. et al. (2018) 'Review of the status and mass changes of Himalayan–Karakoram glaciers', *Journal of Glaciology*, 64(243), pp. 61–74.

Azam, M.F. et al. (2019) 'Snow and ice melt contributions in a highly glacierized Himalayan basin', *Scientific Reports*, 9, 16131.

Barry, R.G. (1987) 'The cryosphere and global change', in Parry, M.L., Carter, T.R. and Konijn, N.T. (eds.) *The Impact of Climatic Variations on Agriculture*, Vol. 1. Berlin: Springer, pp. 109–126.

Barry, R.G. (2002) *The Cryosphere: Past, Present and Future*. London: Arnold.

Benn, D.I. and Evans, D.J.A. (2010) *Glaciers and Glaciation*. 2nd edn. London: Hodder Education.

Berthier, E., Arnaud, Y., Baratoux, D., Vincent, C. and Rémy, F. (2007) 'Remote sensing estimates of glacier mass balances in the Himachal Pradesh (Western Himalaya, India)', *Remote Sensing of Environment*, 108(3), pp. 327–338.

Bhambri, R., Bolch, T., Chaujar, R.K. and Kulshreshtha, S. (2011) 'Glacier changes in the Indian Himalaya: 1960–2006', *Remote Sensing of Environment*, 114(11), pp. 2336–2347.

Birthal, P.S., Negi, D.S. and Kumar, S. (2015) 'Inefficiency of Indian agriculture under climate change', *Agricultural Economics Research Review*, 28(2), pp. 203–216.

Bolch, T. et al. (2012) 'The state and fate of Himalayan glaciers', *Science*, 336(6079), pp. 310–314.

Bolch, T., Kulkarni, A., Kääb, A., Huggel, C., Paul, F., Cogley, J.G., Frey, H., Kargel, J.S., Fujita, K., Scheel, M., Bajracharya, S. and Stoffel, M. (2012) 'The state and fate of Himalayan glaciers', *Science*, 336(6079), pp. 310–314. https://doi.org/10.1126/science.1215828

Bolch, T., Menounos, B. and Wheate, R. (2010) 'Landsat-based inventory of glaciers in western Canada, 1985–2005', *Remote Sensing of Environment*, 114(1), pp. 127–137.

Bookhagen, B. and Burbank, D.W. (2005) 'Abnormal monsoon years and their control on erosion and sediment flux in the high, arid northwest Himalaya', *Earth and Planetary Science Letters*, 231(1–2), pp. 131–146.

Bookhagen, B. and Burbank, D.W. (2010) 'Toward a complete Himalayan hydrological budget', *Journal of Geophysical Research*, 115(F3).

Cogley, J.G. et al. (2011) *Glossary of Glacier Mass Balance and Related Terms*. Paris: UNESCO-IHP.

Cuffey, K.M. and Paterson, W.S.B. (2010) *The Physics of Glaciers*. 4th edn. Oxford: Academic Press.

Dimri, A.P. et al. (2020) 'Western disturbances: A review', *Reviews of Geophysics*, 58(1), e2019RG000657.

Dingman, S.L. (2015) *Physical Hydrology*. 3rd edn. Long Grove, IL: Waveland Press.

Dobhal, D.P., Mehta, M. and Srivastava, D. (2013) 'Retreating and thinning of Gangotri Glacier', *Current Science*, 105(3), pp. 37–49.

Dyurgerov, M.B. (2001) 'Mountain and subpolar glaciers show an increase in sensitivity to climate warming', *Journal of Hydrology*, 282, pp. 164–176. https://doi.org/10.1016/S0022-1694(03)00259-3

Dyurgerov, M.B. and Meier, M.F. (2005) *Glaciers and the Changing Earth System*. Boulder: INSTAAR, University of Colorado.

Environmental Science & Technology (2015) *Climate Change Risk for Hydropower Schemes in Himalayan Region*. Available at: https://pubs.acs.org/doi/10.1021/es502719t (Accessed: 1 January 2026).

Foggin, J.M. (2016) 'Mountain ecosystems', in *Reference Module in Earth Systems and Environmental Sciences*. Amsterdam: Elsevier. https://doi.org/10.1016/B978-0-12-409548-9.09199-5

Frey, H., Paul, F. and Strozzi, T. (2012) 'On the suitability of the SRTM DEM and ASTER GDEM for the compilation of topographic parameters in glacier inventories', *International Journal of Applied Earth Observation and Geoinformation*, 18, pp. 480–490.

Gardelle, J., Berthier, E. and Arnaud, Y. (2012) 'Slight mass gain of Karakoram glaciers', *Nature Geoscience*, 5, pp. 322–325.

Gascoin, S. et al. (2020) 'The ESA Snow CCI project', *Remote Sensing of Environment*, 245, 111735.

Government of India, Ministry of Earth Sciences (2020) *Assessment of Climate Change over the Indian Region*. Singapore: Springer Nature.

Hall, D.K., Riggs, G.A. and Salomonson, V.V. (2015) *MODIS Snow and Sea Ice Products*. NASA.

Hewitt, K. (2005) 'The Karakoram anomaly?', *The Cryosphere*, 3, pp. 247–265.

Hock, R. (2003) 'Temperature index melt modelling in mountain areas', *Journal of Hydrology*, 282(1–4), pp. 104–115.

ICIMOD (2011) *Glacier Status in the Hindu Kush–Himalayan Region*. Kathmandu: ICIMOD.

ICIMOD (2021) *Glacier Lake Inventory of the Hindu Kush Himalaya*. Kathmandu: ICIMOD.

Immerzeel, W.W., van Beek, L.P.H. and Bierkens, M.F.P. (2010) 'Climate change will affect the Asian water towers', *Science*, 328(5984), pp. 1382–1385.

India Water Portal (2026) *Glacier melt threatens water reserves in Satluj basin*. Discussion of climate projections suggesting glacier loss and implications for hydropower water availability in the basin. India Water Portal

IPCC (2022) *Climate Change 2022: Impacts, Adaptation and Vulnerability*. Cambridge: Cambridge University Press.

Jain, S.K., Goswami, A. and Saraf, A.K. (2020) 'Snow cover variability in the Indian Himalaya', *Climate Dynamics*, 54, pp. 2873–2891.

Joseph, T. (2010) *Multivariate statistical analysis: Concepts and applications*. New Delhi: PHI Learning Pvt. Ltd.

Kääb, A. (2005) 'Combination of SRTM3 and repeat ASTER data for deriving alpine glacier flow velocities in the Bhutan Himalaya', *Remote Sensing of Environment*, 94(4), pp. 463–474.

Kääb, A. et al. (2012) ‘Contrasting patterns of glacier mass change’, *Nature*, 488, pp. 495–498.

Knight, J. and Harrison, S. (2022) ‘Climate sensitivity and cryospheric systems’, in Shroder, J.F. (ed.) *Treatise on Geomorphology*. 2nd edn. Amsterdam: Academic Press, pp. 616–628.

Kumar, V., Singh, P. and Singh, V.P. (2007) ‘Snow and glacier melt contribution in the Beas River at Pandoh Dam, Himachal Pradesh, India’, *Hydrological Sciences Journal*, 52(2), pp. 376–388.

Matsuo, K. and Heki, K. (2010) ‘Time-variable ice loss in Asian high mountains from satellite gravimetry’, *Earth and Planetary Science Letters*, 290(1–2), pp. 30–36.

Mishra, V. (2025) *Climate change affects hydropower generation*. India Water Portal (online). Available at: https://www.indiawaterportal.org/climate-change/climate/climate-change-affects-hydropower-generation (Accessed: 1 January 2026).

Mishra, V. et al. (2018) *Runoff components of glacierized Himalayan basins: Implications for hydropower*. Journal of Hydrology, 560, pp. 182–195. DOI: 10.1016/j.jhydrol.2018.03.045.

National Institute of Hydrology (2010) *Snow and glacier contribution in the Satluj River at Bhakra Dam*. Estimation of percent contribution of snow and glacier melt to annual flows at Bhakra reservoir, illustrating importance for hydropower. India Water Portal

National Institute of Hydrology (2010) *Snow and glacier contribution in the Satluj River at Bhakra Dam*. Estimation of percent contribution of snow and glacier melt to annual flows at Bhakra reservoir, illustrating importance for hydropower. India Water Portal

Owen, L.A., Derbyshire, E. and Fort, M. (1998) ‘Observations on rock glaciers in the Himalayas and Karakoram Mountains of northern Pakistan and India’, *Geomorphology*, 26(1–3), pp. 199–213.

Pant, G.B. et al. (2018) *Climate Change in the Himalayas*. Cham: Springer.

Paterson, W.S.B. (1994) *The Physics of Glaciers*. 3rd edn. Oxford: Pergamon Press.

Paul, F. et al. (2013) 'On the accuracy of glacier outlines', *Annals of Glaciology*, 54, pp. 171–182.

Paul, F., Huggel, C. and Kääb, A. (2004) 'Combining satellite multispectral image data and a digital elevation model for mapping of debris-covered glaciers', *Remote Sensing of Environment*, 89(4), pp. 510–518.

Prasad, V., Kulkarni, A.V., Pradeep, S., Pratibha, S., Shirsat, T., Arya, A.R. and Tawde, S.A., with Orr, A. and Bannister, D. (2019) *Study of glacier loss and meltwater contribution in the Satluj basin*, India Science Wire – reported by media. Details on projected glacier disappearance and impacts on stream flow and hydropower availability. Down To Earth

Pritchard, H.D. (2019) 'Asia's shrinking glaciers', *Nature*, 569, pp. 649–654.

Purohit, B., Bhatt, C.M. and Kulkarni, A.V. (2022) 'Climate change implications for hydropower', Current Science, 122(5), pp. 567–574.

Quincey, D.J., Richardson, S.D., Luckman, A., Lucas, R.M., Reynolds, J.M., Hambrey, M.J. and Glasser, N.F. (2007) 'Early recognition of glacial lake hazards in the Himalaya using remote sensing datasets', *Global and Planetary Change*, 56(1–2), pp. 137–152.

Raup, B., Kääb, A., Kargel, J.S., Bishop, M.P., Hamilton, G., Lee, E., Paul, F., Rau, F., Soltesz, D., Khalsa, S.J.S., Beedle, M. and Helm, C. (2007) 'Remote sensing and GIS technology in the Global Land Ice Measurements from Space (GLIMS) Project', *Computers & Geosciences*, 33(1), pp. 104–125.

Schaefli, B., Manso, P., Fischer, M., Huss, M. and Farinotti, D. (2019) *The role of glacier retreat for Swiss hydropower production*. Renewable Energy, 132, pp. 615–627. DOI: 10.1016/j.renene.2018.07.104.

Sharma, D.C. (2026) *Study suggests half of all glaciers in Satluj basin could vanish by 2050*, *The Wire Science* – reporting on observed glacier retreat, decreasing glacier area and potential long-term effects on flow regimes. The Wire Science

Singh, D., Singh, S. and Jain, S.K. (2021) 'Hydrology of the Satluj River Basin', *Environmental Earth Sciences*, 80(23).

Singh, P. and Jain, S.K. (2002) 'Snow and glacier melt contribution in the Satluj River at Bhakra Dam in the western Himalayan region', *Hydrological Sciences Journal*, 47(1), pp. 93–106.

Su, X., Li, Z., Zhang, Y., Li, Y. and Xu, J. (2020) *The impact of glacier shrinkage on energy production from hydropower–solar complementarity in alpine river basins*. Science of The Total Environment, 719, 137488. DOI: 10.1016/j.scitotenv.2020.137488.

Turney, S. (2022) 'Pearson correlation coefficient: definition, formula and interpretation', *Scribbr*. Available at: https://www.scribbr.com/statistics/pearson-correlation-coefficient/ (Accessed: 15 August 2025).

Wagnon, P. et al. (2007) 'Four years of mass balance measurements', *Journal of Glaciology*, 53(183), pp. 603–611.

World Bank (2022) *Climate Change and Development Report for India*. Washington, DC: World Bank.

Zemp, M. et al. (2019) 'Global glacier mass changes', *Nature*, 568, pp. 382–386.

ANNEXURE-I
GLACIER INVENTORY OF THE SPITI BASIN

Sr. No.	Glacier ID	Aspect	Area in Sqkm		
			2000	2011	2020
1	1	N	0.06	0.06	0.06
2	2	NE	0.34	0.34	0.31
3	3	SE	1.53	1.53	1.43
4	4	NE	0.68	0.68	0.61
5	5	NE	7.58	7.58	7.56
6	6	N	8.12	8.12	8.00
7	7	SE	0.28	0.28	0.24
8	8	SE	0.15	0.15	0.14
9	9	E	1.43	1.43	1.28
10	10	NW	0.27	0.27	0.25
11	11	W	0.27	0.27	0.22
12	12	SE	6.46	6.46	6.31
13	13	E	8.12	8.12	7.80
14	14	SE	1.62	1.62	1.36
15	15	N	14.02	14.02	14.02
16	16	SE	0.74	0.74	0.67
17	17	NE	7.21	7.21	7.21
18	18	N	0.34	0.34	0.34
19	19	NE	0.26	0.26	0.26
20	20	SE	0.44	0.44	0.42
21	21	NE	6.22	6.22	6.17
22	22	NE	3.35	3.35	3.29
23	23	SE	0.08	0.08	0.08
24	24	N	12.33	12.33	12.30
25	25	NE	1.55	1.55	1.45
26	26	NE	2.70	2.70	2.46
27	27	SE	0.42	0.42	0.40
28	28	NE	0.17	0.17	0.11
29	29	NE	1.04	1.04	0.99
30	30	N	0.46	0.46	0.46
31	31	E	1.82	1.82	1.82
32	32	E	0.53	0.53	0.40
33	33	NE	0.44	0.44	0.35
34	34	N	8.56	8.56	8.05
35	35	SE	0.75	0.75	0.54
36	36	N	0.62	0.62	0.57
37	37	NE	0.20	0.20	0.16
38	38	NE	0.34	0.34	0.31
39	3	N	0.48	1.53	N/A

40	40	NE	0.54	0.54	0.52
41	41	NW	0.15	0.15	0.13
42	42	NE	1.79	1.79	1.77
43	43	NE	1.04	1.04	0.91
44	44	NE	2.06	2.06	2.06
45	45	NE	1.81	1.81	1.81
46	46	N	0.64	0.64	0.47
47	47	N	0.27	0.27	0.26
48	48	N	0.23	0.23	0.17
49	49	NE	2.99	2.99	2.97
50	50	N	4.27	4.27	4.26
51	51	NE	2.06	2.06	1.94
52	52	NE	0.38	0.38	0.36
53	53	SE	0.32	0.32	0.27
54	54	NE	0.32	0.32	0.32
55	55	E	0.39	0.39	0.35
56	56	SE	2.12	2.12	1.96
57	57	NE	0.21	0.21	0.17
58	58	N	1.20	1.20	1.08
59	59	NW	0.69	0.69	0.53
60	60	N	3.92	3.92	3.53
61	61	N	0.47	0.47	0.38
62	62	W	0.10	0.10	0.10
63	63	N	1.24	1.24	1.02
64	64	N	0.31	0.31	0.22
65	65	N	0.30	0.30	0.26
66	66	N	0.23	0.23	0.22
67	67	N	0.31	0.31	0.28
68	68	N	0.47	0.47	0.38
69	69	SE	11.38	11.38	11.14
70	70	SE	0.67	0.67	0.67
71	71	S	1.13	1.13	0.97
72	72	NE	2.40	2.40	2.15
73	73	E	1.10	1.10	0.94
74	74	NE	0.73	0.73	0.62
75	75	SE	0.88	0.88	0.84
76	76	SE	1.87	1.87	1.84
77	77	SE	2.34	2.34	2.32
78	78	NE	0.31	0.31	0.22
79	79	NE	0.49	0.49	0.40
80	80	N	0.84	0.84	0.76
81	81	NE	0.52	0.52	0.41
82	82	NW	0.38	0.38	0.35
83	83	NE	0.21	0.21	0.20

84	84	W	0.26	0.26	0.25
85	85	SE	0.51	0.51	0.50
86	86	N	0.46	0.46	0.46
87	87	SE	0.34	0.34	0.32
88	88	N	5.36	5.36	5.31
89	89	N	3.69	3.69	3.69
90	90	N	1.09	1.09	1.03
91	91	E	0.96	0.96	0.96
92	92	N	0.29	0.29	0.29
93	93	N	0.62	0.62	0.57
94	94	SE	0.22	0.22	0.11
95	95	SE	0.22	0.22	0.19
96	96	NE	8.40	8.40	8.34
97	96	N	0.17	8.40	8.34
98	98	N	1.04	1.04	0.92
99	99	NE	0.60	0.60	0.53
100	100	N	1.77	1.77	1.65
101	101	N	1.13	1.13	1.10
102	102	N	0.29	0.29	0.22
103	103	N	0.24	0.24	0.22
104	104	NE	0.57	0.57	0.56
105	105	NW	1.24	1.24	1.23
106	106	N	0.23	0.23	0.21
107	107	N	0.62	0.62	0.57
108	108	N	0.42	0.42	0.40
109	109	N	0.81	0.81	0.79
110	110	E	0.25	0.25	0.21
111	111	E	0.14	0.14	0.13
112	112	N	0.38	0.38	0.36
113	113	NW	0.13	0.13	0.11
114	114	N	0.50	0.50	0.45
115	115	NE	0.41	0.41	0.35
116	116	NE	1.22	1.22	1.21
117	117	NE	4.48	4.48	4.46
118	118	N	0.86	0.86	0.69
119	119	SE	0.69	0.69	0.69
120	120	N	0.54	0.54	0.50
121	121	NE	0.36	0.36	0.35
122	122	NE	0.69	0.69	0.69
123	123	N	0.99	0.99	0.91
124	124	N	0.40	0.40	0.32
125	125	NE	0.31	0.31	0.21
126	126	NE	4.29	4.29	4.18
127	127	N	0.42	0.42	0.35

128	128	N	2.16	2.16	1.89
129	129	NW	0.16	0.16	0.14
130	130	NE	0.24	0.24	0.21
131	131	N	0.57	0.57	0.51
132	132	NE	0.73	0.73	0.72
133	133	N	1.16	1.16	1.03
134	134	N	0.82	0.82	0.70
135	135	N	0.31	0.31	0.27
136	136	SW	0.69	0.69	0.66
137	137	SW	0.15	0.15	0.14
138	138	N	1.75	1.75	1.75
139	139	NE	0.98	0.98	0.84
140	140	N	2.33	2.33	2.12
141	141	N	0.67	0.67	0.57
142	142	NW	0.08	0.08	0.08
143	143	N	0.88	0.88	0.87
144	144	N	0.13	0.13	0.07
145	145	NE	1.08	1.08	1.06
146	146	N	3.40	3.40	3.40
147	147	NW	2.80	2.80	2.75
148	148	N	0.24	0.24	0.24
149	149	SW	0.40	0.40	0.40
150	150	N	7.21	7.21	6.99
151	151	N	0.62	0.62	0.48
152	152	N	0.36	0.36	0.29
153	153	NE	1.05	1.05	0.91
154	154	NE	0.25	0.25	0.19
155	155	N	0.47	0.47	0.45
156	156	N	0.37	0.37	0.31
157	157	N	0.19	0.19	0.18
158	158	N	0.86	0.86	0.82
159	159	NE	0.53	0.53	0.49
160	160	E	0.19	0.19	0.18
161	161	N	0.12	0.12	0.12
162	162	N	0.04	0.04	0.04
163	163	N	0.28	0.28	0.26
164	164	N	0.23	0.23	0.19
165	165	N	0.17	0.17	0.16
166	166	N	0.08	0.08	0.07
167	167	NW	0.21	0.21	0.17
168	168	N	0.16	0.16	0.15
169	169	N	0.15	0.15	0.14
170	170	N	0.14	0.14	0.13
171	171	N	0.14	0.14	0.10

172	172	N	0.10	0.10	0.05
173	173	N	0.06	N/A	0.05
174	174	N	0.28	0.28	0.19
175	175	N	0.34	0.34	0.27
176	176	N	0.15	0.15	0.13
177	177	NW	0.15	0.15	0.05
178	178	NE	0.12	0.12	0.11
179	179	N	0.17	0.17	0.17
180	180	N	0.13	0.13	0.12
181	181	N	0.28	0.28	0.27
182	182	N	0.23	0.23	0.13
183	183	NW	0.14	0.14	0.08
184	184	NW	0.14	0.14	0.07
185	185	NW	0.54	0.54	0.37
186	186	N	0.30	0.30	0.30
187	187	NE	0.15	0.15	0.13
188	188	NW	0.46	0.46	0.46
189	189	NE	0.80	0.80	0.77
190	190	N	0.44	0.44	0.36
191	191	N	0.08	0.08	0.06
192	192	N	0.11	0.11	0.09
193	193	NE	0.28	0.28	0.22
194	194	N	0.65	0.65	0.36
195	195	NW	0.26	0.26	0.23
196	196	N	0.64	0.64	0.57
197	197	NW	0.20	0.20	0.20
198	198	SW	0.68	0.68	0.68
199	199	SW	1.55	1.55	1.56
200	200	W	0.62	0.62	0.55
201	201	N	1.09	1.09	1.09
202	202	N	2.91	2.91	2.38
203	203	NW	0.21	0.21	0.12
204	204	NW	0.13	0.13	0.11
205	205	NE	1.25	1.25	0.85
206	206	N	0.48	0.48	0.37
207	207	N	2.20	2.20	2.06
208	208	N	0.46	0.46	0.46
209	209	N	0.35	0.35	0.32
210	210	N	1.17	1.17	1.10
211	211	NW	0.79	0.79	0.75
212	212	NW	0.44	0.44	0.40
213	213	NE	0.10	0.10	0.07
214	214	NE	0.58	0.58	0.54
215	215	N	3.96	3.96	3.96

216	216	NE	1.07	1.07	1.02
217	217	NE	0.61	0.61	0.59
218	218	NE	0.62	0.62	0.62
219	219	SW	0.70	0.70	0.62
220	220	NW	0.67	0.67	0.43
221	221	S	0.59	0.59	0.54
222	222	S	0.62	0.62	0.62
223	223	E	0.21	0.21	0.16
224	224	SE	0.09	0.09	0.08
225	225	NE	3.64	3.64	3.57
226	226	NE	1.12	1.12	1.09
227	227	NE	2.01	2.01	1.82
228	228	N	0.85	0.85	0.78
229	229	SE	0.33	0.33	0.28
230	230	N	0.22	0.22	0.20
231	231	N	0.14	0.14	0.13
232	232	NE	0.05	0.05	0.05
233	233	NE	0.68	0.68	0.68
234	234	SE	0.72	0.72	0.72
235	235	N	0.18	0.18	0.17
236	236	NW	0.37	0.37	0.35
237	237	NE	0.15	0.15	0.16
238	238	NE	1.00	1.00	0.96
239	239	N	0.70	0.70	0.63
240	240	N	1.32	1.32	1.18
241	241	N	1.03	1.03	0.88
242	242	NE	1.06	1.06	0.87
243	243	S	1.33	1.33	0.84
244	244	NW	0.47	0.47	0.42
245	245	E	0.55	0.55	0.52
246	246	N	0.41	0.41	0.37
247	247	N	0.70	0.70	0.70
248	248	NW	0.10	0.10	0.09
249	249	NE	0.83	0.83	0.71
250	250	SE	0.32	0.32	0.31
251	251	N	2.70	2.70	2.53
252	252	N	0.51	0.51	0.46
253	253	N	0.66	0.66	0.59
254	254	SE	0.32	0.32	0.22
255	255	E	0.97	0.97	0.84
256	256	N	1.48	1.48	1.33
257	257	NE	0.18	0.18	0.15
258	258	NE	1.37	1.37	1.30
259	259	S	0.34	0.34	0.25

260	260	S	0.26	0.26	0.18
261	261	E	0.10	0.10	0.08
262	262	N	0.08	0.08	0.05
263	263	NW	0.53	0.53	0.46
264	264	N	0.29	0.29	0.25
265	265	NE	0.83	0.83	0.74
266	266	N	1.21	1.21	1.08
267	267	N	0.25	0.25	0.24
268	268	NW	0.07	0.07	0.06
269	269	NE	0.13	0.13	0.12
270	270	E	0.25	0.25	0.18
271	271	NW	0.32	0.32	0.30
272	272	N	0.39	0.39	0.37
273	273	E	0.47	0.47	0.43
274	274	NE	2.46	2.46	2.35
275	275	E	1.00	1.00	0.95
276	276	E	1.36	1.36	1.14
277	277	SW	0.35	0.35	0.33
278	278	N	6.61	6.61	6.47
279	279	N	0.36	0.36	0.33
280	280	N	4.19	4.19	4.08
281	281	N	0.41	0.41	0.39
282	282	E	0.22	0.22	0.21
283	283	E	0.14	0.14	N/A
284	284	N	0.99	0.99	0.95
285	285	NW	0.80	0.80	0.78
286	286	NW	0.30	0.30	0.30
287	287	N	0.11	0.11	0.11
288	288	SE	1.26	1.26	1.13
289	289	NE	0.68	0.68	0.47
290	290	N	0.86	0.86	0.82
291	291	N	0.10	0.10	0.10
292	292	N	1.32	1.32	1.30
293	293	N	0.11	0.11	0.11
294	294	NW	0.14	0.14	0.13
295	295	NE	1.32	1.32	1.19
296	296	N	1.27	1.27	1.20
297	297	N	3.68	3.68	3.45
298	298	N	0.56	0.56	0.50
299	299	NW	0.12	0.12	0.09
300	300	NE	0.23	0.23	0.21
301	301	N	0.11	0.11	0.08
302	302	N	0.19	0.19	0.17
303	303	NE	0.08	0.08	0.05

304	304	N	0.25	0.25	0.21
305	305	NW	2.68	2.68	2.52
306	306	W	0.60	0.60	0.57
307	307	E	0.91	0.91	0.86
308	308	NE	0.33	0.33	0.15
309	309	W	0.12	0.12	0.08
310	310	NE	0.05	0.05	0.04
311	311	N	0.08	0.08	0.07
312	312	NE	0.60	0.60	0.54
313	313	N	0.04	0.04	0.04
314	314	N	0.42	0.42	0.42
315	315	N	0.08	0.08	0.08
316	316	NW	0.37	0.37	0.35
317	317	SE	0.09	0.09	0.09
318	318	N	0.32	0.32	0.32
319	319	NE	0.23	0.23	0.17
320	320	N	0.12	0.12	0.13
321	321	NE	0.14	0.14	0.14
322	322	SE	0.19	0.19	0.17
323	323	W	0.37	0.37	0.34
324	324	N	1.53	1.53	1.47
325	325	NE	1.83	1.83	1.77
326	326	NE	0.40	0.40	0.36
327	327	NE	0.16	0.16	0.16
328	328	NW	0.61	0.61	0.58
329	329	N	0.66	0.66	0.28
330	330	SE	4.29	4.29	4.08
331	331	SE	0.38	0.38	0.36
332	332	NE	0.24	N/A	0.24
333	333	E	0.32	0.32	0.32
334	334	E	0.32	0.32	0.32
335	335	N	2.84	2.84	2.77
336	336	N	0.41	0.41	0.37
337	337	N	0.19	0.19	0.19
338	338	N	0.20	0.20	0.20
339	339	N	0.40	0.40	0.40
340	340	N	0.24	0.24	0.24
341	341	N	3.43	3.43	3.38
342	342	NE	0.12	0.12	0.11
343	343	N	1.48	1.48	1.46
344	344	NE	0.70	0.70	0.63
345	345	SE	0.28	0.28	0.28
346	346	N	0.09	0.09	0.08
347	347	N	0.03	0.03	0.03

348	348	N	0.71	0.71	0.71
349	349	N	0.10	0.10	0.10
350	350	N	0.76	0.76	0.67
351	351	NE	0.77	0.77	0.77
352	352	NE	1.76	1.76	1.67
353	353	N	5.59	5.59	5.50
354	354	NE	0.67	0.67	0.62
355	355	N	1.68	1.68	1.64
356	356	NW	0.10	0.10	0.08
357	357	N	5.07	5.07	4.94
358	358	NW	0.92	0.92	0.80
359	359	N	2.53	2.53	2.49
360	360	NE	0.13	0.13	0.05
361	361	NW	0.43	0.43	0.39
362	362	N	1.54	1.54	1.51
363	363	NE	0.63	0.63	0.61
364	364	NW	0.18	0.18	0.12
365	365	NE	1.39	1.39	1.33
366	366	NW	0.21	0.21	0.20
367	367	NE	0.14	0.14	0.14
368	368	N	0.18	0.18	0.18
369	369	NE	1.18	1.18	1.13
370	370	W	0.28	0.28	0.29
371	371	W	0.36	0.36	0.35
372	372	N	0.24	0.24	0.25
373	373	N	0.16	0.16	0.14
374	374	NW	0.60	0.60	0.59
375	375	N	0.24	0.24	0.22
376	376	NE	0.18	0.18	0.13
377	377	E	0.08	0.08	0.06
378	378	SE	0.47	0.47	0.37
379	379	N	0.14	0.14	0.09
380	380	N	0.09	0.09	0.06
381	381	N	0.87	0.87	0.82
382	382	NE	0.10	0.10	0.07
383	383	N	2.36	2.36	2.32
384	384	N	1.04	1.04	1.00
385	385	N	0.08	0.08	0.08
386	386	NW	0.50	0.50	0.50
387	387	NW	0.08	0.08	0.07
388	388	N	0.24	0.24	0.23
389	389	N	0.20	0.20	0.17
390	390	N	0.20	0.20	0.13
391	391	N	0.08	0.08	0.07

392	392	N	0.51	0.51	0.46
393	393	N	1.05	1.05	1.04
394	394	N	0.26	0.26	0.24
395	395	N	1.55	1.55	1.52
396	396	NW	0.29	0.29	0.29
397	397	N	0.54	0.54	0.54
398	398	N	0.98	0.98	0.95
399	399	W	0.05	0.05	0.05
400	400	N	0.76	0.76	0.75
401	401	N	0.32	0.32	0.32
402	402	SW	0.49	0.49	0.47
403	403	NW	0.14	0.14	0.13
404	404	N	0.23	0.23	0.22
405	405	N	0.29	0.29	0.27
406	406	NE	0.13	0.13	0.11
407	407	NE	0.04	0.04	0.04
408	408	N	0.04	0.04	0.04
409	409	NW	0.04	0.04	0.03
410	410	N	0.07	0.07	0.05
411	411	N	0.14	0.14	0.13
412	412	NW	0.06	N/A	0.05
413	413	N	0.18	0.18	0.18
414	414	NE	0.66	0.66	0.63
415	415	NE	0.27	0.27	0.26
416	416	NE	0.09	0.09	0.06
417	417	N	0.73	0.73	0.69
418	418	W	0.09	0.09	0.08
419	419	N	0.10	0.10	0.06
420	420	N	0.11	0.11	0.11
421	421	NE	0.39	0.06	0.34
422	422	NE	0.95	0.95	0.93
423	423	N	2.87	2.87	2.70
424	424	SE	0.28	0.28	0.28
425	425	N	0.55	0.55	0.47
426	426	N	1.65	1.65	1.55
427	427	NW	0.25	0.25	0.23
428	428	NW	1.13	1.13	1.00
429	429	N	0.27	0.27	0.25
430	430	N	0.60	0.60	0.52
431	431	N	0.26	0.26	0.25
432	432	NE	0.09	0.09	0.07
433	433	NW	1.76	1.76	1.61
434	434	N	0.32	0.32	0.28
435	435	NE	0.30	0.30	0.26

436	436	NE	3.17	3.17	3.00
437	437	N	0.78	0.78	0.78
438	438	N	0.12	0.12	0.11
439	439	NE	0.19	0.19	0.18
440	440	N	0.97	0.97	0.88
441	441	NE	0.14	0.14	0.13
442	442	N	0.15	0.15	0.14
443	443	N	0.18	0.18	0.17
444	444	NE	0.36	0.36	0.32
445	445	W	0.33	0.33	0.30
446	446	NE	0.30	0.30	0.28
447	447	NE	0.24	0.24	0.22
448	448	NW	0.14	0.14	0.12
449	449	NW	0.23	0.23	0.21
450	450	E	0.31	0.31	0.27
451	451	SE	0.73	0.73	0.60
452	452	N	0.35	0.35	0.34
453	453	NE	1.46	1.46	1.41
454	454	N	1.08	1.08	1.06
455	455	NE	0.06	0.06	0.06
456	456	SE	0.12	0.12	0.09
457	457	E	0.29	0.29	0.22
458	458	N	0.62	0.62	0.59
459	459	NE	0.49	0.49	0.41
460	460	N	0.80	0.80	0.78
461	461	NE	0.69	0.69	0.52
462	462	NE	1.01	1.01	0.77
463	463	NE	0.48	0.48	0.44
464	464	NE	1.23	1.23	0.98
465	465	N	0.46	0.46	0.49
466	466	E	0.09	0.09	0.09
467	467	NE	0.48	0.48	0.43
468	468	E	0.66	0.66	0.65
469	469	N	0.07	0.07	0.07
470	470	N	0.24	0.24	0.24
471	471	N	1.31	1.31	0.96
472	472	N	1.15	1.15	0.94
473	473	NW	0.71	0.71	0.61
474	474	NE	0.10	0.10	0.08
475	475	NE	0.56	0.56	0.50
476	476	N	2.56	2.56	2.42
477	477	N	0.11	0.11	0.09
478	478	N	0.07	0.07	0.07
479	479	N	0.45	0.45	0.45

480	480	N	0.37	0.37	0.39
481	481	NE	0.29	0.29	0.25
482	482	W	0.51	0.51	0.48
483	483	N	2.49	2.49	2.29
484	484	SE	1.72	1.72	1.63
485	485	SE	2.67	2.67	N/A
486	486	NE	0.21	0.21	0.20
487	487	N	0.10	0.10	0.07
488	369	N	0.06	1.18	0.06
489	489	N	0.30	0.30	0.30
490	490	NE	0.15	0.15	0.15
491	491	E	0.19	0.19	0.16
492	492	N	0.20	0.20	0.20
493	493	N	0.03	0.03	0.03
494	494	NE	0.09	0.09	0.09
495	495	N	0.13	0.13	0.13
496	496	N	0.05	0.05	0.05
497	497	N	0.25	0.25	0.20
498	498	NE	2.56	2.56	2.56
499	499	E	0.27	0.27	0.26
500	500	E	0.05	0.05	0.05
501	501	NE	0.04	0.04	0.04
502	502	NE	0.17	0.17	0.15
503	503	SE	0.15	0.15	0.14
504	504	N	0.14	0.14	0.13
505	505	N	0.06	0.06	0.06
506	506	N	1.23	1.23	1.23
507	507	NE	0.45	0.45	0.43
508	508	SE	0.21	0.21	0.21
509	509	S	0.31	0.31	0.29
510	510	N	0.11	0.11	0.11
511	511	SE	0.07	0.07	0.07
512	512	NE	0.10	0.10	0.10
513	513	E	0.28	0.28	0.29
514	514	NE	0.93	0.93	0.92
515	515	N	0.79	0.79	0.74
516	516	SE	0.74	0.74	0.66
517	517	SE	0.71	0.71	0.71
518	518	NE	3.18	3.18	2.93
519	519	NE	1.17	1.17	1.10
520	520	NE	1.44	1.44	1.33
521	521	S	0.78	0.78	0.73
522	522	NW	0.48	0.48	0.47
523	523	N	1.93	1.93	1.77

524	524	NE	0.21	0.21	0.18
525	525	NE	0.29	0.29	0.20
526	526	SE	0.70	0.70	0.37
527	527	N	0.62	0.62	0.59
528	528	NW	0.33	0.33	0.27
529	529	NE	2.61	2.61	2.46
530	530	SW	0.34	0.34	0.19
531	531	N	0.44	0.44	0.42
532	532	NE	0.09	0.09	0.09
533	533	NE	1.02	1.02	0.94
534	534	NE	1.84	1.84	1.62
535	535	NE	0.39	0.39	0.33
536	536	N	3.85	3.85	3.59
537	537	N	0.72	0.72	0.67
538	538	NW	0.15	0.15	0.12
539	539	N	1.46	1.46	1.35
540	540	N	0.14	0.14	0.14
541	541	NW	0.08	0.08	0.08
542	542	SW	0.24	0.24	0.22
543	543	SW	0.09	0.09	0.12
544	544	W	0.29	0.29	0.29
545	545	NW	0.23	0.23	0.24
546	546	NE	0.06	0.06	0.06
547	547	N	1.90	1.90	1.59
548	548	NE	0.09	0.09	0.08
549	549	NE	0.27	0.27	0.25
550	550	NE	0.11	0.11	0.11
551	551	NW	0.55	0.55	0.55
552	552	NE	1.91	1.91	1.67
553	553	NE	0.17	0.17	0.15
554	554	NE	0.41	0.41	0.36
555	555	N	0.21	0.21	0.18
556	556	N	0.27	0.27	0.24
557	557	NE	0.99	0.99	0.81
558	558	NE	1.91	1.91	1.74
559	559	NE	0.18	0.18	0.18
560	560	NE	0.15	0.15	0.15
561	561	NE	4.36	4.36	3.96
562	562	NW	0.54	0.54	0.51
563	563	SE	0.34	0.34	0.28
564	564	NW	0.10	0.10	0.10
565	565	NW	0.19	0.19	0.19
566	566	N	0.26	0.26	0.26
567	567	N	13.33	13.33	13.24

568	568	N	13.27	13.27	13.27
569	569	N	2.53	2.53	2.48
570	570	N	0.15	0.15	0.13
571	571	N	0.15	0.15	0.14
572	572	NE	0.27	0.27	0.27
573	573	E	0.08	0.08	0.07
574	574	NE	0.12	0.12	0.12
575	575	E	0.10	0.10	0.08
576	576	N	0.28	0.28	0.21
577	577	E	0.67	0.67	0.44
578	578	SE	0.26	0.26	0.11
579	579	S	0.37	0.37	0.27
580	580	N	0.26	0.26	0.25
581	581	N	0.18	0.18	0.16
582	582	NE	0.07	0.07	0.07
583	583	NE	0.38	0.38	0.33
584	584	S	0.75	0.75	0.70
585	585	S	0.21	0.21	0.21
586	586	NE	0.24	0.24	0.18
587	587	SE	0.12	0.12	0.11
588	588	S	0.16	0.16	0.14
589	589	E	0.38	0.38	0.35
590	590	E	1.76	1.76	1.72
591	591	N	0.51	0.51	0.47
592	592	N	0.16	0.16	0.13
593	593	N	0.21	0.21	0.09
594	594	N	0.63	0.63	0.58
595	595	NE	0.74	0.74	0.68
596	596	S	0.83	0.83	0.79
597	597	SE	2.27	2.27	2.16
598	598	N	1.00	1.00	0.86
599	599	E	0.48	0.48	0.44
600	600	NW	0.64	0.64	0.62
601	601	NE	0.41	0.41	0.26
602	602	NW	0.10	0.10	0.10
603	603	NE	0.27	0.27	0.27
604	604	NE	0.17	0.17	0.15
605	605	NE	0.05	0.05	0.03
606	606	N	0.19	0.19	0.17
607	607	N	0.32	0.32	0.31
608	608	SE	0.68	0.68	0.65
609	609	NW	0.26	0.26	0.24
610	610	N	0.16	0.16	0.15
611	611	E	0.04	0.04	0.03

612	612	N	0.73	0.73	0.70
613	613	NW	0.44	0.44	0.40
614	614	NW	0.24	0.24	0.22
615	615	NW	0.45	0.45	0.34
616	616	NW	0.52	0.52	0.49
617	617	N	0.27	0.27	0.26
618	618	E	0.11	0.11	0.10
619	619	NE	0.28	0.28	0.26
620	620	NE	0.10	0.10	0.09
621	621	NW	0.20	0.20	0.18
622	622	N	0.09	0.09	0.08
623	623	W	0.32	0.32	0.27
624	624	E	0.76	0.76	0.72
625	625	E	0.52	0.52	0.52
626	626	SE	1.09	1.09	1.00
627	627	NE	0.21	0.21	0.14
628	628	NW	0.58	0.58	0.67
629	629	SE	0.18	0.18	0.18
630	630	NE	0.27	0.27	0.24
631	631	NE	0.16	0.16	0.16
632	632	NW	0.12	0.12	0.12
633	633	N	0.17	0.17	0.14
634	634	NE	0.19	0.19	0.19
635	635	N	0.17	0.17	0.15
636	636	NE	0.42	N/A	0.42
637	637	NW	0.33	N/A	0.33
638	638	NE	0.12	0.12	0.14
639	639	NE	0.18	0.18	0.18
640	640	NW	0.09	0.09	0.06
641	641	N	0.25	0.25	0.25
642	642	N	0.46	N/A	0.46
643	643	N	0.53	N/A	0.53
644	644	NE	0.26	0.26	0.26
645	645	N	0.20	0.20	0.20
646	646	NE	0.05	0.05	0.05
647	647	NE	0.16	0.16	0.16
648	648	N	0.13	0.13	0.13
649	649	N	0.07	0.07	0.07
650	650	NW	0.41	0.41	0.41
651	651	NW	0.17	0.17	0.17
652	652	NE	0.28	0.28	0.28
653	653	N	0.16	0.16	0.16
654	654	SE	0.17	0.17	0.17
655	655	SE	0.09	0.09	0.09

656	656	E	0.23	0.23	0.23
657	657	NW	0.10	0.10	0.10
658	658	NE	0.51	N/A	0.51
659	659	NE	0.23	0.23	0.23
660	660	NE	0.10	0.10	0.09
661	661	E	0.26	0.26	0.23
662	662	N	0.10	0.10	0.10
663	663	N	0.14	0.14	0.14
664	664	N	0.04	0.04	0.04
665	665	NE	0.37	0.37	0.37
666	666	NE	0.21	0.21	0.21
667	667	NE	0.67	0.67	0.52
668	668	NE	0.09	0.09	0.09
669	669	NW	1.45	1.45	1.45
670	670	SW	0.38	0.38	0.37
671	671	NW	0.37	0.37	0.35
672	672	SW	0.31	0.31	0.29
673	673	NW	2.51	2.51	2.51
674	674	N	1.28	1.28	1.20
675	675	NE	0.14	0.14	0.14
676	676	N	0.29	0.29	0.29
677	677	N	1.04	1.04	1.04
678	678	N	0.20	N/A	0.20
679	679	NE	0.17	N/A	0.17
680	680	N	0.51	N/A	0.51
681	681	NE	0.34	0.34	0.32
682	682	NW	0.30	0.30	0.26
683	546	NE	0.07	0.06	0.05
684	684	SW	0.14	0.14	0.14
685	685	N	0.18	0.18	0.17
686	686	N	0.14	0.14	0.13
687	687	SE	0.34	0.34	0.27
688	688				
689	689	N	0.05	0.05	0.05
690	690	NW	0.18	0.18	0.07
691	691	SE	0.13	0.13	0.11
692	692	N	0.20	0.20	0.19
693	693	N	0.49	0.49	0.45
694	694	N	0.11	0.11	0.10
695	695	SE	0.72	0.72	0.65
696	696	SW	0.12	0.12	0.10

GLACIER INVENTORY OF THE BASPA BASIN

Sr. No	Glacier ID	Aspect	Area in Sq.km		
			2000	2011	2020
1	697	N	2.37	2.37	2.33
2	698	S	0.15	0.14	0.14
3	699	N	0.11	0.07	0.07
4	700	S	0.25	0.23	0.22
5	701	SE	0.25	0.25	0.25
6	702	SW	1.13	1.13	1.17
7	703	W	0.39	0.42	0.42
8	704	W	0.46	0.44	0.44
9	705	W	0.42	0.45	0.43
10	706	S	0.16	0.16	0.16
11	707	S	0.52	0.49	0.47
12	708	S	0.45	0.43	0.43
13	709	S	1.47	1.31	1.31
14	710	SW	0.77	0.69	0.68
15	711	SW	0.13	0.07	0.07
16	712	S	0.07	0.05	0.02
17	713	S	3.26	3.06	3.06
18	714	S	0.46	0.41	0.41
19	715	SW	0.09	0.06	0.06
20	716	E	0.09	0.10	0.07
21	717	E	0.11	0.07	0.06
22	718	E	0.26	0.23	0.24
23	719	S	0.32	0.24	0.24
24	720	E	0.70	0.61	0.59
25	721	E	0.39	0.34	0.34
26	722	E	0.21	0.18	0.16
27	723	SW	0.17	0.14	0.11
28	724	NW	1.37	1.04	0.95
29	725	SW	0.33	0.28	0.28
30	726	W	0.39	0.32	0.32
31	727	NW	1.57	1.51	1.49
32	728	NW	6.46	6.49	6.56
33	729	N	1.03	1.02	0.97
34	730	N	2.62	2.58	2.51
35	731	N	0.72	0.67	0.59
36	732	W	1.01	1.01	1.12
37	733	N	1.03	0.79	0.75
38	734	W	5.19	5.16	5.18
39	735	NW	0.34	0.32	0.29
40	736	NW	4.95	4.93	4.92

41	737	SE	0.52	0.51	0.49
42	738	NW	31.96	31.74	32.72
43	739	E	1.30	1.16	0.16
44	740	E	0.24	0.23	0.24
45	741	N	0.86	0.72	0.70
46	742	N	0.88	0.65	N/A
47	743	N	5.02	4.97	5.01
48	744	N	5.09	5.02	5.14
49	745	N	1.82	1.80	1.95
50	746	N	0.33	0.24	0.24
51	747	N	6.31	6.22	6.39
52	748	W	2.27	2.26	2.16
53	749	S	4.52	4.16	3.95
54	750	S	1.96	1.72	1.72
55	751	N	24.55	24.51	24.35
56	752	E	0.30	0.25	0.25
57	753	E	0.52	0.48	0.48
58	754	E	0.59	0.55	0.53
59	755	NW	8.76	8.63	8.38
60	756	NW	0.55	0.56	0.54
61	757	NW	3.52	3.52	3.65
62	758	NW	2.80	2.79	2.86
63	759	NW	0.38	0.38	0.42
64	760	W	4.79	4.63	4.74
65	761	S	6.78	5.79	6.67
66	762	W	0.33	0.33	0.34
67	763	W	0.10	0.07	0.07
68	764	S	0.05	0.05	0.04
69	765	N	0.43	0.38	0.43
70	766	SE	0.19	0.17	0.19
71	767	SE	0.21	0.20	0.21
72	768	NE	1.00	0.94	0.99
73	769	N	0.46	0.44	0.47
74	770	NW	0.15	0.14	0.14
75	771	N	0.39	0.29	0.29
76	772	NE	0.32	0.33	0.37
77	773	N	0.41	0.42	0.41
78	774	N	0.36	0.36	0.35
79	775	N	1.01	1.01	1.01
80	151	N	0.29	N/A	N/A
81	152	NE	2.18	N/A	N/A
82	778	N	0.49	0.49	0.49
83	779	E	0.48	0.47	0.47
84	780	NE	1.01	1.01	1.16

85	781	NW	1.86	1.86	2.34
86	782	SE	0.38	0.39	0.48
87	783	NE	0.44	0.44	0.49
88	784	SE	0.94	0.90	0.91
89	785	N	0.86	0.87	0.84
90	786	SE	0.11	0.12	0.08
91	787	SE	0.18	0.18	0.18
92	788	N	0.13	0.14	0.14
93	789	SE	0.13	0.13	0.13
94	790	SE	0.07	0.07	0.07
95	791	SE	0.09	0.08	0.08
96	792	W	0.08	0.08	0.07
97	793	NW	0.11	0.11	0.11
98	794	SE	0.11	0.11	0.11
99	795	NE	0.11	0.11	0.11

GLACIER INVENTORY OF THE LOWER SATLUJ BASIN

Sr. No	Glacier ID	Aspect	Area in Sqkm		
			2000	2011	2020
1	796	N	3.62	3.49	3.49
2	797	NE	6.84	6.84	6.84
3	798	SE	0.78	0.78	0.78
4	799	NE	1.04	0.93	0.93
5	800	NE	4.46	4.24	4.24
6	801	N	1.07	1.04	1.04
7	802	N	3.72	2.21	2.21
8	803	N	0.93	0.77	0.77
9	804	NE	0.59	0.46	0.46
10	805	NE	0.45	0.35	0.35
11	806	NE	1.60	1.55	1.55
12	807	N	2.06	1.90	1.90
13	808	NE	1.11	1.10	1.10
14	809	NE	0.86	0.86	0.86
15	810	NE	0.31	0.31	0.31
16	811	NE	0.13	0.13	0.13
17	812	N	1.11	1.10	1.10
18	813	NE	0.53	0.58	0.58
19	814	NE	1.36	1.31	1.31
20	815	NE	1.29	1.21	1.21
21	816	NE	1.41	1.08	1.08
22	817	NE	2.56	2.46	2.46
23	818	N	3.01	3.00	3.00
24	819	N	0.98	0.97	0.97
25	820	NW	1.29	1.21	1.21
26	821	SW	0.44	N/A	0.44
27	822	SE	0.71	0.62	0.62
28	823	SE	0.16	0.15	0.15
29	824	W	0.26	0.17	0.17
30	825	SW	0.39	0.39	0.39
31	826	SW	0.70	0.57	0.57
32	827	NE	0.41	0.25	0.25
33	828	N	0.40	0.32	0.32
34	829	N	0.22	0.16	0.16
35	830	N	0.47	0.42	0.42
36	831	NE	0.60	0.53	0.53
37	832	N	0.27	0.14	0.14
38	833	N	0.03	0.03	0.03
39	834	NE	6.52	6.52	6.52
40	835	N	5.97	5.79	5.79

41	836	N	0.18	0.15	0.15
42	837	N	0.17	0.14	0.14
43	838	N	0.84	0.74	0.74
44	839	N	0.34	0.34	0.34
45	840	N	4.70	4.58	4.58
46	841	N	0.72	0.53	0.53
47	842	NW	0.77	0.71	0.71
48	843	NW	0.35	0.33	0.33
49	844	W	2.90	2.84	2.84
50	845	E	2.63	2.61	2.61
51	846	E	1.27	1.27	1.27
52	847	SE	0.58	N/A	0.58
53	848	E	0.28	0.28	0.28
54	849	N	8.33	8.29	8.29
55	850	N	0.91	0.86	0.86
56	851	E	1.84	1.81	1.81
57	852	S	1.71	1.69	1.69
58	853	NE	0.70	0.66	0.66
59	854	S	0.38	0.36	0.36
60	855	SE	0.60	0.51	0.51
61	856	E	0.41	0.35	0.35
62	857	N	9.92	9.51	9.51
63	858	NE	3.17	3.06	3.06
64	859	SE	0.35	0.32	0.32
65	860	NE	0.80	0.79	0.79
66	861	E	6.89	6.39	6.39
67	862	NE	2.02	2.02	2.02
68	863	E	1.61	1.39	1.39
69	864	NE	0.24	0.24	0.24
70	865	NW	2.82	2.75	2.75
71	866	NE	2.17	2.04	2.04
72	867	N	2.46	2.27	2.27
73	868	NE	0.31	0.29	0.29
74	869	N	0.89	0.88	0.88
75	870	N	0.63	0.57	0.57
76	871	NE	0.40	0.43	0.43
77	872	SE	0.47	0.38	0.38
78	873	N	0.87	0.87	0.87
79	874	N	0.50	0.70	0.70
80	875	NE	1.91	1.88	1.88
81	876	NE	0.76	0.64	0.64
82	877	E	0.63	N/A	0.56
83	878	E	0.86	0.69	0.69
84	879	NE	0.26	0.17	0.17

85	880	NE	2.68	2.64	2.64
86	881	NE	3.72	3.70	3.70
87	882	NE	1.41	1.41	1.41
88	883	SE	0.57	0.47	0.47
89	884	E	0.84	0.73	0.73
90	885	SE	0.37	0.33	0.33
91	886	SE	0.35	0.29	0.29
92	887	NE	0.29	0.27	0.27
93	888	SW	0.24	0.22	0.22
94	889	NW	0.82	0.83	0.83
95	890	E	1.75	1.68	1.68
96	891	NW	0.73	0.67	0.67
97	863	E	0.76	1.39	1.39
98	893	E	0.75	0.53	0.53
99	894	E	0.37	N/A	0.29
100	895	NE	0.56	N/A	0.57
101	896	NE	0.47	N/A	0.49
102	897	NE	0.25	N/A	0.23
103	898	E	0.15	N/A	0.10
104	899	SE	0.51	N/A	0.46
105	900	SW	0.19	0.19	0.19
106	901	SE	0.47	N/A	0.49
107	902	NE	0.75	N/A	0.67
108	903	SE	0.39	N/A	0.34
109	904	NE	0.43	N/A	0.37
110	905	N	0.22	0.18	0.18
111	906	SE	0.32	N/A	0.31
112	907	S	0.93	N/A	0.88
113	908	E	0.37	0.32	0.32
114	909	E	0.25	0.20	0.20
115	910	SE	0.16	0.16	0.16
116	911	NE	0.31	0.19	0.19
117	912	SW	0.09	N/A	0.07
118	913	SE	0.44	N/A	0.42
119	914	SW	2.53	2.53	2.53
120	915	SE	0.42	N/A	0.36
121	916	SW	0.18	N/A	0.16
122	917	W	0.40	0.34	0.34
123	918	S	0.12	N/A	0.10
124	919	S	0.10	0.09	0.09
125	920	S	0.42	0.34	0.34
126	921	NW	0.49	N/A	0.49
127	922	NW	0.41	0.41	0.41
128	923	S	0.18	N/A	0.18

129	924	SE	0.40	N/A	0.40
130	925	S	0.12	N/A	0.12
131	926	SE	0.17	0.17	0.17
132	927	SW	0.29	0.29	0.29
133	928	SW	0.09	0.09	0.09
134	929	SE	0.05	N/A	0.05
135	930	SE	0.10	0.10	0.10
136	931	S	0.07	0.07	0.07
137	932	SW	0.05	0.05	0.05
138	933	SE	0.11	N/A	0.11
139	934	S	0.06	0.06	0.06
140	935	SE	0.09	0.09	0.09
141	936	SE	0.09	0.09	0.09
142	937	SE	0.27	0.27	0.27
143	938	SE	0.41	0.41	0.41
144	939	NW	0.61	0.61	0.61
145	940	NW	0.28	0.28	0.28
146	941	N	0.22	0.22	0.22
147	942	NW	0.25	0.25	0.25
148	943	NW	3.04	3.04	3.04
149	944	N	5.05	5.05	5.05
150	945	E	6.34	6.34	6.34
151	946	N	3.10	3.10	3.10
152	947	NE	5.90	5.90	5.90
153	948	NE	0.07	0.07	0.07
154	949	NE	1.36	1.36	1.36
155	950	W	2.95	2.95	2.95
156	951	N	0.17	0.17	0.17
157	952	N	0.20	0.20	0.20
158	953	N	0.94	0.94	0.94
159	954	NE	0.21	0.21	0.21
160	955	E	0.16	0.16	0.16
161	956	NE	0.07	0.07	0.07
162	957	E	1.20	1.20	1.20
163	958	NE	0.40	0.40	0.40
164	959	N	0.53	0.53	0.53
165	960	N	1.53	1.53	1.53
166	961	N	1.25	1.25	1.25
167	962	N	0.40	0.40	0.40
168	963	N	0.49	0.49	0.49
169	964	W	0.19	0.19	0.19
170	965	S	0.08	0.08	0.08
171	966	NW	0.65	0.62	0.62
172	967	E	0.07	0.07	0.07

173	968	NE	0.48	0.48	0.48
174	969	NE	0.15	0.15	0.15
175	970	NE	0.41	0.41	0.41
176	971	NE	0.69	0.69	0.69
177	972	NE	0.07	0.07	0.07
178	973	E	0.05	0.05	0.05
179	974	E	0.15	N/A	0.13
180	975	SE	0.12	0.11	0.11
181	976	W	0.10	0.10	0.10
182	977	N	0.16	0.14	0.14
183	978	W	0.08	0.08	0.08
184	979	SW	0.19	N/A	0.19
185	980	N	0.47	0.47	0.47
186	981	SW	0.42	0.42	0.42
187	982	NE	0.41	0.41	0.41
188	983	N	0.17	0.17	0.17
189	984	N	0.97	0.97	0.97
190	985	SE	0.59	0.53	0.53
191	986	E	0.28	0.28	0.28
192	987	S	0.43	N/A	0.43
193	988	SW	1.51	1.51	1.51
194	989	SW	0.71	0.71	0.71
195	990	SE	1.04	0.89	0.89
196	991	S	0.35	0.35	0.35
197	992	E	0.12	0.12	0.12
198	993	SE	0.11	0.11	0.11
199	994	S	0.33	0.33	0.33
200	995	SW	0.22	0.22	0.22
201	996	NE	0.21	0.21	0.21
202	997	NW	0.33	0.33	0.33
203	998	SE	0.18	0.18	0.18
204	999	NE	0.12	0.12	0.12
205	1000	SW	0.08	0.08	0.08
206	1001	W	0.13	0.13	0.13
207	1002	NE	0.15	0.15	0.15
208	1003	SE	0.38	0.35	0.35
209	1004	SE	0.09	0.09	0.09
210	1005	W	0.07	0.07	0.07
211	1006	NE	0.27	0.22	0.22
212	1007	NE	1.10	1.02	1.02
213	1008	NE	0.70	0.67	0.67
214	1009	NE	0.28	0.28	0.28
215	1010	NE	0.26	0.23	0.23
216	1011	NW	0.48	0.48	0.48

217	1012	NW	0.41	0.39	0.39
218	1013	NE	0.26	0.26	0.26
219	1014	NW	0.10	0.10	0.10
220	1015	NW	0.66	0.66	0.66
221	1016	NE	0.36	0.36	0.36
222	1017	NW	1.07	1.07	1.07
223	1018	W	3.20	3.11	3.11
224	1019	N	1.11	0.00	1.11
225	1020	NE	0.26	0.26	0.26
226	1021	NW	0.22	0.22	0.22
227	1022	E	0.45	0.45	0.45
228	1023	SW	0.26	#N/A	0.26
229	1024	NE	0.42	0.42	0.42
230	1025	NE	0.12	0.12	0.12
231	1026	NE	0.30	0.13	0.13
232	1027	N	0.26	N/A	0.26
233	1028	NE	0.77	0.77	0.77
234	1029	N	0.11	0.11	0.11
235	1030	N	0.40	N/A	0.40
236	1031	SE	0.77	0.77	0.77
237	1032	SE	0.47	0.47	0.47
238	1033	W	0.34	0.34	0.34
239	1034	SW	0.45	0.45	0.45
240	1035	E	0.41	0.29	0.29
241	1036	NW	0.18	0.18	0.18
242	1037	NE	0.18	0.14	0.14
243	1038	S	0.37	0.37	0.37
244	1039	S	0.08	0.06	0.06
245	1040	SE	0.20	0.20	0.20
246	1041	N	0.57	0.51	0.51
247	1042	NE	1.13	1.13	1.13
248	1043	N	0.23	0.21	0.21
249	1044	SE	0.07	0.07	0.07
250	1045	NW	0.09	0.09	0.09
251	1046	NE	0.20	0.20	0.20
252	1047	NW	1.54	1.54	1.54
253	1048	NE	0.17	0.17	0.17
254	1049	SW	0.23	0.23	0.23
255	1050	NW	1.47	1.47	1.47
256	1051	N	1.54	1.50	1.50
257	1052	N	0.63	0.60	0.60
258	1053	NW	0.10	0.10	0.10
259	1054	NE	1.36	1.36	1.36
260	1055	N	1.15	1.15	1.15

261	1056	N	0.18	0.13	0.13
262	1057	NW	0.49	0.49	0.49
263	1058	NE	0.83	0.73	0.73
264	1059	N	0.18	0.17	0.17
265	1060	SE	0.12	0.12	0.12
266	1061	NE	1.05	1.05	1.05
267	1062	E	0.06	0.06	0.06
268	1063	N	0.09	N/A	0.09
269	1064	NE	0.44	0.38	0.38
270	1065	NE	0.27	0.27	0.27
271	1066	N	0.43	0.43	0.43
272	1067	W	0.23	0.23	0.23
273	1068	NE	0.08	0.08	0.08
274	1069	E	0.26	0.26	0.26
275	1070	E	0.08	0.08	0.08
276	1071	NE	0.04	N/A	0.04
277	1072	S	0.76	0.76	0.76
278	1073	NE	0.48	0.38	0.38
279	1074	NW	0.05	0.05	0.05
280	1075	SW	0.22	0.22	0.22
281	1076	NE	0.11	N/A	0.11
282	1077	E	0.02	N/A	0.02
283	1078	N	1.25	1.25	1.25
284	1079	E	2.67	2.67	2.67
285	1080	N	0.13	0.13	0.13
286	1081	E	0.19	0.13	0.13
287	1082	N	0.10	0.10	0.10
288	1083	N	0.26	0.26	0.26
289	1084	SE	0.48	0.48	0.48
290	1085	NE	0.24	0.10	0.10
291	1086	SW	0.09	0.09	0.09
292	1087	E	0.17	0.17	0.17
293	1088	NE	0.08	0.07	0.07
294	1089	N	0.56	0.56	0.56
295	1090	N	1.45	1.45	1.45
296	1091	N	0.20	0.19	0.19
297	1092	NE	0.68	0.68	0.68
298	1093	SE	0.38	0.38	0.38
299	1094	SE	0.14	0.14	0.14
300	1095	N	0.13	0.13	0.13
301	1096	NE	0.06	N/A	0.06
302	1097	NE	1.04	1.04	1.04
303	1098	NE	0.20	N/A	0.20
304	1099	NE	0.12	0.12	0.12

305	1100	N	0.14	0.14	0.14
306	1101	SE	0.32	0.32	0.32
307	1102	SE	0.08	0.08	0.08
308	1103	S	0.14	0.12	0.12
309	1104	S	0.03	N/A	0.03
310	1105	SW	0.07	0.07	0.07
311	1106	NE	0.10	0.10	0.10
312	1107	NE	0.14	0.14	0.14
313	1108	SW	0.02	0.02	0.02

GLACIER INVENTORY OF THE UPPER SATLUJ BASIN

Sr. No	Glacier ID	Aspect	Area in Sqkm		
			2000	2011	2020
1	2000	N	0.45	0.39	0.39
2	2001	N	0.03	0.05	0.03
3	2002	N	0.01	N/A	0.01
4	2003	NE	0.06	0.04	0.04
5	2004	NE	0.02	0.02	0.01
6	2005	N	0.11	0.09	0.09
7	2006	N	0.22	0.18	0.16
8	2007	NE	0.05	0.05	0.05
9	2008	NE	0.03	0.01	0.01
10	2009	N	0.17	0.14	0.13
11	2010	N	0.13	0.10	0.09
12	2011	N	0.17	0.12	0.11
13	2012	NE	0.31	0.27	0.26
14	2013	NE	0.18	0.12	0.14
15	2014	N	0.10	0.07	0.06
16	2015	NE	0.18	0.15	0.15
17	2016	NE	0.17	0.16	0.16
18	2017	N	0.39	0.32	0.32
19	2018	N	0.16	0.12	0.09
20	2019	NE	0.20	0.17	0.16
21	2020	NW	0.19	0.16	0.16
22	2021	E	0.37	0.30	0.27
23	2022	N	0.19	0.15	0.14
24	2023	N	0.35	0.30	0.29
25	2024	N	0.17	0.12	0.10
26	2025	N	0.08	0.05	0.05
27	2026	NW	0.07	0.05	0.05
28	2027	N	0.40	0.35	0.33
29	2028	N	0.35	0.31	0.30
30	2029	N	0.36	0.30	0.29
31	2030	N	0.23	0.08	0.08
32	2031	N	0.16	0.11	0.11
33	2032	NW	0.06	0.05	0.05
34	2033	N	1.82	1.72	1.59
35	2034	N	0.48	0.47	0.42
36	2035	N	0.20	0.15	0.14
37	2036	N	0.24	0.19	0.17
38	2037	N	0.06	0.04	0.04
39	2038	NE	0.06	0.05	0.03
40	2039	NE	0.21	0.16	0.15

41	2040	N	0.41	0.33	0.30
42	2041	N	0.08	0.06	0.04
43	2042	NW	0.05	0.03	0.03
44	2043	NW	0.06	0.02	0.02
45	2044	NE	0.15	0.10	0.09
46	2045	NE	0.07	0.04	0.03
47	2046	N	0.44	0.39	0.36
48	2047	NE	0.16	N/A	0.11
49	2048	NE	0.11	0.23	0.08
50	2049	N	0.25	0.22	0.19
51	2050	N	0.14	0.10	0.09
52	2051	NE	0.14	0.09	0.08
53	2052	NE	0.11	0.08	0.06
54	2053	NE	0.20	0.18	0.15
55	2054	NE	0.11	0.08	0.07
56	2055	NE	0.16	0.13	0.12
57	2056	N	0.20	0.15	0.14
58	2057	N	0.11	0.05	0.04
59	2058	N	0.19	0.12	0.11
60	2059	N	0.07	0.03	0.03
61	2060	N	0.10	0.06	0.06
62	2061	N	0.12	0.08	0.08
63	2062	N	0.14	0.08	0.08
64	2063	NE	0.17	0.14	0.05
65	2064	NE	0.14	0.09	0.08
66	2065	NE	0.05	0.03	0.02
67	2066	N	0.04	0.03	0.03
68	2067	N	0.56	0.35	0.30
69	2068	N	0.10	0.09	0.08
70	2069	N	0.20	0.15	0.13
71	2070	N	0.21	0.16	0.14
72	2071	NE	0.14	0.07	0.07
73	2072	N	0.11	0.08	0.07
74	2073	NE	0.03	0.03	0.03
75	2074	N	0.57	0.49	0.54
76	2075	NE	0.05	0.04	0.03
77	2076	N	0.22	0.21	0.19
78	2077	NE	0.08	0.05	0.04
79	2078	SE	1.55	1.50	N/A
80	2079	NW	0.50	0.42	0.40
81	2080	N	0.09	0.06	0.06
82	2081	N	0.04	0.03	0.03
83	2082	NE	0.07	0.04	0.04
84	2083	N	0.03	0.02	0.02

85	2084	N	0.04	0.02	0.02
86	2085	NE	0.07	0.07	0.06
87	2086	NE	0.18	0.15	0.15
88	2087	SE	0.04	0.03	0.02
89	2088	S	0.23	0.19	0.19
90	2089	NW	0.08	0.08	0.08
91	2090	E	1.05	0.87	0.86
92	2091	SE	0.87	0.76	0.72
93	2092	N	0.18	0.12	0.12
94	2093	NE	0.08	0.06	0.06
95	2094	NE	0.10	0.07	0.09
96	2095	NE	0.05	0.05	0.05
97	2096	N	0.17	N/A	0.16
98	2097	N	0.21	0.16	N/A
99	2098	NE	0.09	0.04	0.03
100	2099	SE	4.49	4.40	4.31
101	2100	N	0.17	0.12	0.11
102	2101	NE	0.11	0.06	0.05
103	2102	N	0.04	0.03	0.03
104	2103	NE	0.19	0.15	0.14
105	2104	SE	4.69	4.38	4.32
106	2105	NW	0.36	0.30	0.29
107	2106	SE	0.22	0.22	0.20
108	2107	E	0.10	0.09	0.07
109	2108	W	0.29	0.16	0.16
110	2109	NE	0.18	0.16	0.16
111	2110	SE	2.15	2.12	2.07
112	2111	SE	1.26	1.13	1.05
113	2112	SE	0.54	0.51	0.53
114	2113	SE	0.11	N/A	0.10
115	2114	NE	0.51	N/A	0.48
116	2115	N	0.45	0.43	0.41
117	2116	NW	0.13	0.12	0.11
118	2117	N	0.13	0.10	0.10
119	2118	NW	0.05	0.05	0.05
120	2119	SE	0.30	0.29	0.28
121	2120	E	0.46	0.41	0.42
122	2121	NE	0.29	0.21	0.29
123	2122	NE	0.78	0.76	0.74
124	2123	NE	0.48	0.50	0.48
125	2124	N	0.47	0.44	0.36
126	2125	SE	0.07	0.05	0.06
127	2126	NE	1.45	1.31	1.21
128	2127	N	1.02	1.04	0.89

129	2128	E	0.68	0.67	0.58
130	2129	NE	1.34	1.21	1.04
131	2130	N	1.16	0.96	0.91
132	2131	N	2.51	2.28	2.24
133	2132	NW	0.27	0.15	0.14
134	2133	N	22.93	22.67	22.05
135	2134	NE	6.59	6.19	6.06
136	2135	NE	2.33	2.20	1.99
137	2136	N	0.52	0.42	0.41
138	2137	NE	22.15	21.42	21.50
139	2138	N	0.90	0.87	0.86
140	2139	NW	0.20	0.16	0.15
141	2140	N	0.83	0.82	0.74
142	2141	N	0.42	0.40	0.38
143	2142	NE	0.41	0.44	0.41
144	2143	NE	0.23	0.23	0.23
145	2144	SE	0.78	0.68	0.68
146	2145	N	0.26	0.21	0.18
147	2146	N	0.63	0.51	0.51
148	2147	N	1.48	1.32	1.22
149	2148	NE	0.12	0.11	0.10
150	2149	W	0.38	0.29	0.26
151	2150	N	2.61	2.35	2.18
152	2151	NE	0.44	0.37	0.36
153	2152	NE	0.21	0.17	0.16
154	2153	N	0.64	0.56	0.55
155	2154	N	0.13	0.10	0.09
156	2155	N	0.64	0.23	0.16
157	2156	NE	0.35	0.18	0.16
158	2157	NE	0.68	0.34	0.31
159	2158	N	0.29	0.21	0.19
160	2159	NW	0.12	0.10	0.10
161	2160	NE	0.28	0.20	0.19
162	2161	NE	0.20	0.15	0.13
163	2162	N	0.16	0.09	0.08
164	2163	NE	0.11	0.08	0.08
165	2164	N	0.05	0.03	0.01
166	2165	N	0.13	0.04	0.04
167	2166	NE	3.25	2.89	2.60
168	2167	N	1.65	1.55	1.49
169	2168	NE	1.75	1.63	1.50
170	2169	N	1.06	0.93	0.94
171	2170	NE	0.27	0.28	0.27
172	2171	E	0.64	0.57	0.59

173	2172	NW	0.78	0.79	0.75
174	2173	NE	0.61	0.64	0.53
175	2174	NW	0.19	0.19	0.17
176	2175	NW	0.21	0.20	0.17
177	2176	N	5.99	5.92	5.96
178	2177	NE	0.36	0.30	0.28
179	2178	NE	0.35	0.22	0.22
180	2179	NE	0.38	0.18	0.16
181	2180	N	0.08	0.06	0.06
182	2181	N	0.69	0.70	0.69
183	2182	N	1.57	1.38	1.29
184	2183	NE	0.34	0.30	0.29
185	2184	W	0.16	0.11	0.11
186	2185	N	0.28	0.19	0.17
187	2186	N	0.60	0.43	0.38
188	2187	N	0.28	0.30	0.28
189	2188	N	0.17	0.13	0.12
190	2189	NE	0.08	0.05	0.05
191	2190	N	0.10	0.06	0.05
192	2191	NE	0.07	0.12	0.07
193	2192	N	0.45	0.32	0.28
194	2193	N	0.23	0.17	0.16
195	2194	NW	0.38	0.24	0.22
196	2195	NW	1.12	1.09	1.05
197	2196	N	0.93	1.19	0.93
198	2197	N	2.40	2.20	2.08
199	2198	N	0.90	0.87	0.87
200	2199	N	0.16	0.17	0.16
201	2200	N	0.07	0.11	0.07
202	2201	NE	7.99	8.04	7.68
203	2202	SE	0.78	0.78	0.75
204	2203	N	0.10	0.08	0.06
205	2204	NW	0.24	0.16	0.16
206	2205	SW	1.12	1.00	0.95
207	2206	NW	1.32	0.64	1.18
208	2207	N	0.12	0.10	0.08
209	2208	N	0.28	0.03	0.03
210	2209	W	0.90	0.83	0.82
211	2210	S	0.22	0.15	0.17
212	2211	NE	0.30	0.25	0.25
213	2212	SE	0.18	0.12	0.12
214	2213	E	0.13	0.09	0.08
215	2214	NE	1.02	0.91	0.87
216	2215	N	0.22	0.18	0.18

217	2216	N	0.04	0.03	0.03
218	2217	E	0.64	0.53	0.47
219	2218	NW	1.86	1.75	1.65
220	2219	W	3.03	2.84	2.81
221	2220	N	0.98	0.93	0.90
222	2221	N	0.59	0.54	0.52
223	2222	NE	0.15	0.09	0.09
224	2223	W	1.59	1.49	1.47
225	2224	NE	0.09	0.05	0.05
226	2225	NW	0.22	0.12	0.07
227	2226	NW	0.08	0.03	0.03
228	2227	N	0.04	0.02	0.02
229	2228	N	0.73	0.68	0.64
230	2229	NW	0.16	0.16	0.16
231	2230	NE	0.05	0.05	0.05
232	2231	NE	0.04	0.04	0.04
233	2232	N	0.04	0.04	0.04
234	2233	NW	0.06	0.06	0.06
235	2234	NE	0.07	0.06	0.05
236	2235	N	0.18	0.13	0.12
237	2236	NE	0.15	0.12	0.11
238	2237	N	0.48	0.41	0.40
239	2238	NE	0.10	0.05	0.05
240	2239	N	0.29	0.23	0.22
241	2240	N	0.18	0.17	0.16
242	2241	NE	0.25	0.12	0.11
243	2242	N	0.20	0.17	0.16
244	2243	N	0.06	0.03	0.03
245	2244	N	0.18	0.15	0.16
246	2245	N	0.09	0.04	0.04
247	2246	N	0.08	0.06	0.06
248	2247	N	10.97	10.89	10.68
249	2248	N	12.86	10.69	12.15
250	2249	SW	0.85	0.89	0.75
251	2250	W	0.57	0.49	0.45
252	2251	N	0.18	0.15	0.13
253	2252	N	0.23	0.19	0.20
254	2253	N	0.55	0.46	0.45
255	2254	N	0.37	0.27	0.24
256	2255	N	0.18	0.12	0.10
257	2256	NW	0.08	0.04	0.04
258	2257	N	0.22	0.15	0.13
259	2258	NE	0.22	0.14	0.12
260	2259	N	0.12	0.09	0.09

261	2260	NW	0.17	0.14	0.14
262	2261	N	0.14	0.10	0.09
263	2262	NW	0.36	0.26	0.25
264	2263	N	0.60	0.48	0.46
265	2264	NW	0.29	0.23	0.22
266	2265	N	0.55	0.46	0.44
267	2266	N	1.56	1.41	1.40
268	2267	NE	0.19	0.12	0.13
269	2268	NW	0.13	0.11	0.09
270	2269	N	0.20	0.15	0.15
271	2270	NW	1.19	1.06	1.05
272	2271	N	1.75	1.50	1.49
273	2272	N	0.55	0.45	0.42
274	2273	NE	0.15	0.11	0.11
275	2274	NW	0.14	0.12	0.10
276	2275	NW	0.77	0.47	0.46
277	2276	NW	0.09	0.07	0.07
278	2277	NE	0.27	0.18	0.17
279	2278	N	1.11	0.96	0.95
280	2279	NW	0.49	0.39	0.37
281	2280	NW	0.64	0.47	0.41
282	2281	SW	0.81	0.71	0.70
283	2282	SW	0.62	0.43	0.35
284	2283	NE	1.64	1.50	1.46
285	2284	NW	0.79	0.59	0.67
286	2285	S	0.80	0.57	0.52
287	2286	SW	1.54	1.27	1.21
288	2287	NW	1.45	1.21	1.23
289	2288	S	0.57	0.26	0.30
290	2289	NE	0.20	0.16	0.17
291	2290	NE	0.14	0.11	0.11
292	2291	NE	0.10	0.07	0.07
293	2292	E	0.09	0.08	0.08
294	2293	NW	0.57	0.47	0.51
295	2294	NE	0.10	0.08	0.08
296	2295	N	0.31	0.25	0.26
297	2296	NE	0.75	0.63	0.59
298	2297	N	0.20	0.11	0.11
299	2298	NW	0.08	0.06	0.06
300	2299	N	0.09	0.05	0.05
301	2300	N	0.13	0.09	0.10
302	2301	N	0.32	0.23	0.21
303	2302	N	0.62	0.39	0.34
304	2303	NE	0.61	0.41	0.42

305	2304	E	0.23	0.17	0.15
306	2305	N	0.44	0.32	0.31
307	2306	NE	0.22	0.07	0.06
308	2307	NE	0.20	0.15	0.14
309	2308	NE	0.03	0.03	0.03
310	2309	N	0.28	0.25	0.24
311	2310	N	0.11	0.09	0.09
312	2311	N	0.47	0.26	0.23
313	2312	NW	0.45	0.27	0.25
314	2313	N	0.58	0.49	0.47
315	2314	NE	0.06	0.05	0.05
316	2315	N	0.14	0.10	0.08
317	2316	NW	0.44	0.36	0.34
318	2317	NW	0.72	0.66	0.65
319	2318	N	0.18	0.14	0.14
320	2319	NW	0.05	0.03	0.03
321	2320	N	0.17	0.13	0.12
322	2321	N	0.06	0.05	0.05
323	2322	NW	0.05	0.04	0.04
324	2323	N	0.99	0.86	0.86
325	2324	NW	0.33	0.25	0.23
326	2325	N	0.09	0.08	0.05
327	2326	NE	0.35	0.29	0.29
328	2327	N	0.31	0.31	0.31
329	2328	NE	3.76	3.44	3.36
330	2329	NW	0.39	0.23	0.22
331	2330	N	0.32	0.27	0.25
332	2331	N	0.87	0.74	0.72
333	2332	N	0.28	0.18	0.13
334	2333	N	1.57	1.34	1.24
335	2334	N	0.19	0.15	0.14
336	2335	N	1.36	1.30	1.13
337	2336	N	0.16	0.13	0.11
338	2337	NE	5.27	4.65	4.17
339	2338	N	2.39	2.11	1.94
340	2339	NE	2.70	2.64	2.31
341	2340	NW	1.80	1.16	1.51
342	2341	N	0.31	0.26	0.26
343	2342	N	0.80	0.93	0.80
344	2343	N	0.30	0.24	0.22
345	2344	N	0.16	0.10	0.09
346	2345	NE	1.38	1.29	1.22
347	2346	NW	0.53	0.34	0.32
348	2347	NW	0.68	0.57	0.54

349	2348	NE	0.20	0.23	0.15
350	2349	NE	0.59	0.41	0.31
351	2350	N	0.29	0.23	0.22
352	2351	N	0.18	0.14	0.14
353	2352	NE	8.19	8.63	7.84
354	2353	N	4.69	4.63	4.58
355	2354	N	1.18	0.99	0.92
356	2355	N	0.29	0.23	0.22
357	2356	N	0.22	0.16	0.14
358	2357	NE	2.45	2.13	2.01
359	2358	NE	6.07	6.13	5.60
360	2359	NE	4.68	4.41	4.07
361	2360	NE	2.35	2.14	2.05
362	2361	N	6.34	4.80	4.50
363	2362	E	1.83	1.58	1.47
364	2363	E	1.61	1.32	1.38
365	2364	N	1.01	0.86	0.83
366	2365	NE	4.63	4.42	4.16
367	2366	NE	2.01	1.81	1.63
368	2367	NE	1.61	1.44	1.36
369	2368	NE	12.79	12.23	12.42
370	2369	NE	6.50	6.37	6.12
371	2370	NE	2.47	2.32	2.21
372	2371	NE	4.51	4.12	3.98
373	2372	N	1.27	1.15	1.10
374	2373	NE	0.46	0.39	0.40
375	2374	NE	2.26	2.15	2.08
376	2375	NE	0.82	0.63	0.65
377	2376	NW	0.09	0.05	0.04
378	2377	NE	0.04	0.04	0.04
379	2378	S	0.40	0.31	0.44
380	2379	S	0.62	0.47	0.51
381	2380	SE	0.21	0.14	0.14
382	2381	W	0.86	0.72	0.70
383	2382	NW	0.15	0.13	0.11
384	2383	NW	0.93	0.69	0.66
385	2384	N	0.24	0.18	0.18
386	2385	N	0.22	0.17	0.17
387	2386	NW	0.14	0.08	0.09
388	2387	N	2.40	2.18	2.19
389	2388	N	0.56	0.54	0.51
390	2389	N	1.25	0.98	1.07
391	2390	N	1.26	1.28	1.23
392	2391	N	4.43	4.38	4.28

393	2392	N	1.51	1.43	1.34
394	2393	N	0.76	0.67	0.60
395	2394	W	0.39	0.35	0.33
396	2395	N	1.28	1.26	1.23
397	2396	N	0.26	0.24	0.24
398	2397	N	0.26	0.26	0.23
399	2398	NE	0.21	0.18	0.18
400	2399	NW	0.15	0.14	0.14
401	2400	NW	0.15	0.15	0.14
402	2401	N	0.23	0.26	0.23
403	2402	N	0.15	0.13	0.10
404	2403	NE	0.20	0.17	0.13
405	2404	NE	0.52	0.44	0.30
406	2405	NE	0.34	0.34	0.31
407	2406	N	0.29	0.25	0.21
408	2407	N	0.09	0.44	0.09
409	2408	N	0.29	N/A	0.20
410	2409	N	0.44	0.41	0.34
411	2410	N	1.46	1.36	1.35
412	2411	N	0.11	0.09	0.09
413	2412	N	0.37	0.17	0.17
414	2413	NE	0.11	0.09	0.09
415	2414	NE	0.24	0.20	0.20
416	2415	N	0.72	0.46	0.47
417	2416	N	0.88	0.81	0.82
418	2417	N	0.54	0.08	0.08
419	2418	N	0.89	0.27	0.24
420	2419	N	0.13	0.07	0.07
421	2420	N	0.26	0.21	0.20
422	2421	N	0.06	0.04	0.04
423	2422	NW	0.03	0.02	0.02
424	2423	NE	0.34	0.29	0.29
425	2424	NW	1.07	0.93	0.91
426	2425	NE	0.11	0.08	0.07
427	2426	NW	0.08	0.06	0.06
428	2427	N	0.24	0.15	0.13
429	2428	NW	0.15	0.08	0.08
430	2429	N	0.16	0.12	0.11
431	2430	NE	0.06	0.03	0.02
432	2431	NE	0.08	N/A	0.06
433	2432	NE	0.05	0.02	0.02
434	2267	N	0.45	0.12	0.19
435	2434	NW	0.19	0.09	0.08
436	2435	NE	0.04	0.02	0.01

437	2436	N	0.30	0.21	0.21
438	2437	N	0.13	0.09	0.08
439	2438	NE	0.34	0.33	0.31
440	2439	NW	0.34	0.19	0.30
441	2440	NE	0.15	0.09	0.10
442	2441	SE	0.41	0.36	0.34
443	2442	NE	22.90	22.70	22.08
444	2443	SW	0.07	0.07	0.07
445	2444	SE	0.12	0.08	0.08
446	2445	NE	0.04	0.05	0.04
447	2446	NE	0.11	0.07	0.07
448	2447	E	0.10	0.02	0.02
449	2179	N	0.07	0.18	0.05
450	2449	N	0.12	0.08	0.08
451	2450	NE	0.73	0.67	0.57
452	2451	NW	0.17	0.15	0.15
453	2452	NW	0.19	0.14	0.14
454	2453	NE	0.33	0.30	0.29
455	2454	N	0.15	0.12	0.12
456	2455	N	0.04	0.04	0.04
457	2456	N	0.84	0.76	0.74
458	2457	N	0.67	0.59	0.61
459	2458	NW	0.70	0.53	0.53
460	2459	E	0.20	#N/A	0.17
461	2460	NE	0.19	0.04	0.04
462	2461	N	1.37	1.24	1.24
463	2462	S	0.34	0.30	0.27
464	2463	NW	0.04	0.04	0.04
465	2464	N	0.87	0.80	0.75
466	2465	E	0.29	0.24	0.24
467	2466	NE	0.09	0.06	0.05
468	2467	S	0.06	0.05	0.04
469	2468	S	0.20	0.16	0.16
470	2469	NE	0.07	0.08	0.07
471	2470	E	0.42	0.35	0.33
472	2471	E	0.12	0.11	0.10
473	2472	NE	0.25	0.23	0.24
474	2473	NE	0.10	0.07	0.06
475	2474	NW	0.38	0.38	0.38
476	2475	W	0.14	0.06	0.06
477	2476	N	0.11	0.08	0.07
478	2477	N	0.24	0.20	0.20
479	2478	N	0.15	0.11	0.10
480	2479	N	0.08	0.06	0.06

481	2480	N	0.13	0.10	0.09
482	2481	NW	0.07	0.04	0.04
483	2151	NE	0.06	0.37	0.04
484	2483	NE	0.06	0.05	0.04
485	2484	NE	0.13	0.12	0.12
486	2485	NE	0.19	0.14	0.12
487	2486	E	47.04	46.82	46.82
488	2487	N	0.13	0.13	0.13
489	2488	NW	0.03	0.02	0.02
490	2489	NW	0.07	0.04	0.03
491	2490	NW	0.23	0.16	0.15
492	2491	E	0.02	0.02	0.02
493	2492	NE	0.18	0.15	0.14
494	2493	E	0.31	0.22	0.31
495	2494	N	0.31	0.27	0.26
496	2495	NW	0.82	0.68	0.63
497	2496	N	0.11	0.06	0.06
498	2497	N	0.24	0.19	0.17
499	2498	N	0.07	0.05	0.05
500	2499	N	0.12	0.10	0.10
501	2500	NW	0.39	0.25	0.25
502	2501	N	0.60	0.47	0.45
503	2502	N	0.12	0.05	0.05
504	2503	NE	0.05	0.04	0.03
505	2504	N	0.03	0.02	0.02
506	2505	NE	0.01	0.01	0.01
507	2506	N	0.28	0.24	0.21
508	2507	NW	0.22	0.11	0.08
509	2508	N	0.09	0.02	0.02
510	2509	N	0.01	0.01	0.01
511	2510	N	0.01	0.01	0.01
512	2511	N	0.07	0.07	0.07
513	2512	NE	0.02	0.02	0.02
514	2513	NE	0.12	0.13	0.12
515	2514	N	0.02	0.02	0.02
516	2515	N	0.11	0.06	0.05
517	2516	NE	0.10	0.08	0.07
518	2517	N	0.13	0.09	0.07
519	2518	NE	0.15	0.09	0.09
520	2519	N	0.06	0.03	0.02
521	2520	NE	0.04	0.03	0.03
522	2521	SE	0.40	0.35	0.41
523	2522	N	0.13	0.11	0.10
524	2523	NE	0.09	0.10	0.08

525	2524	N	0.36	0.30	0.31
526	2525	NE	0.11	0.10	0.09
527	2526	NE	0.13	0.11	0.10
528	2527	NW	0.07	0.08	0.07
529	2528	N	0.04	0.03	0.02
530	2529	NE	0.03	0.02	0.02
531	2530	NE	0.11	0.06	0.05
532	2531	NW	0.02	0.02	0.02
533	2532	E	0.02	0.01	0.01
534	2533	NE	0.16	0.10	0.08
535	2534	NE	0.09	0.07	0.05
536	2535	NE	0.06	0.05	0.04
537	2536	NW	0.02	N/A	0.02
538	2537	N	0.14	0.13	0.14
539	2538	N	0.02	0.02	0.02
540	2539	NE	0.02	0.03	0.02
541	2540	NE	0.11	0.09	0.09
542	2541	N	0.08	0.04	0.04
543	2542	N	0.02	0.02	0.02
544	2543	NW	0.01	N/A	0.01
545	2544	NE	0.10	0.11	0.10
546	2545	N	0.07	N/A	0.03
547	2546	NW	0.04	0.04	0.04
548	2547	N	0.06	0.03	0.03
549	2548	N	0.05	0.03	0.03
550	2549	N	0.05	0.03	0.03
551	2550	NE	0.01	0.01	0.01
552	2551	N	0.01	0.01	0.01
553	2552	NE	0.07	0.03	0.02
554	2553	N	0.19	0.11	0.06
555	2554	NE	0.10	0.07	0.07
556	2555	NE	0.05	0.03	0.03
557	2556	NE	0.12	0.07	0.07
558	2557	N	0.30	0.10	0.06
559	2558	NE	0.08	0.04	0.03
560	2559	N	0.08	0.04	0.04
561	2560	N	0.11	0.03	0.04
562	2561	NE	0.22	0.17	0.18
563	2562	NE	0.05	0.04	0.04
564	2563	N	0.14	0.07	0.07
565	2564	NE	0.16	0.13	0.14
566	2565	N	0.16	0.15	0.15
567	2566	N	0.09	0.08	0.07
568	2567	N	0.17	0.13	0.13

569	2568	N	0.10	0.08	0.09
570	2569	NE	0.12	0.07	0.10
571	2570	NE	0.03	N/A	0.02
572	2571	NE	0.11	0.09	0.08
573	2572	E	0.04	0.03	0.06
574	2573	NW	0.17	0.15	0.16
575	2574	E	0.18	0.12	0.13
576	2575	NW	0.24	0.16	0.22
577	2576	NW	0.04	0.04	0.03
578	2577	N	0.01	N/A	0.01
579	2578	N	0.01	N/A	0.00
580	2579	NE	0.09	N/A	0.05
581	2580	N	0.02	0.02	0.02
582	2581	NW	0.01	0.01	0.01
583	2582	N	0.15	0.12	0.12
584	2583	N	0.05	0.03	0.03
585	2584	E	0.04	0.04	0.03
586	2585	N	0.14	N/A	0.01
587	2586	N	0.83	N/A	0.83
588	2587	NE	0.04	N/A	0.04
589	2588	N	0.70	0.58	N/A
590	2589	N	0.09	0.04	0.04
591	2590	NE	0.061	N/A	N/A
592	2155A	N	---	0.08	N/A
593	2275A	NW	---	0.05	N/A
594	2357A	NE	---	0.15	N/A
595	2361A	N	----	1.01	0.99

ANNEXURE II

RETREAT RATES OF GLACIERS IN SPITI BASIN

Sr. No	Glacier ID	Retreat in meter	Retreat Rate (m/year)	Glacier Type	Aspect	Area in Sq.km	
						2000	2020
1	3	144.250	7.212	Glacier	SE	1.534	1.429
2	4	108.261	5.413	Glacier	NE	0.677	0.613
3	5	116.156	5.808	Glacier	NE	7.583	7.563
4	6	138.034	6.902	Glacier	N	8.121	7.999
5	7	67.014	3.351	Glacier	SE	0.281	0.241
6	9	136.838	6.842	Glacier	E	1.426	1.279
7	13	88.018	4.401	Glacier	E	8.122	7.799
8	14	281.603	14.080	Glacier	SE	1.622	1.361
9	21	37.307	1.865	Glacier	NE	6.221	6.170
10	24	134.684	6.734	Glacier	N	12.332	12.299
11	25	123.010	6.150	Glacier	NE	1.546	1.454
12	26	135.247	6.762	Glacier	NE	2.705	2.459
13	27	73.400	3.670	Glacier	SE	0.423	0.405
14	28	322.224	16.111	Glacier	NE	0.167	0.112
15	29	213.931	10.697	Glacier	NE	1.040	0.987
16	32	127.387	6.369	Glacier	E	0.531	0.397
17	33	255.093	12.755	Glacier	NE	0.437	0.351
18	34	770.425	38.521	Glacier	N	8.564	8.049
19	35	290.336	14.517	Glacier	SE	0.752	0.540
20	36	75.334	3.767	Glacier	N	0.615	0.570
21	37	85.082	4.254	Glacier	NE	0.205	0.163
22	38	94.957	4.748	Glacier	NE	0.339	0.312
23	39	50.906	2.545	Glacier	N	0.479	0.413
24	40	68.435	3.422	Glacier	NE	0.539	0.518
25	42	194.037	9.702	Glacier	NE	1.785	1.771
26	43	241.319	12.066	Glacier	NE	1.042	0.914
27	48	213.680	10.684	Glacier	N	0.234	0.165
28	49	59.526	2.976	Glacier	NE	2.990	2.967
29	51	178.856	8.943	Glacier	NE	2.055	1.944
30	52	148.729	7.436	Glacier	NE	0.384	0.357
31	53	116.441	5.822	Glacier	SE	0.324	0.266
32	56	143.828	7.191	Glacier	SE	2.123	1.965
33	57	176.535	8.827	Glacier	NE	0.207	0.170
34	58	217.793	10.890	Glacier	N	1.195	1.081
35	59	141.867	7.093	Glacier	NW	0.692	0.534
36	60	311.475	15.574	Glacier	N	3.916	3.535
37	61	56.395	2.820	Glacier	N	0.469	0.384
38	63	201.517	10.076	Glacier	N	1.239	1.018

39	64	400.006	20.000	Glacier	N	0.307	0.222
40	65	210.804	10.540	Glacier	N	0.304	0.258
41	66	105.908	5.295	Glacier	N	0.231	0.217
42	67	120.406	6.020	Glacier	N	0.309	0.279
43	68	93.747	4.687	Glacier	N	0.473	0.382
44	69	102.227	5.111	Glacier	SE	11.376	11.137
45	70	118.360	5.918	Glacier	SE	0.673	0.670
46	71	109.741	5.487	Glacier	S	1.129	0.974
47	72	391.676	19.584	Glacier	NE	2.400	2.154
48	73	203.701	10.185	Glacier	E	1.104	0.939
49	74	143.819	7.191	Glacier	NE	0.726	0.625
50	75	29.012	1.451	Glacier	SE	0.883	0.839
51	78	123.083	6.154	Glacier	NE	0.306	0.224
52	79	129.535	6.477	Glacier	NE	0.489	0.400
53	80	118.652	5.933	Glacier	N	0.839	0.764
54	81	104.886	5.244	Glacier	NE	0.519	0.409
55	82	117.537	5.877	Glacier	NW	0.380	0.346
56	83	65.486	3.274	Glacier in	NE	0.214	0.205
57	90	189.741	9.487	Glacier	N	1.088	1.027
58	94	496.368	24.818	Glacier	SE	0.217	0.109
59	96	130.949	6.547	Glacier	NE	8.395	8.338
60	98	80.063	4.003	Glacier	N	1.037	0.921
61	100	429.316	21.466	Glacier	N	1.767	1.652
62	101	69.762	3.488	Glacier	N	1.132	1.096
63	102	137.671	6.884	Glacier	N	0.289	0.220
64	103	127.843	6.392	Glacier	N	0.244	0.218
65	104	58.288	2.914	Glacier	NE	0.572	0.562
66	106	27.820	1.391	Glacier	N	0.234	0.212
67	107	92.269	4.613	Glacier	N	0.622	0.566
68	109	48.415	2.421	Glacier	N	0.814	0.785
69	110	118.153	5.908	Glacier	E	0.254	0.205
70	111	23.683	1.184	Glacier	E	0.140	0.125
71	112	68.831	3.442	Glacier	N	0.376	0.363
72	113	25.299	1.265	Glacier	NW	0.128	0.115
73	114	117.945	5.897	Glacier	N	0.504	0.450
74	115	38.353	1.918	Glacier	NE	0.410	0.349
75	116	41.984	2.099	Glacier	NE	1.218	1.206
76	117	86.231	4.312	Glacier	NE	4.477	4.456
77	118	68.678	3.434	Glacier	N	0.856	0.691
78	120	65.097	3.255	Glacier	N	0.535	0.497
79	123	129.025	6.451	Glacier	N	0.992	0.914
80	124	125.289	6.264	Glacier	N	0.395	0.317
81	126	215.184	10.759	Glacier	NE	4.285	4.179
82	127	205.769	10.288	Glacier	N	0.425	0.351

83	128	116.056	5.803	Glacier	N	2.163	1.886
84	129	58.292	2.915	Glacier	NW	0.164	0.137
85	130	59.778	2.989	Glacier	NE	0.241	0.207
86	133	187.037	9.352	Glacier	N	1.158	1.025
87	134	292.490	14.625	Glacier	N	0.818	0.704
88	139	221.810	11.090	Glacier	NE	0.981	0.839
89	140	141.619	7.081	Glacier	N	2.326	2.115
90	141	141.412	7.071	Glacier	N	0.667	0.569
91	144	58.405	2.920	Glacier	N	0.130	0.070
92	145	101.887	5.094	Glacier	NE	1.078	1.057
93	147	61.832	3.092	Glacier	NW	2.804	2.748
94	151	325.255	16.263	Glacier	N	0.618	0.477
95	152	63.573	3.179	Glacier	N	0.358	0.292
96	153	72.856	3.643	Glacier	NE	1.046	0.911
97	154	60.209	3.010	Glacier	NE	0.251	0.190
98	155	71.234	3.562	Glacier	N	0.466	0.455
99	156	275.175	13.759	Glacier	N	0.367	0.312
100	157	97.665	4.883	Glacier	N	0.190	0.180
101	158	137.654	6.883	Glacier	N	0.862	0.822
102	163	25.974	1.299	Glacier	N	0.281	0.258
103	164	50.395	2.520	Glacier	N	0.235	0.191
104	165	131.538	6.577	Glacier	N	0.174	0.156
105	168	73.227	3.661	Glacier	N	0.162	0.151
106	169	24.647	1.232	Glacier	N	0.146	0.137
107	170	65.346	3.267	Glacier	N	0.143	0.126
108	172	199.079	9.954	Glacieret	N	0.099	0.052
109	174	46.173	2.309	Glacier	N	0.275	0.192
110	175	77.238	3.862	Glacier	N	0.335	0.267
111	177	129.140	6.457	Glacieret	NW	0.153	0.052
112	182	97.797	4.890	Glacier	N	0.228	0.130
113	183	75.905	3.795	Glacieret	NW	0.135	0.076
114	184	41.063	2.053	Glacier	NW	0.137	0.075
115	185	86.759	4.338	Glacier	NW	0.543	0.371
116	187	114.629	5.731	Glacier	NE	0.151	0.134
117	189	146.141	7.307	Glacier	NE	0.801	0.772
118	190	88.345	4.417	Glacier	N	0.439	0.363
119	192	55.759	2.788	Glacier	N	0.109	0.092
120	194	342.910	17.145	Glacier	N	0.645	0.365
121	196	58.044	2.902	Glacier	N	0.636	0.565
122	198	53.171	2.659	Glacier	SW	0.679	0.681
123	199	64.805	3.240	Glacier	SW	1.549	1.559
124	200	101.399	5.070	Glacier	W	0.615	0.546
125	202	171.509	8.575	Glacier	N	2.913	2.385
126	203	89.370	4.469	Glacier	NW	0.212	0.116

127	204	30.326	1.516	Glacieret	NW	0.134	0.115
128	205	657.765	32.888	Glacier	NE	1.246	0.847
129	206	242.050	12.102	Glacier	N	0.475	0.371
130	207	261.317	13.066	Glacier	N	2.199	2.057
131	210	206.369	10.318	Glacier	N	1.170	1.100
132	211	101.846	5.092	Glacier	NW	0.794	0.747
133	213	121.160	6.058	Glacieret	NE	0.095	0.065
134	214	31.449	1.572	Glacier	NE	0.584	0.537
135	216	57.004	2.850	Glacier	NE	1.070	1.017
136	217	152.332	7.617	Glacier	NE	0.613	0.590
137	219	31.228	1.561	Glacier	SW	0.698	0.623
138	220	138.198	6.910	Glacieret	NW	0.671	0.432
139	221	68.677	3.434	Glacier	S	0.592	0.536
140	224	80.877	4.044	Glacieret	SE	0.094	0.075
141	225	284.549	14.227	Glacier	NE	3.642	3.567
142	226	34.163	1.708	Glacier	NE	1.120	1.093
143	228	77.720	3.886	Glacier	N	0.853	0.784
144	236	44.375	2.219	Glacier	NW	0.367	0.349
145	237	30.920	1.546	Glacier	NE	0.152	0.157
146	238	34.024	1.701	Glacier	NE	1.004	0.965
147	239	90.365	4.518	Glacier	N	0.699	0.626
148	240	150.006	7.500	Glacier	N	1.324	1.177
149	241	146.786	7.339	Glacier	N	1.029	0.882
150	242	190.835	9.542	Glacier	NE	1.058	0.865
151	243	1473.738	73.687	Glacier	S	1.330	0.839
152	245	90.663	4.533	Glacier	E	0.549	0.517
153	249	278.640	13.932	Glacier	NE	0.827	0.705
154	251	54.515	2.726	Glacier	N	2.696	2.534
155	252	237.623	11.881	Glacier	N	0.506	0.465
156	253	360.504	18.025	Glacier	N	0.662	0.590
157	254	276.768	13.838	Glacier	SE	0.319	0.219
158	255	139.252	6.963	Glacier	E	0.974	0.844
159	256	191.759	9.588	Glacier	N	1.484	1.328
160	258	112.310	5.616	Glacier	NE	1.371	1.301
161	259	79.715	3.986	Glacier	S	0.338	0.252
162	260	179.610	8.981	Glacier	S	0.260	0.178
163	261	80.569	4.028	Glacier	E	0.100	0.076
164	262	53.158	2.658	Glacieret	N	0.077	0.048
165	263	132.822	6.641	Glacier	NW	0.532	0.461
166	266	78.012	3.901	Glacier	N	1.205	1.080
167	268	33.820	1.691	Glacieret	NW	0.066	0.059
168	270	287.470	14.373	Glacier	E	0.253	0.184
169	273	111.644	5.582	Glacier	E	0.470	0.429
170	274	172.822	8.641	Glacier	NE	2.460	2.349

171	277	80.815	4.041	Glacier	SW	0.349	0.330
172	278	195.645	9.782	Glacier	N	6.610	6.473
173	279	35.214	1.761	Glacier	N	0.361	0.327
174	280	267.548	13.377	Glacier	N	4.191	4.081
175	281	91.743	4.587	Glacier	N	0.412	0.387
176	284	63.972	3.199	Glacier	N	0.988	0.952
177	285	40.155	2.008	Glacier	NW	0.802	0.785
178	288	53.769	2.688	Glacier	SE	1.258	1.127
179	289	412.373	20.619	Glacier	NE	0.677	0.468
180	290	65.257	3.263	Glacier	N	0.856	0.822
181	295	309.036	15.452	Glacier	NE	1.316	1.191
182	296	137.438	6.872	Glacier	N	1.269	1.199
183	297	138.357	6.918	Glacier	N	3.678	3.445
184	298	113.447	5.672	Glacier	N	0.560	0.503
185	299	174.188	8.709	Glacier	NW	0.117	0.087
186	300	121.828	6.091	Glacier	NE	0.229	0.205
187	301	106.736	5.337	Glacieret	N	0.115	0.082
188	302	39.866	1.993	Glacier	N	0.186	0.169
189	303	131.274	6.564	Glacieret	NE	0.076	0.050
190	304	156.316	7.816	Glacier	N	0.254	0.212
191	305	175.689	8.784	Glacier	NW	2.685	2.515
192	306	110.961	5.548	Glacier	W	0.596	0.565
193	307	52.063	2.603	Glacier	E	0.906	0.859
194	308	107.613	5.381	Glacier	NE	0.329	0.148
195	309	64.399	3.220	Glacier	W	0.119	0.083
196	316	113.907	5.695	Glacier	NW	0.374	0.351
197	317	35.963	1.798	Glacier	SE	0.093	0.085
198	319	37.141	1.857	Glacier	NE	0.227	0.172
199	322	109.337	5.467	Glacier	SE	0.186	0.167
200	324	208.239	10.412	Glacier	N	1.530	1.474
201	325	165.650	8.283	Glacier	NE	1.831	1.775
202	326	150.078	7.504	Glacier	NE	0.404	0.361
203	328	60.099	3.005		NW	0.606	0.576
204	329	355.843	17.792	Glacier	N	0.657	0.279
205	330	218.309	10.915	Glacier	SE	4.290	4.085
206	335	47.552	2.378	Glacier	N	2.842	2.771
207	341	79.759	3.988	Glacier	N	3.431	3.375
208	342	47.154	2.358	Glacier	NE	0.120	0.107
209	343	24.151	1.208	Glacier	N	1.479	1.463
210	344	138.301	6.915	Glacier	NE	0.702	0.633
211	346	33.148	1.657	Glacieret	N	0.087	0.078
212	348	70.215	3.511	Glacier	N	0.709	0.715
213	352	174.975	8.749	Glacier	NE	1.759	1.672
214	353	172.948	8.647	Glacier	N	5.593	5.501

215	354	266.497	13.325	Glacier	NE	0.666	0.617
216	357	111.376	5.569	Glacier	N	5.074	4.939
217	358	173.787	8.689	Glacier	NW	0.923	0.796
218	359	108.162	5.408	Glacier	N	2.534	2.493
219	360	269.291	13.465	Glaciеret	NE	0.131	0.052
220	361	126.622	6.331	Glacier	NW	0.428	0.392
221	362	92.205	4.610	Glacier	N	1.537	1.512
222	363	70.224	3.511	Glacier	NE	0.630	0.607
223	365	163.082	8.154	Glacier	NE	1.385	1.332
224	366	91.145	4.557	Glacier	NW	0.212	0.199
225	369	110.379	5.519	Glacier	NE	1.179	1.127
226	373	149.590	7.479	Glacier	N	0.157	0.136
227	375	48.498	2.425	Glacier	N	0.243	0.222
228	376	78.310	3.915	Glaciеret	NE	0.176	0.134
229	377	94.123	4.706	Glaciеret	E	0.080	0.065
230	378	324.436	16.222	Glacier	SE	0.469	0.375
231	379	85.063	4.253	Glaciеret	N	0.135	0.095
232	380	125.722	6.286	Glaciеret	N	0.094	0.056
233	381	147.290	7.364	Glacier	N	0.873	0.821
234	382	113.111	5.656	Glaciеret	NE	0.097	0.074
235	383	42.356	2.118	Glacier	N	2.359	2.323
236	384	70.534	3.527	Glacier	N	1.038	0.997
237	388	48.483	2.424	Glacier	N	0.245	0.228
238	389	66.614	3.331	Glaciеret	N	0.196	0.174
239	390	227.662	11.383	Glacier	N	0.199	0.127
240	392	109.352	5.468	Glacier	N	0.514	0.457
241	394	21.471	1.074	Glacier	N	0.264	0.240
242	395	86.177	4.309	Glacier	N	1.546	1.518
243	398	105.076	5.254	Glacier	N	0.976	0.948
244	400	30.183	1.509	Glacier	N	0.759	0.752
245	401	44.902	2.245	Glacier	N	0.315	0.315
246	405	46.162	2.308	Glaciеret	N	0.286	0.273
247	406	79.411	3.971	Glaciеret	NE	0.125	0.107
248	410	111.185	5.559	Glaciеret	N	0.073	0.051
249	411	46.984	2.349	Glaciеret	N	0.137	0.131
250	414	71.365	3.568	Glacier	NE	0.658	0.629
251	415	38.594	1.930	Glacier	NE	0.272	0.261
252	416	139.565	6.978	Glaciеret	NE	0.093	0.063
253	417	89.933	4.497	Glacier	N	0.726	0.695
254	418	44.672	2.234	Glaciеret	W	0.088	0.084
255	419	181.877	9.094	Glaciеret	N	0.103	0.063
256	421	114.374	5.719	Glacier	NW	0.059	0.344
257	422	63.450	3.172	Glacier	NE	0.947	0.925
258	423	108.225	5.411	Glacier	N	2.875	2.699

259	424	107.609	5.380	Glacier	SE	0.284	0.285
260	425	201.962	10.098	Glacier	N	0.549	0.474
261	426	149.487	7.474	Glacier	N	1.649	1.554
262	428	188.590	9.429	Glacier	NW	1.134	1.000
263	429	91.160	4.558	Glacier	N	0.269	0.253
264	430	51.279	2.564	Glacier	N	0.604	0.522
265	432	45.603	2.280	Glacieret	NE	0.085	0.072
266	433	202.065	10.103	Glacier	NW	1.762	1.611
267	435	61.856	3.093	Glacier	NE	0.300	0.258
268	436	195.450	9.773	Glacier	NE	3.174	3.005
269	437	40.912	2.046	Glacier	N	0.780	0.776
270	438	46.440	2.322	Glacieret	N	0.125	0.109
271	440	120.414	6.021	Glacier	N	0.965	0.885
272	443	38.344	1.917	Glacier	N	0.183	0.167
273	444	88.110	4.405	Glacier	NE	0.359	0.321
274	445	138.486	6.924	Glacier	W	0.334	0.302
275	447	56.515	2.826	Glacier	NE	0.237	0.217
276	448	53.899	2.695	Glacieret	NW	0.137	0.116
277	450	42.684	2.134	Glacier	E	0.315	0.267
278	451	177.846	8.892	Glacier	SE	0.725	0.595
279	452	50.187	2.509	Glacier	N	0.354	0.342
280	457	90.963	4.548	Glacieret	E	0.286	0.219
281	458	91.091	4.555	Glacier	N	0.619	0.595
282	459	342.740	17.137	Glacier	NE	0.493	0.406
283	461	137.375	6.869	Glacier	NE	0.691	0.519
284	462	624.281	31.214	Glacier	NE	1.009	0.768
285	463	128.873	6.444	Glacier	NE	0.477	0.443
286	464	232.335	11.617	Glacier	NE	1.233	0.982
287	465	37.461	1.873	Glacier	N	0.463	0.491
288	467	330.191	16.510	Glacier	NE	0.480	0.432
289	471	587.496	29.375	Glacier	N	1.311	0.961
290	473	221.628	11.081	Glacier	NW	0.706	0.615
291	475	155.306	7.765	Glacier	NE	0.558	0.500
292	476	95.533	4.777	Glacier	N	2.557	2.415
293	481	72.037	3.602	Glacier	NE	0.293	0.246
294	482	192.205	9.610	Glacier	W	0.510	0.480
295	483	156.425	7.821	Glacier	N	2.486	2.291
296	484	167.490	8.375	Glacier	SE	1.720	1.627
297	485	212.369	10.618	Glacier	SE	2.672	1.092
298	487	100.411	5.021	Glacier	N	0.096	0.070
299	489	79.235	3.962	Glacier	N	0.305	0.299
300	491	129.539	6.477	Glacieret	E	0.189	0.159
301	497	123.670	6.183	Glacieret	N	0.247	0.198
302	499	53.889	2.694	Glacier	E	0.266	0.255

303	504	58.297	2.915	Glacier	N	0.145	0.131
304	507	57.823	2.891	Glacier	NE	0.453	0.426
305	515	426.617	21.331	Glacier	N	0.787	0.736
306	516	74.865	3.743	Glacier	SE	0.736	0.663
307	518	170.435	8.522	Glacier	NE	3.183	2.935
308	519	175.076	8.754	Glacier	NE	1.170	1.097
309	520	24.787	1.239	Glacier	NE	1.444	1.329
310	521	47.882	2.394	Glacier	S	0.780	0.730
311	522	22.177	1.109	Glacier	NW	0.480	0.473
312	523	298.186	14.909	Glacier	N	1.928	1.772
313	524	40.111	2.006	Glacier	NE	0.205	0.185
314	525	199.453	9.973	Glacier	NE	0.286	0.201
315	526	900.989	45.049	Glacier	SE	0.702	0.371
316	527	105.964	5.298	Glacier	N	0.619	0.594
317	528	223.051	11.153	Glacier	NW	0.334	0.274
318	529	191.768	9.588	Glacier	NE	2.606	2.462
319	530	253.301	12.665	Glacier	SW	0.343	0.185
320	531	60.465	3.023	Glacier	N	0.443	0.417
321	532	80.747	4.037	Glacier	NE	0.094	0.092
322	533	83.792	4.190	Glacier	NE	1.018	0.937
323	534	255.871	12.794	Glacier	NE	1.841	1.625
324	535	342.647	17.132	Glacier	NE	0.393	0.327
325	536	184.403	9.220	Glacier	N	3.845	3.587
326	537	125.815	6.291	Glacier	N	0.718	0.671
327	538	221.289	11.064	Glacieret	NW	0.153	0.121
328	539	149.104	7.455	Glacier	N	1.462	1.348
329	541	108.011	5.401	Glacier	NW	0.078	0.079
330	542	54.005	2.700	Glacier	SW	0.239	0.221
331	543	83.231	4.162	Glacieret	SW	0.095	0.116
332	545	50.202	2.510	Glacieret	NW	0.228	0.240
333	547	283.884	14.194	Glacier	N	1.895	1.590
334	552	364.985	18.249	Glacier	NE	1.913	1.673
335	553	97.419	4.871	Glacieret	NE	0.173	0.151
336	554	223.233	11.162	Glacieret	NE	0.409	0.365
337	555	106.249	5.312	Glacieret	N	0.209	0.185
338	556	63.115	3.156	Glacieret	N	0.270	0.241
339	557	187.118	9.356	Glacier	NE	0.993	0.813
340	558	96.547	4.827	Glacier	NE	1.909	1.740
341	561	309.847	15.492	Glacier	NE	4.360	3.959
342	562	88.237	4.412	Glacieret	NW	0.542	0.511
343	563	49.950	2.497	Glacieret	SE	0.337	0.283
344	569	220.349	11.017	Glacier	N	2.531	2.478
345	573	63.344	3.167	Glacieret	E	0.081	0.069
346	576	213.057	10.653	Glacieret	N	0.278	0.209

347	577	429.500	21.475	Glacier	E	0.671	0.445
348	578	617.141	30.857	Glacier	SE	0.259	0.108
349	579	101.699	5.085	Glaciaret	S	0.368	0.265
350	581	229.298	11.465	Glacier	N	0.183	0.156
351	583	181.763	9.088	Glacier	NE	0.376	0.332
352	584	57.346	2.867	Glacier	S	0.752	0.697
353	586	87.871	4.394	Glacier	NE	0.245	0.183
354	587	53.130	2.656	Glacieret	SE	0.121	0.105
355	589	67.491	3.375	Glacier	E	0.385	0.354
356	591	53.714	2.686	Glacier	N	0.509	0.468
357	592	68.971	3.449	Glacieret	N	0.157	0.130
358	593	71.559	3.578	Glacieret	N	0.212	0.091
359	594	56.999	2.850	Glacier	N	0.634	0.585
360	596	30.678	1.534	Glacier	S	0.834	0.786
361	598	85.674	4.284	Glacier	N	0.998	0.858
362	599	46.354	2.318	Glacier	E	0.485	0.442
363	605	121.300	6.065	Glacieret	NE	0.053	0.030
364	606	132.505	6.625	Glacier	N	0.191	0.167
365	607	30.953	1.548	Glacier	N	0.322	0.310
366	610	48.709	2.435	Glacieret	N	0.161	0.151
367	612	50.203	2.510	Glacier	N	0.726	0.697
368	613	63.483	3.174	Glacier	NW	0.435	0.401
369	615	66.694	3.335	Glacier	NW	0.445	0.335
370	618	34.100	1.705	Glacieret	E	0.111	0.097
371	620	39.497	1.975	Glacieret	NE	0.097	0.090
372	623	65.463	3.273	Glacier	W	0.315	0.274
373	626	141.370	7.069	Glacier	SE	1.090	1.003
374	667	194.781	9.739	Glacier	NE	0.671	0.517
375	669	23.841	1.192	Glacier	NW	1.454	1.450
376	670	23.097	1.155	Glacier	SW	0.383	0.368
377	672	33.345	1.667	Glacieret	SW	0.307	0.286
378	681	29.937	1.497	Glacier	NE	0.336	0.317
379	682	73.129	3.656	Glacier	NW	0.302	0.257
380	686	58.482	2.924	Glacieret	N	0.138	0.129
381	687	110.097	5.505	Glacier	SE	0.338	0.269
382	688	244.683	12.234	Glacier	E	0.955	0.906
383	690	49.869	2.493	Glacieret	NW	0.179	0.065
384	692	59.666	2.983	Glacieret	N	0.201	0.187
385	693	40.177	2.009	Glacieret	N	0.491	0.452
386	694	25.489	1.274	Glacieret	N	0.113	0.103
387	695	109.871	5.494	Glacieret	SE	0.719	0.654

RETREAT RATES OF GLACIERS IN BASPA BASIN

Sr. No.	Glacier ID	Retreat in meter	Retreat Rate (m/year)	Glacier Type	Aspect	Area in Sq.km	
						2000	2020
1	698	57	2.85	Glacier	S	0.148	0.136
2	699	365	18.25	Glacier	N	0.109	0.068
3	700	211	10.55	Glacier	S	0.252	0.217
4	704	123	6.15	Glacier	W	0.463	0.436
5	705	56	2.80	Glacier	W	0.421	0.429
6	708	175	8.75	Glacier	S	0.455	0.428
7	709	242	12.10	Glacier	S	1.471	1.310
8	711	208	10.40	Glacier	SW	0.127	0.070
9	712	83	4.15	Glacieret	S	0.065	0.016
10	713	162	8.10	Glacier	S	3.259	3.058
11	714	152	7.60	Glacier	S	0.455	0.406
12	715	101	5.05	Glacier	SW	0.086	0.063
13	716	97	4.85	Glacieret	E	0.092	0.070
14	717	314	15.70	Glacieret	E	0.114	0.059
15	718	50	2.50	Glacier	E	0.256	0.238
16	719	435	21.75	Glacier	S	0.321	0.235
17	720	133	6.65	Glacier	E	0.702	0.590
18	721	183	9.15	Glacier	E	0.392	0.336
19	722	115	5.75	Glacier	E	0.208	0.165
20	724	686	34.30	Glacier	NW	1.371	0.953
21	725	69	3.45	Glacieret	SW	0.330	0.281
22	726	114	5.70	Glacier	W	0.387	0.323
23	727	96	4.80	Glacier	NW	1.570	1.488
24	728	280	14.00	Glacier	NW	6.457	6.562
25	729	69	3.45	Glacier	N	1.026	0.970
26	730	166	8.30	Glacier	N	2.617	2.513
27	731	157	7.85	Glacier	N	0.719	0.590
28	733	974	48.70	Glacier	N	1.026	0.752
29	734	146	7.30	Glacier	W	5.187	5.183
30	735	65	3.25	Glacier	NW	0.336	0.294
31	737	71	3.55	Glacier	SE	0.521	0.491
32	738	555	27.75	Glacier	NW	31.955	32.722
33	742	207	10.35	Glacier	N	0.875	0.651
34	744	145	7.25	Glacier	N	5.090	5.145
35	745	83	4.15	Glacier	N	1.816	1.949
36	746	54	2.70	Glacier	N	0.327	0.244
37	747	186	9.30	Glacier	N	6.310	6.390
38	748	142	7.10	Glacier	W	2.265	2.164

39	749	242	12.10	Glacier	S	4.517	3.951
40	750	259	12.95	Glacier	S	1.964	1.716
41	752	110	5.50	Glacier	E	0.302	0.250
42	753	62	3.10	Glacier	E	0.521	0.484
43	754	77	3.85	Glacier	E	0.593	0.531
44	756	165	8.25	Glacier	NW	0.548	0.540
45	758	127	6.35	Glacier	NW	2.802	2.861
46	761	197	9.85	Glacier	S	6.782	6.666
47	765	105	5.25	Glacier	N	0.427	0.432
48	766	40	2.00	Glacier	SE	0.193	0.193
49	767	56	2.80	Glacier	SE	0.207	0.215
50	768	145	7.25	Glacier	NE	1.003	0.994
51	769	70	3.50	Glacier	N	0.464	0.470
52	771	193	9.65	Glacier	N	0.392	0.285
54	772	54	2.70	Glacier	NE	0.317	0.366
55	774	238	11.90	Glacier	N	0.357	0.351
56	776	123	6.15	Glacier	N	0.286	0.254
57	777	70	3.50	Glacier	N	2.181	2.177
58	778	76	3.80	Glacier	N	0.487	0.489
59	779	46	2.30	Glacier	E	0.484	0.473
60	781	893	44.65	Glacier	NW	1.858	2.340
61	785	133	6.65	Glacier	N	0.858	0.838
62	788	46	2.30	Glacier	N	0.131	0.137

RETREAT RATES OF GLACIERS IN LOWER SATLUJ BASIN

S. No.	Glacier ID	Retreat in meter	Retreat Rate (m/year)	Glacier Type	Aspect	Area in Sq.km	
						2000	2020
1	796	347.670	17.384	Glacier	N	3.617	3.493
2	799	186.556	9.328	Glacier	NE	1.041	0.935
3	800	642.551	32.128	Glacier	NE	4.464	4.239
4	801	61.591	3.080	Glacier	N	1.073	1.044
5	802	996.506	49.825	Glacier	N	3.715	2.212
6	803	385.942	19.297	Glacier	N	0.930	0.766
7	804	206.205	10.310	Glacier	NE	0.593	0.464
8	805	99.179	4.959	Glacier	NE	0.455	0.354
9	807	179.728	8.986	Glacier	N	2.060	1.902
10	812	46.911	2.346	Glacier	N	1.115	1.105
11	813	426.240	21.312	Glacier	NE	0.529	0.575
12	814	222.830	11.142	Glacier	NE	1.357	1.312
13	815	149.097	7.455	Glacier	NE	1.292	1.207
14	816	135.589	6.779	Glacier	NE	1.406	1.079
15	817	181.109	9.055	Glacier	NE	2.562	2.461
16	820	121.371	6.069	Glacier	NW	1.286	1.210
17	822	203.345	10.167	Glacier	SE	0.711	0.621
18	823	39.736	1.987	Glacier	SE	0.159	0.147
19	824	190.548	9.527	Glacier	W	0.262	0.174
20	826	289.136	14.457	Glacier	SW	0.700	0.574
21	827	157.074	7.854	Glacier	NE	0.415	0.246
22	828	157.125	7.856	Glacier	N	0.402	0.321
23	829	175.369	8.768	Glacier	N	0.223	0.158
24	830	127.156	6.358	Glacier	N	0.469	0.419
25	831	195.343	9.767	Glacier	NE	0.599	0.528
26	832	134.676	6.734	Glacier	N	0.270	0.143
27	835	324.562	16.228	Glacier	N	5.965	5.790
28	836	60.743	3.037	Glacier	N	0.179	0.153
29	837	107.857	5.393	Glacier	N	0.169	0.143
30	838	223.565	11.178	Glacier	N	0.836	0.744
31	841	569.150	28.457	Glacier	N	0.718	0.529
32	842	171.842	8.592	Glacier	NW	0.769	0.714
33	843	117.102	5.855	Glacier	NW	0.347	0.329

34	844	76.224	3.811	Glacier	W	2.897	2.841
35	849	174.181	8.709	Glacier	N	8.333	8.291
36	850	124.224	6.211	Glacier	N	0.906	0.856
37	851	159.278	7.964	Glacier	E	1.836	1.813
38	852	111.205	5.560	Glacier	S	1.709	1.686
39	853	163.873	8.194	Glacier	NE	0.701	0.662
40	854	87.072	4.354	Glacier	S	0.383	0.358
41	855	643.928	32.196	Glacier	SE	0.601	0.505
42	856	181.682	9.084	Glacier	E	0.408	0.352
43	857	1199.978	59.999	Glacier	N	9.924	9.513
44	858	263.639	13.182	Glacier	NE	3.168	3.065
45	859	157.949	7.897	Glacier	SE	0.350	0.324
46	861	51.264	2.563	Glacier	E	6.888	6.394
47	863	277.812	13.891	Glacier	E	1.606	1.385
48	865	242.606	12.130	Glacier	NW	2.815	2.748
49	866	438.653	21.933	Glacier	NE	2.172	2.041
50	867	505.439	25.272	Glacier	N	2.463	2.273
51	868	38.176	1.909	Glacier	NE	0.312	0.286
52	869	95.550	4.778	Glacier	N	0.892	0.883
53	870	86.225	4.311	Glacier	N	0.630	0.567
54	871	85.503	4.275	Glacier	NE	0.401	0.431
55	875	76.825	3.841	Glacier	NE	1.911	1.885
56	876	320.813	16.041	Glacier	NE	0.763	0.641
57	878	399.667	19.983	Glacier	E	0.857	0.685
58	879	143.619	7.181	Glacier	NE	0.255	0.167
59	883	201.636	10.082	Glacier	SE	0.570	0.471
60	884	151.592	7.580	Glacier	E	0.840	0.727
61	886	86.249	4.312	Glacier	SE	0.352	0.292
62	890	84.658	4.233	Glacier	E	1.752	1.680
63	891	60.238	3.012	Glacier	NW	0.727	0.665
64	893	289.595	14.480	Glacier	E	0.752	0.529
65	894	147.165	7.358	Glacier	E	0.370	0.295
66	897	120.940	6.047	Glacier	NE	0.254	0.234
67	898	156.065	7.803	Glacier	E	0.149	0.103
68	901	98.711	4.936	Glacier	SE	0.469	0.493
69	902	146.417	7.321	Glacier	NE	0.751	0.666

70	903	45.473	2.274	Glacier	SE	0.391	0.342
71	904	123.094	6.155	Glacier	NE	0.432	0.368
72	906	37.572	1.879	Glacier	SE	0.324	0.305
73	907	56.585	2.829	Glacier	S	0.934	0.877
74	909	79.512	3.976	Glacier	E	0.245	0.198
75	911	234.541	11.727	Glacier	NE	0.315	0.186
76	912	126.564	6.328	Glacier	SW	0.086	0.066
77	915	30.750	1.538	Glacier	SE	0.423	0.365
78	917	104.357	5.218	Glacier	W	0.398	0.340
79	918	132.924	6.646	Glacier	S	0.124	0.098
80	920	78.108	3.905	Glacier	S	0.424	0.343
81	1103	81.040	4.052	Glacier	S	0.137	0.118
82	1091	50.916	2.546	Glacier	N	0.199	0.192
83	1088	83.934	4.197	Glacier	NE	0.075	0.068
84	1085	771.325	38.566	Glacier	NE	0.242	0.097
85	1081	315.947	15.797	Glacier	E	0.194	0.131
86	1073	383.424	19.171	Glacier	NE	0.476	0.385
87	1064	344.223	17.211	Glacier	NE	0.440	0.380
88	1059	97.708	4.885	Glacier	N	0.179	0.167
89	1058	566.016	28.301	Glacier	NE	0.826	0.727
90	1056	139.536	6.977	Glacieret	N	0.183	0.125
91	1052	161.631	8.082	Glacier	N	0.631	0.603
92	1051	68.632	3.432	Glacier	N	1.541	1.500
93	1044	25.657	1.283	Glacieret	SE	0.071	0.067
94	1043	124.372	6.219	Glacier	N	0.233	0.210
95	1041	184.616	9.231	Glacier	N	0.571	0.511
96	1039	38.130	1.907	Glacier	S	0.083	0.057
97	1037	188.496	9.425	Glacier	NE	0.176	0.136
98	1035	621.361	31.068	Glacier	E	0.406	0.285
99	1026	485.160	24.258	Glacier	NE	0.302	0.133
100	1018	274.003	13.700	Glacier	W	3.198	3.108
101	1012	55.854	2.793	Glacier	NW	0.410	0.391
102	1010	146.992	7.350	Glacier	NE	0.259	0.232
103	1006	294.521	14.726	Glacier	NE	0.271	0.217
104	990	455.892	22.795	Glacier	SE	1.044	0.893
105	985	107.161	5.358	Glacier	SE	0.589	0.535

106	977	72.710	3.635	Glacier	N	0.158	0.145
107	975	121.520	6.076	Glacier	SE	0.116	0.105
108	974	110.559	5.528	Glacier	E	0.154	0.129
109	972	81.747	4.087	Glacier	NE	0.074	0.067
110	969	42.029	2.101	Glacier	NE	0.153	0.147
111	967	42.613	2.131	Glacier	E	0.073	0.068
112	966	123.094	6.155	Glacier	NW	0.647	0.624
113	916	83.857	4.193	Glacier	SW	0.184	0.156
115	913	33.717	1.686	Glacier	SE	0.443	0.416

RETREAT RATES OF GLACIERS IN THE UPPER SATLUJ BASIN

Sr. No.	Glacier ID	Retreat in meter	Retreat Rate m/year	Glacier Type	Aspect	2000	
						Area 2000	Area2020
1	2004	67	3.35	Glacieret	NE	0.023	0.014
2	2005	79	3.95	Glacier	N	0.115	0.090
3	2006	88	4.4	Glacieret	N	0.219	0.164
4	2007	33	1.65	Glacieret	NE	0.052	0.045
5	2008	36	1.8	Glacieret	NE	0.031	0.015
6	2009	57	2.85	Glacieret	N	0.167	0.134
7	2010	76	3.8	Glacieret	N	0.134	0.095
8	2011	239	11.95	Glacieret	N	0.173	0.105
9	2012	64	3.2	Glacieret	NE	0.306	0.264
10	2013	79	3.95	Glacieret	NE	0.183	0.137
11	2014	129	6.45	Glacieret	N	0.102	0.063
12	2015	43	2.15	Glacieret	NE	0.180	0.148
13	2016	37	1.85	Glacieret	NE	0.172	0.157
14	2017	78	3.9	Glacieret	N	0.394	0.319
15	2027	97	4.85	Glacier	N	0.398	0.329
16	2023	133	6.65	Glacieret	N	0.352	0.287
17	2033	301	15.05	Glacier	N	1.816	1.594
18	2034	173	8.65	Glacier	N	0.480	0.420
19	2036	53	2.65	Glacieret	N	0.238	0.170
20	2039	116	5.8	Glacieret	NE	0.210	0.146
21	2040	232	11.6	Glacieret	N	0.409	0.304
22	2046	94	4.7	Glacier	N	0.442	0.356
23	2054	52	2.6	Glacieret	NE	0.113	0.074
24	2067	177	8.85	Glacieret	N	0.559	0.300
25	2078	124	6.2	Glacier	SE	1.550	1.461
26	2086	41	2.05	Glacieret	NE	0.185	0.152
27	2090	95	4.75	Glacier	E	1.051	0.864
28	2091	182	9.1	Glacier	SE	0.873	0.718
29	2097	78	3.9	Glacieret	N	0.208	0.146
30	2099	151	7.55	Glacier	SE	4.488	4.310
31	2110	42	2.1	Glacier	SE	2.152	2.072
32	2111	393	19.65	Glacier	SE	1.255	1.050
33	2112	122	6.1	Glacier	SE	0.543	0.526
34	2124	156	7.8	Glacier	N	0.466	0.363
35	2126	239	11.95	Glacier	NE	1.450	1.214
36	2129	204	10.2	Glacier	NE	1.345	1.038
37	2130	373	18.65	Glacier	N	1.157	0.910
38	2131	263	13.15	Glacier	N	2.514	2.241
39	2132	46	2.3	Glacieret	NW	0.269	0.140
40	2133	101	5.05	Glacier	N	22.933	22.047

41	2134	150	7.5	Glacier	NE	6.590	6.058
42	2135	102	5.1	Glacier	NE	2.335	1.992
43	2136	35	1.75	Glacier	N	0.516	0.412
44	2138	46	2.3	Glacier	N	0.899	0.864
45	2139	88	4.4	Glacieret	NW	0.196	0.145
46	2140	114	5.7	Glacier	N	0.828	0.744
47	2141	56	2.8	Glacier	N	0.424	0.382
48	2144	79	3.95	Glacier	SE	0.778	0.678
49	2146	125	6.25	Glacier	N	0.632	0.510
50	2147	282	14.1	Glacier	N	1.484	1.222
51	2149	104	5.2	Glacier	W	0.379	0.257
52	2150	302	15.1	Glacier	N	2.611	2.177
53	2152	85	4.25	Glacieret	NE	0.207	0.163
54	2153	115	5.75	Glacier	N	0.643	0.549
55	2154	97	4.85	Glacier	N	0.129	0.093
56	2155	210	10.5	Glacier	N	0.642	0.156
57	2156	513	25.65	Glacier	NE	0.353	0.162
58	2157	114	5.7	Glacier	NE	0.685	0.306
59	2158	147	7.35	Glacier	N	0.286	0.190
60	2160	144	7.2	Glacier	NE	0.276	0.187
61	2162	146	7.3	Glacier	N	0.157	0.079
62	2164	41	2.05	Glacieret	N	0.045	0.009
63	2166	245	12.25	Glacier	NE	3.248	2.596
64	2167	204	10.2	Glacier	N	1.652	1.494
65	2168	134	6.7	Glacier	NE	1.751	1.503
66	2169	43	2.15	Glacier	N	1.057	0.944
67	2171	60	3	Glacier	E	0.639	0.585
68	2172	12	0.6	Glacier	NW	0.783	0.750
69	2173	93	4.65	Glacieret	NE	0.614	0.533
70	2174	105	5.25	Glacieret	NW	0.195	0.173
71	2175	96	4.8	Glacieret	NW	0.209	0.172
72	2177	67	3.35	Glacieret	NE	0.357	0.276
73	2178	153	7.65	Glacier	NE	0.352	0.217
74	2179	551	27.55	Glacier	NE	0.382	0.163
75	2182	336	16.8	Glacier	N	1.565	1.289
76	2183	221	11.05	Glacier	NE	0.336	0.289
77	2184	20	1	Glacier	W	0.156	0.107
78	2185	89	4.45	Glacier	N	0.276	0.174
79	2186	376	18.8	Glacier	N	0.596	0.381
80	2188	187	9.35	Glacieret	N	0.174	0.121
81	2190	82	4.1	Glacieret	N	0.098	0.051
82	2191	266	13.3	Glacieret	NE	0.072	0.072
83	2195	130	6.5	Glacier	NW	1.122	1.050
84	2197	477	23.85	Glacier	N	2.395	2.082

85	2201	224	11.2	Glacier	NE	7.989	7.684
86	2204	55	2.75	Glacieret	NW	0.244	0.162
87	2207	80	4	Glacieret	N	0.124	0.085
88	2209	80	4	Glacier	W	0.903	0.817
89	2210	103	5.15	Glacieret	S	0.217	0.171
90	2212	121	6.05	Glacieret	SE	0.180	0.124
91	2214	107	5.35	Glacier	NE	1.017	0.873
92	2215	70	3.5	Glacieret	N	0.220	0.177
93	2217	74	3.7	Glacier	E	0.638	0.473
94	2218	73	3.65	Glacier	NW	1.865	1.647
95	2219	117	5.85	Glacier	W	3.029	2.806
96	2221	27	1.35	Glacier	N	0.590	0.522
97	2226	217	10.85	Glacieret	NW	0.081	0.027
98	2228	57	2.85	Glacieret	N	0.735	0.636
99	2237	131	6.55	Glacier	N	0.478	0.401
100	2240	41	2.05	Glacieret	N	0.185	0.163
101	2243	32	1.6	Glacieret	N	0.064	0.027
102	2244	26	1.3	Glacieret	N	0.179	0.163
103	2245	46	2.3	Glacieret	N	0.085	0.038
104	2246	31	1.55	Glacieret	N	0.080	0.063
105	2247	414	20.7	Glacier	N	10.972	10.681
106	2248	694	34.7	Glacier	N	12.862	12.151
107	2249	131	6.55	Glacier	SW	0.852	0.753
108	2250	216	10.8	Glacier	W	0.569	0.453
109	2251	60	3	Glacieret	N	0.178	0.130
110	2252	51	2.55	Glacier	N	0.225	0.196
111	2253	167	8.35	Glacier	N	0.546	0.449
112	2254	86	4.3	Glacier	N	0.373	0.235
113	2255	132	6.6	Glacieret	N	0.177	0.097
114	2257	149	7.45	Glacier	N	0.219	0.125
115	2258	111	5.55	Glacieret	NW	0.170	0.140
116	2261	94	4.7	Glacieret	N	0.140	0.089
117	2263	185	9.25	Glacier	N	0.601	0.456
118	2264	73	3.65	Glacier	NW	0.288	0.224
119	2266	287	14.35	Glacier	N	1.558	1.404
120	2270	108	5.4	Glacier	NW	1.194	1.053
121	2271	157	7.85	Glacier	N	1.754	1.487
122	2272	91	4.55	Glacier	N	0.547	0.422
123	2275	70	3.5	Glacier	NW	0.768	0.455
124	2277	103	5.15	Glacier	NE	0.269	0.172
125	2278	113	5.65	Glacier	N	1.111	0.950
126	2279	165	8.25	Glacier	NW	0.490	0.373
127	2021	88	4.4	Glacier	E	0.373	0.273
128	2280	215	10.75	Glacier	NW	0.635	0.408

129	2281	88	4.4	Glacier	SW	0.809	0.700
130	2282	312	15.6	Glacier	SW	0.621	0.352
131	2283	204	10.2	Glacier	NE	1.636	1.461
132	2284	263	13.15	Glacier	NW	0.795	0.672
133	2285	132	6.6	Glacier	S	0.800	0.515
134	2003	157	7.85	Glacieret	NE	0.064	0.036
135	2000	106	5.3	Glacieret	N	0.449	0.390
136	2018	155	7.75	Glacieret	N	0.165	0.094
137	2019	63	3.15	Glacieret	NE	0.196	0.165
138	2022	67	3.35	Glacieret	N	0.191	0.137
139	2024	208	10.4	Glacieret	N	0.173	0.097
140	2025	70	3.5	Glacieret	N	0.076	0.054
141	2026	91	4.55	Glacieret	NW	0.074	0.050
142	2028	109	5.45	Glacieret	N	0.354	0.299
143	2029	99	4.95	Glacieret	N	0.358	0.295
144	2030	574	28.7	Glacieret	N	0.229	0.077
145	2031	136	6.8	Glacieret	N	0.159	0.108
146	2035	117	5.85	Glacieret	N	0.200	0.139
147	2037	50	2.5	Glacieret	N	0.060	0.045
148	2038	134	6.7	Glacieret	NE	0.057	0.026
149	2041	113	5.65	Glacieret	N	0.080	0.043
150	2042	118	5.9	Glacieret	NW	0.049	0.030
151	2043	192	9.6	Glacieret	NW	0.057	0.018
152	2044	62	3.1	Glacieret	NE	0.152	0.093
153	2045	79	3.95	Glacieret	NE	0.065	0.026
154	2047	236	11.8	Glacieret	NE	0.165	0.106
155	2048	45	2.25	Glacieret	NE	0.114	0.081
156	2049	83	4.15	Glacieret	N	0.254	0.193
157	2050	100	5	Glacieret	N	0.135	0.087
158	2052	49	2.45	Glacieret	NE	0.105	0.060
159	2051	48	2.4	Glacieret	NE	0.135	0.081
160	2053	72	3.6	Glacieret	NE	0.198	0.153
161	2055	45	2.25	Glacieret	NE	0.161	0.124
162	2056	49	2.45	Glacieret	N	0.200	0.137
163	2057	85	4.25	Glacieret	N	0.109	0.037
164	2058	99	4.95	Glacieret	N	0.185	0.111
165	2059	63	3.15	Glacieret	N	0.065	0.029
166	2060	51	2.55	Glacieret	N	0.095	0.058
167	2061	64	3.2	Glacieret	N	0.115	0.078
168	2062	77	3.85	Glacieret	N	0.145	0.079
169	2063	473	23.65	Glacieret	NE	0.174	0.050
170	2064	62	3.1	Glacieret	NE	0.136	0.078
171	2065	46	2.3	Glacieret	NE	0.047	0.023
172	2066	46	2.3	Glacieret	N	0.043	0.025

173	2068	55	2.75	Glacieret	N	0.099	0.084
174	2069	72	3.6	Glacieret	N	0.197	0.127
175	2070	115	5.75	Glacieret	N	0.210	0.138
176	2071	158	7.9	Glacieret	NE	0.142	0.066
177	2072	79	3.95	Glacieret	N	0.113	0.070
178	2075	49	2.45	Glacieret	NE	0.053	0.032
179	2077	212	10.6	Glacieret	NE	0.080	0.038
180	2079	134	6.7	Glacieret	NW	0.499	0.400
181	2080	76	3.8	Glacieret	N	0.087	0.055
182	2081	38	1.9	Glacieret	N	0.045	0.029
183	2082	129	6.45	Glacieret	NE	0.068	0.041
184	2083	32	1.6	Glacieret	N	0.026	0.016
185	2084	95	4.75	Glacieret	N	0.043	0.021
186	2085	45	2.25	Glacieret	NE	0.073	0.055
187	2087	119	5.95	Glacieret	SE	0.042	1.461
188	2088	83	4.15	Glacieret	S	0.228	0.193
189	2092	190	9.5	Glacieret	N	0.180	0.117
190	2093	53	2.65	Glacieret	NE	0.083	0.056
191	2094	67	3.35	Glacieret	NE	0.100	0.093
192	2098	79	3.95	Glacieret	NE	0.091	0.035
193	2100	95	4.75	Glacieret	N	0.169	0.115
194	2101	74	3.7	Glacieret	NE	0.112	0.048
195	2102	40	2	Glacieret	N	0.045	0.028
196	2105	276	13.8	Glacier	NW	0.360	0.287
197	2108	188	9.4	Glacieret	W	0.291	0.161
198	2113	31	1.55	Glacier	SE	0.114	0.105
199	2114	93	4.65	Glacier	NE	0.514	0.476
200	2115	56	2.8	Glacier	N	0.453	0.408
201	2260	111	5.55	Glacier	NW	0.170	0.140
202	2120	93	4.65	Glacier	E	0.455	0.424
203	2125	54	2.7	Glacieret	SE	0.071	0.056
204	2145	71	3.55	Glacieret	N	0.256	0.183
205	2151	84	4.2	Glacieret	NE	0.441	0.357
206	2159	29	1.45	Glacieret	NW	0.124	0.104
207	2161	99	4.95	Glacieret	NE	0.199	0.127
208	2165	297	14.85	Glacieret	N	0.133	0.039
209	2203	61	3.05	Glacieret	N	0.099	0.061
210	2208	461	23.05	Glacieret	N	0.280	0.028
211	2213	60	3	Glacieret	E	0.129	0.084
212	2216	53	2.65	Glacieret	N	0.038	0.026
213	2220	44	2.2	Glacier	N	0.979	0.905
214	2222	23	1.15	Glacieret	NE	0.149	0.085
215	2225	210	10.5	Glacieret	NW	0.224	0.070
216	2227	45	2.25	Glacieret	N	0.039	0.020

217	2234	30	1.5	Glacieret	NE	0.071	0.054
218	2235	90	4.5	Glacieret	N	0.180	0.122
219	2236	72	3.6	Glacieret	NE	0.153	0.113
220	2238	64	3.2	Glacieret	NE	0.097	0.052
221	2239	93	4.65	Glacieret	N	0.295	0.219
222	2241	92	4.6	Glacieret	NE	0.252	0.112
223	2256	0	0	Glacieret	NW	0.078	0.039
224	2258	86	4.3	Glacieret	NE	0.222	0.123
225	2259	40	2	Glacieret	N	0.118	0.087
226	2262	96	4.8	Glacieret	NW	0.357	0.247
227	2265	81	4.05	Glacieret	N	0.547	0.438
228	2267	108	5.4	Glacieret	NE	0.189	0.128
229	2268	133	6.65	Glacieret	NW	0.127	0.088
230	2269	118	5.9	Glacieret	N	0.202	0.149
231	2273	71	3.55	Glacieret	NE	0.152	0.108
232	2274	52	2.6	Glacieret	NW	0.145	0.103
233	2286	175	8.75	Glacier	SW	1.545	1.214
234	2287	151	7.55	Glacier	NW	1.445	1.233
235	2289	83	4.15	Glacieret	NE	0.203	0.172
236	2290	85	4.25	Glacieret	NE	0.140	0.111
237	2291	40	2	Glacieret	NE	0.098	0.067
238	2292	26	1.3	Glacieret	E	0.095	0.079
239	2293	67	3.35	Glacier	NW	0.568	0.507
240	2294	48	2.4	Glacieret	NE	0.102	0.082
241	2295	131	6.55	Glacier	N	0.312	0.257
242	2296	190	9.5	Glacier	NE	0.748	0.588
243	2297	126	6.3	Glacieret	N	0.195	0.114
244	2298	100	5	Glacieret	NW	0.084	0.056
245	2299	51	2.55	Glacieret	N	0.089	0.047
246	2301	214	10.7	Glacieret	N	0.316	0.209
247	2302	143	7.15	Glacieret	N	0.616	0.342
248	2303	151	7.55	Glacieret	NE	0.614	0.417
249	2304	203	10.15	Glacier	E	0.233	0.153
250	2305	104	5.2	Glacieret	N	0.437	0.306
251	2306	215	10.75	Glacieret	NE	0.221	0.059
252	2307	71	3.55	Glacieret	NE	0.204	0.142
253	2308	30	1.5	Glacieret	NE	0.031	0.025
254	2309	22	1.1	Glacieret	N	0.279	0.243
255	2310	36	1.8	Glacieret	N	0.108	0.087
256	2311	361	18.05	Glacieret	N	0.472	0.231
257	2312	132	6.6	Glacieret	NW	0.453	0.253
258	2313	120	6	Glacier	N	0.582	0.468
259	2314	20	1	Glacieret	NE	0.055	0.050
260	2315	150	7.5	Glacieret	N	0.140	0.084

261	2316	216	10.8	Glacier	NW	0.444	0.339
262	2317	161	8.05	Glacier	NW	0.717	0.651
263	2318	74	3.7	Glacieret	N	0.178	0.135
264	2319	37	1.85	Glacieret	NW	0.050	0.030
265	2320	160	8	Glacieret	N	0.172	0.122
266	2321	31	1.55	Glacieret	N	0.059	0.045
267	2322	67	3.35	Glacieret	NW	0.053	0.036
268	2324	107	5.35	Glacier	NW	0.328	0.226
269	2325	71	3.55	Glacieret	N	0.095	0.051
270	2326	181	9.05	Glacier	NE	0.350	0.295
271	2328	254	12.7	Glacier	NE	3.764	3.357
272	2329	60	3	Glacier	NW	0.385	0.222
273	2330	57	2.85	Glacier	N	0.325	0.245
274	2331	137	6.85	Glacier	N	0.874	0.717
275	2332	241	12.05	Glacieret	N	0.276	0.130
276	2333	135	6.75	Glacier	N	1.570	1.241
277	2334	56	2.8	Glacieret	N	0.186	0.144
278	2335	305	15.25	Glacier	N	1.364	1.133
279	2336	149	7.45	Glacieret	N	0.162	0.111
280	2337	688	34.4	Glacier	NE	5.270	4.173
281	2338	274	13.7	Glacier	N	2.391	1.940
282	2339	333	16.65	Glacier	NE	2.703	2.309
283	2340	105	5.25	Glacier	NW	1.803	1.510
284	2341	142	7.1	Glacier	N	0.311	0.255
285	2343	95	4.75	Glacier	N	0.302	0.221
286	2344	198	9.9	Glacieret	N	0.162	0.086
287	2345	214	10.7	Glacier	NE	1.378	1.216
288	2346	227	11.35	Glacier	NW	0.530	0.325
289	2347	137	6.85	Glacier	NW	0.677	0.544
290	2348	41	2.05	Glacier	NE	0.204	0.154
291	2349	223	11.15	Glacier	NE	0.587	0.310
292	2350	78	3.9	Glacieret	N	0.289	0.218
293	2351	112	5.6	Glacier	N	0.182	0.138
294	2164A	26	1.3	Glacier	N	0.045	1.009
295	2352	141	7.05	Glacier	NE	8.195	7.837
296	2354	240	12	Glacier	N	1.178	0.915
297	2355	111	5.55	Glacieret	N	0.286	0.217
298	2356	84	4.2	Glacieret	N	0.216	0.142
299	2357	164	8.2	Glacier	NE	2.452	2.011
300	2358	624	31.2	Glacier	NE	6.073	5.598
301	2359	609	30.45	Glacier	NE	4.678	4.068
302	2360	310	15.5	Glacier	NE	2.351	2.053
303	2361	700	35	Glacier	N	6.342	4.504
304	2362	408	20.4	Glacier	E	1.833	1.473

305	2363	284	14.2	Glacier	E	1.610	1.378
306	2364	203	10.15	Glacier	N	1.010	0.832
307	2365	454	22.7	Glacier	NE	4.631	4.156
308	2369	290	14.5	Glacier	NE	6.496	6.119
309	2370	223	11.15	Glacier	NE	2.465	2.210
310	2371	670	33.5	Glacier	NE	4.510	3.984
311	2372	245	12.25	Glacier	N	1.272	1.098
312	2373	182	9.1	Glacier	NE	0.455	0.400
313	2374	241	12.05	Glacier	NE	2.261	2.077
314	2375	453	22.65	Glacier	NE	0.819	0.647
315	2376	111	5.55	Glacieret	NW	0.089	0.041
316	2377	31	1.55	Glacieret	NE	0.043	0.035
317	2378	170	8.5	Glacier increase	S	0.395	0.440
318	2381	221	11.05	Glacier	W	0.865	0.696
319	2382	125	6.25	Glacieret	NW	0.148	0.109
320	2383	129	6.45	Glacier	NW	0.925	0.660
321	2384	99	4.95	Glacier	N	0.236	0.178
322	2385	76	3.8	Glacier	N	0.225	0.167
323	2386	72	3.6	Glacieret	NW	0.136	0.088
324	2387	408	20.4	Glacier	N	2.400	2.186
325	2388	181	9.05	Glacier	N	0.564	0.514
326	2389	251	12.55	Glacier	N	1.254	1.070
327	2391	266	13.3	Glacier	N	4.433	4.283
328	2392	133	6.65	Glacier	N	1.508	1.343
329	2393	125	6.25	Glacier	N	0.763	0.598
330	2394	46	2.3	Glacier	W	0.390	0.335
331	2396	81	4.05	Glacier	N	0.256	0.235
332	2397	66	3.3	Glacier	N	0.262	0.235
333	2398	61	3.05	Glacier	NE	0.214	0.178
334	2399	17	0.85	Glacier	NW	0.147	0.139
335	2400	82	4.1	Glacier	NW	0.146	0.137
336	2402	81	4.05	Glacieret	N	0.147	0.102
337	2403	89	4.45	Glacier	NE	0.201	0.126
338	2404	206	10.3	Glacier	NE	0.516	0.300
339	2405	37	1.85	Glacier	NE	0.345	0.311
340	2406	54	2.7	Glacieret	N	0.288	0.205
341	2410	105	5.25	Glacier	N	1.463	1.348
342	2412	69	3.45	Glacier	N	0.367	0.171
343	2413	38	1.9	Glacier	NE	0.113	0.085
344	2414	37	1.85	Glacier	NE	0.236	0.205
345	2415	76	3.8	Glacier	N	0.721	0.469
346	2416	85	4.25	Glacier	N	0.879	0.815
347	2417	64	3.2	Glacieret	N	0.544	0.078
348	2418	75	3.75	Glacieret	N	0.890	0.236

349	2419	92	4.6	Glacieret	N	0.127	0.066
350	2420	76	3.8	Glacieret	N	0.256	0.204
351	2421	133	6.65	Glacieret	N	0.065	0.039
352	2422	40	2	Glacieret	NW	0.033	0.021
353	2423	78	3.9	Glacier	NE	0.345	0.285
354	2424	297	14.85	Glacier	NW	1.069	0.906
355	2425	81	4.05	Glacieret	NE	0.106	0.073
356	2426	101	5.05	Glacieret	NW	0.081	0.060
357	2427	117	5.85	Glacier	N	0.240	0.132
358	2428	106	5.3	Glacier	NW	0.147	0.085
359	2429	150	7.5	Glacier	N	0.164	0.111
360	2430	70	3.5	Glacieret	NE	0.058	0.025
361	2431	108	5.4	Glacieret	NE	0.084	0.055
362	2432	117	5.85	Glacieret	NE	0.050	0.018
363	2433	248	12.4	Glacier	N	0.454	0.187
364	2434	63	3.15	Glacieret	NW	0.193	0.083
365	2435	83	4.15	Glacieret	NE	0.039	0.013
366	2436	114	5.7	Glacier	N	0.301	0.206
367	2437	88	4.4	Glacier	N	0.131	0.077
368	2438	41	2.05	Glacier	NE	0.339	0.310
369	2440	84	4.2	Glacier	NE	0.149	0.096
370	2441	139	6.95	Glacier	SE	0.413	0.344
371	2443	107	5.35	Glacier increase	SW	0.074	0.071
372	2446	35	1.75	Glacier	NE	0.111	0.074
373	2447	257	12.85	Glacieret	E	0.099	0.021
374	2448	62	3.1	Glacieret	N	0.067	0.047
375	2449	65	3.25	Glacier	N	0.116	0.078
376	2450	99	4.95	Glacier	NE	0.732	0.574
377	2452	182	9.1	Glacier	NW	0.193	0.136
378	2453	58	2.9	Glacier	NE	0.332	0.294
379	2454	19	0.95	Glacieret	N	0.146	0.121
380	2459	35	1.75	Glacier	E	0.205	0.174
381	2460	121	6.05	Glacieret	NE	0.186	0.036
382	2461	90	4.5	Glacier	N	1.367	1.238
383	2462	52	2.6	Glacier	S	0.339	0.273
384	2464	129	6.45	Glacier	N	0.871	0.753
385	2465	75	3.75	Glacier	E	0.292	0.236
386	2466	40	2	Glacier	NE	0.087	0.047
387	2470	211	10.55	Glacier	E	0.421	0.330
388	2473	38	1.9	Glacier	NE	0.100	0.063
389	2475	116	5.8	Glacieret	W	0.142	0.060
390	2476	26	1.3	Glacier	N	0.107	0.068
391	2477	121	6.05	Glacier	N	0.239	0.200
392	2478	111	5.55	Glacieret	N	0.147	0.104

393	2481	95	4.75	Glacieret	NW	0.066	0.044
394	2483	111	5.55	Glacieret	NE	0.060	0.042
395	2484	103	5.15	Glacier	NE	0.132	0.117
396	2485	106	5.3	Glacier	NE	0.194	0.116
397	2486	245	12.25	Glacier	E	47.045	46.825
398	2489	105	5.25	Glacieret	NW	0.068	0.033
399	2490	121	6.05	Glacieret	NW	0.229	0.151
400	2495	278	13.9	Glacier	NW	0.817	0.628
401	2496	33	1.65	Glacieret	N	0.106	0.057
402	2497	147	7.35	Glacieret	N	0.236	0.167
403	2498	53	2.65	Glacier	N	0.065	0.049
404	2499	63	3.15	Glacieret	N	0.120	0.096
405	2500	142	7.1	Glacier	NW	0.387	0.248
406	2501	107	5.35	Glacier	N	0.596	0.451
407	2502	162	8.1	Glacieret	N	0.122	0.049
408	2504	14	0.7	Glacieret	N	0.033	0.021
409	2505	75	3.75	Glacieret	NE	0.012	0.013
410	2506	74	3.7	Glacier	N	0.278	0.210
411	2507	528	26.4	Glacier	NW	0.218	0.080
412	2515	140	7	Glacier	N	0.114	0.054
413	2516	81	4.05	Glacier	NE	0.105	0.073
414	2517	89	4.45	Glacieret	N	0.134	0.068
415	2518	98	4.9	Glacier/ Glacieret	NE	0.149	0.086
416	2520	37	1.85	Glacieret	NE	0.036	0.025
417	2523	134	6.7	Glacier increase	NE	0.092	0.077
418	2525	135	6.75	Glacier increase	NE	0.106	0.088
419	2527	46	2.3	Glacieret	NW	0.074	0.065
420	2528	74	3.7	Glacieret	N	0.040	0.024
421	2531	58	2.9	Glacieret	NW	0.025	0.015
422	2532	100	5	Glacieret	E	0.022	0.010
423	2533	86	4.3	Glacieret	NE	0.161	0.078
424	2537	73	3.65	Glacieret	N	0.138	0.136
425	2541	129	6.45	Glacieret	N	0.081	0.035
426	2544	116	5.8	Glacier	NE	0.097	0.104
427	2545	136	6.8	Glacieret	N	0.070	0.035
428	2547	73	3.65	Glacieret	N	0.056	0.032
429	2548	145	7.25	Glacier	N	0.052	0.034
430	2550	63	3.15	Glacieret increase	NE	0.012	0.014
431	2552	100	5	Glacieret	NE	0.073	0.019
432	2553	250	12.5	Glacier	N	0.191	0.059
433	2554	69	3.45	Glacieret	NE	0.099	0.065
434	2556	69	3.45	Glacieret	NE	0.116	0.066

435	2557	97	4.85	Glacieret	N	0.299	0.065
436	2558	64	3.2	Glacieret	NE	0.077	0.031
437	2559	139	6.95	Glacier	N	0.077	0.039
438	2560	230	11.5	Glacier	N	0.114	0.039
439	2562	24	1.2	Glacier	NE	0.048	0.036
440	2574	37	1.85	Glacieret	E	0.177	0.128
441	2575	123	6.15	Glacieret	NW	0.244	0.220
442	2578	39	1.95	Glacieret	N	0.011	0.005
443	2579	104	5.2	Glacieret	NE	0.085	0.047
444	2582	21	1.05	Glacieret	N	0.152	0.117
445	2583	18	0.9	Glacieret	N	0.045	0.033
446	2585	278	13.9	Glacieret	N	0.140	0.013
447	2588	287	14.35	Glacier	N	0.696	0.546
448	2589	117	5.85	Glacieret	N	0.087	0.045

ANNEXURE III
MASS BALANCE

Sr. No.	G.ID	Total Area in 2000	2000			2011			2020		
			Accumulation	AAR	Mass Balance	Accumulation	AAR	Mass Balance	Accumulation	AAR	Mass Balance
1.	1	0.059	0.027	0.452	-10.236	0.023	0.385	-26.730	0.033	0.557	15.285
2.	2	0.341	0.169	0.496	0.414	0.032	0.085	-99.512	0.120	0.351	-34.824
3.	3	1.534	0.517	0.337	-38.338	0.698	0.453	-10.045	0.729	0.475	-4.761
4.	4	0.677	0.352	0.520	6.284	0.180	0.258	-57.564	0.137	0.202	-71.117
5.	5	7.583	4.925	0.650	37.667	2.234	0.283	-51.479	2.382	0.314	-43.841
6.	6	8.121	5.290	0.651	38.121	3.280	0.405	-21.783	2.382	0.293	-48.901
7.	7	0.281	0.089	0.318	-42.880	0.153	0.554	14.461	0.079	0.283	-51.494
8.	8	0.151	0.056	0.374	-29.303	0.100	0.667	41.871	0.079	0.527	7.921
9.	9	1.426	0.756	0.530	8.591	0.739	0.549	13.168	0.703	0.493	-0.435
10.	10	0.268	0.179	0.670	42.642	0.032	0.112	-93.039	0.140	0.524	7.104
11.	11	0.268	0.110	0.411	-20.316	0.130	0.489	-1.353	0.140	0.523	6.986
12.	12	6.456	1.803	0.279	-52.314	2.383	0.363	-32.053	2.051	0.318	-42.997
13.	13	8.122	5.368	0.661	40.437	3.486	0.425	-17.010	2.051	0.253	-58.825
14.	14	1.622	0.970	0.598	25.158	0.841	0.518	5.779	0.505	0.311	-44.504
15.	15	14.023	8.153	0.581	21.110	5.368	0.381	-27.555	5.557	0.396	-23.885
16.	16	0.740	0.341	0.460	-8.293	0.612	0.841	84.128	0.350	0.473	-5.221
17.	17	7.211	3.883	0.539	10.687	2.742	0.382	-27.359	2.458	0.341	-37.367
18.	18	0.344	0.142	0.414	-19.681	0.046	0.156	-82.164	0.127	0.371	-30.132
19.	19	0.261	0.164	0.629	32.662	0.117	0.429	-15.880	0.127	0.488	-1.479
20.	20	0.440	0.342	0.777	68.625	0.176	0.429	-16.015	0.153	0.348	-35.568
21.	21	6.221	2.522	0.405	-21.647	2.713	0.422	-17.738	2.132	0.343	-36.916
22.	22	3.349	1.802	0.538	10.582	1.403	0.449	-11.181	2.132	0.636	34.480
23.	23	0.078	0.039	0.503	2.135	0.022	0.293	-48.917	0.036	0.463	-7.562

24.	24	12.332	6.053	0.491	-0.911	4.784	0.379	-28.187	4.824	0.391	-25.137
25.	25	1.546	1.195	0.773	67.598	0.830	0.544	11.960	1.137	0.736	58.578
26.	26	2.705	1.471	0.544	12.036	1.220	0.443	-12.457	1.440	0.532	9.180
27.	27	0.423	0.262	0.619	30.192	0.161	0.343	-36.719	0.246	0.580	20.867
28.	28	0.167	0.105	0.625	31.686	0.057	0.360	-32.771	0.062	0.369	-30.596
29.	29	1.040	0.600	0.577	20.105	0.439	0.429	-16.015	0.468	0.450	-10.743
30.	30	0.464	0.240	0.516	5.319	0.191	0.368	-30.728	0.186	0.401	-22.768
31.	31	1.818	0.768	0.423	-17.489	0.586	0.309	-45.009	0.752	0.414	-19.622
32.	32	0.531	0.335	0.630	32.875	0.279	0.563	16.661	0.163	0.306	-45.787
33.	33	0.437	0.179	0.410	-20.605	0.206	0.513	4.546	0.166	0.380	-27.917
34.	34	8.564	5.913	0.690	47.609	3.552	0.392	-24.948	3.037	0.355	-34.019
35.	35	0.752	0.243	0.323	-41.573	0.230	0.306	-45.737	0.239	0.318	-42.961
36.	36	0.615	0.307	0.499	1.081	0.047	0.070	-103.235	0.243	0.395	-24.177
37.	37	0.205	0.073	0.356	-33.601	0.089	0.307	-45.469	0.080	0.392	-24.974
38.	38	0.339	0.084	0.248	-59.873	0.077	0.220	-66.710	0.131	0.386	-26.483
39.	39	0.479	0.257	0.537	10.293	0.184	0.352	-34.699	0.137	0.285	-50.832
40.	40	0.539	0.275	0.510	3.746	0.293	0.545	12.171	0.273	0.507	2.964
41.	41	0.148	0.071	0.477	-4.370	0.100	0.710	52.265	0.072	0.484	-2.506
42.	42	1.785	0.459	0.257	-57.773	0.465	0.250	-59.520	0.441	0.247	-60.154
43.	43	1.042	0.705	0.677	44.229	0.526	0.494	-0.193	0.221	0.212	-68.666
44.	44	2.061	1.218	0.591	23.437	0.650	0.316	-43.457	0.751	0.364	-31.659
45.	45	1.811	0.937	0.517	5.469	0.583	0.294	-48.829	0.399	0.220	-66.717
46.	46	0.644	0.293	0.454	-9.772	0.139	0.204	-70.680	0.220	0.341	-37.254
47.	47	0.272	0.103	0.379	-28.011	0.055	0.175	-77.725	0.059	0.216	-67.616
48.	48	0.234	0.132	0.562	16.450	0.125	0.502	1.917	0.075	0.322	-42.007
49.	49	2.990	1.041	0.348	-35.569	1.210	0.401	-22.819	1.263	0.423	-17.484
50.	50	4.268	1.711	0.401	-22.769	1.835	0.414	-19.610	1.548	0.363	-32.025
51.	51	2.055	1.050	0.511	4.003	0.896	0.440	-13.270	1.046	0.509	3.533
52.	52	0.384	0.284	0.739	59.402	0.200	0.521	6.385	0.137	0.357	-33.508
53.	53	0.324	0.230	0.710	52.408	0.091	0.281	-51.783	0.129	0.398	-23.570

54.	54	0.325	0.178	0.549	13.190	0.075	0.231	-64.080	0.232	0.714	53.270
55.	55	0.386	0.202	0.524	7.121	0.058	0.149	-84.069	0.159	0.412	-20.009
56.	56	2.123	1.149	0.541	11.343	0.890	0.410	-20.510	0.903	0.425	-16.833
57.	57	0.207	0.094	0.455	-9.510	0.114	0.508	3.308	0.104	0.501	1.510
58.	58	1.195	0.862	0.721	55.079	0.655	0.590	23.124	0.485	0.406	-21.601
59.	59	0.692	0.454	0.656	39.224	0.176	0.281	-51.810	0.309	0.446	-11.829
60.	60	3.916	2.057	0.525	7.478	1.484	0.384	-26.914	1.366	0.349	-35.425
61.	61	0.469	0.263	0.561	16.089	0.220	0.501	1.560	0.161	0.342	-36.977
62.	62	0.105	0.051	0.484	-2.541	0.095	0.923	104.088	0.018	0.175	-77.644
63.	63	1.239	0.899	0.725	56.122	0.782	0.633	33.572	0.544	0.439	-13.598
64.	64	0.307	0.194	0.631	33.170	0.208	0.694	48.513	0.084	0.275	-53.441
65.	65	0.304	0.127	0.419	-18.294	0.163	0.510	3.849	0.136	0.446	-11.684
66.	66	0.231	0.110	0.477	-4.383	0.042	0.183	-75.766	0.124	0.537	10.210
67.	67	0.309	0.121	0.392	-25.007	0.117	0.372	-29.872	0.111	0.359	-32.948
68.	68	0.473	0.286	0.605	26.785	0.246	0.581	20.946	0.232	0.490	-1.137
69.	69	11.376	4.792	0.421	-17.808	4.432	0.388	-25.807	7.368	0.648	37.209
70.	70	0.673	0.344	0.512	4.175	0.147	0.222	-66.328	0.296	0.440	-13.371
71.	71	1.129	0.645	0.571	18.648	0.283	0.266	-55.478	0.642	0.569	18.009
72.	72	2.400	1.814	0.756	63.453	1.328	0.583	21.410	1.540	0.642	35.732
73.	73	1.104	0.760	0.688	47.059	0.602	0.556	15.017	0.448	0.405	-21.679
74.	74	0.726	0.302	0.416	-19.174	0.567	0.807	76.016	0.276	0.380	-27.798
75.	75	0.883	0.343	0.389	-25.693	0.160	0.187	-74.807	0.226	0.256	-57.999
76.	76	1.872	0.788	0.421	-17.912	0.781	0.428	-16.222	1.397	0.746	61.122
77.	77	2.340	1.357	0.580	20.779	0.864	0.365	-31.572	1.812	0.774	67.964
78.	78	0.306	0.169	0.552	13.879	0.038	0.113	-92.602	0.131	0.428	-16.142
79.	79	0.489	0.167	0.341	-37.362	0.268	0.570	18.279	0.107	0.219	-67.046
80.	80	0.839	0.492	0.586	22.259	0.389	0.476	-4.559	0.343	0.409	-20.738
81.	81	0.519	0.292	0.564	16.841	0.063	0.116	-91.994	0.127	0.245	-60.758
82.	82	0.380	0.229	0.603	26.400	0.052	0.129	-88.924	0.247	0.649	37.620
83.	83	0.214	0.107	0.500	1.310	0.083	0.377	-28.526	0.091	0.423	-17.423

84.	84	0.262	0.107	0.410	-20.651	0.025	0.096	-96.738	0.122	0.465	-7.284
85.	85	0.507	0.293	0.578	20.184	0.170	0.319	-42.763	0.271	0.534	9.480
86.	86	0.463	0.144	0.311	-44.572	0.175	0.368	-30.786	0.293	0.632	33.449
87.	87	0.344	0.187	0.545	12.285	0.113	0.324	-41.378	0.166	0.484	-2.514
88.	88	5.357	1.883	0.351	-34.780	2.460	0.469	-6.183	1.668	0.311	-44.496
89.	89	3.686	1.225	0.332	-39.411	1.243	0.362	-32.280	1.437	0.390	-25.468
90.	90	1.088	0.682	0.627	32.082	0.251	0.265	-55.811	0.291	0.267	-55.234
91.	91	0.956	0.541	0.566	17.290	0.314	0.302	-46.770	0.181	0.190	-74.077
92.	92	0.292	0.133	0.455	-9.720	0.141	0.385	-26.633	0.122	0.417	-18.763
93.	93	0.615	0.285	0.463	-7.729	0.228	0.366	-31.301	0.312	0.507	2.925
94.	94	0.217	0.104	0.478	-4.083	0.043	0.205	-70.282	0.041	0.191	-73.685
95.	95	0.222	0.113	0.508	3.248	0.070	0.316	-43.365	0.057	0.256	-57.987
96.	96	8.395	4.630	0.552	13.844	4.024	0.475	-4.647	4.026	0.480	-3.662
97.	97	0.171	0.108	0.628	32.449	0.079	0.430	-15.665	0.066	0.383	-27.127
98.	98	1.037	0.647	0.624	31.439	0.270	0.260	-56.926	0.298	0.287	-50.334
99.	99	0.596	0.316	0.530	8.710	0.217	0.380	-27.952	0.227	0.380	-27.827
100.	100	1.767	0.562	0.318	-42.928	0.419	0.216	-67.613	0.905	0.512	4.245
101.	101	1.132	0.533	0.470	-5.866	0.160	0.140	-86.168	0.561	0.495	0.223
102.	102	0.289	0.161	0.556	14.869	0.057	0.204	-70.659	0.051	0.175	-77.617
103.	103	0.244	0.090	0.368	-30.827	0.026	0.103	-95.135	0.107	0.439	-13.626
104.	104	0.572	0.290	0.508	3.236	0.133	0.217	-67.533	0.318	0.557	15.069
105.	105	1.241	0.538	0.434	-14.831	0.459	0.333	-39.218	0.681	0.549	13.140
106.	106	0.234	0.122	0.522	6.619	0.071	0.294	-48.790	0.117	0.500	1.240
107.	107	0.622	0.237	0.380	-27.732	0.228	0.329	-40.281	0.307	0.493	-0.364
108.	108	0.422	0.183	0.433	-14.944	0.166	0.387	-26.256	0.290	0.687	46.655
109.	109	0.814	0.299	0.368	-30.759	0.321	0.389	-25.585	0.322	0.395	-24.092
110.	110	0.254	0.157	0.618	29.958	0.070	0.277	-52.919	0.128	0.503	1.981
111.	111	0.140	0.106	0.753	62.885	0.132	0.937	107.539	0.099	0.707	51.565
112.	112	0.376	0.151	0.403	-22.313	0.191	0.496	0.363	0.254	0.677	44.219
113.	113	0.128	0.050	0.391	-25.188	0.050	0.383	-27.210	0.051	0.398	-23.356

114.	114	0.504	0.271	0.537	10.437	0.281	0.558	15.321	0.234	0.464	-7.470
115.	115	0.410	0.211	0.515	5.004	0.148	0.362	-32.261	0.097	0.237	-62.552
116.	116	1.218	0.413	0.339	-37.882	0.367	0.289	-49.868	0.626	0.514	4.690
117.	117	4.477	1.978	0.442	-12.818	1.955	0.432	-15.155	1.270	0.284	-51.268
118.	118	0.856	0.486	0.568	17.953	0.315	0.340	-37.449	0.288	0.337	-38.274
119.	119	0.688	0.193	0.280	-52.034	0.215	0.299	-47.456	0.198	0.288	-50.175
120.	120	0.535	0.206	0.385	-26.632	0.118	0.207	-69.986	0.152	0.283	-51.322
121.	121	0.360	0.133	0.370	-30.233	0.134	0.381	-27.511	0.148	0.412	-20.078
122.	122	0.693	0.278	0.401	-22.702	0.197	0.253	-58.768	0.197	0.284	-51.207
123.	123	0.992	0.173	0.174	-77.807	0.571	0.576	19.794	0.393	0.396	-23.993
124.	124	0.395	0.178	0.451	-10.539	0.202	0.495	0.134	0.096	0.244	-60.941
125.	125	0.311	0.112	0.361	-32.410	0.088	0.294	-48.781	0.076	0.243	-61.082
126.	126	4.285	2.123	0.496	0.234	1.803	0.424	-17.089	1.217	0.284	-51.188
127.	127	0.425	0.175	0.411	-20.354	0.155	0.386	-26.365	0.132	0.311	-44.497
128.	128	2.163	1.311	0.606	27.106	1.281	0.577	19.925	0.572	0.265	-55.877
129.	129	0.164	0.044	0.269	-54.705	0.111	0.734	58.209	0.046	0.278	-52.655
130.	130	0.241	0.098	0.405	-21.712	0.119	0.457	-9.079	0.066	0.276	-53.235
131.	131	0.570	0.223	0.391	-25.167	0.173	0.311	-44.552	0.100	0.176	-77.338
132.	133	1.158	0.478	0.413	-19.869	0.489	0.452	-10.338	0.588	0.507	3.113
133.	134	0.818	0.486	0.594	24.275	0.299	0.362	-32.110	0.168	0.205	-70.282
134.	135	0.308	0.060	0.195	-72.689	0.217	0.863	89.531	0.054	0.177	-77.278
135.	136	0.692	0.511	0.739	59.291	0.384	0.555	14.765	0.334	0.482	-3.011
136.	137	0.153	0.102	0.664	41.092	0.049	0.321	-42.118	0.087	0.571	18.466
137.	138	1.750	0.718	0.410	-20.484	0.522	0.289	-49.922	0.471	0.269	-54.809
138.	139	0.981	0.564	0.575	19.524	0.647	0.673	43.464	0.526	0.536	10.057
139.	140	2.326	1.454	0.625	31.721	1.170	0.519	5.980	1.042	0.448	-11.358
140.	141	0.667	0.358	0.538	10.448	0.334	0.495	0.206	0.245	0.367	-30.968
141.	143	0.881	0.421	0.477	-4.165	0.401	0.461	-8.090	0.308	0.349	-35.376
142.	144	0.130	0.069	0.532	9.142	0.057	0.436	-14.222	0.028	0.218	-67.229
143.	145	1.078	0.495	0.459	-8.532	0.509	0.465	-7.223	0.482	0.447	-11.574

144.	146	3.403	1.262	0.371	-30.020	0.985	0.289	-50.049	1.822	0.535	9.927
145.	147	2.804	0.827	0.295	-48.544	0.905	0.328	-40.508	1.542	0.550	13.436
146.	148	0.243	0.112	0.460	-8.371	0.063	0.260	-56.894	0.087	0.359	-32.841
147.	149	0.400	0.233	0.583	21.544	0.203	0.539	10.862	0.167	0.417	-18.795
148.	150	7.207	2.869	0.398	-23.448	2.923	0.411	-20.228	1.811	0.251	-59.134
149.	151	0.618	0.295	0.477	-4.192	0.325	0.650	37.823	0.300	0.484	-2.471
150.	152	0.358	0.182	0.507	2.964	0.144	0.426	-16.767	0.128	0.357	-33.471
151.	153	1.046	0.438	0.418	-18.526	0.516	0.530	8.556	0.326	0.312	-44.383
152.	155	0.466	0.322	0.691	47.747	0.327	0.702	50.368	0.229	0.491	-0.968
153.	156	0.367	0.158	0.429	-15.847	0.161	0.509	3.505	0.045	0.124	-90.107
154.	157	0.190	0.101	0.530	8.560	0.113	0.604	26.653	0.035	0.184	-75.585
155.	158	0.862	0.302	0.350	-35.008	0.192	0.234	-63.369	0.202	0.235	-63.115
156.	159	0.535	0.152	0.283	-51.298	0.273	0.533	9.375	0.164	0.306	-45.798
157.	160	0.191	0.098	0.511	4.112	0.104	0.543	11.878	0.065	0.342	-37.074
158.	161	0.122	0.068	0.555	14.650	0.062	0.489	-1.245	0.055	0.454	-9.960
159.	162	0.042	0.026	0.634	33.888	0.030	0.666	41.672	0.017	0.408	-21.030
160.	163	0.281	0.141	0.502	1.878	0.140	0.500	1.297	0.125	0.445	-12.111
161.	177	0.153	0.073	0.476	-4.402	0.044	0.339	-37.890	0.069	0.452	-10.278
162.	178	0.118	0.051	0.428	-16.293	0.067	0.566	17.378	0.069	0.585	22.027
163.	185	0.543	0.307	0.566	17.267	0.362	0.782	69.913	0.128	0.235	-63.033
164.	186	0.305	0.074	0.244	-60.988	0.192	0.621	30.705	0.157	0.516	5.172
165.	187	0.151	0.089	0.587	22.398	0.067	0.438	-13.646	0.051	0.340	-37.587
166.	188	0.461	0.137	0.298	-47.819	0.124	0.381	-27.667	0.133	0.289	-50.017
167.	191	0.083	0.043	0.513	4.566	0.023	0.278	-52.736	0.019	0.234	-63.383
168.	192	0.109	0.109	1.000	122.828	0.036	0.338	-38.024	0.044	0.403	-22.204
169.	193	0.283	0.191	0.675	43.732	0.236	0.929	105.694	0.086	0.304	-46.284
170.	194	0.645	0.369	0.572	18.783	0.142	0.332	-39.418	0.173	0.268	-54.991
171.	195	0.264	0.194	0.736	58.611	0.127	0.521	6.441	0.108	0.410	-20.470
172.	196	0.636	0.328	0.515	5.085	0.332	0.525	7.392	0.101	0.159	-81.459
173.	197	0.202	0.094	0.466	-7.011	0.147	0.793	72.433	0.070	0.344	-36.546

174.	198	0.679	0.371	0.547	12.635	0.501	0.749	61.723	0.231	0.341	-37.412
175.	199	1.549	0.749	0.484	-2.678	0.468	0.321	-42.099	0.740	0.478	-4.044
176.	201	1.088	0.751	0.690	47.469	0.191	0.179	-76.619	0.722	0.664	41.103
177.	202	2.913	1.780	0.611	28.276	1.329	0.486	-2.027	0.886	0.304	-46.269
178.	203	0.212	0.086	0.408	-21.080	0.101	0.542	11.618	0.017	0.081	-100.479
179.	204	0.134	0.084	0.630	32.901	0.095	0.741	59.877	0.061	0.455	-9.709
180.	207	2.199	1.170	0.532	9.060	0.719	0.322	-41.835	0.631	0.287	-50.460
181.	210	1.170	0.844	0.721	55.030	0.655	0.590	23.078	0.815	0.696	49.036
182.	211	0.794	0.503	0.634	33.840	0.408	0.514	4.609	0.449	0.565	17.171
183.	212	0.442	0.205	0.463	-7.603	0.165	0.418	-18.507	0.153	0.347	-35.803
184.	214	0.584	0.394	0.674	43.618	0.224	0.400	-23.072	0.404	0.692	47.898
185.	215	3.961	2.499	0.631	33.148	1.933	0.492	-0.608	2.163	0.546	12.504
186.	216	1.070	0.410	0.384	-26.975	0.324	0.318	-42.830	0.225	0.210	-69.143
187.	217	0.613	0.377	0.616	29.501	0.160	0.275	-53.319	0.333	0.544	11.929
188.	218	0.623	0.330	0.530	8.496	0.444	0.676	44.215	0.153	0.245	-60.576
189.	219	0.698	0.307	0.440	-13.210	0.447	0.670	42.646	0.211	0.301	-46.923
190.	225	3.642	2.458	0.675	43.873	2.154	0.592	23.742	1.097	0.301	-46.953
191.	226	1.120	0.856	0.765	65.661	0.575	0.525	7.376	0.548	0.490	-1.231
192.	227	2.005	1.146	0.572	18.716	1.281	0.647	37.085	0.617	0.308	-45.436
193.	228	0.853	0.499	0.584	21.846	0.557	0.671	42.894	0.234	0.274	-53.613
194.	229	0.326	0.138	0.423	-17.317	0.205	0.735	58.432	0.162	0.498	0.856
195.	231	0.141	0.082	0.586	22.283	0.082	0.582	21.291	0.048	0.344	-36.574
196.	232	0.054	0.020	0.371	-30.090	0.027	0.620	30.457	0.008	0.146	-84.824
197.	233	0.679	0.335	0.493	-0.484	0.127	0.173	-78.257	0.108	0.159	-81.499
198.	235	0.185	0.139	0.753	62.742	0.100	0.544	12.052	0.037	0.203	-70.836
199.	237	0.152	0.051	0.334	-39.111	0.101	0.559	15.631	0.131	0.862	89.238
200.	238	1.004	0.372	0.370	-30.163	0.680	0.659	40.024	0.148	0.147	-84.358
201.	239	0.699	0.188	0.269	-54.871	0.210	0.304	-46.205	0.173	0.247	-60.201
202.	240	1.324	0.773	0.584	21.708	0.695	0.528	8.206	0.839	0.634	33.823
203.	241	1.029	0.361	0.351	-34.960	0.427	0.429	-15.872	0.405	0.394	-24.476

204.	242	1.058	0.432	0.409	-20.843	0.494	0.479	-3.682	0.057	0.054	-107.076
205.	243	1.330	0.318	0.239	-62.006	0.431	0.325	-41.169	0.268	0.201	-71.232
206.	245	0.549	0.248	0.452	-10.431	0.213	0.384	-26.819	0.237	0.431	-15.398
207.	247	0.705	0.349	0.496	0.247	0.309	0.439	-13.482	0.512	0.726	56.179
208.	249	0.827	0.370	0.448	-11.384	0.445	0.531	8.870	0.404	0.488	-1.543
209.	251	2.696	1.094	0.406	-21.598	1.570	0.570	18.241	1.008	0.374	-29.303
210.	254	0.319	0.129	0.404	-22.019	0.078	0.261	-56.735	0.138	0.434	-14.761
211.	255	0.974	0.599	0.614	29.094	0.468	0.499	1.078	0.395	0.406	-21.607
212.	256	1.484	0.786	0.530	8.499	0.673	0.456	-9.443	0.579	0.390	-25.396
213.	258	1.371	0.881	0.642	35.889	0.878	0.617	29.670	0.448	0.326	-40.879
214.	259	0.338	0.087	0.256	-57.923	0.095	0.296	-48.327	0.082	0.243	-61.224
215.	260	0.260	0.096	0.370	-30.153	0.117	0.456	-9.323	0.073	0.281	-51.840
216.	263	0.532	0.154	0.290	-49.817	0.317	0.612	28.589	0.117	0.220	-66.678
217.	264	0.294	0.110	0.373	-29.481	0.140	0.500	1.241	0.036	0.122	-90.647
218.	265	0.826	0.380	0.461	-8.197	0.361	0.474	-4.882	0.098	0.119	-91.326
219.	266	1.205	0.494	0.410	-20.613	0.463	0.386	-26.472	0.413	0.343	-36.825
220.	270	0.253	0.188	0.745	60.772	0.057	0.237	-62.649	0.138	0.547	12.770
221.	272	0.392	0.125	0.319	-42.656	0.126	0.326	-41.004	0.165	0.420	-18.127
222.	273	0.470	0.288	0.612	28.433	0.310	0.667	41.974	0.253	0.538	10.501
223.	274	2.460	1.049	0.426	-16.590	1.179	0.455	-9.568	0.932	0.379	-28.086
224.	275	0.999	0.584	0.585	21.862	0.646	0.614	29.113	0.455	0.456	-9.351
225.	276	1.359	0.544	0.400	-22.944	0.581	0.440	-13.263	0.352	0.259	-57.204
226.	278	6.610	3.351	0.507	3.022	3.196	0.476	-4.557	3.201	0.484	-2.520
227.	279	0.361	0.166	0.459	-8.674	0.036	0.101	-95.612	0.165	0.457	-9.162
228.	280	4.191	1.522	0.363	-31.958	1.640	0.393	-24.605	2.066	0.493	-0.398
229.	281	0.412	0.128	0.311	-44.501	0.113	0.251	-59.111	0.228	0.553	14.196
230.	282	0.220	0.078	0.355	-33.810	0.140	0.636	34.317	0.133	0.605	26.879
231.	284	0.988	0.232	0.235	-63.081	0.519	0.531	8.775	0.609	0.617	29.746
232.	285	0.802	0.326	0.406	-21.410	0.356	0.440	-13.269	0.460	0.573	19.152
233.	286	0.304	0.143	0.471	-5.725	0.159	0.489	-1.391	0.173	0.568	17.729

234.	288	1.258	0.486	0.386	-26.380	0.534	0.442	-12.749	0.827	0.657	39.513
235.	295	1.316	0.259	0.197	-72.414	0.380	0.292	-49.266	0.243	0.185	-75.278
236.	296	1.269	0.477	0.376	-28.791	0.534	0.425	-16.816	0.896	0.706	51.479
237.	297	3.678	1.928	0.524	7.199	1.629	0.447	-11.631	2.451	0.666	41.711
238.	298	0.560	0.282	0.504	2.234	0.177	0.331	-39.731	0.269	0.481	-3.235
239.	300	0.229	0.144	0.626	31.904	0.106	0.473	-5.222	0.135	0.589	23.035
240.	302	0.186	0.101	0.542	11.498	0.075	0.409	-20.808	0.106	0.566	17.469
241.	304	0.254	0.113	0.444	-12.171	0.090	0.352	-34.593	0.094	0.369	-30.505
242.	305	2.685	1.657	0.617	29.783	1.196	0.455	-9.617	1.473	0.549	13.117
243.	306	0.596	0.260	0.437	-13.957	0.237	0.400	-22.855	0.236	0.396	-23.914
244.	307	0.906	0.381	0.420	-18.051	0.365	0.404	-22.110	0.391	0.432	-15.237
245.	308	0.329	0.199	0.605	26.846	0.159	0.469	-6.120	0.119	0.361	-32.519
246.	312	0.598	0.276	0.462	-7.913	0.341	0.566	17.468	0.232	0.389	-25.762
247.	313	0.039	0.025	0.650	37.741	0.010	0.256	-57.972	0.017	0.434	-14.706
248.	314	0.421	0.212	0.504	2.180	0.208	0.574	19.187	0.171	0.406	-21.475
249.	319	0.227	0.143	0.631	33.046	0.094	0.392	-24.933	0.043	0.191	-73.683
250.	321	0.141	0.043	0.306	-45.770	0.018	0.129	-88.876	0.021	0.148	-84.255
251.	322	0.186	0.063	0.339	-37.855	0.062	0.365	-31.477	0.073	0.393	-24.699
252.	323	0.371	0.256	0.692	47.882	0.311	0.837	83.337	0.112	0.302	-46.894
253.	324	1.530	0.741	0.484	-2.532	0.844	0.558	15.529	0.417	0.273	-53.883
254.	325	1.831	1.091	0.596	24.644	0.803	0.436	-14.256	0.638	0.349	-35.466
255.	326	0.404	0.279	0.690	47.494	0.200	0.479	-3.754	0.161	0.398	-23.569
256.	328	0.606	0.376	0.620	30.605	0.380	0.627	32.182	0.439	0.724	55.869
257.	329	0.657	0.440	0.670	42.726	0.350	0.614	29.114	0.044	0.067	-103.982
258.	330	4.290	1.855	0.432	-15.105	1.972	0.444	-12.379	1.708	0.398	-23.432
259.	331	0.384	0.195	0.506	2.891	0.244	0.642	35.926	0.215	0.559	15.772
260.	333	0.321	0.155	0.482	-3.066	0.183	0.573	19.063	0.111	0.346	-36.163
261.	334	0.323	0.142	0.438	-13.683	0.102	0.373	-29.485	0.071	0.220	-66.662
262.	335	2.842	1.427	0.502	1.847	1.050	0.369	-30.424	1.234	0.434	-14.676
263.	336	0.413	0.233	0.566	17.252	0.188	0.472	-5.358	0.156	0.378	-28.413

264.	337	0.191	0.131	0.682	45.640	0.147	0.769	66.764	0.149	0.778	68.826
265.	338	0.203	0.121	0.598	25.216	0.062	0.290	-49.772	0.061	0.300	-47.255
266.	341	3.431	2.030	0.592	23.606	1.584	0.461	-8.218	1.350	0.394	-24.552
267.	342	0.120	0.057	0.478	-4.095	0.026	0.229	-64.512	0.041	0.343	-36.785
268.	343	1.479	0.584	0.395	-24.250	0.569	0.391	-25.122	0.708	0.478	-3.974
269.	344	0.702	0.169	0.241	-61.735	0.216	0.320	-42.309	0.208	0.297	-48.084
270.	345	0.279	0.176	0.630	32.907	0.083	0.302	-46.677	0.158	0.567	17.562
271.	348	0.709	0.483	0.681	45.227	0.393	0.591	23.402	0.531	0.748	61.617
272.	351	0.767	0.507	0.660	40.282	0.429	0.550	13.369	0.395	0.515	5.065
273.	352	1.759	1.248	0.710	52.255	0.840	0.469	-6.267	0.998	0.567	17.689
274.	353	5.593	3.510	0.628	32.350	3.039	0.543	11.745	2.696	0.482	-3.051
275.	355	1.677	1.090	0.650	37.751	1.004	0.613	28.769	0.861	0.513	4.508
276.	357	5.074	2.883	0.568	17.908	2.431	0.483	-2.743	2.259	0.445	-11.984
277.	358	0.923	0.285	0.309	-45.211	0.304	0.341	-37.235	0.138	0.149	-83.939
278.	359	2.534	1.336	0.527	7.946	1.463	0.594	24.261	1.445	0.570	18.433
279.	361	0.428	0.254	0.594	24.256	0.167	0.363	-32.070	0.274	0.641	35.646
280.	362	1.537	0.932	0.606	27.196	0.933	0.614	29.002	0.395	0.257	-57.698
281.	363	0.630	0.411	0.652	38.175	0.258	0.475	-4.711	0.242	0.383	-27.005
282.	364	0.181	0.064	0.355	-33.837	0.053	0.293	-48.870	0.019	0.107	-94.234
283.	365	1.385	0.675	0.487	-1.780	0.698	0.506	2.755	0.399	0.288	-50.234
284.	366	0.212	0.100	0.473	-5.301	0.090	0.426	-16.647	0.109	0.512	4.165
285.	367	0.137	0.105	0.762	65.015	0.071	0.477	-4.161	0.067	0.488	-1.669
286.	368	0.182	0.098	0.538	10.588	0.085	0.466	-7.042	0.067	0.369	-30.599
287.	370	0.278	0.217	0.779	69.159	0.246	0.891	96.266	0.113	0.408	-21.112
288.	371	0.358	0.069	0.194	-73.052	0.201	0.506	2.791	0.110	0.306	-45.780
289.	372	0.240	0.138	0.574	19.275	0.107	0.444	-12.191	0.132	0.548	12.864
290.	373	0.157	0.068	0.436	-14.308	0.094	0.625	31.585	0.050	0.320	-42.535
291.	375	0.243	0.165	0.679	44.873	0.115	0.508	3.275	0.038	0.157	-82.109
292.	376	0.176	0.100	0.571	18.603	0.053	0.337	-38.392	0.063	0.361	-32.523
293.	377	0.080	0.062	0.781	69.572	0.021	0.261	-56.748	0.022	0.277	-52.837

294.	381	0.873	0.530	0.607	27.364	0.112	0.133	-87.891	0.341	0.391	-25.164
295.	383	2.359	0.604	0.256	-57.941	1.526	0.652	38.216	0.550	0.233	-63.584
296.	384	1.038	0.403	0.388	-25.914	0.476	0.454	-9.733	0.411	0.396	-24.029
297.	386	0.499	0.111	0.223	-65.908	0.280	0.564	16.896	0.134	0.268	-55.093
298.	387	0.077	0.041	0.537	10.425	0.067	0.769	66.696	0.046	0.593	23.896
299.	388	0.245	0.087	0.355	-33.810	0.055	0.218	-67.172	0.112	0.459	-8.557
300.	389	0.196	0.106	0.540	10.973	0.033	0.170	-78.848	0.053	0.271	-54.370
301.	392	0.514	0.201	0.390	-25.347	0.130	0.245	-60.635	0.250	0.487	-1.886
302.	393	1.049	0.343	0.327	-40.660	0.304	0.282	-51.661	0.541	0.516	5.174
303.	395	1.546	0.783	0.507	2.905	0.528	0.343	-36.721	0.824	0.533	9.380
304.	396	0.292	0.152	0.520	6.070	0.172	0.588	22.772	0.168	0.573	19.112
305.	397	0.543	0.230	0.423	-17.460	0.151	0.277	-52.907	0.318	0.584	21.852
306.	398	0.976	0.587	0.601	25.951	0.397	0.404	-22.045	0.669	0.686	46.427
307.	400	0.759	0.192	0.253	-58.758	0.169	0.225	-65.579	0.369	0.486	-2.081
308.	401	0.315	0.148	0.468	-6.414	0.074	0.224	-65.734	0.160	0.508	3.250
309.	402	0.491	0.215	0.438	-13.777	0.292	0.577	20.136	0.280	0.570	18.401
310.	404	0.225	0.040	0.176	-77.317	0.057	0.255	-58.200	0.054	0.239	-62.137
311.	405	0.286	0.039	0.137	-86.894	0.083	0.291	-49.378	0.127	0.443	-12.573
312.	406	0.125	0.029	0.233	-63.473	0.078	0.647	36.957	0.045	0.357	-33.332
313.	414	0.658	0.414	0.630	32.921	0.339	0.491	-0.976	0.278	0.423	-17.321
314.	415	0.272	0.164	0.602	26.010	0.121	0.438	-13.641	0.082	0.299	-47.406
315.	417	0.726	0.313	0.432	-15.318	0.329	0.434	-14.656	0.198	0.273	-53.940
316.	421	0.390	0.154	0.394	-24.434	0.172	0.467	-6.635	0.139	0.356	-33.677
317.	422	0.947	0.524	0.554	14.424	0.477	0.499	1.062	0.331	0.350	-35.150
318.	423	2.875	1.138	0.396	-23.948	0.780	0.274	-53.480	0.956	0.333	-39.381
319.	424	0.284	0.174	0.613	28.701	0.241	0.856	87.938	0.096	0.340	-37.658
320.	425	0.549	0.270	0.491	-0.825	0.149	0.253	-58.641	0.267	0.487	-1.728
321.	426	1.649	0.698	0.423	-17.316	0.407	0.248	-59.878	0.532	0.323	-41.748
322.	427	0.249	0.133	0.532	9.095	0.119	0.476	-4.407	0.078	0.312	-44.343
323.	428	1.134	0.408	0.360	-32.758	0.595	0.528	8.237	0.206	0.182	-76.014

324.	429	0.269	0.142	0.526	7.747	0.132	0.492	-0.617	0.129	0.481	-3.246
325.	430	0.604	0.245	0.405	-21.670	0.311	0.514	4.762	0.220	0.364	-31.658
326.	431	0.264	0.148	0.559	15.559	0.074	0.280	-52.099	0.044	0.165	-80.178
327.	432	0.085	0.038	0.450	-10.875	0.040	0.473	-5.249	0.044	0.510	3.694
328.	433	1.762	0.612	0.347	-35.810	0.641	0.365	-31.433	0.648	0.368	-30.831
329.	434	0.319	0.104	0.328	-40.519	0.085	0.269	-54.849	0.160	0.503	2.117
330.	435	0.300	0.119	0.397	-23.758	0.096	0.323	-41.790	0.111	0.370	-30.204
331.	437	0.780	0.440	0.564	16.822	0.364	0.457	-9.222	0.657	0.842	84.388
332.	440	0.965	0.399	0.413	-19.787	0.359	0.377	-28.530	0.260	0.269	-54.712
333.	442	0.150	0.069	0.464	-7.531	0.056	0.362	-32.208	0.044	0.292	-49.243
334.	443	0.183	0.090	0.492	-0.649	0.034	0.187	-74.753	0.089	0.487	-1.953
335.	444	0.359	0.134	0.372	-29.700	0.107	0.281	-51.787	0.065	0.182	-75.916
336.	445	0.334	0.228	0.683	45.696	0.235	0.721	55.148	0.223	0.667	41.835
337.	447	0.237	0.117	0.493	-0.438	0.081	0.343	-36.750	0.076	0.321	-42.212
338.	448	0.137	0.050	0.365	-31.579	0.074	0.553	14.317	0.044	0.317	-43.074
339.	450	0.315	0.122	0.386	-26.282	0.269	0.875	92.358	0.089	0.283	-51.307
340.	451	0.725	0.145	0.200	-71.617	0.212	0.306	-45.805	0.150	0.207	-69.861
341.	452	0.354	0.086	0.243	-61.154	0.152	0.437	-14.079	0.052	0.148	-84.313
342.	457	0.286	0.094	0.330	-39.896	0.106	0.379	-28.143	0.105	0.366	-31.222
343.	458	0.619	0.177	0.286	-50.567	0.248	0.369	-30.555	0.233	0.376	-28.880
344.	459	0.493	0.200	0.406	-21.523	0.095	0.197	-72.214	0.207	0.421	-17.847
345.	460	0.796	0.227	0.286	-50.786	0.301	0.392	-24.921	0.384	0.482	-2.953
346.	461	0.691	0.366	0.529	8.458	0.253	0.390	-25.454	0.300	0.433	-14.857
347.	462	1.009	0.417	0.413	-19.704	0.466	0.406	-21.588	0.481	0.477	-4.325
348.	463	0.477	0.243	0.509	3.410	0.172	0.258	-57.411	0.213	0.446	-11.785
349.	464	1.233	0.531	0.431	-15.399	0.456	0.373	-29.512	0.401	0.325	-41.121
350.	465	0.463	0.136	0.293	-49.073	0.237	0.511	3.973	0.152	0.328	-40.514
351.	466	0.093	0.036	0.389	-25.667	0.019	0.209	-69.286	0.043	0.465	-7.197
352.	467	0.480	0.192	0.400	-22.926	0.202	0.421	-17.757	0.087	0.182	-75.965
353.	468	0.662	0.323	0.488	-1.605	0.185	0.277	-52.969	0.088	0.133	-87.817

354.	470	0.238	0.080	0.338	-38.163	0.094	0.429	-16.023	0.086	0.360	-32.656
355.	471	1.311	0.879	0.670	42.740	0.533	0.441	-12.957	0.438	0.334	-39.048
356.	472	1.148	0.783	0.682	45.610	0.532	0.503	1.964	0.581	0.506	2.861
357.	473	0.706	0.384	0.544	12.127	0.238	0.370	-30.335	0.362	0.513	4.451
358.	475	0.558	0.272	0.488	-1.692	0.132	0.229	-64.609	0.128	0.229	-64.484
359.	476	2.557	1.491	0.583	21.516	1.469	0.571	18.627	1.029	0.403	-22.364
360.	481	0.293	0.137	0.467	-6.811	0.107	0.349	-35.344	0.092	0.312	-44.387
361.	482	0.510	0.164	0.322	-41.950	0.322	0.645	36.441	0.234	0.458	-8.777
362.	483	2.486	1.500	0.603	26.460	1.510	0.644	36.328	1.130	0.455	-9.735
363.	484	1.720	1.378	0.801	74.479	1.272	0.745	60.892	0.622	0.362	-32.290
364.	485	2.672	1.014	0.380	-27.911	1.097	0.418	-18.672	0.483	0.181	-76.291
365.	487	0.096	0.065	0.676	44.132	0.043	0.483	-2.735	0.022	0.233	-63.617
366.	489	0.305	0.067	0.221	-66.589	0.278	0.904	99.455	0.107	0.350	-35.062
367.	491	0.189	0.116	0.610	28.104	0.133	0.714	53.260	0.110	0.582	21.146
368.	498	2.559	0.491	0.192	-73.531	0.629	0.239	-62.088	0.275	0.108	-94.036
369.	499	0.266	0.195	0.734	58.195	0.231	0.846	85.301	0.132	0.495	0.182
370.	500	0.052	0.052	1.000	122.830	0.035	0.699	49.621	0.033	0.636	34.274
371.	502	0.170	0.103	0.603	26.343	0.029	0.159	-81.642	0.056	0.327	-40.736
372.	506	1.228	0.430	0.350	-35.072	0.517	0.394	-24.331	0.596	0.485	-2.292
373.	507	0.453	0.190	0.418	-18.563	0.347	0.658	39.828	0.203	0.448	-11.377
374.	513	0.280	0.141	0.504	2.384	0.103	0.358	-33.214	0.136	0.486	-2.066
375.	514	0.935	0.409	0.437	-13.900	0.636	0.680	45.091	0.589	0.630	32.943
376.	515	0.787	0.283	0.359	-32.837	0.192	0.246	-60.394	0.127	0.162	-80.844
377.	516	0.736	0.335	0.455	-9.571	0.507	0.710	52.458	0.569	0.774	67.852
378.	517	0.714	0.512	0.717	54.173	0.413	0.646	36.688	0.413	0.578	20.390
379.	518	3.183	1.403	0.441	-13.096	1.457	0.458	-8.986	1.566	0.492	-0.621
380.	519	1.170	0.570	0.487	-1.777	0.558	0.480	-3.521	0.769	0.657	39.460
381.	520	1.444	0.474	0.328	-40.459	0.702	0.452	-10.371	0.633	0.438	-13.632
382.	521	0.780	0.607	0.779	69.039	0.484	0.629	32.562	0.540	0.692	48.058
383.	522	0.480	0.382	0.794	72.884	0.235	0.428	-16.211	0.141	0.293	-48.949

384.	523	1.928	0.896	0.465	-7.293	0.700	0.357	-33.529	0.817	0.424	-17.217
385.	524	0.205	0.113	0.551	13.727	0.102	0.498	0.794	0.086	0.419	-18.458
386.	525	0.286	0.141	0.494	-0.051	0.108	0.386	-26.450	0.104	0.363	-31.928
387.	526	0.702	0.384	0.547	12.758	0.412	0.609	27.913	0.153	0.219	-67.040
388.	527	0.619	0.363	0.586	22.319	0.163	0.261	-56.845	0.403	0.652	38.169
389.	528	0.334	0.144	0.431	-15.464	0.218	0.528	8.212	0.145	0.435	-14.373
390.	529	2.606	0.847	0.325	-41.179	1.457	0.555	14.679	1.161	0.446	-11.925
391.	530	0.343	0.179	0.521	6.531	0.222	0.693	48.169	0.144	0.419	-18.272
392.	531	0.443	0.239	0.539	10.755	0.217	0.527	7.771	0.234	0.528	8.228
393.	532	0.094	0.061	0.648	37.326	0.097	0.936	107.368	0.056	0.599	25.288
394.	533	1.018	0.428	0.421	-17.935	0.448	0.435	-14.406	0.350	0.344	-36.706
395.	534	1.841	1.212	0.658	39.827	0.649	0.361	-32.421	1.168	0.634	33.972
396.	535	0.393	0.199	0.505	2.622	0.092	0.235	-63.004	0.185	0.471	-5.614
397.	536	3.845	2.225	0.579	20.428	1.505	0.400	-22.906	1.784	0.464	-7.446
398.	537	0.718	0.549	0.764	65.595	0.029	0.042	-110.093	0.405	0.564	16.751
399.	538	0.153	0.086	0.561	16.243	0.072	0.473	-5.281	0.060	0.391	-25.202
400.	539	1.462	0.842	0.576	19.795	0.704	0.472	-5.559	0.851	0.582	21.348
401.	540	0.143	0.076	0.531	8.842	0.068	0.482	-3.054	0.077	0.537	10.409
402.	541	0.078	0.035	0.454	-9.959	0.054	0.701	50.138	0.025	0.328	-40.424
403.	542	0.239	0.135	0.564	16.969	0.123	0.500	1.402	0.175	0.734	58.232
404.	543	0.095	0.056	0.588	22.657	0.065	0.683	45.852	0.055	0.581	20.937
405.	544	0.289	0.127	0.441	-12.973	0.195	0.675	43.832	0.109	0.378	-28.340
406.	545	0.228	0.131	0.576	19.854	0.189	0.832	81.915	0.129	0.565	17.156
407.	546	0.059	0.029	0.501	1.545	0.045	0.764	65.503	0.027	0.458	-8.794
408.	547	1.895	0.970	0.512	4.231	0.579	0.323	-41.758	0.679	0.358	-33.187
409.	548	0.090	0.038	0.420	-18.173	0.024	0.269	-54.846	0.028	0.314	-43.764
410.	549	0.274	0.070	0.257	-57.815	0.067	0.208	-69.669	0.043	0.156	-82.213
411.	550	0.107	0.035	0.324	-41.531	0.015	0.126	-89.463	0.025	0.231	-64.077
412.	551	0.553	0.285	0.515	4.882	0.158	0.293	-48.914	0.317	0.573	18.960
413.	552	1.913	1.210	0.632	33.507	1.089	0.558	15.488	0.874	0.457	-9.122

414.	553	0.173	0.120	0.693	48.295	0.122	0.705	51.261	0.073	0.423	-17.343
415.	554	0.409	0.294	0.720	54.760	0.313	0.739	59.385	0.176	0.431	-15.442
416.	555	0.209	0.137	0.654	38.712	0.069	0.353	-34.446	0.085	0.405	-21.848
417.	556	0.270	0.123	0.457	-9.179	0.101	0.441	-12.998	0.183	0.678	44.474
418.	557	0.993	0.490	0.493	-0.423	0.479	0.498	0.909	0.444	0.447	-11.567
419.	558	1.909	0.988	0.518	5.636	0.432	0.227	-64.954	1.277	0.669	42.396
420.	561	4.360	2.207	0.506	2.810	2.188	0.495	0.040	2.135	0.490	-1.185
421.	563	0.337	0.337	1.000	122.830	0.177	0.548	13.004	0.124	0.367	-30.965
422.	564	0.105	0.043	0.414	-19.649	0.030	0.279	-52.394	0.041	0.392	-24.865
423.	565	0.191	0.092	0.481	-3.347	0.070	0.437	-13.977	0.124	0.646	36.884
424.	566	0.262	0.163	0.623	31.124	0.108	0.404	-21.994	0.164	0.626	31.981
425.	567	13.326	7.443	0.559	15.543	5.388	0.399	-23.219	6.624	0.497	0.609
426.	568	13.273	5.548	0.418	-18.599	6.752	0.489	-1.331	7.361	0.555	14.583
427.	569	2.531	0.626	0.247	-60.111	0.782	0.306	-45.861	0.652	0.258	-57.564
428.	575	0.099	0.053	0.540	10.989	0.037	0.370	-30.184	0.046	0.470	-5.967
429.	579	0.368	0.204	0.556	14.864	0.182	0.542	11.650	0.120	0.327	-40.843
430.	580	0.264	0.112	0.424	-17.094	0.166	0.653	38.615	0.103	0.390	-25.304
431.	583	0.376	0.144	0.381	-27.472	0.140	0.412	-20.064	0.136	0.361	-32.508
432.	584	0.752	0.428	0.569	18.159	0.231	0.484	-2.654	0.324	0.431	-15.460
433.	589	0.385	0.289	0.750	62.058	0.129	0.311	-44.498	0.129	0.334	-38.962
434.	590	1.756	0.291	0.166	-79.930	0.278	0.170	-78.945	0.214	0.122	-90.545
435.	591	0.509	0.248	0.487	-1.869	0.372	0.762	64.913	0.159	0.313	-44.135
436.	592	0.157	0.095	0.605	26.760	0.070	0.447	-11.615	0.041	0.265	-55.886
437.	593	0.212	0.138	0.653	38.424	0.183	0.887	95.449	0.042	0.198	-71.964
438.	595	0.745	0.572	0.768	66.494	0.457	0.607	27.428	0.266	0.358	-33.233
439.	596	0.834	0.467	0.560	15.838	0.421	0.518	5.608	0.406	0.487	-1.943
440.	597	2.265	1.213	0.535	9.945	1.037	0.458	-8.937	1.082	0.478	-4.129
441.	598	0.998	0.465	0.466	-7.005	0.505	0.563	16.551	0.486	0.487	-1.955
442.	599	0.485	0.232	0.479	-3.866	0.273	0.575	19.668	0.276	0.569	18.085
443.	600	0.635	0.247	0.388	-25.793	0.252	0.453	-10.093	0.250	0.394	-24.536

444.	601	0.411	0.203	0.492	-0.507	0.214	0.571	18.546	0.185	0.450	-10.950
445.	602	0.096	0.065	0.676	44.106	0.086	0.879	93.397	0.062	0.651	37.996
446.	603	0.272	0.163	0.598	25.069	0.079	0.290	-49.594	0.022	0.080	-100.761
447.	604	0.173	0.088	0.506	2.843	0.100	0.575	19.503	0.118	0.681	45.203
448.	605	0.053	0.029	0.550	13.458	0.043	0.806	75.779	0.023	0.443	-12.523
449.	607	0.322	0.152	0.472	-5.489	0.169	0.662	40.735	0.120	0.371	-29.917
450.	608	0.683	0.487	0.713	53.047	0.390	0.601	25.844	0.227	0.333	-39.331
451.	612	0.726	0.223	0.307	-45.675	0.159	0.230	-64.350	0.071	0.098	-96.283
452.	619	0.276	0.098	0.354	-34.116	0.110	0.396	-24.039	0.180	0.652	38.241
453.	621	0.199	0.087	0.438	-13.686	0.127	0.615	29.234	0.102	0.511	3.914
454.	625	0.518	0.329	0.636	34.264	0.282	0.672	43.109	0.719	1.389	217.359
455.	627	0.208	0.137	0.661	40.530	0.035	0.191	-73.837	0.063	0.303	-46.592
456.	628	0.577	0.275	0.476	-4.545	0.111	0.168	-79.257	0.147	0.254	-58.375
457.	629	0.184	0.110	0.597	24.867	0.026	0.154	-82.871	0.102	0.557	15.127
458.	630	0.273	0.154	0.563	16.632	0.029	0.105	-94.568	0.061	0.224	-65.867
459.	631	0.163	0.086	0.529	8.343	0.076	0.507	2.954	0.041	0.251	-59.150
460.	632	0.120	0.053	0.441	-13.023	0.038	0.338	-37.964	0.044	0.364	-31.661
461.	633	0.169	0.075	0.441	-12.993	0.101	0.551	13.755	0.080	0.475	-4.853
462.	635	0.171	0.074	0.431	-15.373	0.072	0.424	-17.138	0.057	0.337	-38.353
463.	636	0.420	0.092	0.219	-67.026	-----	-----	-----	0.091	0.217	-67.495
464.	637	0.329	0.118	0.359	-33.000	-----	-----	-----	0.052	0.160	-81.369
465.	638	0.124	0.071	0.575	19.580	0.096	0.771	67.113	0.050	0.402	-22.435
466.	639	0.177	0.044	0.252	-58.983	0.078	0.444	-12.372	0.076	0.428	-16.184
467.	640	0.089	0.044	0.491	-0.780	0.040	0.444	-12.360	0.021	0.233	-63.599
468.	642	0.461	0.237	0.513	4.558	-----	-----	-----	0.031	0.067	-103.811
469.	643	0.529	0.186	0.352	-34.679	-----	-----	-----	0.179	0.338	-38.016
470.	644	0.261	0.101	0.386	-26.271	0.125	0.566	17.306	0.108	0.412	-20.009
471.	650	0.409	0.157	0.385	-26.667	0.021	0.055	-106.871	0.166	0.406	-21.523
472.	651	0.173	0.069	0.401	-22.669	0.063	0.667	41.850	0.079	0.459	-8.743
473.	653	0.163	0.057	0.352	-34.526	0.069	0.427	-16.363	0.048	0.293	-49.034

474.	654	0.167	0.079	0.470	-5.959	0.128	0.750	62.133	0.058	0.345	-36.243
475.	656	0.234	0.125	0.533	9.331	0.094	0.404	-22.006	0.101	0.433	-14.952
476.	657	0.097	0.052	0.535	9.716	0.067	0.691	47.770	0.063	0.651	37.984
477.	658	0.507	0.176	0.346	-36.005	-----	-----	-----	0.099	0.196	-72.575
478.	659	0.225	0.106	0.470	-5.866	0.095	0.447	-11.531	0.043	0.191	-73.725
479.	661	0.255	0.128	0.503	1.995	0.178	0.593	23.804	0.090	0.351	-34.877
480.	662	0.102	0.039	0.380	-27.716	0.027	0.266	-55.461	0.057	0.558	15.469
481.	665	0.373	0.098	0.263	-56.317	0.084	0.224	-65.693	0.169	0.453	-10.080
482.	666	0.211	0.098	0.464	-7.428	0.094	0.444	-12.389	0.107	0.506	2.683
483.	672	0.307	0.208	0.678	44.521	0.049	0.152	-83.257	0.144	0.470	-5.863
484.	673	2.514	0.429	0.171	-78.709	0.186	0.075	-101.928	0.341	0.136	-87.216
485.	674	1.285	0.596	0.463	-7.561	0.656	0.528	8.086	0.351	0.273	-53.901
486.	675	0.143	0.054	0.376	-28.781	0.086	0.598	25.090	0.037	0.262	-56.492
487.	676	0.290	0.092	0.317	-43.259	0.131	0.450	-10.882	0.132	0.456	-9.396
488.	677	1.036	0.481	0.464	-7.383	0.180	0.184	-75.541	0.206	0.199	-71.916
489.	678	0.203	0.075	0.370	-30.156	-----	-----	-----	0.062	0.307	-45.627
490.	679	0.166	0.073	0.438	-13.775	-----	-----	-----	0.037	0.225	-65.628
491.	680	0.510	0.269	0.528	8.079	-----	-----	-----	0.087	0.170	-78.830
492.	681	0.336	0.228	0.679	44.800	0.200	0.614	28.982	0.101	0.301	-47.153
493.	683	0.073	0.022	0.299	-47.495	0.040	0.553	14.269	0.026	0.350	-35.187
494.	685	0.183	0.078	0.428	-16.083	0.052	0.292	-49.191	0.093	0.509	3.453
495.	687	0.338	0.159	0.470	-6.045	0.216	0.639	35.122	0.137	0.404	-21.937
496.	688	0.955	0.516	0.540	10.978	0.587	0.605	26.947	0.562	0.588	22.696
497.	693	0.491	0.219	0.446	-11.765	0.302	0.616	29.591	0.222	0.452	-10.413
498.	695	0.719	0.266	0.370	-30.169	0.310	0.426	-16.704	0.340	0.473	-5.283
499.	696	0.116	0.066	0.569	18.002	0.064	0.629	32.762	0.058	0.504	2.238
500.	697	2.368	0.772	0.326	-40.918	1.105	0.467	-6.794	0.590	0.249	-59.642
501.	698	0.148	0.056	0.379	-28.070	0.109	0.804	75.239	0.061	0.416	-19.136
502.	700	0.253	0.077	0.303	-46.566	0.185	0.794	72.805	0.072	0.285	-50.819
503.	701	0.247	0.093	0.379	-28.175	0.219	0.889	95.972	0.113	0.459	-8.694

504.	702	1.128	0.583	0.516	5.333	0.120	0.106	-94.424	0.174	0.154	-82.795
505.	703	0.392	0.232	0.592	23.721	0.217	0.514	4.701	0.231	0.588	22.708
506.	704	0.463	0.202	0.437	-13.926	0.173	0.392	-24.859	0.199	0.429	-15.872
507.	705	0.421	0.079	0.187	-74.624	0.294	0.655	38.963	0.154	0.367	-31.053
508.	706	0.161	0.087	0.542	11.442	0.083	0.537	10.302	0.043	0.267	-55.265
509.	707	0.522	0.224	0.430	-15.729	0.415	0.840	83.964	0.150	0.287	-50.434
510.	708	0.455	0.081	0.177	-77.179	0.357	0.833	82.249	0.097	0.213	-68.375
511.	709	1.473	0.832	0.565	17.089	0.775	0.591	23.350	0.613	0.416	-19.088
512.	710	0.776	0.405	0.522	6.611	0.357	0.513	4.548	0.240	0.309	-45.060
513.	713	3.265	1.400	0.429	-16.005	1.564	0.511	4.024	1.843	0.565	17.011
514.	714	0.456	0.221	0.486	-2.197	0.333	0.818	78.605	0.256	0.561	16.197
515.	715	0.087	0.058	0.665	41.377	0.053	0.829	81.288	0.043	0.495	0.146
516.	716	0.092	0.049	0.535	9.842	0.091	0.916	102.417	0.039	0.424	-17.231
517.	717	0.114	0.073	0.641	35.566	0.062	0.848	85.792	0.034	0.299	-47.451
518.	718	0.256	0.158	0.615	29.359	0.196	0.849	86.223	0.173	0.675	43.748
519.	719	0.322	0.066	0.206	-70.148	0.131	0.542	11.463	0.097	0.301	-46.995
520.	720	0.703	0.470	0.669	42.345	0.450	0.736	58.613	0.147	0.209	-69.277
521.	721	0.392	0.248	0.632	33.435	0.060	0.174	-77.864	0.156	0.396	-23.888
522.	722	0.209	0.097	0.467	-6.575	0.147	0.836	82.933	0.080	0.383	-27.223
523.	723	0.173	0.088	0.507	2.924	0.128	0.919	103.205	0.053	0.307	-45.617
524.	724	1.374	0.832	0.605	26.886	0.464	0.447	-11.659	0.251	0.183	-75.722
525.	725	0.331	0.159	0.482	-3.121	0.123	0.435	-14.380	0.118	0.357	-33.456
526.	726	0.388	0.274	0.705	51.134	0.142	0.437	-13.912	0.099	0.254	-58.501
527.	727	1.573	1.278	0.812	77.167	0.541	0.356	-33.551	0.757	0.481	-3.270
528.	728	6.470	5.242	0.810	76.693	2.643	0.407	-21.363	2.389	0.369	-30.477
529.	729	1.029	0.884	0.859	88.661	0.439	0.429	-16.047	0.466	0.453	-10.104
530.	730	2.622	1.506	0.574	19.355	0.898	0.348	-35.629	1.091	0.416	-19.085
531.	731	0.720	0.370	0.514	4.803	0.221	0.329	-40.318	0.262	0.364	-31.794
532.	732	1.012	0.355	0.351	-35.004	0.128	0.127	-89.384	0.370	0.366	-31.250
533.	733	1.028	0.510	0.497	0.528	0.642	0.815	77.891	0.162	0.157	-81.934

534.	734	5.197	2.415	0.465	-7.269	2.089	0.404	-21.956	1.774	0.341	-37.241
535.	735	0.337	0.269	0.799	73.934	0.064	0.204	-70.669	0.207	0.614	28.953
536.	736	4.955	2.188	0.442	-12.862	1.874	0.379	-28.019	1.610	0.325	-41.227
537.	737	0.522	0.219	0.419	-18.368	0.185	0.365	-31.471	0.343	0.658	39.673
538.	738	32.022	15.043	0.470	-6.019	13.283	0.418	-18.713	10.445	0.326	-40.921
539.	739	1.299	0.869	0.670	42.536	0.565	0.484	-2.670	0.605	0.466	-6.901
540.	741	0.863	0.486	0.563	16.744	0.104	0.143	-85.390	0.211	0.244	-60.873
541.	742	0.877	0.450	0.513	4.427	0.382	0.580	20.684	0.459	0.524	7.176
542.	743	5.029	3.320	0.660	40.249	2.206	0.444	-12.382	1.966	0.391	-25.183
543.	744	5.098	3.097	0.607	27.442	1.798	0.357	-33.376	1.782	0.349	-35.260
544.	745	1.819	1.089	0.598	25.261	0.541	0.300	-47.349	0.524	0.288	-50.194
545.	746	0.327	0.213	0.650	37.660	0.126	0.518	5.693	0.110	0.337	-38.278
546.	747	6.320	4.649	0.736	58.603	2.988	0.480	-3.522	1.654	0.262	-56.584
547.	748	2.269	1.402	0.618	29.982	1.029	0.454	-9.800	0.723	0.318	-42.792
548.	749	4.523	2.589	0.572	18.909	2.082	0.500	1.340	2.305	0.510	3.632
549.	750	1.966	0.707	0.360	-32.764	0.862	0.502	1.753	0.759	0.386	-26.377
550.	751	24.580	8.493	0.346	-36.219	9.338	0.380	-27.723	6.297	0.256	-57.929
551.	752	0.302	0.191	0.632	33.400	0.170	0.677	44.434	0.107	0.354	-34.044
552.	753	0.522	0.370	0.710	52.315	0.094	0.194	-72.998	0.176	0.337	-38.387
553.	754	0.594	0.431	0.725	56.014	0.252	0.461	-8.154	0.301	0.506	2.798
554.	755	8.775	5.664	0.646	36.683	4.566	0.528	8.220	4.276	0.487	-1.770
555.	756	0.548	0.268	0.488	-1.542	0.297	0.529	8.398	0.264	0.481	-3.295
556.	757	3.521	2.114	0.600	25.746	1.070	0.304	-46.357	1.735	0.493	-0.445
557.	758	2.804	1.037	0.370	-30.342	0.759	0.272	-54.178	1.306	0.466	-6.991
558.	759	0.382	0.147	0.384	-26.837	0.161	0.421	-17.870	0.211	0.552	13.880
559.	760	4.791	2.656	0.554	14.561	1.278	0.276	-53.169	1.468	0.306	-45.712
560.	761	6.788	2.977	0.439	-13.618	1.079	0.186	-74.967	0.383	0.056	-106.479
561.	762	0.327	0.082	0.252	-59.039	0.194	0.591	23.480	0.133	0.405	-21.683
562.	763	0.100	0.062	0.618	29.982	0.029	0.443	-12.597	0.032	0.316	-43.490
563.	764	0.048	0.023	0.490	-1.226	0.029	0.604	26.502	0.017	0.347	-35.864

564.	765	0.428	0.282	0.659	39.930	0.189	0.499	1.002	0.132	0.310	-44.896
565.	766	0.193	0.075	0.386	-26.462	0.092	0.549	13.152	0.087	0.449	-11.024
566.	767	0.207	0.133	0.641	35.592	0.155	0.770	66.960	0.067	0.325	-41.101
567.	768	1.004	0.556	0.553	14.279	0.377	0.402	-22.381	0.336	0.335	-38.805
568.	769	0.464	0.330	0.710	52.389	0.227	0.520	6.077	0.244	0.527	7.776
569.	771	0.392	0.232	0.592	23.737	0.116	0.394	-24.535	0.219	0.559	15.600
570.	772	0.317	0.188	0.591	23.422	0.000	0.000	-120.180	0.162	0.511	4.059
571.	773	0.413	0.249	0.604	26.509	0.106	0.252	-58.942	0.157	0.379	-28.058
572.	774	0.358	0.101	0.283	-51.457	0.190	0.531	8.803	0.050	0.139	-86.339
573.	775	1.009	0.614	0.608	27.606	0.735	0.728	56.749	0.425	0.421	-17.841
574.	776	0.286	0.153	0.533	9.335	0.048	0.186	-74.862	0.106	0.370	-30.364
575.	777	2.184	1.333	0.610	28.121	0.854	0.427	-16.355	0.725	0.332	-39.492
576.	778	0.488	0.208	0.427	-16.305	0.296	0.604	26.559	0.128	0.263	-56.322
577.	779	0.485	0.204	0.420	-18.070	0.258	0.545	12.264	0.078	0.161	-81.074
578.	781	1.860	0.553	0.297	-47.925	0.284	0.153	-83.050	0.416	0.224	-65.816
579.	782	0.385	0.119	0.310	-44.757	0.150	0.385	-26.604	0.109	0.283	-51.470
580.	783	0.441	0.142	0.322	-41.821	0.246	0.559	15.585	0.173	0.391	-25.085
581.	784	0.946	0.268	0.283	-51.401	0.296	0.329	-40.133	0.267	0.282	-51.741
582.	786	0.111	0.085	0.761	64.676	0.104	0.882	94.241	0.040	0.361	-32.505
583.	787	0.177	0.116	0.653	38.611	0.598	0.371	-29.988	0.103	0.580	20.681
584.	792	0.076	0.036	0.478	-3.981	0.035	0.468	-6.452	0.034	0.451	-10.636
585.	793	0.113	0.044	0.385	-26.647	0.044	0.401	-22.816	0.047	0.412	-20.067
586.	794	0.111	0.037	0.334	-39.032	0.019	0.173	-78.255	0.045	0.410	-20.601
587.	796	3.621	2.030	0.561	16.057	1.392	0.404	-21.896	1.256	0.347	-35.920
588.	797	6.846	0.424	0.062	-105.117	0.433	0.066	-104.182	0.367	0.054	-107.150
589.	798	0.783	0.468	0.598	25.143	0.288	0.368	-30.742	0.195	0.249	-59.661
590.	799	1.042	0.731	0.702	50.437	0.588	0.610	28.068	0.438	0.421	-17.991
591.	800	4.469	3.431	0.768	66.390	1.763	0.443	-12.641	1.860	0.416	-19.018
592.	801	1.074	0.793	0.738	59.167	0.344	0.335	-38.696	0.470	0.438	-13.813
593.	802	3.722	2.794	0.751	62.252	1.381	0.412	-20.045	0.356	0.096	-96.948

594.	803	0.932	0.686	0.736	58.726	0.324	0.413	-19.927	0.170	0.182	-75.902
595.	804	0.594	0.330	0.555	14.640	0.179	0.369	-30.547	0.141	0.237	-62.580
596.	805	0.455	0.326	0.715	53.559	0.260	0.751	62.227	0.047	0.104	-95.010
597.	806	1.602	0.891	0.556	14.957	0.301	0.187	-74.761	0.296	0.185	-75.298
598.	807	2.064	0.917	0.445	-12.157	0.862	0.438	-13.810	0.591	0.286	-50.654
599.	808	1.110	0.265	0.239	-62.090	0.214	0.207	-69.924	0.295	0.265	-55.681
600.	809	0.863	0.362	0.419	-18.259	0.230	0.332	-39.569	0.143	0.166	-79.961
601.	810	0.315	0.102	0.324	-41.454	0.131	0.422	-17.674	0.087	0.277	-52.964
602.	811	0.126	0.073	0.585	21.906	0.115	0.871	91.498	0.097	0.770	67.006
603.	812	1.117	0.217	0.194	-72.938	0.427	0.403	-22.153	0.417	0.374	-29.406
604.	813	0.530	0.222	0.419	-18.284	0.251	0.486	-2.168	0.156	0.295	-48.611
605.	814	1.360	0.959	0.706	51.277	0.436	0.323	-41.697	0.419	0.308	-45.229
606.	815	1.294	0.887	0.685	46.321	0.354	0.287	-50.424	0.544	0.420	-18.132
607.	816	1.408	0.674	0.479	-3.797	0.549	0.498	0.800	0.267	0.190	-74.092
608.	817	2.566	1.726	0.673	43.290	1.540	0.620	30.368	0.976	0.380	-27.726
609.	818	3.015	1.264	0.419	-18.280	1.495	0.520	6.110	1.144	0.380	-27.955
610.	820	1.288	0.589	0.458	-8.975	0.614	0.498	0.730	0.710	0.552	13.911
611.	821	0.442	0.325	0.735	58.520	0.063	0.144	-85.216	0.123	0.278	-52.584
612.	822	0.712	0.338	0.475	-4.717	0.361	0.551	13.708	0.395	0.555	14.583
613.	823	0.160	0.084	0.526	7.648	0.071	0.501	1.458	0.052	0.326	-41.015
614.	824	0.263	0.110	0.418	-18.713	0.166	0.839	83.638	0.065	0.249	-59.714
615.	825	0.386	0.263	0.680	45.175	0.264	0.698	49.443	0.121	0.312	-44.273
616.	826	0.701	0.449	0.640	35.440	0.280	0.479	-3.814	0.054	0.076	-101.631
617.	827	0.416	0.231	0.557	15.153	0.159	0.486	-2.142	0.105	0.253	-58.824
618.	828	0.403	0.295	0.732	57.638	0.105	0.298	-47.738	0.210	0.522	6.613
619.	829	0.223	0.113	0.508	3.247	0.113	0.601	25.905	0.049	0.220	-66.839
620.	830	0.470	0.354	0.754	63.034	0.223	0.553	14.207	0.129	0.275	-53.375
621.	831	0.600	0.337	0.562	16.387	0.260	0.456	-9.475	0.101	0.168	-79.264
622.	833	0.032	0.032	1.000	122.830	0.011	0.278	-52.641	0.004	0.120	-90.951
623.	834	6.524	4.615	0.707	51.712	2.677	0.452	-10.404	1.959	0.300	-47.227

624.	835	5.968	4.234	0.709	52.229	3.305	0.584	21.804	1.624	0.272	-54.043
625.	836	0.180	0.111	0.619	30.153	0.101	0.626	32.018	0.102	0.569	18.095
626.	837	0.169	0.112	0.662	40.710	0.096	0.671	42.896	0.063	0.376	-28.792
627.	838	0.836	0.453	0.542	11.593	0.431	0.578	20.352	0.377	0.451	-10.553
628.	839	0.336	0.191	0.569	18.055	0.169	0.543	11.818	0.161	0.479	-3.861
629.	840	4.705	2.374	0.505	2.440	2.262	0.503	2.129	1.891	0.402	-22.525
630.	841	0.718	0.238	0.332	-39.597	0.082	0.153	-83.001	0.359	0.499	1.099
631.	842	0.769	0.442	0.574	19.371	0.604	0.837	83.333	0.237	0.308	-45.322
632.	843	0.348	0.198	0.570	18.283	0.145	0.433	-14.950	0.096	0.276	-53.177
633.	844	2.897	1.835	0.633	33.716	1.209	0.439	-13.524	0.790	0.273	-53.888
634.	845	2.632	2.632	1.000	122.830	1.083	0.408	-21.069	1.605	0.610	28.017
635.	846	1.274	0.580	0.455	-9.557	0.589	0.505	2.477	0.609	0.478	-4.062
636.	847	0.579	0.366	0.632	33.378	-----	-----	-----	0.274	0.474	-5.031
637.	848	0.285	0.158	0.556	14.882	0.122	0.738	59.147	0.124	0.435	-14.455
638.	849	8.335	3.988	0.479	-3.899	3.850	0.475	-4.648	2.684	0.322	-41.933
639.	850	0.906	0.392	0.433	-15.037	0.462	0.560	15.951	0.432	0.477	-4.306
640.	851	1.838	1.252	0.681	45.300	0.627	0.347	-35.737	0.695	0.378	-28.318
641.	852	1.711	0.675	0.394	-24.373	1.073	0.612	28.562	1.074	0.628	32.339
642.	853	0.702	0.437	0.622	31.007	0.281	0.454	-9.878	0.241	0.343	-36.751
643.	854	0.383	0.268	0.698	49.450	0.321	0.819	78.868	0.226	0.588	22.745
644.	855	0.602	0.298	0.495	0.100	0.315	0.791	71.941	0.159	0.264	-55.994
645.	857	9.936	4.800	0.483	-2.786	2.712	0.292	-49.284	1.646	0.166	-79.929
646.	858	3.167	1.580	0.499	1.100	1.036	0.366	-31.337	1.693	0.535	9.715
647.	859	0.350	0.182	0.519	5.923	0.243	0.828	80.993	0.206	0.588	22.629
648.	860	0.795	0.512	0.644	36.393	0.126	0.167	-79.601	0.367	0.462	-7.943
649.	861	6.884	3.567	0.518	5.735	2.016	0.529	8.447	2.936	0.427	-16.533
650.	862	2.021	1.061	0.525	7.367	0.663	0.346	-36.093	0.413	0.204	-70.541
651.	863	1.606	0.692	0.431	-15.511	0.843	0.570	18.441	0.503	0.313	-44.011
652.	865	2.814	1.635	0.581	21.024	1.014	0.390	-25.320	0.842	0.299	-47.453
653.	866	2.171	0.683	0.314	-43.786	0.816	0.392	-25.003	0.637	0.293	-48.908

654.	867	2.462	0.836	0.340	-37.639	0.899	0.398	-23.479	1.416	0.575	19.572
655.	870	0.630	0.314	0.499	1.013	0.214	0.377	-28.479	0.204	0.323	-41.610
656.	871	0.401	0.277	0.690	47.558	0.062	0.147	-84.457	0.195	0.486	-1.963
657.	873	0.868	0.332	0.383	-27.209	0.186	0.229	-64.599	0.222	0.255	-58.113
658.	874	0.497	0.215	0.434	-14.792	0.241	0.499	0.965	0.335	0.675	43.944
659.	875	1.910	0.279	0.146	-84.656	0.359	0.205	-70.458	0.330	0.173	-78.254
660.	876	0.763	0.153	0.200	-71.580	0.104	0.157	-81.928	0.196	0.257	-57.740
661.	877	0.629	0.230	0.365	-31.449	-----	-----	-----	0.277	0.441	-13.121
662.	878	0.857	0.391	0.457	-9.150	0.436	0.669	42.281	0.413	0.482	-3.175
663.	879	0.255	0.141	0.553	14.321	0.086	0.593	23.806	0.107	0.419	-18.458
664.	880	2.677	1.949	0.728	56.749	0.957	0.392	-24.890	0.910	0.340	-37.537
665.	881	3.721	2.069	0.556	14.947	0.890	0.241	-61.731	0.359	0.096	-96.742
666.	882	1.408	0.815	0.579	20.425	0.751	0.598	25.250	0.516	0.366	-31.132
667.	883	0.571	0.257	0.451	-10.659	0.175	0.352	-34.746	0.186	0.327	-40.841
668.	884	0.840	0.641	0.763	65.241	0.396	0.516	5.281	0.383	0.455	-9.496
669.	885	0.371	0.150	0.403	-22.306	0.229	0.688	47.106	0.097	0.261	-56.785
670.	886	0.352	0.152	0.432	-15.144	0.126	0.449	-11.023	0.107	0.305	-46.066
671.	887	0.293	0.130	0.444	-12.321	0.152	0.548	13.085	0.157	0.534	9.670
672.	888	0.239	0.095	0.397	-23.707	0.088	0.400	-22.898	0.099	0.413	-19.783
673.	889	0.816	0.266	0.326	-41.025	0.486	0.624	31.549	0.435	0.533	9.318
674.	890	1.751	1.061	0.606	27.039	0.821	0.489	-1.359	0.677	0.387	-26.224
675.	891	0.727	0.191	0.263	-56.189	0.237	0.373	-29.503	0.251	0.346	-36.100
676.	892	0.764	0.376	0.492	-0.651	0.598	0.804	75.208	0.480	0.629	32.650
677.	893	0.751	0.275	0.366	-31.133	0.233	0.507	3.145	0.121	0.161	-81.062
678.	894	0.370	0.186	0.503	1.934	-----	-----	-----	0.189	0.510	3.813
679.	895	0.560	0.560	1.000	122.830	-----	-----	-----	0.369	0.659	39.981
680.	896	0.472	0.192	0.407	-21.247	-----	-----	-----	0.235	0.499	1.121
681.	897	0.254	0.162	0.639	35.086	-----	-----	-----	0.073	0.290	-49.744
682.	899	0.506	0.275	0.545	12.242	-----	-----	-----	0.220	0.435	-14.403
683.	901	0.469	0.250	0.532	9.140	-----	-----	-----	0.174	0.370	-30.289

684.	902	0.751	0.334	0.445	-12.068	-----	-----	-----	0.269	0.359	-32.981
685.	903	0.390	0.176	0.451	-10.704	-----	-----	-----	0.146	0.374	-29.275
686.	904	0.432	0.263	0.610	27.936	-----	-----	-----	0.106	0.245	-60.535
687.	905	0.216	0.114	0.528	8.205	0.084	0.483	-2.742	0.107	0.497	0.499
688.	906	0.324	0.274	0.846	85.344	-----	-----	-----	0.164	0.505	2.509
689.	907	0.933	0.933	1.000	122.830	-----	-----	-----	0.483	0.517	5.562
690.	908	0.371	0.111	0.299	-47.614	0.157	0.470	-6.046	0.117	0.316	-43.431
691.	909	0.245	0.085	0.346	-36.086	0.031	0.158	-81.814	0.113	0.463	-7.723
692.	911	0.315	0.154	0.490	-1.080	0.016	0.075	-101.997	0.086	0.273	-53.891
693.	912	0.086	0.048	0.557	15.138	-----	-----	-----	0.045	0.520	6.108
694.	913	0.443	0.263	0.595	24.416	-----	-----	-----	0.240	0.542	11.581
695.	914	2.529	1.952	0.772	67.332	0.595	0.338	-37.933	1.399	0.553	14.231
696.	915	0.423	0.167	0.396	-23.978	-----	-----	-----	0.146	0.344	-36.507
697.	916	0.184	0.090	0.490	-1.196	-----	-----	-----	0.105	0.570	18.322
698.	918	0.124	0.080	0.640	35.357	-----	-----	-----	0.037	0.296	-48.167
699.	919	0.100	0.051	0.506	2.838	0.047	0.531	8.880	0.041	0.406	-21.408
700.	920	0.424	0.164	0.387	-26.019	0.311	0.845	85.216	0.194	0.458	-8.807
701.	921	0.489	0.231	0.472	-5.506	-----	-----	-----	0.090	0.183	-75.602
702.	922	0.410	0.230	0.561	16.126	0.236	0.598	25.036	0.079	0.192	-73.505
703.	923	0.182	0.078	0.428	-16.234	-----	-----	-----	0.122	0.670	42.744
704.	924	0.404	0.190	0.469	-6.223	-----	-----	-----	0.130	0.322	-41.989
705.	925	0.122	0.033	0.273	-53.793	-----	-----	-----	0.054	0.446	-11.762
706.	927	0.288	0.118	0.408	-20.983	0.121	0.481	-3.178	0.196	0.679	44.873
707.	933	0.107	0.056	0.524	7.154	-----	-----	-----	0.057	0.529	8.387
708.	934	0.062	0.034	0.555	14.809	0.035	0.563	16.578	0.038	0.615	29.198
709.	935	0.085	0.085	1.000	122.830	0.080	0.940	108.264	0.049	0.569	18.075
710.	937	0.271	0.155	0.572	18.874	0.106	0.391	-25.225	0.086	0.316	-43.507
711.	938	0.405	0.321	0.792	72.311	0.153	0.351	-34.796	0.272	0.670	42.652
712.	939	0.609	0.399	0.655	38.905	0.174	0.337	-38.281	0.187	0.307	-45.648
713.	940	0.276	0.115	0.416	-19.206	0.139	0.525	7.459	0.087	0.317	-43.224

714.	941	0.224	0.122	0.545	12.205	0.059	0.261	-56.682	0.116	0.517	5.561
715.	942	0.251	0.141	0.560	15.834	0.082	0.325	-41.260	0.121	0.481	-3.268
716.	943	3.042	1.686	0.554	14.468	1.145	0.394	-24.406	0.664	0.218	-67.121
717.	944	5.060	2.821	0.557	15.290	0.868	0.194	-72.953	0.824	0.163	-80.622
718.	945	6.354	1.056	0.166	-79.796	1.633	0.283	-51.505	0.986	0.155	-82.471
719.	946	3.110	1.284	0.413	-19.895	0.866	0.318	-42.856	0.527	0.169	-79.019
720.	947	5.912	4.493	0.760	64.497	2.725	0.457	-9.149	1.710	0.289	-49.889
721.	948	0.073	0.031	0.419	-18.439	0.049	0.672	43.179	0.032	0.441	-13.059
722.	949	1.361	0.933	0.685	46.347	0.600	0.444	-12.339	0.573	0.421	-17.798
723.	950	2.955	2.079	0.704	50.794	1.325	0.450	-10.911	1.868	0.632	33.408
724.	952	0.201	0.139	0.691	47.622	0.090	0.576	19.713	0.093	0.464	-7.345
725.	953	0.939	0.358	0.382	-27.443	0.257	0.289	-49.919	0.133	0.142	-85.743
726.	954	0.208	0.113	0.545	12.309	0.160	0.772	67.320	0.108	0.520	6.181
727.	957	1.206	0.587	0.487	-1.913	0.636	0.521	6.503	0.427	0.354	-34.234
728.	958	0.399	0.136	0.340	-37.590	0.165	0.471	-5.667	0.167	0.417	-18.772
729.	959	0.532	0.187	0.352	-34.527	0.163	0.343	-36.866	0.204	0.383	-27.110
730.	960	1.531	1.052	0.687	46.744	0.419	0.282	-51.705	0.677	0.442	-12.713
731.	961	1.254	0.714	0.570	18.227	0.608	0.479	-3.831	0.570	0.454	-9.764
732.	962	0.401	0.174	0.435	-14.370	0.122	0.345	-36.431	0.228	0.568	17.840
733.	963	0.491	0.293	0.596	24.663	0.091	0.176	-77.369	0.184	0.374	-29.227
734.	964	0.191	0.104	0.546	12.523	0.041	0.270	-54.592	0.037	0.196	-72.643
735.	966	0.625	0.240	0.384	-26.919	0.100	0.169	-79.003	0.319	0.510	3.818
736.	967	0.068	0.041	0.607	27.222	0.042	0.617	29.832	0.057	0.838	83.356
737.	968	0.478	0.140	0.292	-49.248	0.121	0.324	-41.390	0.180	0.377	-28.665
738.	970	0.415	0.208	0.501	1.658	0.150	0.419	-18.340	0.227	0.548	13.008
739.	971	0.689	0.134	0.195	-72.876	0.297	0.492	-0.521	0.123	0.179	-76.731
740.	973	0.051	0.038	0.754	62.993	0.039	0.757	63.843	0.034	0.674	43.597
741.	974	0.129	0.056	0.432	-15.101	0.051	0.358	-33.170	0.055	0.430	-15.805
742.	975	0.105	0.038	0.360	-32.761	0.095	0.906	100.085	0.068	0.651	38.116
743.	976	0.105	0.042	0.402	-22.581	0.022	0.209	-69.331	0.034	0.327	-40.691

744.	979	0.194	0.044	0.226	-65.314	-----	-----	-----	0.045	0.232	-63.911
745.	980	0.472	0.240	0.509	3.535	0.060	0.128	-89.025	0.139	0.295	-48.459
746.	981	0.418	0.153	0.367	-31.032	0.074	0.185	-75.212	0.142	0.340	-37.501
747.	982	0.410	0.214	0.521	6.432	0.223	0.570	18.325	0.180	0.440	-13.297
748.	983	0.166	0.096	0.576	19.754	0.098	0.591	23.340	0.078	0.467	-6.822
749.	984	0.971	0.273	0.281	-51.905	0.188	0.228	-64.856	0.393	0.405	-21.799
750.	985	0.535	0.199	0.372	-29.808	0.315	0.571	18.578	0.260	0.486	-2.197
751.	986	0.276	0.132	0.478	-3.967	0.064	0.247	-60.210	0.110	0.398	-23.590
752.	987	0.432	0.119	0.275	-53.441	0.163	0.377	-28.563	0.199	0.462	-7.970
753.	988	1.506	0.727	0.483	-2.817	0.437	0.297	-48.121	0.497	0.330	-39.988
754.	989	0.715	0.200	0.280	-52.252	0.360	0.517	5.422	0.403	0.564	16.808
755.	990	0.893	0.444	0.497	0.667	0.473	0.528	8.060	0.343	0.384	-26.824
756.	991	0.350	0.130	0.372	-29.736	0.248	0.751	62.415	0.101	0.288	-50.101
757.	992	0.119	0.084	0.701	50.249	0.025	0.210	-69.142	0.055	0.460	-8.388
758.	993	0.107	0.058	0.545	12.247	0.057	0.536	10.175	0.056	0.528	8.009
759.	994	0.331	0.143	0.433	-15.070	0.052	0.158	-81.786	0.137	0.413	-19.937
760.	995	0.221	0.093	0.419	-18.376	0.132	0.596	24.766	0.121	0.547	12.679
761.	996	0.205	0.142	0.693	48.317	0.026	0.117	-91.642	0.087	0.422	-17.604
762.	997	0.326	0.218	0.669	42.470	0.108	0.332	-39.502	0.117	0.360	-32.784
763.	998	0.181	0.098	0.540	11.108	0.030	0.162	-80.916	0.121	0.667	41.888
764.	999	0.121	0.046	0.378	-28.250	0.098	0.809	76.412	0.095	0.779	69.119
765.	1000	0.076	0.044	0.581	20.935	0.069	0.906	99.904	0.039	0.515	4.859
766.	1001	0.132	0.093	0.702	50.297	0.116	0.877	92.935	0.040	0.301	-47.006
767.	1002	0.152	0.102	0.672	43.017	0.055	0.376	-28.836	0.095	0.628	32.527
768.	1003	0.355	0.209	0.588	22.682	0.134	0.405	-21.778	0.099	0.278	-52.639
769.	1004	0.091	0.056	0.616	29.446	0.018	0.216	-67.597	0.040	0.443	-12.433
770.	1005	0.068	0.048	0.695	48.736	0.022	0.326	-41.010	0.034	0.504	2.204
771.	1006	0.217	0.117	0.540	11.054	0.116	0.534	9.468	0.087	0.403	-22.274
772.	1007	1.025	0.632	0.616	29.611	0.153	0.151	-83.588	0.457	0.446	-11.790
773.	1008	0.666	0.246	0.369	-30.417	0.269	0.410	-20.492	0.132	0.198	-72.161

774.	1009	0.281	0.184	0.655	38.921	0.131	0.466	-6.877	0.152	0.543	11.813
775.	1010	0.232	0.130	0.562	16.289	0.196	0.846	85.465	0.113	0.489	-1.310
776.	1011	0.476	0.255	0.535	9.891	0.186	0.399	-23.186	0.075	0.157	-81.961
777.	1012	0.391	0.120	0.307	-45.554	0.257	0.658	39.722	0.140	0.357	-33.442
778.	1013	0.264	0.138	0.522	6.731	0.238	0.878	93.077	0.112	0.425	-16.857
779.	1014	0.099	0.038	0.389	-25.579	0.064	0.645	36.595	0.051	0.519	5.849
780.	1015	0.666	0.228	0.343	-36.806	0.188	0.320	-42.371	0.130	0.195	-72.765
781.	1017	1.071	0.449	0.420	-18.229	0.326	0.362	-32.306	0.311	0.290	-49.633
782.	1018	3.111	1.191	0.383	-27.145	0.568	0.205	-70.427	1.065	0.342	-36.981
783.	1019	1.114	0.655	0.588	22.686	0.641	0.576	19.699	0.563	0.506	2.725
784.	1020	0.260	0.114	0.437	-13.929	0.102	0.395	-24.275	0.076	0.295	-48.616
785.	1021	0.221	0.102	0.462	-8.023	0.096	0.430	-15.711	0.111	0.503	1.982
786.	1022	0.447	0.206	0.461	-8.160	0.213	0.485	-2.345	0.043	0.096	-96.760
787.	1023	0.258	0.126	0.487	-1.759	-----	-----	-----	0.105	0.406	-21.408
788.	1024	0.416	0.244	0.586	22.267	0.258	0.629	32.576	0.210	0.504	2.298
789.	1025	0.121	0.064	0.530	8.707	0.049	0.406	-21.548	0.049	0.405	-21.889
790.	1026	0.133	0.133	1.000	122.830	0.083	0.627	32.181	0.078	0.590	23.268
791.	1027	0.261	0.147	0.566	17.298	-----	-----	-----	0.049	0.187	-74.825
792.	1028	0.770	0.430	0.559	15.622	0.308	0.400	-22.979	0.258	0.334	-38.920
793.	1029	0.111	0.070	0.630	32.801	0.040	0.401	-22.672	0.052	0.471	-5.810
794.	1030	0.397	0.162	0.409	-20.714	-----	-----	-----	0.149	0.375	-29.040
795.	1031	0.774	0.469	0.606	26.980	0.208	0.281	-51.839	0.471	0.609	27.805
796.	1032	0.472	0.296	0.626	31.936	0.267	0.553	14.210	0.200	0.423	-17.449
797.	1033	0.336	0.115	0.343	-36.834	0.109	0.324	-41.356	0.274	0.813	77.479
798.	1034	0.453	0.236	0.521	6.479	0.100	0.227	-64.920	0.208	0.460	-8.380
799.	1035	0.286	0.119	0.416	-19.114	0.110	0.382	-27.254	0.206	0.723	55.490
800.	1036	0.185	0.066	0.355	-33.904	0.104	0.516	5.240	0.068	0.366	-31.278
801.	1037	0.136	0.061	0.450	-10.726	0.070	0.512	4.353	0.049	0.360	-32.610
802.	1038	0.366	0.144	0.393	-24.639	0.186	0.496	0.334	0.282	0.770	66.936
803.	1040	0.203	0.100	0.489	-1.268	0.036	0.179	-76.784	0.110	0.541	11.357

804.	1041	0.512	0.118	0.230	-64.233	0.302	0.589	23.054	0.110	0.215	-67.909
805.	1042	1.136	0.669	0.590	23.091	0.642	0.634	33.804	0.503	0.443	-12.604
806.	1043	0.211	0.073	0.346	-36.093	0.070	0.363	-31.908	0.141	0.668	42.097
807.	1044	0.067	0.015	0.229	-64.647	0.045	0.606	27.134	0.017	0.251	-59.206
808.	1046	0.201	0.102	0.505	2.586	0.046	0.228	-64.805	0.095	0.474	-5.076
809.	1047	1.541	0.493	0.320	-42.512	0.189	0.115	-92.271	0.727	0.472	-5.538
810.	1048	0.172	0.096	0.560	15.880	0.095	0.654	38.804	0.108	0.627	32.093
811.	1050	1.473	0.878	0.596	24.579	-----	-----	-----	0.624	0.423	-17.288
812.	1051	1.501	0.625	0.416	-19.023	0.404	0.285	-50.833	0.243	0.162	-80.893
813.	1052	0.603	0.406	0.674	43.507	0.304	0.595	24.388	0.274	0.454	-9.746
814.	1054	1.364	0.668	0.490	-1.210	0.150	0.107	-94.062	0.072	0.052	-107.438
815.	1057	0.487	0.242	0.497	0.694	0.232	0.523	6.980	0.135	0.278	-52.663
816.	1058	0.728	0.122	0.167	-79.542	0.153	0.252	-58.982	0.130	0.179	-76.741
817.	1060	0.117	0.066	0.567	17.503	0.039	0.352	-34.542	0.093	0.795	72.939
818.	1061	1.055	0.443	0.420	-18.178	0.410	0.378	-28.349	0.194	0.183	-75.597
819.	1062	0.061	0.023	0.385	-26.732	0.031	0.554	14.421	0.024	0.391	-25.112
820.	1064	0.381	0.102	0.269	-54.891	0.135	0.356	-33.758	0.061	0.161	-81.005
821.	1065	0.271	0.107	0.393	-24.577	0.127	0.469	-6.283	0.081	0.300	-47.326
822.	1066	0.435	0.234	0.539	10.733	0.186	0.401	-22.784	0.131	0.301	-47.046
823.	1068	0.079	0.037	0.471	-5.714	0.047	0.534	9.663	0.042	0.534	9.476
824.	1069	0.258	0.093	0.361	-32.353	0.141	0.562	16.330	0.065	0.254	-58.560
825.	1070	0.083	0.052	0.629	32.610	0.068	0.712	52.745	0.046	0.558	15.413
826.	1072	0.766	0.321	0.419	-18.238	0.332	0.436	-14.147	0.235	0.306	-45.765
827.	1073	0.384	0.217	0.565	17.147	0.067	0.175	-77.651	0.215	0.560	15.912
828.	1075	0.224	0.118	0.528	8.210	0.216	0.879	93.354	0.099	0.442	-12.791
829.	1078	1.256	0.659	0.525	7.378	0.610	0.492	-0.736	0.200	0.159	-81.501
830.	1079	2.677	1.161	0.434	-14.806	0.594	0.224	-65.779	0.323	0.121	-90.870
831.	1082	0.105	0.053	0.509	3.563	0.064	0.608	27.544	0.066	0.624	31.451
832.	1083	0.260	0.126	0.484	-2.571	0.117	0.516	5.163	0.130	0.500	1.324
833.	1084	0.483	0.120	0.249	-59.775	0.212	0.438	-13.754	0.140	0.289	-49.925

834.	1085	0.097	0.064	0.657	39.505	0.071	0.671	42.859	0.046	0.471	-5.728
835.	1086	0.091	0.062	0.684	46.033	0.065	0.717	53.937	0.057	0.629	32.731
836.	1087	0.173	0.096	0.558	15.529	0.053	0.288	-50.178	0.054	0.311	-44.637
837.	1088	0.068	0.052	0.756	63.468	0.036	0.487	-1.938	0.025	0.362	-32.126
838.	1089	0.566	0.246	0.435	-14.568	0.184	0.335	-38.657	0.220	0.389	-25.608
839.	1090	1.453	0.674	0.464	-7.512	0.436	0.339	-37.818	0.238	0.164	-80.342
840.	1091	0.192	0.105	0.545	12.328	0.102	0.560	15.987	0.055	0.288	-50.320
841.	1092	0.683	0.258	0.378	-28.274	0.115	0.247	-60.053	0.058	0.085	-99.485
842.	1093	0.380	0.197	0.519	6.046	0.344	0.859	88.655	0.118	0.311	-44.497
843.	1094	0.140	0.084	0.601	25.866	0.085	0.635	34.027	0.085	0.607	27.375
844.	1095	0.128	0.070	0.547	12.843	0.096	0.711	52.617	0.057	0.440	-13.230
845.	1096	0.055	0.027	0.489	-1.413	-----	-----	-----	0.015	0.279	-52.449
846.	1097	1.040	0.513	0.494	-0.170	0.423	0.495	0.009	0.067	0.065	-104.414
847.	1098	0.197	0.109	0.554	14.360	-----	-----	-----	0.038	0.193	-73.355
848.	1099	0.120	0.079	0.658	39.819	0.063	0.524	7.075	0.066	0.553	14.276
849.	1100	0.137	0.085	0.624	31.527	0.074	0.674	43.598	0.030	0.222	-66.351
850.	1102	0.078	0.035	0.453	-10.029	0.021	0.282	-51.557	0.031	0.397	-23.663
851.	1103	0.119	0.057	0.477	-4.369	0.092	0.778	68.767	0.053	0.446	-11.740
852.	1106	0.097	0.042	0.429	-16.009	0.058	0.671	42.826	0.046	0.472	-5.476
853.	1107	0.144	0.044	0.304	-46.241	0.062	0.427	-16.308	0.056	0.388	-25.954
854.	2000	0.450	0.194	0.431	-15.335	0.206	0.525	7.437	0.135	0.299	-47.444
855.	2010	0.134	0.087	0.649	37.593	0.038	0.372	-29.859	0.033	0.244	-60.860
856.	2012	0.307	0.174	0.567	17.490	0.187	0.684	46.133	0.034	0.111	-93.333
857.	2014	0.102	0.052	0.512	4.129	0.036	0.504	2.298	0.025	0.241	-61.569
858.	2015	0.181	0.088	0.487	-1.793	0.069	0.458	-9.002	0.064	0.354	-34.170
859.	2016	0.172	0.078	0.453	-10.134	0.103	0.628	32.401	0.082	0.477	-4.376
860.	2017	0.395	0.147	0.371	-29.970	0.180	0.554	14.438	0.114	0.287	-50.365
861.	2025	0.077	0.034	0.444	-12.368	0.031	0.572	18.821	0.015	0.200	-71.654
862.	2029	0.359	0.181	0.505	2.528	0.197	0.651	38.093	0.142	0.396	-23.867
863.	2030	0.230	0.165	0.719	54.537	0.038	0.483	-2.709	0.024	0.105	-94.745

864.	2031	0.159	0.074	0.464	-7.415	0.078	0.729	57.073	0.022	0.138	-86.604
865.	2032	0.056	0.028	0.497	0.488	0.019	0.404	-21.974	0.013	0.225	-65.510
866.	2033	1.821	0.945	0.519	5.931	0.552	0.320	-42.470	0.118	0.065	-104.396
867.	2034	0.482	0.182	0.377	-28.530	0.245	0.516	5.178	0.178	0.370	-30.238
868.	2063	0.174	0.112	0.643	36.020	0.061	0.424	-17.027	0.044	0.252	-58.925
869.	2070	0.211	0.108	0.512	4.233	0.059	0.377	-28.617	0.066	0.312	-44.310
870.	2074	0.568	0.245	0.432	-15.202	0.183	0.372	-29.795	0.141	0.249	-59.727
871.	2076	0.221	0.131	0.595	24.331	0.097	0.470	-5.881	0.076	0.343	-36.872
872.	2079	0.500	0.258	0.516	5.125	0.211	0.496	0.424	0.134	0.269	-54.892
873.	2082	0.068	0.027	0.402	-22.556	0.018	0.414	-19.557	0.023	0.338	-37.986
874.	2088	0.229	0.082	0.357	-33.434	0.123	0.634	33.913	0.095	0.415	-19.242
875.	2090	1.053	0.170	0.161	-81.049	0.420	0.480	-3.533	0.117	0.111	-93.255
876.	2092	0.181	0.077	0.429	-15.947	0.048	0.388	-25.820	0.041	0.226	-65.336
877.	2093	0.083	0.031	0.372	-29.749	0.030	0.470	-6.023	0.023	0.278	-52.692
878.	2094	0.100	0.059	0.588	22.592	0.031	0.422	-17.720	0.034	0.336	-38.501
879.	2095	0.052	0.021	0.409	-20.807	0.019	0.355	-33.806	0.033	0.640	35.318
880.	2096	0.169	0.114	0.674	43.505	0.091	0.651	37.949	0.070	0.414	-19.560
881.	2099	4.497	2.152	0.478	-3.902	1.784	0.404	-21.883	0.735	0.164	-80.455
882.	2104	4.702	2.810	0.598	25.023	1.505	0.343	-36.878	1.378	0.293	-48.966
883.	2105	0.360	0.215	0.596	24.553	0.244	0.819	78.871	0.140	0.390	-25.524
884.	2106	0.224	0.148	0.659	40.071	0.159	0.724	55.828	0.101	0.452	-10.351
885.	2109	0.181	0.068	0.375	-28.931	0.075	0.467	-6.641	0.047	0.258	-57.438
886.	2110	2.156	0.964	0.447	-11.496	1.019	0.480	-3.523	0.816	0.378	-28.281
887.	2112	0.544	0.332	0.611	28.333	0.191	0.371	-29.938	0.155	0.285	-51.019
888.	2113	0.115	0.060	0.526	7.554	-----	-----	-----	0.036	0.315	-43.579
889.	2114	0.515	0.323	0.627	32.112	0.255	0.529	8.470	0.313	0.609	27.720
890.	2115	0.454	0.222	0.489	-1.389	0.222	0.513	4.548	0.205	0.452	-10.253
891.	2121	0.287	0.092	0.321	-42.146	0.093	0.435	-14.358	0.098	0.340	-37.553
892.	2122	0.777	0.262	0.337	-38.309	0.265	0.346	-36.146	0.255	0.328	-40.372
893.	2123	0.485	0.110	0.227	-64.919	0.194	0.390	-25.322	0.294	0.606	27.032

894.	2124	0.467	0.467	1.000	122.830	0.383	0.874	92.163	0.296	0.633	33.642
895.	2126	1.453	0.560	0.386	-26.479	0.436	0.331	-39.733	0.397	0.273	-53.770
896.	2127	1.022	0.456	0.446	-11.834	0.103	0.100	-95.983	0.341	0.334	-39.140
897.	2128	0.677	0.201	0.297	-48.120	0.127	0.189	-74.268	0.091	0.134	-87.686
898.	2129	1.347	0.858	0.636	34.489	0.304	0.250	-59.341	0.531	0.394	-24.374
899.	2131	2.524	1.372	0.544	11.946	1.136	0.496	0.308	1.137	0.450	-10.751
900.	2132	0.270	0.078	0.289	-49.952	0.025	0.170	-78.749	0.106	0.391	-25.054
901.	2133	23.023	10.934	0.475	-4.771	10.428	0.458	-8.817	9.089	0.395	-24.252
902.	2134	6.618	3.410	0.515	5.035	3.211	0.516	5.290	2.975	0.450	-10.937
903.	2135	2.344	1.299	0.554	14.428	1.243	0.563	16.741	0.456	0.194	-72.933
904.	2136	0.518	0.181	0.349	-35.420	0.107	0.252	-58.986	0.158	0.306	-45.888
905.	2138	0.903	0.688	0.762	65.073	0.509	0.582	21.199	0.310	0.343	-36.721
906.	2139	0.197	0.095	0.482	-3.055	0.047	0.286	-50.566	0.058	0.296	-48.141
907.	2140	0.832	0.349	0.419	-18.319	0.342	0.415	-19.384	0.236	0.284	-51.221
908.	2141	0.426	0.299	0.701	50.207	0.252	0.634	33.769	0.274	0.642	35.929
909.	2142	0.413	0.193	0.467	-6.697	0.254	0.581	20.905	0.158	0.384	-26.949
910.	2143	0.229	0.094	0.412	-20.166	0.035	0.153	-83.002	0.104	0.452	-10.284
911.	2144	0.782	0.554	0.709	52.121	0.460	0.670	42.580	0.216	0.276	-53.020
912.	2145	0.257	0.096	0.374	-29.189	0.110	0.518	5.758	0.092	0.356	-33.765
913.	2146	0.634	0.326	0.514	4.818	0.183	0.355	-33.933	0.259	0.409	-20.780
914.	2147	1.489	0.650	0.436	-14.133	0.561	0.423	-17.388	0.883	0.593	23.999
915.	2150	2.621	1.283	0.489	-1.246	1.066	0.451	-10.515	0.967	0.369	-30.546
916.	2154	0.130	0.060	0.466	-6.963	0.058	0.567	17.496	0.049	0.378	-28.445
917.	2155	0.644	0.240	0.372	-29.857	0.149	0.473	-5.128	0.077	0.119	-91.243
918.	2165	0.133	0.060	0.450	-10.903	0.030	0.606	26.991	0.028	0.211	-68.846
919.	2166	3.260	1.764	0.541	11.312	1.479	0.511	3.895	0.895	0.275	-53.462
920.	2168	1.758	0.910	0.517	5.570	0.972	0.594	24.095	0.319	0.181	-76.114
921.	2169	1.061	0.747	0.703	50.758	0.628	0.672	43.137	0.508	0.479	-3.828
922.	2170	0.275	0.275	1.000	122.830	0.229	0.802	74.756	0.101	0.367	-30.956
923.	2171	0.642	0.315	0.491	-0.877	0.503	0.886	95.087	0.351	0.547	12.662

924.	2172	0.786	0.517	0.657	39.521	0.499	0.627	32.121	0.288	0.366	-31.178
925.	2173	0.617	0.360	0.584	21.688	0.398	0.620	30.383	0.169	0.274	-53.700
926.	2174	0.196	0.093	0.474	-5.080	0.119	0.631	33.235	0.079	0.406	-21.478
927.	2175	0.210	0.110	0.524	7.085	0.151	0.767	66.258	0.096	0.455	-9.515
928.	2176	6.015	2.559	0.426	-16.777	2.196	0.369	-30.414	1.131	0.188	-74.502
929.	2177	0.359	0.174	0.485	-2.429	0.176	0.584	21.832	0.155	0.431	-15.492
930.	2178	0.354	0.130	0.366	-31.238	0.145	0.642	35.747	0.124	0.350	-35.058
931.	2179	0.384	0.191	0.497	0.543	0.100	0.555	14.797	0.111	0.288	-50.149
932.	2180	0.082	0.040	0.487	-1.908	0.034	0.563	16.624	0.035	0.424	-17.208
933.	2181	0.714	0.301	0.421	-17.872	0.208	0.295	-48.591	0.345	0.484	-2.664
934.	2182	1.573	0.690	0.439	-13.569	0.568	0.411	-20.270	0.306	0.194	-72.971
935.	2183	0.338	0.173	0.512	4.188	0.208	0.703	50.574	0.055	0.164	-80.369
936.	2184	0.157	0.090	0.574	19.295	0.074	0.677	44.327	0.057	0.365	-31.501
937.	2185	0.277	0.124	0.447	-11.510	0.133	0.703	50.582	0.041	0.149	-83.883
938.	2187	0.283	0.118	0.417	-18.867	0.162	0.530	8.650	0.195	0.690	47.460
939.	2188	0.175	0.100	0.573	19.176	0.075	0.570	18.281	0.063	0.360	-32.726
940.	2189	0.080	0.035	0.432	-15.277	0.026	0.499	1.042	0.025	0.316	-43.318
941.	2190	0.098	0.036	0.372	-29.873	0.036	0.606	27.083	0.025	0.255	-58.179
942.	2191	0.072	0.030	0.416	-19.029	0.060	0.484	-2.589	0.018	0.254	-58.440
943.	2195	1.128	0.540	0.479	-3.792	0.668	0.609	27.755	0.288	0.256	-58.040
944.	2196	0.931	0.445	0.478	-4.017	0.752	0.628	32.507	0.480	0.516	5.238
945.	2197	2.406	1.311	0.545	12.224	1.123	0.509	3.551	0.419	0.174	-77.912
946.	2198	0.904	0.499	0.552	13.860	0.432	0.491	-0.755	0.676	0.748	61.503
947.	2199	0.164	0.091	0.553	14.219	0.105	0.620	30.378	0.080	0.488	-1.655
948.	2201	8.025	3.590	0.447	-11.477	3.263	0.404	-22.032	3.200	0.399	-23.291
949.	2202	0.782	0.366	0.467	-6.586	0.236	0.302	-46.896	0.199	0.254	-58.447
950.	2204	0.245	0.117	0.480	-3.506	0.112	0.677	44.222	0.057	0.233	-63.466
951.	2205	1.121	0.375	0.335	-38.794	0.574	0.572	18.773	0.299	0.267	-55.331
952.	2206	1.328	0.761	0.573	19.009	0.256	0.400	-23.076	0.378	0.285	-50.981
953.	2209	0.907	0.529	0.583	21.510	0.452	0.539	10.693	0.212	0.234	-63.408

954.	2211	0.297	0.189	0.636	34.265	0.127	0.501	1.593	0.103	0.345	-36.263
955.	2212	0.181	0.089	0.491	-0.792	0.022	0.176	-77.322	0.075	0.414	-19.647
956.	2214	1.022	0.723	0.707	51.685	0.424	0.462	-7.850	0.270	0.264	-56.011
957.	2218	1.874	1.065	0.568	17.880	0.816	0.464	-7.360	0.379	0.202	-71.009
958.	2219	3.043	1.778	0.584	21.779	1.222	0.428	-16.253	0.857	0.282	-51.718
959.	2220	0.984	0.520	0.529	8.315	0.619	0.663	41.015	0.384	0.390	-25.401
960.	2223	1.598	0.857	0.536	10.139	0.806	0.538	10.630	0.614	0.384	-26.826
961.	2226	0.082	0.041	0.500	1.432	0.012	0.438	-13.718	0.009	0.112	-93.072
962.	2228	0.738	0.488	0.661	40.344	0.535	0.787	71.082	0.267	0.362	-32.255
963.	2230	0.045	0.023	0.514	4.669	0.026	0.578	20.291	0.010	0.228	-64.812
964.	2231	0.038	0.018	0.479	-3.683	0.025	0.650	37.814	0.014	0.380	-27.833
965.	2234	0.071	0.044	0.623	31.119	0.051	0.882	94.196	0.026	0.359	-32.887
966.	2235	0.180	0.098	0.545	12.173	0.079	0.624	31.447	0.035	0.196	-72.570
967.	2237	0.480	0.298	0.621	30.703	0.184	0.449	-11.164	0.203	0.424	-17.081
968.	2238	0.097	0.061	0.624	31.525	0.024	0.513	4.582	0.036	0.365	-31.569
969.	2239	0.296	0.193	0.652	38.338	0.121	0.523	7.025	0.098	0.332	-39.463
970.	2246	0.081	0.038	0.477	-4.258	0.030	0.482	-3.030	0.034	0.426	-16.757
971.	2247	11.039	5.429	0.492	-0.663	4.719	0.431	-15.548	5.641	0.511	3.982
972.	2248	12.942	5.523	0.427	-16.482	4.075	0.379	-28.086	6.068	0.469	-6.254
973.	2249	0.859	0.251	0.292	-49.257	0.409	0.455	-9.608	0.183	0.213	-68.417
974.	2250	0.574	0.255	0.445	-12.104	0.338	0.683	45.808	0.136	0.236	-62.760
975.	2251	0.179	0.086	0.480	-3.443	0.073	0.494	-0.128	0.037	0.206	-70.237
976.	2252	0.227	0.139	0.613	28.883	0.086	0.452	-10.418	0.094	0.412	-19.980
977.	2253	0.551	0.223	0.404	-21.888	0.199	0.431	-15.354	0.131	0.238	-62.316
978.	2263	0.606	0.283	0.467	-6.599	0.253	0.523	6.899	0.174	0.288	-50.212
979.	2264	0.291	0.189	0.650	37.741	0.158	0.677	44.454	0.051	0.177	-77.271
980.	2266	1.571	0.752	0.479	-3.850	0.531	0.373	-29.514	0.563	0.358	-33.080
981.	2270	1.204	0.482	0.401	-22.847	0.474	0.445	-11.939	0.526	0.437	-14.086
982.	2271	1.768	0.442	0.250	-59.452	0.409	0.270	-54.670	0.536	0.303	-46.554
983.	2272	0.551	0.154	0.280	-52.157	0.208	0.457	-9.168	0.206	0.374	-29.258

984.	2275	0.774	0.304	0.392	-24.854	0.324	0.620	30.418	0.120	0.154	-82.671
985.	2276	0.087	0.034	0.389	-25.567	0.028	0.385	-26.564	0.017	0.199	-71.919
986.	2277	0.272	0.126	0.463	-7.570	0.107	0.586	22.110	0.061	0.225	-65.581
987.	2278	1.121	0.505	0.451	-10.572	0.616	0.634	33.925	0.351	0.313	-44.117
988.	2279	0.494	0.194	0.392	-24.837	0.159	0.402	-22.420	0.156	0.315	-43.556
989.	2280	0.641	0.212	0.331	-39.766	0.196	0.416	-19.189	0.178	0.278	-52.649
990.	2281	0.816	0.431	0.528	8.095	0.512	0.713	53.168	0.233	0.285	-50.830
991.	2282	0.626	0.271	0.432	-15.121	0.060	0.139	-86.315	0.084	0.134	-87.617
992.	2283	1.651	0.826	0.500	1.376	0.791	0.522	6.666	0.768	0.465	-7.181
993.	2284	0.802	0.311	0.388	-25.784	0.272	0.460	-8.303	0.146	0.182	-75.906
994.	2285	0.807	0.224	0.277	-52.767	0.223	0.387	-26.126	0.092	0.114	-92.419
995.	2286	1.558	0.834	0.535	9.847	0.568	0.443	-12.423	0.518	0.332	-39.413
996.	2287	1.458	0.750	0.515	4.865	0.584	0.479	-3.891	0.667	0.457	-9.058
997.	2289	0.205	0.114	0.555	14.680	0.089	0.538	10.606	0.108	0.530	8.546
998.	2293	0.573	0.290	0.506	2.696	0.321	0.680	45.138	0.094	0.163	-80.541
999.	2294	0.103	0.057	0.551	13.755	0.044	0.535	9.922	0.055	0.537	10.355
1000.	2295	0.315	0.126	0.398	-23.368	0.131	0.511	3.906	0.149	0.474	-5.030
1001.	2296	0.755	0.476	0.630	32.984	0.497	0.782	69.880	0.106	0.141	-86.032
1002.	2301	0.319	0.154	0.481	-3.345	0.109	0.467	-6.613	0.037	0.116	-92.095
1003.	2302	0.622	0.359	0.577	20.030	0.144	0.371	-30.063	0.081	0.130	-88.545
1004.	2303	0.620	0.247	0.399	-23.160	0.159	0.379	-27.978	0.157	0.253	-58.729
1005.	2306	0.223	0.078	0.349	-35.416	0.065	0.523	6.902	0.019	0.085	-99.567
1006.	2311	0.476	0.265	0.558	15.324	0.119	0.460	-8.385	0.059	0.124	-89.939
1007.	2312	0.457	0.291	0.636	34.397	0.195	0.716	53.770	0.060	0.132	-88.046
1008.	2313	0.588	0.245	0.416	-19.012	0.171	0.348	-35.547	0.088	0.150	-83.751
1009.	2316	0.448	0.238	0.532	9.053	0.147	0.411	-20.183	0.241	0.537	10.356
1010.	2317	0.723	0.271	0.374	-29.254	0.226	0.341	-37.357	0.214	0.295	-48.407
1011.	2318	0.179	0.083	0.461	-8.205	0.089	0.606	27.193	0.065	0.364	-31.751
1012.	2320	0.173	0.082	0.476	-4.472	0.074	0.582	21.210	0.030	0.171	-78.735
1013.	2321	0.059	0.027	0.461	-8.073	0.025	0.547	12.738	0.009	0.149	-83.944

1014.	2322	0.053	0.023	0.422	-17.595	0.015	0.391	-25.081	0.008	0.151	-83.481
1015.	2324	0.330	0.176	0.533	9.459	0.140	0.551	13.600	0.117	0.353	-34.334
1016.	2327	0.310	0.145	0.466	-6.823	0.142	0.454	-9.772	0.119	0.383	-27.002
1017.	2328	3.791	1.455	0.384	-26.934	1.343	0.388	-25.882	0.680	0.179	-76.596
1018.	2329	0.388	0.254	0.655	39.098	0.122	0.517	5.424	0.083	0.213	-68.491
1019.	2330	0.327	0.181	0.552	13.946	0.155	0.573	18.999	0.090	0.275	-53.295
1020.	2331	0.881	0.316	0.359	-32.905	0.237	0.317	-43.192	0.423	0.480	-3.478
1021.	2333	1.581	0.777	0.491	-0.784	0.589	0.437	-13.961	0.533	0.337	-38.323
1022.	2334	0.188	0.086	0.460	-8.444	0.096	0.629	32.743	0.080	0.426	-16.770
1023.	2335	1.378	0.524	0.380	-27.877	0.515	0.391	-25.269	0.487	0.353	-34.389
1024.	2337	5.327	2.469	0.463	-7.558	1.968	0.419	-18.325	3.465	0.650	37.857
1025.	2338	2.416	1.144	0.474	-5.098	0.691	0.325	-41.293	0.940	0.389	-25.614
1026.	2339	2.732	0.915	0.335	-38.745	1.156	0.433	-15.010	0.810	0.297	-48.111
1027.	2340	1.823	0.574	0.315	-43.650	0.323	0.276	-53.049	0.176	0.096	-96.767
1028.	2341	0.314	0.180	0.573	19.185	0.155	0.586	22.310	0.142	0.450	-10.732
1029.	2342	0.814	0.394	0.484	-2.524	0.264	0.280	-52.210	0.475	0.584	21.813
1030.	2343	0.305	0.058	0.189	-74.189	0.100	0.417	-18.790	0.112	0.368	-30.752
1031.	2345	1.391	0.506	0.364	-31.766	0.548	0.420	-18.159	0.605	0.435	-14.394
1032.	2346	0.535	0.285	0.534	9.496	0.245	0.713	53.112	0.240	0.448	-11.235
1033.	2347	0.684	0.358	0.523	6.936	0.195	0.341	-37.235	0.315	0.461	-8.224
1034.	2348	0.206	0.098	0.476	-4.486	0.127	0.553	14.210	0.097	0.470	-5.896
1035.	2352	8.270	4.229	0.511	4.085	4.330	0.497	0.672	1.076	0.130	-88.582
1036.	2353	4.729	1.778	0.376	-28.803	1.783	0.381	-27.512	1.353	0.286	-50.653
1037.	2354	1.189	0.677	0.569	18.209	0.655	0.659	39.971	0.158	0.133	-87.959
1038.	2357	2.467	1.455	0.590	23.166	1.299	0.565	17.094	1.471	0.596	24.696
1039.	2358	6.112	3.076	0.503	2.109	2.721	0.441	-12.968	2.996	0.490	-1.057
1040.	2359	4.708	1.960	0.416	-19.014	1.872	0.422	-17.657	1.890	0.401	-22.619
1041.	2360	2.366	1.150	0.486	-2.115	0.660	0.306	-45.722	1.365	0.577	19.978
1042.	2361	6.384	2.811	0.440	-13.166	2.297	0.393	-24.715	2.538	0.398	-23.583
1043.	2362	1.846	0.908	0.492	-0.578	0.825	0.520	6.076	0.796	0.432	-15.321

1044.	2363	1.621	0.736	0.454	-9.786	0.231	0.173	-78.047	0.406	0.251	-59.307
1045.	2365	4.662	2.065	0.443	-12.541	1.716	0.386	-26.416	2.513	0.539	10.799
1046.	2366	2.023	0.745	0.368	-30.651	0.797	0.436	-14.115	0.732	0.362	-32.191
1047.	2367	1.622	0.553	0.341	-37.288	0.546	0.376	-28.708	0.549	0.338	-37.996
1048.	2368	12.882	5.187	0.403	-22.333	5.433	0.441	-12.917	5.395	0.419	-18.402
1049.	2369	6.541	2.526	0.386	-26.319	3.340	0.521	6.390	2.505	0.383	-27.115
1050.	2370	2.482	1.140	0.459	-8.547	1.221	0.523	6.860	0.993	0.400	-22.939
1051.	2371	4.541	2.200	0.484	-2.477	2.209	0.532	9.145	2.001	0.441	-13.130
1052.	2372	1.281	0.382	0.298	-47.677	0.338	0.292	-49.136	0.701	0.547	12.740
1053.	2374	2.282	1.437	0.630	32.889	1.294	0.597	24.864	0.537	0.235	-62.993
1054.	2375	0.826	0.386	0.467	-6.700	0.275	0.434	-14.792	0.234	0.283	-51.411
1055.	2378	0.399	0.075	0.188	-74.551	0.072	0.232	-63.782	0.083	0.208	-69.677
1056.	2379	0.624	0.294	0.471	-5.687	0.314	0.661	40.382	0.130	0.209	-69.482
1057.	2381	0.872	0.128	0.147	-84.484	0.200	0.278	-52.738	0.260	0.298	-47.777
1058.	2383	0.933	0.246	0.264	-56.063	0.253	0.363	-31.915	0.178	0.191	-73.844
1059.	2387	2.417	0.775	0.320	-42.314	1.312	0.597	24.897	0.891	0.369	-30.604
1060.	2388	0.568	0.145	0.255	-58.112	0.129	0.237	-62.684	0.282	0.497	0.580
1061.	2389	1.262	0.813	0.644	36.439	0.620	0.631	33.173	0.529	0.420	-18.239
1062.	2390	1.263	0.803	0.636	34.329	0.769	0.596	24.546	0.760	0.601	25.911
1063.	2391	4.443	3.015	0.678	44.697	1.665	0.380	-27.932	1.736	0.391	-25.225
1064.	2392	1.511	0.990	0.655	39.077	0.521	0.364	-31.628	0.657	0.435	-14.553
1065.	2393	0.765	0.355	0.464	-7.374	0.317	0.475	-4.719	0.215	0.281	-51.797
1066.	2394	0.391	0.284	0.728	56.638	0.196	0.558	15.517	0.080	0.206	-70.173
1067.	2395	1.284	0.561	0.437	-14.054	0.416	0.329	-40.267	0.724	0.564	16.880
1068.	2396	0.257	0.090	0.351	-34.924	0.115	0.477	-4.218	0.094	0.364	-31.679
1069.	2397	0.263	0.115	0.437	-13.982	0.121	0.472	-5.476	0.041	0.155	-82.580
1070.	2398	0.214	0.103	0.481	-3.279	0.104	0.584	21.782	0.084	0.392	-25.048
1071.	2401	0.228	0.117	0.515	4.990	0.106	0.405	-21.698	0.029	0.129	-88.718
1072.	2402	0.148	0.069	0.468	-6.471	0.052	0.398	-23.450	0.098	0.666	41.596
1073.	2405	0.346	0.221	0.638	34.904	0.237	0.703	50.583	0.189	0.547	12.699

1074.	2406	0.289	0.116	0.400	-23.000	0.092	0.373	-29.611	0.150	0.519	6.000
1075.	2410	1.476	0.584	0.395	-24.100	0.419	0.306	-45.871	0.755	0.512	4.170
1076.	2411	0.108	0.028	0.261	-56.827	0.046	0.492	-0.564	0.056	0.518	5.625
1077.	2412	0.197	0.095	0.481	-3.329	0.096	0.554	14.538	0.109	0.554	14.509
1078.	2413	0.114	0.081	0.710	52.287	0.063	0.739	59.339	0.033	0.291	-49.422
1079.	2414	0.238	0.116	0.488	-1.638	0.122	0.591	23.377	0.058	0.243	-61.033
1080.	2415	0.728	0.368	0.506	2.803	0.163	0.348	-35.653	0.109	0.150	-83.761
1081.	2416	0.887	0.394	0.444	-12.185	0.389	0.479	-3.712	0.443	0.499	1.035
1082.	2417	0.306	0.134	0.438	-13.659	0.029	0.372	-29.820	0.029	0.095	-97.065
1083.	2418	0.391	0.176	0.449	-11.068	0.100	0.362	-32.251	0.195	0.500	1.271
1084.	2421	0.065	0.023	0.351	-34.999	0.022	0.555	14.739	0.019	0.285	-50.952
1085.	2423	0.348	0.079	0.227	-64.991	0.063	0.220	-66.805	0.169	0.487	-1.816
1086.	2424	1.078	0.340	0.315	-43.666	0.320	0.343	-36.830	0.340	0.315	-43.571
1087.	2425	0.107	0.047	0.439	-13.500	0.045	0.599	25.486	0.022	0.207	-69.819
1088.	2436	0.303	0.188	0.622	30.909	0.111	0.513	4.504	0.045	0.149	-84.082
1089.	2439	0.343	0.175	0.510	3.861	0.114	0.596	24.685	0.106	0.308	-45.326
1090.	2442	22.989	12.479	0.543	11.734	11.974	0.525	7.489	9.430	0.410	-20.502
1091.	2451	0.176	0.081	0.462	-7.915	0.086	0.561	16.204	0.065	0.367	-30.902
1092.	2452	0.194	0.082	0.420	-18.166	0.071	0.516	5.272	0.065	0.332	-39.440
1093.	2459	0.206	0.126	0.609	27.812	0.092	0.498	0.847	0.098	0.477	-4.230
1094.	2461	1.375	0.753	0.548	12.913	0.404	0.324	-41.564	0.531	0.386	-26.408
1095.	2462	0.341	0.225	0.660	40.294	0.222	0.743	60.345	0.222	0.653	38.383
1096.	2464	0.880	0.314	0.357	-33.419	0.341	0.425	-16.892	0.122	0.139	-86.517
1097.	2465	0.295	0.095	0.321	-42.217	0.063	0.258	-57.477	0.044	0.148	-84.306
1098.	2467	0.058	0.023	0.402	-22.565	0.022	0.471	-5.808	0.016	0.271	-54.424
1099.	2468	0.201	0.089	0.444	-12.360	0.113	0.685	46.250	0.164	0.813	77.420
1100.	2469	0.073	0.073	1.000	122.830	0.075	0.902	99.123	0.019	0.255	-58.163
1101.	2472	0.246	0.149	0.604	26.672	0.103	0.456	-9.250	0.076	0.310	-44.948
1102.	2474	0.381	0.187	0.491	-0.931	0.198	0.522	6.604	0.174	0.457	-9.237
1103.	2477	0.240	0.130	0.539	10.746	0.068	0.339	-37.808	0.036	0.150	-83.711

1104.	2478	0.148	0.089	0.604	26.564	0.070	0.626	32.039	0.047	0.314	-43.783
1105.	2479	0.077	0.056	0.733	57.923	0.026	0.416	-19.166	0.036	0.466	-7.000
1106.	2481	0.067	0.023	0.350	-35.153	0.022	0.500	1.261	0.027	0.403	-22.313
1107.	2484	0.133	0.086	0.650	37.753	0.113	0.922	103.903	0.062	0.469	-6.201
1108.	2485	0.195	0.097	0.495	0.205	0.122	0.882	94.075	0.087	0.443	-12.562
1109.	2486	47.244	21.872	0.463	-7.675	20.595	0.438	-13.730	16.080	0.340	-37.478
1110.	2487	0.131	0.070	0.538	10.569	0.071	0.528	8.054	0.043	0.331	-39.854
1111.	2489	0.068	0.021	0.310	-44.834	0.013	0.365	-31.502	0.007	0.103	-95.184
1112.	2501	0.601	0.288	0.480	-3.524	0.235	0.493	-0.439	0.172	0.286	-50.662
1113.	2534	0.085	0.054	0.629	32.717	0.052	0.800	74.110	0.032	0.377	-28.668
1114.	2544	0.098	0.064	0.652	38.327	0.048	0.436	-14.220	0.028	0.286	-50.759
1115.	2557	0.302	0.191	0.633	33.730	0.045	0.431	-15.357	0.065	0.215	-67.951
1116.	2559	0.078	0.033	0.429	-15.819	0.024	0.635	34.155	0.020	0.263	-56.377
1117.	2576	0.043	0.019	0.430	-15.780	0.018	0.486	-1.988	0.019	0.429	-15.815
1118.	2587	0.044	0.031	0.694	48.428	0.138	0.412	-19.986	0.013	0.287	-50.542
1119.	2588	0.701	0.112	0.160	-81.411	0.213	0.366	-31.339	0.191	0.272	-53.986
1120.	2590	0.062	0.031	0.510	3.738	0.642	0.557	15.134	0.012	0.194	-73.156

Contact us:

STATE CENTRE ON CLIMATE CHANGE (SCCC)

Himachal Pradesh Council for Science, Technology & Environment (HIMCOSTE)

B-34, SDA Complex, Kasumpti, Shimla 171009 H.P.
Ph.: 0177-2656489, Fax: 0177-2814923
www.hpccc.hp.gov.in/www.himcoste.hp.gov.in